WAVE INDUCED SEDIMENT TRANSPORT ON INTERTIDAL FLATS IN A FETCH LIMITED ENVIRONMENT, PINE HARBOUR MARINA, AUCKLAND

A thesis
submitted in partial fulfilment
of the requirements for the Degree
of
Master of Science (Technology)
in Earth Sciences
at the University of Waikato

by

Joanne Margaret Hull

University of Waikato
1996

ABSTRACT

This study investigates the nature of sediments and the role of tides, currents, waves and winds in driving sediment transport on the intertidal flats and shallow subtidal areas in the vicinity of Pine Harbour Marina which is situated in a shallow embayment adjoining Tamaki Strait in Hauraki Gulf, northeast North Island, New Zealand. The results from these investigations along with the study of the marina approach channel and dredge spoil dump site are used to examine the causes of sediment infilling the approach channel to the marina. This work was undertaken in support of two resource consents (H/9205 and H/9258) granted to Pine Harbour Marina by the Auckland Regional Council to undertake maintenance dredging to excavate 4,500 m^3 of sediment from the navigation approach channel between June and October 1994.

The sediments of the intertidal and shallow subtidal regions in the vicinity of Pine Harbour Marina were characterised and sediment mixing depths and transport patterns investigated with sedimentation rods, tracer studies, beach surveys and hydrographic surveys. The forcing processes of tide, wave, current and wind in the embayment were also investigated with hydrodynamic monitoring and a wave generation model for fetch limited environments was used to hind cast wave conditions. The data was collected, in conjunction with a monitoring program of the physical impacts of the 1994 dredging, to identify sediment transport pathways and to obtain quantitative sediment volume changes over the intertidal and subtidal channel areas.

Pine Harbour Marina is situated in a fetch limited low wave energy environment, dominated by local wind generated waves. Wave generation model WGEN3DD for limited fetches, was set up to hind cast wave conditions from wind data recorded at the site. The wave climate is characterised by wave heights (H_s) between 0.1 m to 0.4 m, and wave periods (T_s) between 1.0 and 2.0 s. Large wave events are rare, but wave heights (H_s) up to 0.5 m and periods (T_s) of 2.5 s are generated by wind speeds greater than 10 m/s from the northwest where fetch is greatest.

Wind driven circulation is important over the shallow intertidal region. On a day-to-day basis suspended sediment is transported north driven by the prevailing south-westerly winds. However large infrequent storms from the north have a greater impact on sediment transport over short time periods where significant volumes of sediment are entrained beneath high energy waves. Greater sediment transport occurs over the intertidal region than the subtidal region because sediment threshold velocities are more frequently exceeded in the shallower water depths. Thus sediment deposited in the approach channel to Pine Harbour Marina is infrequently entrained as wave orbital velocities are attenuated before they reach the bed in the deeper water.

A sediment tracer experiment was undertaken using artificial fluorescent particles to identify the pattern of fine grained sediment dispersion over the intertidal flats. The dominant sediment transport direction detected was towards the southeast during a westerly storm, and a significant concentration of tracer particles accumulated in the approach channel.

Sediment depth of disturbance rods on the intertidal flats indicate that sediment mixing depths were generally less than 1.5 cm due to shallow disturbance created the movement of small (h = 1.0-1.5 cm) wave ripples. Depth of sediment disturbance increased to between 2.0 and 3.0 cm associated with storm periods. The maximum sediment mixing depth recorded by sedimentation rods was 6.2 cm. Similar mixing depths of 2.5 cm were recorded during mixing depth experiments involving short cores through buried dyed sediment and vertical mixing of fluorescent tracer particles. Fluorescent tracer was mixed to a maximum depth of 17 cm, which was not attributed to wave action but rather to bioturbation.

Six monthly beach surveys indicated 2.5 cm of accretion occurred over the mid tide region on the northern intertidal flats. This volume of sediment accretion accounts for approximately half of the dredgings material dumped on the intertidal flats. The remaining dumped sediment was resuspended by wave action and either transported back into the approach channel to Pine Harbour Marina, or removed from the area in suspension.

Within 9 months of dredging of the approach channel, an average of 0.5 m of sediment deposition occurred along the northern side of the landward 700 m of approach channel. This was estimated to be approximately 5,250 $m^3 \pm 2{,}100\ m^3$ of sediment infilling the channel. The increased rate of sediment infilling the approach channel is attributed to natural sediment accumulation combined with the rapid transportation of some dredgings sediment back into the channel.

Initially dredgings sediment appeared to consolidate *in situ*, but became dispersed as a shallow layer extending up to 100 m over the intertidal flats north of the approach channel. Over the course of the investigation the dredge mounds were observed to be eroded by small drainage channels which became incised into the silty sediment at various locations transporting fine sediment from the dredge mound and intertidal flats into the approach channel. Some 12 months after dredging, the dredge mounds were dissipated and only remnant blocks of gravel to boulder sized fragments of bed rock were left.

This investigation has shown that a significant amount of dredge spoil deposited on the northern intertidal flats during the 1994 dredging operation became transported back into the approach channel within 9 months of the completion of the dredging works. An alternate disposal site for future maintenance dredging works in the approach channel at a further distance from the channel edge would reduce the likelihood of "recycling" of dredged material. Possible alternate disposal options for management of dredge spoil from future maintenance dredging could include: sidecasting disposal further from the channel; offshore disposal site - adjacent or distant; contained disposal; or landfill.

ACKNOWLEDGEMENTS

There are many people who have made a contribution to this thesis who I would like to thank. Firstly thank you to Prof. Terry Healy for initiating and coordinating this project with Pine Harbour Marina. Bruce and Allan Drinkrow, and Elizabeth Kempthorne of Pine Harbour Marina are thanked for the opportunity to undertake this research, and for sponsorship over the course of this study. Thanks also to staff at the marina for assistance in the field, and for the use of equipment and facilities.

My thanks are extended to Dr Terry Hume, for his continued interest and valued advice during the critical stages of this thesis, and to Dr Willem de Lange for computer assistance and editing of drafts.

Thanks to Prof. Kerry Black for advice and guidance during the fluorescent tracer experiment. Jon Marsh of Environmental Tracing Systems in the United Kingdom is thanked for supplying the tracer material and for analysing samples. Thanks also to Sarah Healy and Kerry for setting up the wave model WGEN3DD at Pine Harbour. Alf Harris (Waikato Microscope Unit, Ruakura) is thanked for assistance with SEM work, and Dave McComish (Greenfield Surveyors) for undertaking the beach surveys.

The staff of the Department of Earth Sciences are thanked for assistance in the field and lab. Particular thanks to Dirk and John for help with fieldwork; Ian for answering numerous questions and for his patience in teaching me how to conquer techbase; and Renat for XRD analysis. Thanks also to Dr Vicki Moon, Dr Richard Gormon, Mike, Steve B, Qi, Penny, Elaine and Sydney for general help.

Thanks to fellow masters students Nick, Scott P, Penny, Fiona, Scott S, Brett, Clare and Dave for help in the field, and advice and friendship over the last 18 months. To Dr Joseph Mathew, a big thank you for always having time to answer my questions, offering helpful suggestions and editing drafts.

Most importantly I would like to thank my family and friends for their interest and encouragement, especially over these last few months. Special thanks to Mum and Dad for moral and financial support over my years at varsity, to Grandma for all the goodies (and for keeping my flatmates happy with chocolate chippies), and to Sandie, Karen, Mervyn and Toby. A huge thank you to my chief field assistant Karen and to Mum and Steve who also endured bad weather and mud to help me whenever I called. Finally thanks to Steve for his constant support and encouragement, and for always being there to give me a helping hand.

Thanks, Jo ☺

TABLE OF CONTENTS

CHAPTER SIX: CONCLUSIONS

LIST OF FIGURES

LIST OF TABLES

LIST OF PLATES

CHAPTER ONE: INTRODUCTION

1.1 Introduction

Pine Harbour Marina, located near Beachlands, in south-east Auckland is situated partly on low lying land, and extends some 200 m over intertidal flats on the western side of the Beachlands - Maraetai Peninsula (Figure 1.1). The marina approach channel was dredged to a design depth of between 2.0 and 2.6 m below chart datum (CD) through sandy Holocene marine sediments of the intertidal sand flats, and carved in shore platform Miocene flysch deposits. Since the marina was opened in 1988, sedimentation in the approach channel has been faster than predicted in the hydraulic studies undertaken by Raudkavi (1986). Subsequently, hydrographic surveys of the approach channel in 1993 revealed that depths were reduced by up to 1 m in the area between 300 and 700 m from the entrance to the marina basin, necessitating removal of approximately 4500 m^3 of sediment (Kingett Mitchell & Associates, 1993a).

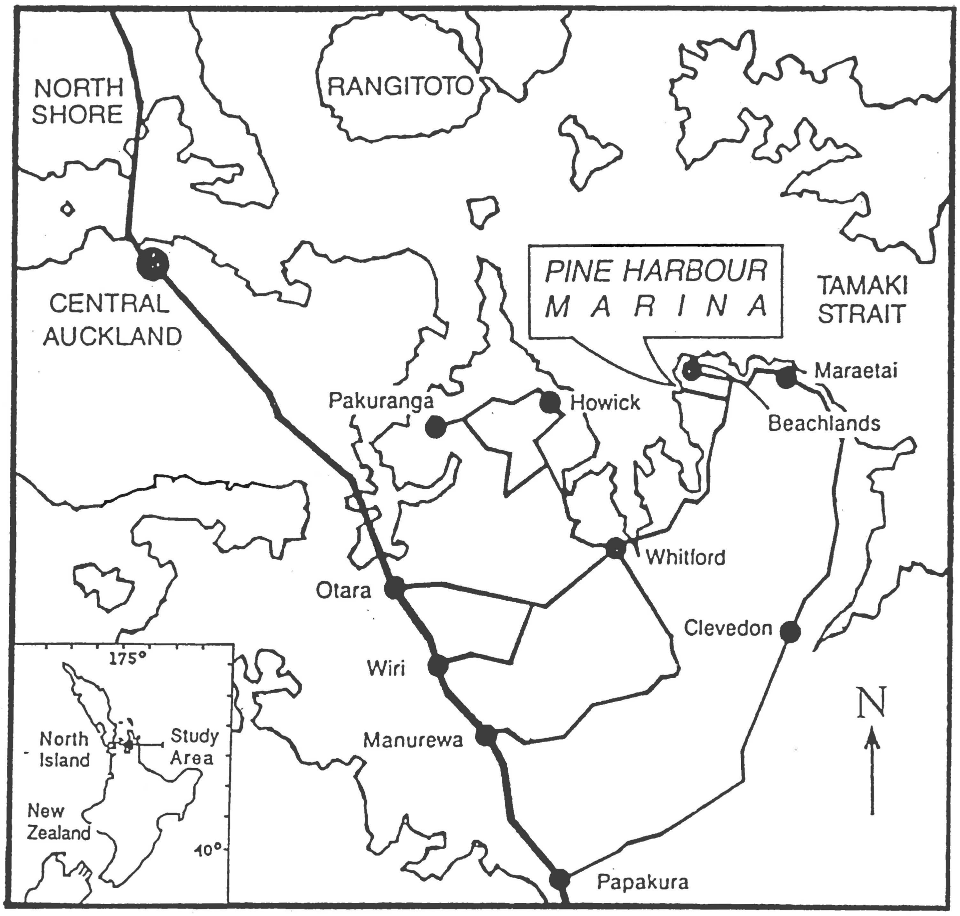

FIGURE 1.1: Location of Pine Harbour Marina in Manukau City, Auckland.

Resource consents were granted in 1994, under the Resource Management Act 1991 (RMA), to Pine Harbour Marina by the Auckland Regional Council to undertake the required maintenance dredging and disposal. The dredging was undertaken using a barge mounted hydraulic back hoe, and the dredged material was deposited on the adjacent sand flats to the north of the channel between June and October 1994. As a condition of the resource consent (as detailed in the Fourth Schedule of the RMA 1991), a monitoring program to assess the effects of the dredging on the environment was undertaken.

The monitoring program was undertaken in conjunction with an investigation into the broader issues of sediment transport pathways on the intertidal flat surrounding the marina approach channel and the processes driving these patterns. An understanding of sediment transport patterns and sedimentation rates in this intertidal fetch-limited environment is fundamental to solving the practical problems of channel sedimentation.

1.2 Objectives

The aims of this research are firstly, to monitor the physical effects of the dredging and disposal of dredgings material on the intertidal sand flats that took place at Pine Harbour Marina, between June and October 1994; and secondly to document the nature and origin of sediments and the sediment transport pathways and rates across the intertidal flats, in order to assist future decision making regarding continuing maintenance dredging of the navigation approach channel to Pine Harbour Marina.

The specific objectives of the research are:

1) To determine the patterns of sediment transport on the intertidal sand flats in the fetch limited environment fronting Pine Harbour Marina.

2) To determine the role of tides, currents, waves, and winds in driving sediment transport at the site.

3) To determine the stability of dredgings at the disposal site and ascertain the role of physical processes in their dispersal.

4) To assess the implications of disrupting the littoral system with dredging and dredge spoil disposal and dispersion on intertidal flats fronting Pine Harbour Marina.

1.3 Thesis structure

In this chapter, the context of the thesis has been introduced. The main issues of the sedimentation problem experienced at Pine Harbour Marina are highlighted, and the reasons why this study was undertaken were stated, along with the specific objectives to be met in this research.

Chapter 2 describes the geographical setting of the study. A brief literature review of previous work undertaken on sediment transport in fetch limited intertidal environments is included.

Chapter 3 investigates the characteristics of the intertidal and subtidal sediments and quantifies any volumetric beach changes that occur as the dredge mound disperses from the dump site, involving the monitoring of sedimentation rods, periodic beach surveys over the intertidal flats and hydrographic surveys over the approach channel.

Chapter 4 examines the forcing processes of tides, currents, waves, and winds in the local region, and involves the use of a wave generation model WGEN3DD.

In Chapter 5 a fluorescent tracer study is presented, the results of which are used to infer sediment transport patterns that occur as a result of the forcing processes over the intertidal flats.

In concluding, Chapter 6 summarises the main findings of the thesis, identifying the sediment transport patterns on the intertidal flats and the processes which drive these patterns. These findings will be applied to the sedimentation problem at Pine Harbour Marina, and be used to offer recommendations for future dredging and disposal options. Finally, areas requiring further research in order to better understand sediment transport in the fetch limited environment in the vicinity of Pine Harbour Marina will be highlighted, along with the potential for future research projects in the region to expand upon this research.

1.4 Study context

Numerous ports, harbours and marinas require ongoing maintenance dredging in order to maintain water depths for the safe and convenient passage of vessels in navigation channels and at berthing and mooring facilities. These developments necessitate dredging, reclamation, and coastal subdivision and earthworks that alter the natural coastal zone processes and impact on processes occurring in these systems. In order to make rational management decisions in controlling coastal development and minimising adverse effects, it is necessary to have an understanding of natural processes and systems operating in these zones, such as sedimentation rates and sediment transport pathways.

The Resource Management Act 1991 (RMA) is New Zealand's governing legislation concerning development of natural resources. The New Zealand Coastal Policy Statement (1994) accompanies the RMA in controlling coastal developments such as dredging, reclamation and coastal subdivisions. The purpose of the Resource Management Act 1991, as set out in Section 5 of the Act, is "...to promote the sustainable management of natural and physical resources". By sustainable management the Act means "...managing the use, development, and protection of natural and physical resources in a way, or at a rate, which enables people and communities to provide for their social, economic, and cultural well being and for their health and safety while: sustaining the potential of natural and physical resources (excluding minerals) to meet the reasonably foreseeable needs of future generations; safeguarding the life-supporting capacity of air, water, soil, and ecosystems; and avoiding, remedying, or mitigating any adverse effects of activities on the environment".

The New Zealand Coastal Policy Statement 1994 was prepared and recommended by the Minister of Conservation. It details policies intended to achieve the purposes of the RMA in relation to the coastal environment of New Zealand. The Coastal Policy Statement includes: national priorities for preservation of the coastline; protection of coastal characteristics with special value to tangata whenua; activities involving subdivision, use or development of coastal environment; the Crowns' interests; matters to be included in all Regional Coastal Plans, and responsibilities of the Minister of Conservation relating to types of activities having significant, or irreversible, adverse effects, and areas of coastal marine area that have specific value; implementation of New Zealand's international obligations; procedures used to review policies and monitor effectiveness, and any other matters relating to the purpose of New Zealand's Coastal Policy Statement. Regional Coastal Plans identify restricted activities, and recognise resources and features unique to each region, with the option of including specific policies to apply to important regional issues.

1.5 Pine Harbour Marina development

1.5.1 Marina development

The Pine Harbour Marina complex covers an area of 20 hectares situated in a shallow mesotidal low wave energy environment of the western side of the Beachlands - Maraetai Peninsula, approximately 1 km south of Beachlands, in Manukau City, Auckland. It is situated in an existing stream valley flat and extends west over the tidal flats. Undulating rural land borders the marina to the north, south and west.

Planning for the 555 berth marina at Pine Harbour commenced in 1984. Approvals were obtained by 1986, and development of Pine Harbour Marina began in 1986. The marina was officially opened and has been in operation since April 1988.

Approximately 440,000 m^3 of material was excavated to form the marina basin which covers an area of around 9 hectares (Wilkens and Davies, 1986). The excavated material was used to form the reclamations, and fill the area behind the marina basin for car and boat parking, and commercial facilities (Shirley, 1991). Breakwaters and seawalls were built from 24,000 m^3 of basalt rock imported from an Auckland quarry. Wave dissipation beaches were also placed at the entrance to the marina to minimise wave energy entering the marina basin (Wilkens and Davies, 1986).

The 1.5 km navigation channel was dredged through Holocene marine sediments in the outer channel and through Miocene flysch deposits of the Waitemata Formation landward (Healy, 1994). The channel's design depth was 2.4 m below CD, relative to the lowest astronomical tide (LAT), at the marina entrance and 2.6 m below CD seaward, to provide all tide access to the marina basin. This required the removal of approximately 130,000 m^3 of "silt" (Wilkens and Davies, 1986). The dredging was carried out using a hydraulic excavator mounted on a barge loading bottom dump barge. The dredged sediment was then disposed of at sea (Shirley, 1991). The marina basin design depth was 2.4 m below CD at the entrance, grading up to 1.9 m below CD landward. The purpose of the channel bottom sloping seawards, was to encourage the migration of accumulated sediment towards the sea as a density current (Raudkavi, 1986; Wilkens and Davies, 1986).

Two existing streams within the land catchment draining toward the marina complex were realigned to discharge to the south of the marina onto the intertidal flats (Bioresearches, 1985).

1.5.2 Pre and post-construction monitoring

In compliance with the original Water Right that was granted for marina construction, a series of pre and post-construction surveys have been carried out. Wilkens and Davies (1986) carried out the original EIA which included a section on hydraulics by Raudkavi (1986). Investigations into the effects of the development on aquatic and terrestrial habitats, and pre-construction surveys were carried out to gather baseline information on the condition of sediments and shellfish (Bioresearches, 1985, 1986). Post-construction surveys for shellfish and sediment quality monitoring took place after six months, twelve months and at two yearly intervals (Bioresearches, 1988, 1989, 1991, 1993). The time interval between later surveys was extended to four years as little change in condition was been found (Bioresearches, 1993).

1.5.3 Sedimentation problem

The approach channel to Pine Harbour Marina suffered sediment deposition affecting navigation, especially in a 300 m sector of the channel between 400 and 700 m from the entrance to the marina basin, within two years of construction (Healy, 1994). A feeder channel to service the boat loading ramp was originally excavated to a depth of 2.0-2.6 m below CD; within two years this channel had completely filled in, involving approximately 3,000 m^3 of sediment deposition (Healy, 1994). Sediments within the channel are typically very fine sand to silt, and are finer than sediment immediately adjacent the channel on the sand flats (Kingett Mitchell & Associates, 1993a). This rate of channel infill was not predicted in the original environmental impact assessment, which predicted 10-15 mm of deposition which would require maintenance dredging at intervals of only about 20 years (Raudkavi, 1986).

Sedimentation within the marina approach channel was greater than originally predicted. Hydrographic soundings of the marina approach channel, undertaken by Kingett Mitchell & Associates, in March and July 1993 indicate that channel water depths were reduced by up to one metre in the landward section of the channel, between the first and second landward navigation markers, when compared to the design depths of 2.4 and 2.6 m respectively below CD (Kingett Mitchell & Associates, 1993a). There was concern for vessel safety when entering or leaving the marina at low tide. Thus maintenance dredging in the landward section of the channel was required in June 1994 for the safe navigation of vessels through the approach channel to Pine Harbour Marina.

Concern was raised by local residents about the source of muddy deposits occasionally blanketing and despoiling the intertidal zone along the shoreline from Beachlands Point to Maraetai Beach. The possibility of this being attributed to the marina dredging operation necessitated investigation.

1.5.4 The 1994 dredging requirement

A minimum channel depth of 2.0 m below CD is required for safe vessel movement into and out of the marina. In 1994 some 4,500 m^3 of sediment was estimated as requiring removal from the approach channel to Pine Harbour Marina. Kingett Mitchell & Associates (1993b) based this volume upon a channel width of 25 m, across which 10 m of width required 0.75 m to be dredged, and 15 m required 0.5 m to be dredged, over a channel length of 300 m.

Under the RMA 1991, permits are required for the disturbance of the seabed and for the release of material to the water column that results from dredging activity, sections 12 and 15 RMA (Kingett Mitchell & Associates, 1993a). The resource consent application was made to the Auckland Regional Council for a consent to carry out dredging of the approach channel to Pine Harbour Marina. Permission to carry out maintenance dredging of the approach channel to the marina was granted in April 1994 via two resource consents: to disturb the seabed during dredging (permit no. H/9205); and to discharge sediment into the water column during dredge disposal (permit no. H/9258). These consents were subject to a number of conditions and required the setup of a monitoring program which took place from April 1994 to December 1995.

The dredging operation took place from June to October 1994, using a hydraulic back hoe excavator which was mounted on a floating barge (Plate 1.1). Dredging took place sporadically over eight weeks, dependant on weather patterns which affected the stability of the barge. The excavated material was side cast onto the adjacent intertidal flats to the north of the approach channel, the dump mound extending the length of the dredged area parallel to the channel (Plate 1.2).

Plate 1.1: Dredging of the approach channel to Pine Harbour Marina was undertaken using a hydraulic back hoe mounted on a floating barge.

Plate 1.2: Dredged sediment excavated from the approach channel to Pine Harbour Marina was dumped on the adjacent intertidal flats north of the channel.

CHAPTER TWO: STUDY SITE AND LITERATURE REVIEW

2.1 Geographical setting

Pine Harbour Marina is located 1 km south of the small rural settlement of Beachlands, in Manukau City, Auckland. The marina is located in a shallow tidal embayment on Tamaki Strait coastline in Hauraki Gulf. Plate 2.1 illustrates the extensive intertidal flats fronting Pine Harbour Marina, and the exposed shore platforms and chenier shell ridges north of the marina approach channel. The different catchment land uses are evident in Plate 2.1, including pastoral farm land, forestry, and earthworks. The embayment is sheltered from the Hauraki Gulf by numerous islands including Rangitoto, Motutapu, Motuihe and Waiheke Islands (Plate 2.2). These landforms also reduce fetch for wave generation in the embayment between Howick and Beachlands Points.

2.1.1 Regional geology

Auckland's regional geology (Figure 2.1) can be broadly characterised into two main groups. Underlying the eastern half of the region are fine grained greywacke basement rocks of the Waipapa Group, deposited in the Triassic (c. 200 m.y.a). These were upthrust during folding and faulting during the Jurassic to form the rugged hills east of Whitford (Kermode, 1992). In the west, the Waitemata Basin filled with a 2 km thick succession of sediments, derived from neighbouring lands, in the Early Miocene (24-15 m.y.a). These sediments consisted of mainly flysch sequences with conglomerate and rare limestone layers (Kermode, 1992). The area was extensively blockfaulted in the late Miocene to Pliocene (7-2 m.y.a), during which the Hunua Ranges and Maraetai Hills were upthrust, while the Manukau Harbour and Waitakere Ranges to the west were downthrown. This raised the greywacke hills to the east of Beachlands, and exposed the Waitemata Formation along the coastline as cliffs. Shore platforms of Waitemata Formation were cut by wave action eroding the cliffs around the Waitemata Harbour (Kermode, 1992). More recently, during the Pleistocene and Holocene (0-2 m.y.a), coastal and shallow marine sediments accumulated in inlets and around islands.

PLATE 2.1: *View to the south towards Waikopua Creek with Pine Harbour Marina in the foreground. Catchment landuse is varied including pastoral farm land and forestry at Whitford. Evidence of earthworks at Whitford Landfill and with expanding subdivisions can be seen in the top right corner.*

PLATE 2.2: *Pine Harbour Marina is located in an embayment between Howick and Beachlands Points adjoining Tamaki Strait and is sheltered from Hauraki Gulf by Beachlands coastline and Rangitito, Motutapu, Motuihe, and Waiheke Islands.*

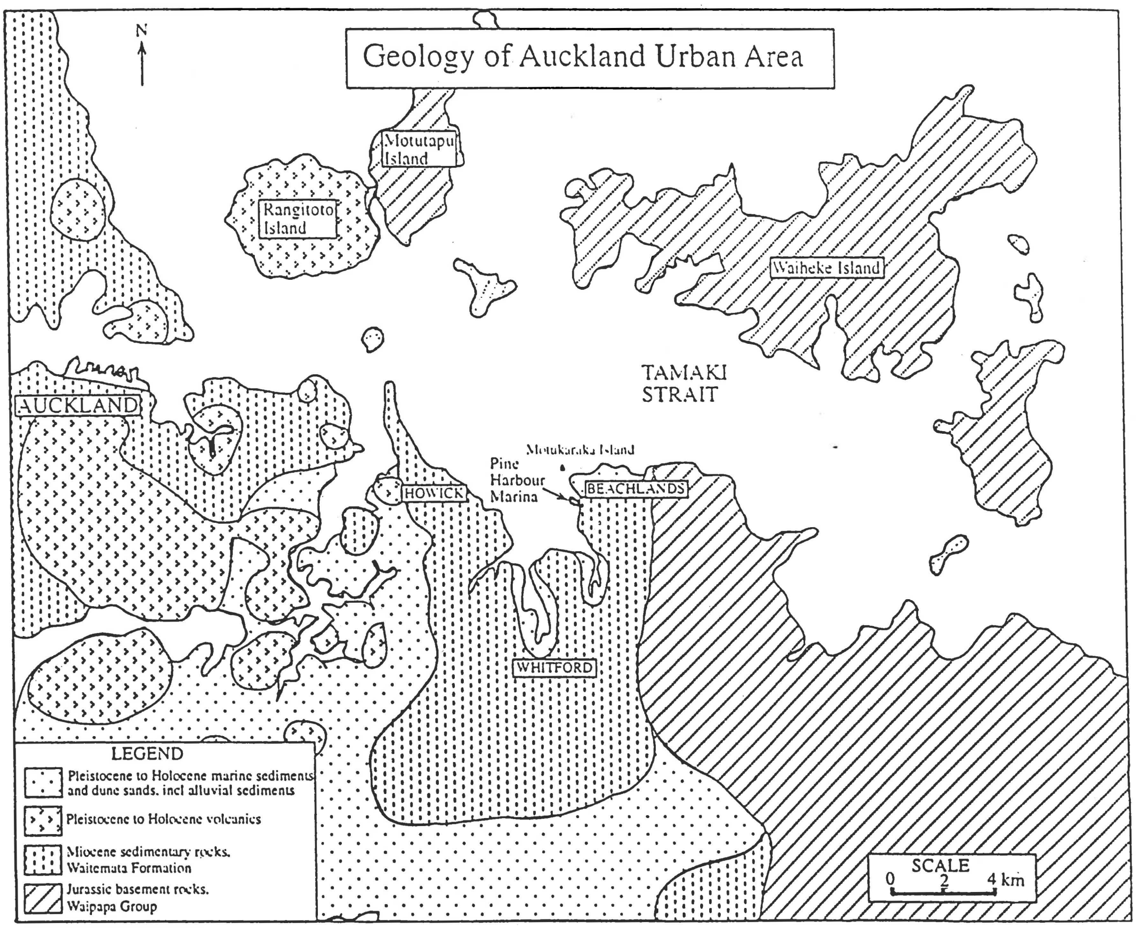

FIGURE 2.1: Geology of Auckland urban area.

2.1.2 Harbour morphology

2.1.2.1 Hauraki Gulf and Tamaki Strait

Pine Harbour Marina is located in a semi-enclosed bay, at the mouth of a shallow inlet which joins Tamaki Strait, in Hauraki Gulf, north-east North Island, New Zealand (Figure 2.2). Hauraki Gulf is a shallow, partially enclosed sea bounded on 3 sides by the North Island of New Zealand and open, on its northern side, to the Pacific Ocean (Harris, 1985). Hauraki Gulf, at the 100 m contour, encloses approximately 10,000 km^2. The gulf is the continuation of a down faulted rift valley, extending from Firth of Thames to the northern tip of Coromandel Peninsula (Bowman & Chiswell, 1982). Tamaki Strait is a drowned river valley creating a narrow waterway (6-10 km wide) connecting Firth of Thames and Waitemata Harbour. Water depths in Tamaki Strait are shallow, on average less than 10 m.

Hauraki Gulf is dotted with numerous islands, both sedimentary and volcanic in origin. The coastline on which Pine Harbour Marina is located is sheltered from ocean swells approaching Hauraki Gulf from the north and north-east by Rangitoto, Motutapu, Motuihe and Waiheke Islands. Fetch is limited by these islands and the coastline around Howick and Beachlands, and restrict wave heights. Shallow water depths in the embayment between Howick and Beachlands Points and in Tamaki Strait (depths reach 4 m approximately 4 km offshore) also restrict the development of large waves.

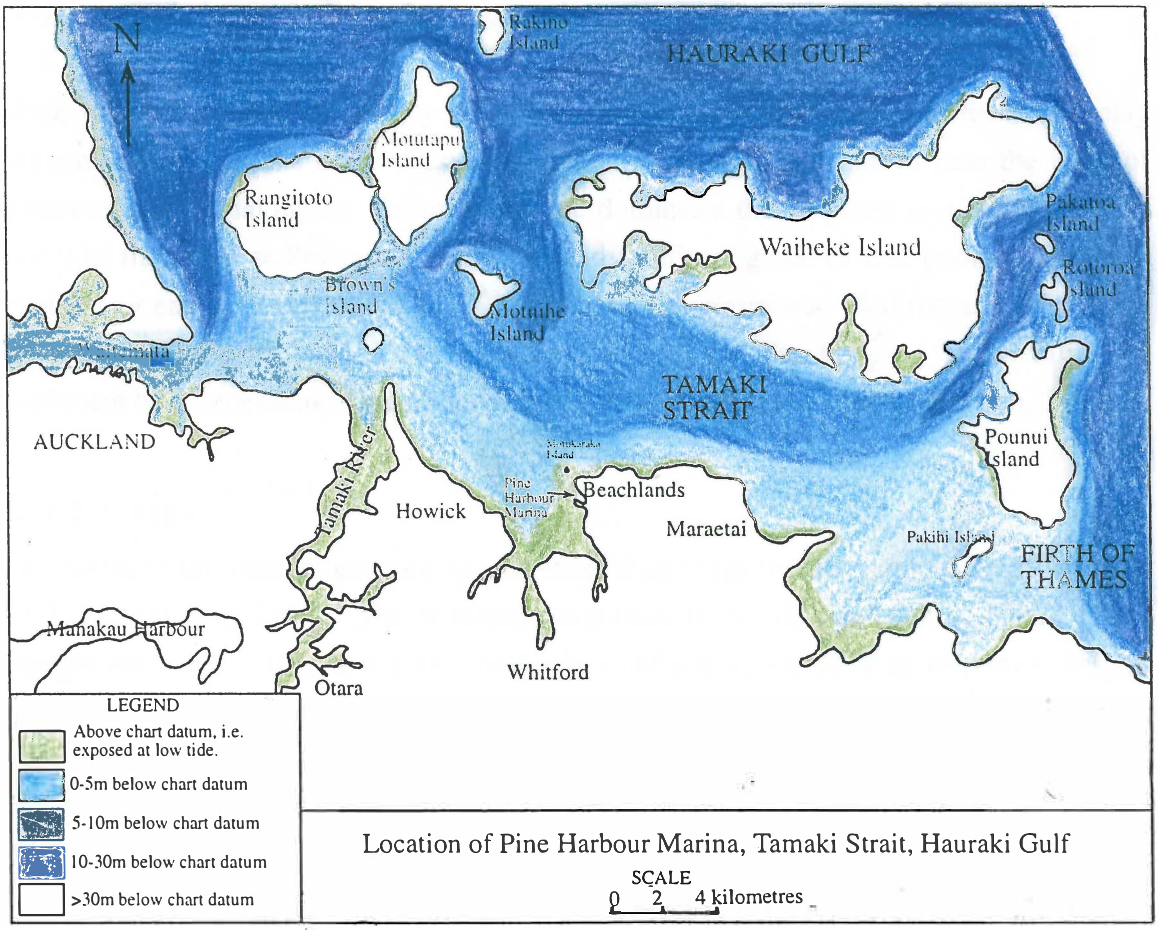

FIGURE 2.2: Water depths in the vicinity of Pine Harbour Marina and Tamaki Strait.

2.1.2.2 *Intertidal flats*

Gently sloping intertidal sand flats extend 1,000-1,400 m from the north-south oriented coastline, covering approximately 60% of the inlet at low tide. Shore platforms of Waitemata Formation extend up to 200 m from the sea cliffs exposed along the northern sector of the Beachlands coastline, and to the south in the upper reaches of the tidal inlet.

Sediments veneering the wave cut shore platforms are comprised of medium to fine sands, with some shell gravel, which grade to coarse silts towards the head of the embayment and offshore. A large chenier shell ridge joins Motukaraka Island to the Beachlands coastline to the north of Pine Harbour Marina.

Tidal inlets or embayments, like estuaries, are areas of active sedimentation receiving fluvial inputs of sediment with the discharge of rivers and streams into the coastal zone. Sediments are also introducted to the marine environment through erosion of the coastline. The Waitemata Formation flysh sequences of sandstones and mudstones forming sea cliffs exposed around the Hauraki Gulf are readily eroded. Evidence for this are the numerous shore platforms of Waitemata Group sediments cut by wave action and subaerial weathering (Gordon, 1993). Flysh sequences of mudstone and sandstone weather to fine silts and sand, and are the principal source of Holocene sediments in the Waitemata Harbour and along the Auckland coastline (Gordon, 1993).

Fine grained sediment is usually dispersed, but once in the marine environment clay minerals flocculate and settle out of suspension in muddy coagulations near the head of estuaries and fluvial inputs. Sediment source dominates the sediment size distribution of the tidal flat where sediment is generally muddy, reflecting source and poorly sorted due to the low energy levels experienced in intertidal environments. Sediments can become consolidated due to biological processes, for example the trapping and binding of sediment by filamentous algae organisms and faecal pellets and mucus (Gordon, 1993).

2.1.2.3 Tides

In Hauraki Gulf tides are essentially semi-diurnal although there is some diurnal variation in height (Harris, 1985). The principal component is the M2 tide (Greig, 1990). Tidal ranges are 1.0 to 3.0 m along the coast. In confined areas, such as estuaries, heights differ. A tide in an embayment such as inner Hauraki Gulf is a co-oscillating tide, and is the result of superpositions of the ocean tidal wave at the entrance, which drives the system, and the reflected wave (Harris, 1985).

S4 electromagnetic current measurements at Pine Harbour Marina indicate that tidal currents are weak (< 20 cm/s) and unable to entrain sediment, however they can transport sediment entrained by wave action in the net direction with tidal assymetry. Tidal currents flow towards the south-east in flood tide and towards the north-west during the stronger ebb tide. Currents in the marina approach channel flow parallel to the channel to the east and west with the tide.

A comparison of tidal elevations predicted from tidal constituents for Auckland and Pine Harbour Marina, using THANAL tidal prediction program, is presented in Figure 2.3. Tides are similar at both sites, although there is some variation in the MSF constituent which creates a fortnightly variation in tidal amplitudes (W. de Lange, pers. comm.). This variation is negligble during the neap tide, but is more pronounced during the spring tide where Auckland's tidal range is greater than for Pine Harbour Marina by approximately 0.1 m. There is no significant difference in the time peak high tide is reached between the two locations, although it appears that high tide at Pine Harbour Marina is reached slightly before high tide in Auckland.

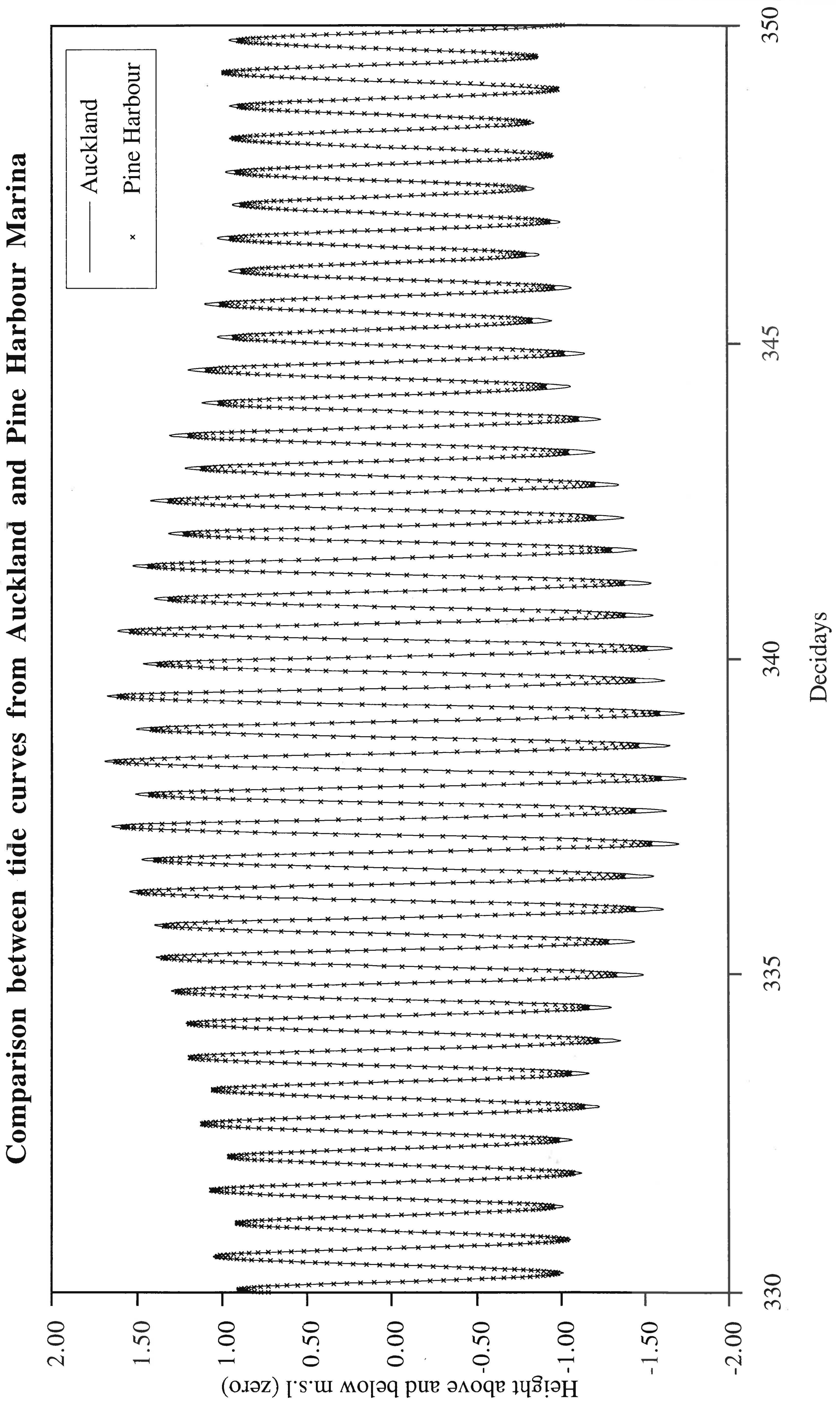

FIGURE 2.3: Comparison of tidal range between Port of Auckland and Pine Harbour Marina predicted using THANAL tidal prediction program.

2.1.2.4 Waves

Beachlands coastline on which Pine Harbour Marina is located is sheltered from ocean swells by surrounding landforms and offshore islands. Local wind generated waves are of primary significance, however fetch is limited in all directions which restricts wave generation. Winds in the Auckland region are predominantly from the south-west, west and north-east (Hurnard, 1980). South-westerly winds prevail especially during the winter, and easterly winds are likely in late summer and autumn. Data from Musick Point (March 1980 to October 1981) indicate that winds from the south-west occur 31.3% of time, with westerly winds occuring 14.3% of the time (Figure 2.4) (Wilkens & Davies, 1986).

No previous waves and current measurements were made in the embayment prior to this investigation which determined that significant wave heights (H_s) are between 0.1 and 0.4 m and wave periods (T_s) 1-3 s. During storms, waves (H_s) generated across the 10 km fetch from the north-west can reach up to 0.5 m. Waves are diffracted from the southern shores of Rangitoto and Motutapu Islands, and are transmitted through the channel between Browns and Motuihe Islands, across north-west Tamaki Strait and onto the western shores of the Beachlands coast. Waves from the north and north-east are excluded by Beachlands coastline and Motukaraka Island.

Waves generated by the prevailing west and south-westerly winds are limited by the short 4 km fetch that extends across the embayment to Howick. Locally generated sea waves from the south-west (H_s = 0.1-0.2 m) dominate the wave climate, and propagate in the direction of the prevailing south-westerly winds (Figure 2.4). Littoral drift is driven by the dominant wind generated waves acting over the tidal flats. Wave energy resultants from the wind energy indicate a northerly component aligned towards 70° (Healy, 1994). Along the Beachlands coastal sector south-westerly wind generated waves drive the littoral drift north from Waikopua Creek to Motukaraka Island (Figure 3.9).

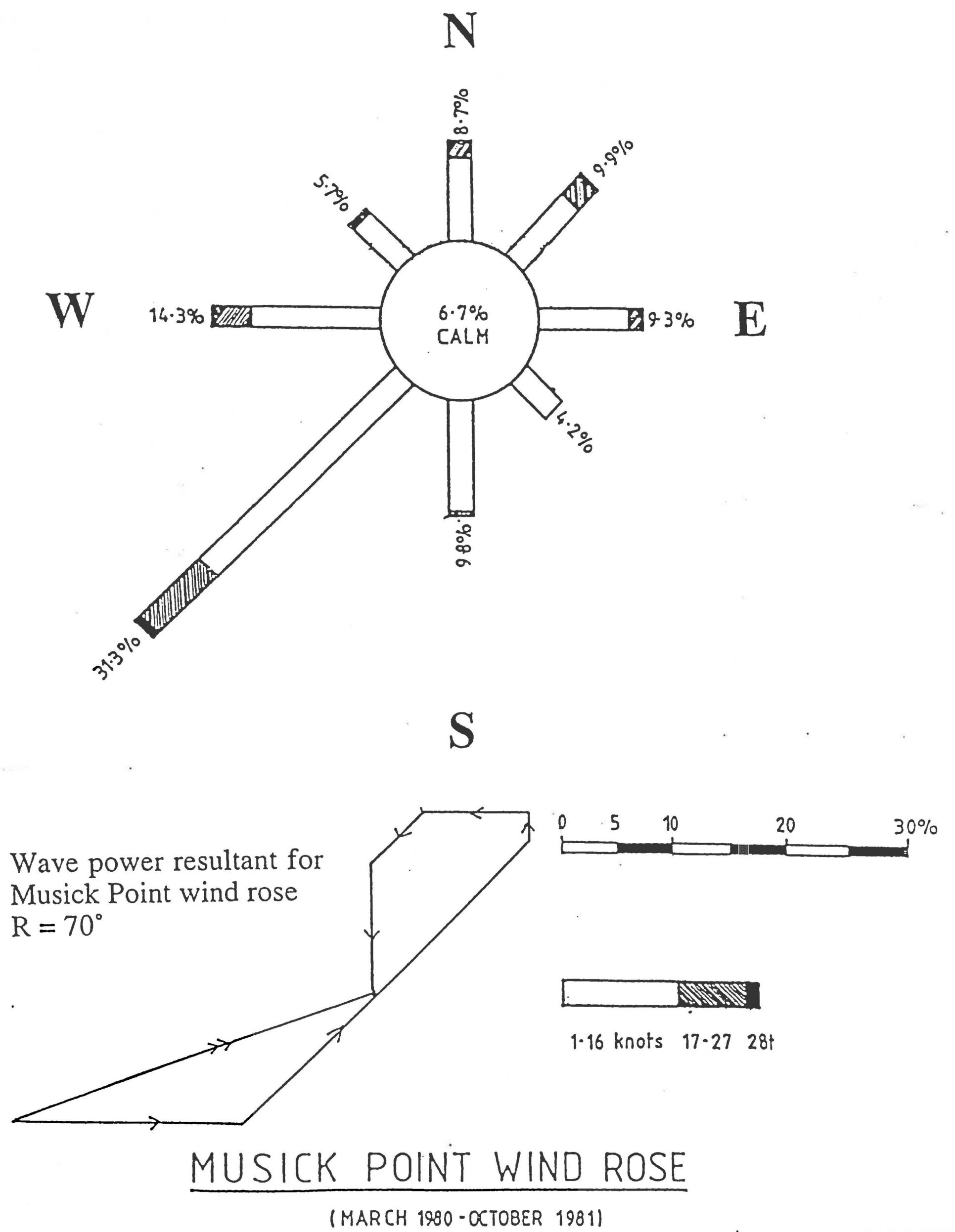

FIGURE 2.4: Wind rose from Musick Point, March 1980 to October 1981 and calculated wave energy resultant aligned towards 70° (Healy, 1994 after Wilkens & Davies, 1986).

2.1.2.5 Currents

Wind driven circulation in Hauraki Gulf is composed of surface currents mainly directed 0-25° left of wind direction except in nearshore regions where currents are modified by local topographic features (Proctor & Greig, 1989). In Tamaki Strait currents are generally orientated along the coast in the same direction as the wind. Proctor & Greig (1989) used a depth-averaged 2D numerical model to simulate tidal conditions under various wind conditions. The model showed that a north-easterly wind generates currents that flow east to west from Beachlands to Howick, the current following the coastline turns towards the south-west as it crosses the embayment before continuing to flow towards Howick in the west. Under south-west and north-west winds the opposite situation occurs, with currents flowing west to east parallel to the coast from Howick to Beachlands, turning towards the north-east as the current encounters the embayment, before continuing east parallel to the Beachlands coastline (Proctor & Greig, 1989).

Tidal currents are weak (<20 cm/s) and are predominantly ebb and flood in the absence of wind up the approach channel and over the tidal flats. The tidal assymetry produces a net current which can transport suspended sediment north. In relatively shallow depths, the water responds rapidly to wind stresses and there is a strong tendency for the surface currents to be aligned with the wind direction (Niedoroda & Swift, 1991). The effect of wind stress on the water surface can enhance or reduce the net current depending on the direction. Strong wind flowing in the same direction as tidal currents will increase the strength of the current. In the opposite situation strong winds opposing the tidal flow may retard current velocities and produce a net current in the opposite direction.

2.1.3 Catchment characteristics and sediment supply

The shallow tidal embayment, in which Pine Harbour Marina is located, receives sediment input from three large catchments, drained by creeks delivering sediment into the coastal system (Figure 3.9). Catchment geology, hydrology and land use determine how much fluvial sediment is input into the tidal inlet. The largest of the catchments, at appproximately 24 km^2, is drained by Turanga Creek, which forms the major channel in the tidal inlet and is joined by the smaller Mangemangeroa Creek, which has a catchment of approximately 11 km^2. The second largest creek to enter the tidal inlet is Waikopua Creek which drains approximately 14 km^2 of catchment. Each of these catchments has underlying Waitemata Formation flysch geology which weathers to mud and sand sized particles. Pastoral land is evident in all catchments, but Waikopua Creek also collects drainage from some forested areas. With the expansion of Auckland's urban area, new subdivisions and land development in these catchments deliver greater quantities of terrestrial sediments to the coastal environment. As pastoral land is developed the protective vegetation layer is removed for earthworks increase the exposure of soils to erosion and wash out with any rainfall events.

2.2 Sediment transport studies in fetch limited environments and intertidal flats

Descriptions of sediment transport in the literature has tended to be biased towards microtidal environments (Short, 1991; Carter, 1988). Studies of processes and morphodynamics on open coasts appear to have received most attention, to the disadvantage of sediment transport studies in environments, such as low wave energy intertidal flats. This research will contribute to a better understanding of sediment transport in fetch limited intertidal environments which are poorly described in the literature.

A high proportion of meso to macro tidal beaches are in sea, or wind wave (fetch limited) environments, owing to the semi protected nature of many macro tidal environments. Fetch is the distance over which the wind blows, the greater the fetch the more the wave will have developed due to the longer period of wind stress applied to the surface of the water (Komar, 1976). Fetch is limited by local topographic features, shape of the coastline, and occurance of offshore islands, which impede the passage of the wind over the water, thus limiting significant wave heights and periods.

Few studies are found in the literature of sediment transport studies on intertidal flats. Many workers (Wright & Short, 1983; Short, 1991; Masselink & Short, 1993) have proposed morphological beach models which accommodate higher wave energies. With decreasing wave energy macro tidal beaches eventually grade into tide dominated tidal flats, however little is known about their dynamics (Short, 1991). Studies of morphologies of beaches indicate that tidal flats occur with the transition to lower wave energy environments and also occur in estuarine conditions (Short, 1991). Beach tidal flats are characterised by a steep coarse grained beachface which abruptly changes into fine grained, very low gradient (0.1 degrees) rippled tidal flats. Depending on the location the flat may be, uniform, accomodate low amplitude bars, or ridge and runnel topographies. These low energy environments are exposed to episodic higher wave energy, the impact of which on the tidal flat will depend on the actual wave climate, the tidal flat gradient and sediment grain size, tide range, and competing tidal currents and wind and wave induced currents.

CHAPTER THREE: THE SEDIMENTS: INTERTIDAL FLATS & MARINA APPROACH CHANNEL

3.1 Introduction

This chapter describes intertidal and subtidal sediments in the vicinity of Pine Harbour Marina, and quantifies volumetric changes in beach and channel sediments which occur as a result of disposing of dredging material from the Pine Harbour Marina approach channel onto the adjacent sandflats. Numerous investigative methods were employed including: sediment sampling and analysis; beach surveys of intertidal flats; probing of intertidal flat sediments; hydrographic surveys of Pine Harbour Marina approach channel; and beach surveys of the dredge mound.

3.2 Intertidal and subtidal sediment characteristics

3.2.1 Textural analysis of surficial sediments

The surficial sediments on the intertidal flats fronting Pine Harbour Marina were extensively sampled in February 1995. 50 samples were collected along 3 lines at approximately the high tide, mid tide and low tide levels (Figure 3.1a). Measurements of bedforms and observations of the dominant biogenic and terrigenous components were made upon sample collection, and the raw data compiled as Appendix 1.1. Nine subtidal samples were also collected by divers from offshore of the marina, around Motukaraka Island and offshore from Sunkist Bay during March 1995 (Figure 3.1a). Channel samples were taken in September 1995 to investigate the texture of sediment infilling the approach channel (Figure 3.1b). Further to this, SCUBA diver observations and descriptions of sediment texture were made along 3 transects offshore from: Sunkist Bay; Motukaraka Island; and between the approach channel to Pine Harbour Marina and Motukaraka Island (Figure 3.1a) during December 1995 (Appendix 1.2).

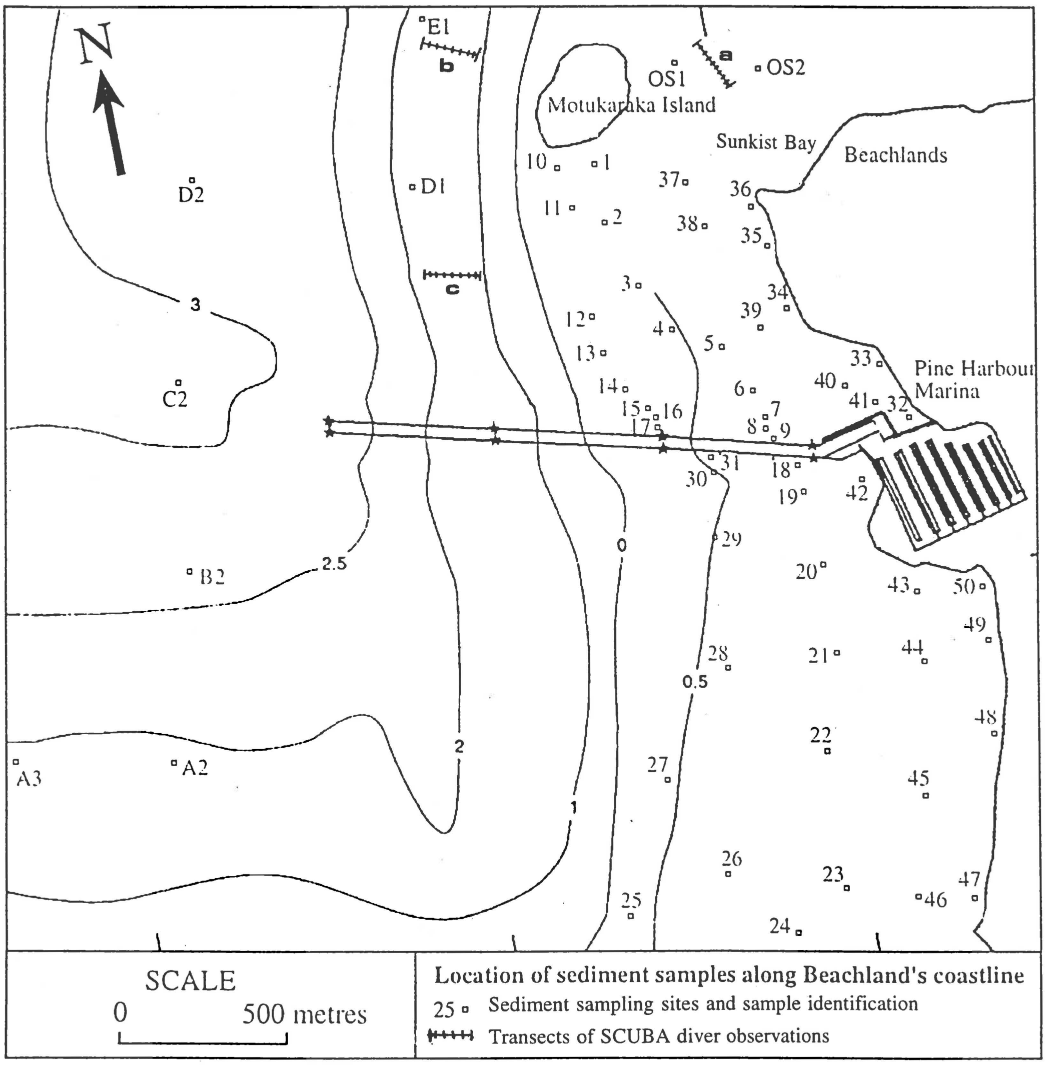

FIGURE 3.1a: Location of intertidal and subtidal sediment sampling sites in the vicinity of Pine Harbour Marina. SCUBA diver transects are represented by lines a, b and c.

Fifty samples from the intertidal flats were analysed following standard textural analysis procedures of Folk (1968) to obtain gravel, sand and mud fraction percentages. The sand fraction of each sample was analysed using the University of Waikato Rapid Sediment Analyser (RSA) to obtain qualitative and descriptive measures of sediment grain size and sorting. The RSA consists of a fall tube, 1.90 m in height, with a pan in the bottom connected to a balance which measures the amount of sediment settling out of the fall tube after the sediment has been released. Release of sediment triggers a timer connected to the balance. Settling velocities of different sized grains vary, with larger grains settling sooner than fine silts. The RSA computer programme calculates the mean grain size, sorting, skewness and percentage of each size class (Appendix 1.3). RSA gives a good indication of hydraulic properties of sediments and allows many samples to be analysed relatively quickly. Results are presented as both moment method and graphical method calculations, however moment method is considered a better representation because it is computational (Folk, 1968).

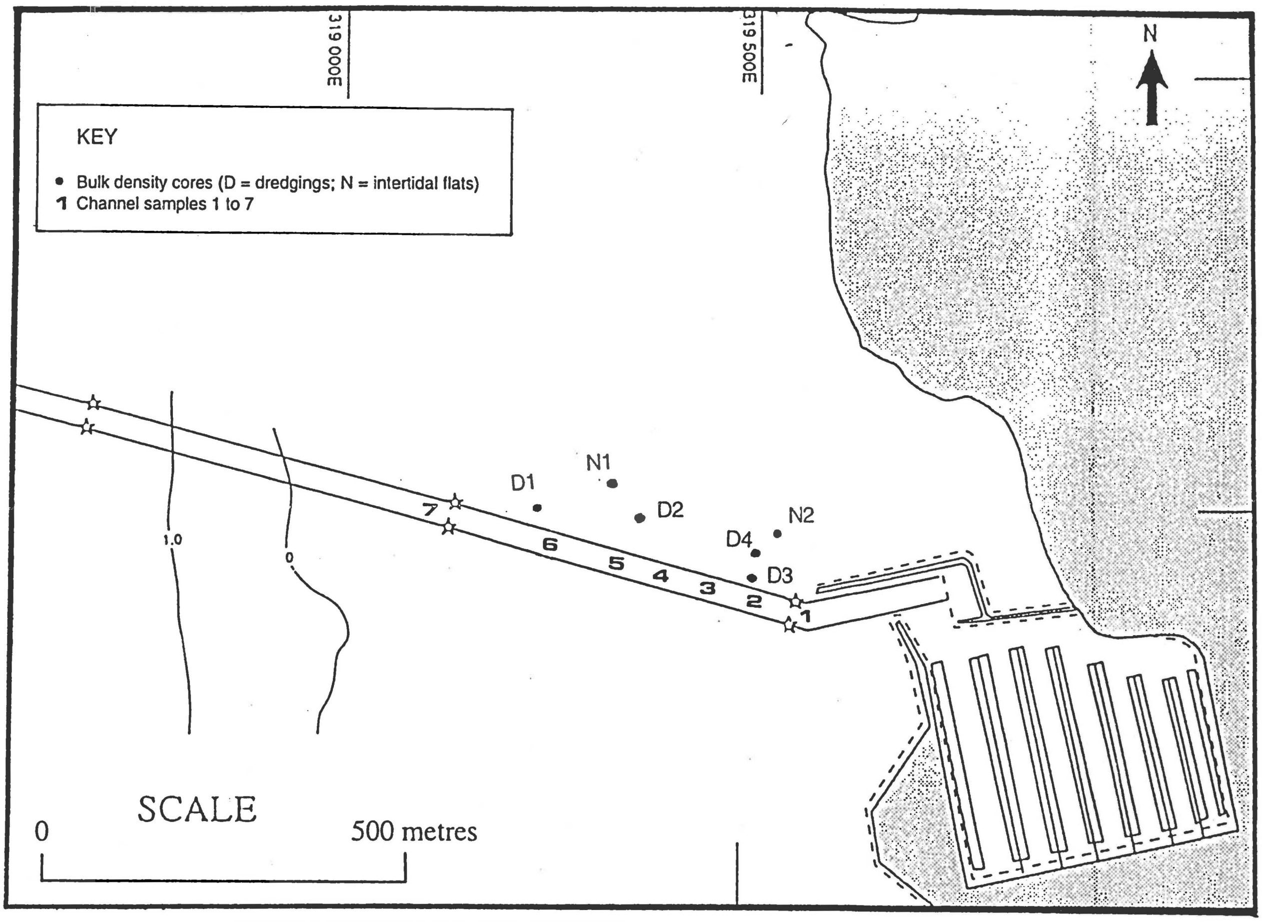

FIGURE 3.1b: Location of channel sediment samples 1 to 7, and location of bulk density cores from dredgings sediment (D) and from natural intertidal flat sediments (N).

Subtidal sediment samples and selected samples from intertidal flats, with mud content greater than 5 %, were analysed following the methodology of Lewis & McConchie (1994) to determine the proportion of clay and silt in the mud fraction, these results are compiled as Appendix 1.4. The weight of each dried subsample is representative of the proportion of the total mud fraction remaining in suspension above that specified depth at that specified time. Temperature affects the viscosity of water and therefore settling velocities. The temperature was noted, as this affects the viscosity of the water, and the sampling depths adjusted accordingly (Lewis and McConchie, 1994).

3.2.2 Results

Mean grain size

A map of the distribution of mean grain sizes of surficial samples is illustrated in Figure 3.2 which shows the dominance of fine sands (2.5 to 3.0 Ø or 0.2 to 0.1 mm). Sediment along the narrow beach face is comprised of coarse sand with a high broken shell gravel component. Sediments become finer offshore. Areas of very fine and muddy sediment occur closer to the head of Waikopua Creek. Muddy sediment is also evident along the northern side of the approach channel to Pine Harbour Marina where the dredgings were dredgings were deposited. Coarse sediments comprise the shell ridges to the north of the approach channel and some shelly-gravel covers the shore platform immediately to the north of the approach channel.

Sorting

Sorting represents the standard deviation or range of grain sizes occurring within a sample. A low standard deviation is typified as a well sorted sample compared to sediment with a high standard deviation, described as poorly sorted. Sorting depends on two major factors which are the size of grains supplied to the system and the environment and processes acting on the grains supplied.

Figure 3.3 illustrates the pattern of surficial sediment sorting across the intertidal sandflats. Sediment was generally better sorted further offshore, and are poorly sorted around the dredging dump-ground, where there was a large range of grain sizes from boulder to gravel sized terrigenous rock fragments, weathered from shore platform, to fine sand and silt and abundant broken shell. The poorest sorted sediments are near the chenier shell ridges and close to where terrigenous inputs are high, such as near eroding cliffs. Poor sorting is common in sediments that are bimodal, that is sediments that have more than one source.

Skewness

Figure 3.4 illustrates the skewness of surficial sediments on the intertidal flats. Skewness represents the symmetry of the particle size distribution, with a positively skewed sediment distribution dominated by fine grains, and vice versa for negative skewed sediment (Boggs, 1987). Sediment distribution curves may be negatively skewed due to fine sands being winnowed and coarse grains left behind in a lag (King, 1972), or from addition of coarse grains, such as broken shell.

At Pine Harbour the texture of surficial sediments on the intertidal flats is dominated by negatively skewed sediment, that is although the mean grain size is fine sand the distribution of sand grains is asymmetric and skewed towards coarser sand grain sizes. The opposite effect is evident along the beach face, where the distribution curve is positively skewed by fine sediments amongst the abundant broken shell material on the beach. Through the mid tide region sediment distribution is near symmetrical.

Ratio of sand to mud

Figure 3.5 demonstrates that the silt and clay content of sediment increases offshore, and silt content of sediment is higher closer to the head of the inlet near Waikopua Creek. Sediment has a high silt and clay content on the northern intertidal flats adjacent to the channel where dredgings material was deposited. The silt and clay content of sediment decreases with distance from the dredgings and percentage of sand in samples increases. This is evidently an effect of the dredgings dispersion from the disposal site, as fine sediment is transported from the dredgings and becomes dispersed over sediment to the north, thereby increasing the clay and silt content of this sandy sediment. Gravel content of sediment is highest close to shore where fluvial inputs are high and sea cliffs are actively eroding.

3.2.3 Discussion

Sediment grain size is similar over most of the intertidal flats, with mean grain size between 2.5 and 3.0 Ø (0.2-0.1 mm) on the lower to mid intertidal regions. Beach sediments and the chenier shell ridge are generally coarser, containing broken shell gravel. Muddy sediment (< 0.1 mm) occurs near the head of the inlet, and around the dredgings where fine silt sized sediment dredged from the approach channel was deposited on the adjacent northern intertidal flats. Offshore sediment is finer, comprised of at least 75 % silt and clay. Grain size distribution shows decreasing sand content with increasing water depth, which is the general pattern observed in low-energy embayments (Blatt *et al.* 1980).

Sediment source is the main control on surficial sediment grain sizes and sorting on the intertidal flats. The abundance of fine sediment distributed over the intertidal and subtidal region is attributed to a greater supply of finer clasts eroded from local catchments and delivered to the littoral system. There is little variation in sediment sorting across the intertidal flats as most sediment is moderately to moderately well sorted Poorly sorted sediments are the result of bimodal sources and occur near the dredgings mound and near streams and cliffs where erosion and fluvial inputs deliver sediment of varying size classes.

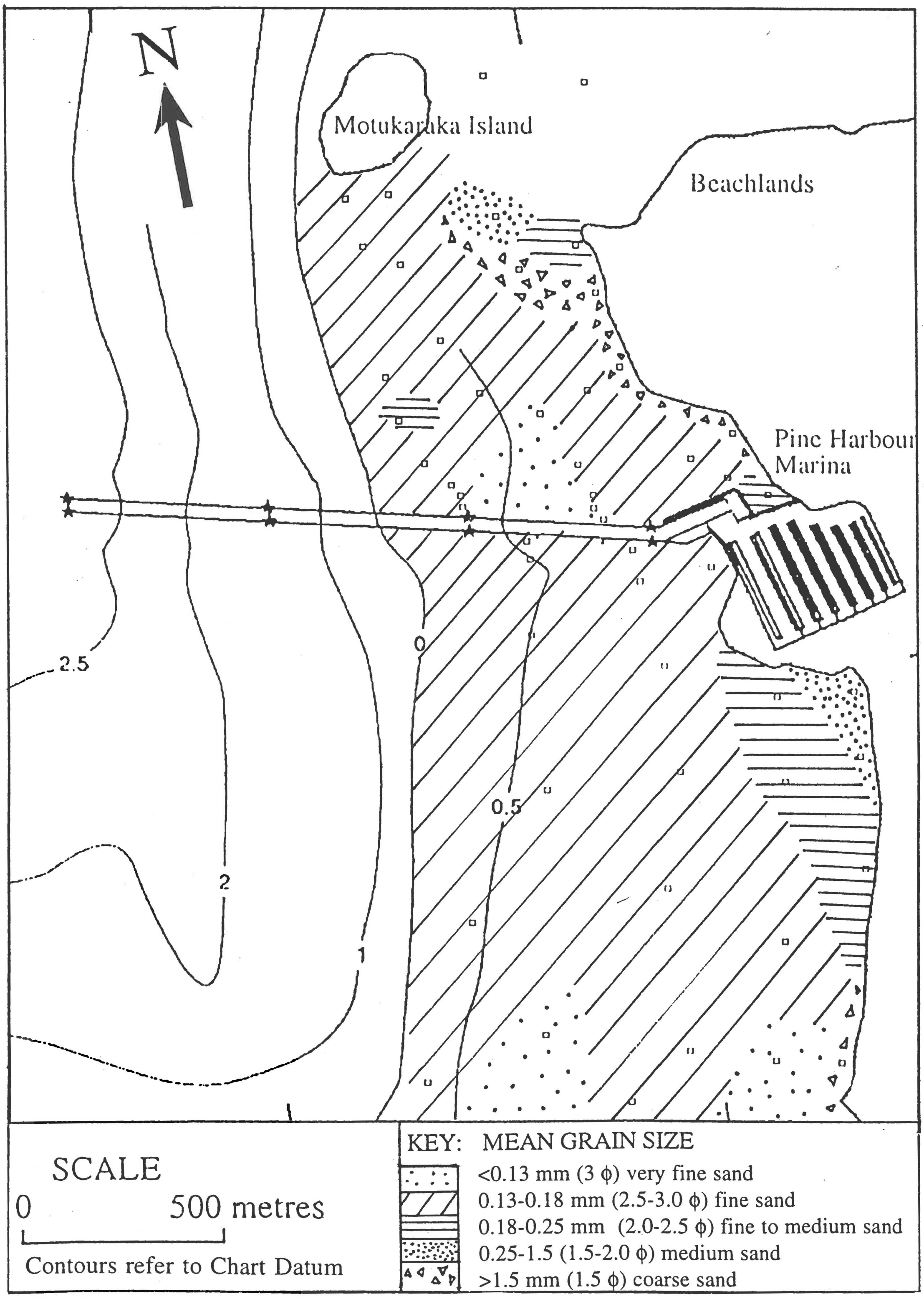

FIGURE 3.2: Spatial distribution of mean grain size of surficial sediments over intertidal flats fronting Pine Harbour Marina

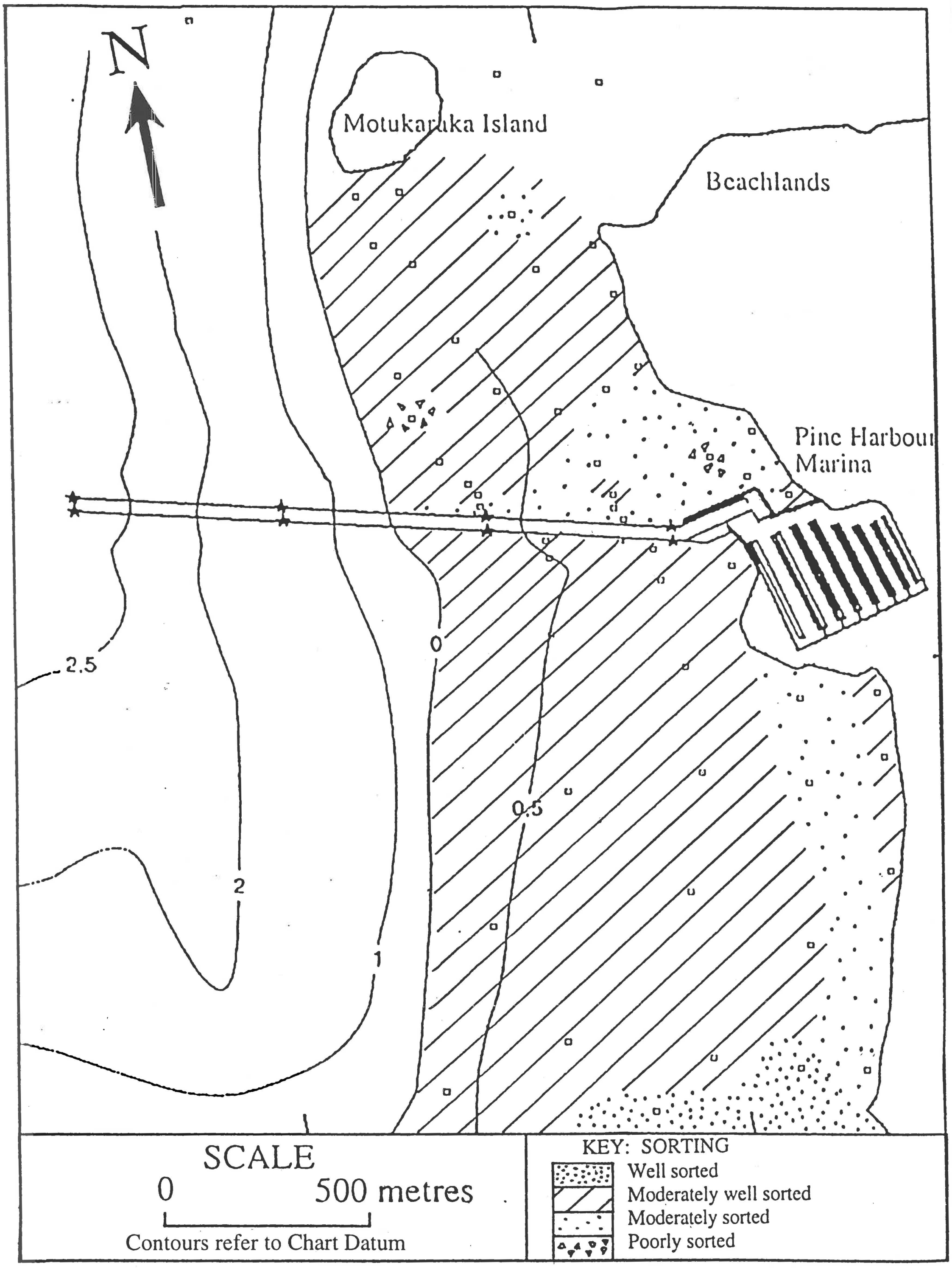

FIGURE 3.3: Pattern of moment method sorting of surficial sediments on intertidal flats fronting Pine Harbour Marina.

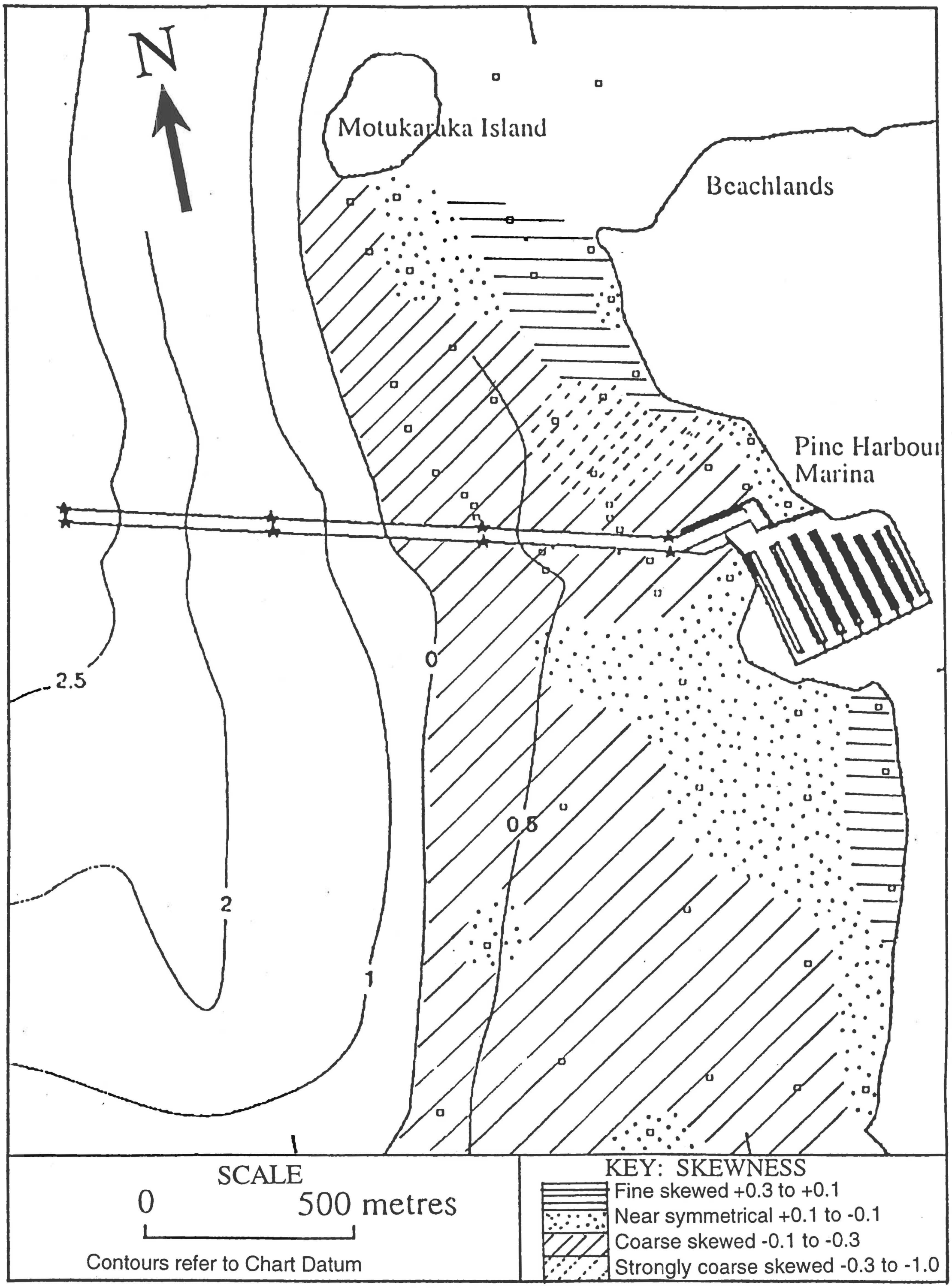

FIGURE 3.4: Variations in moment method skewness of surficial sediments over intertidal flats fronting Pine Harbour Marina.

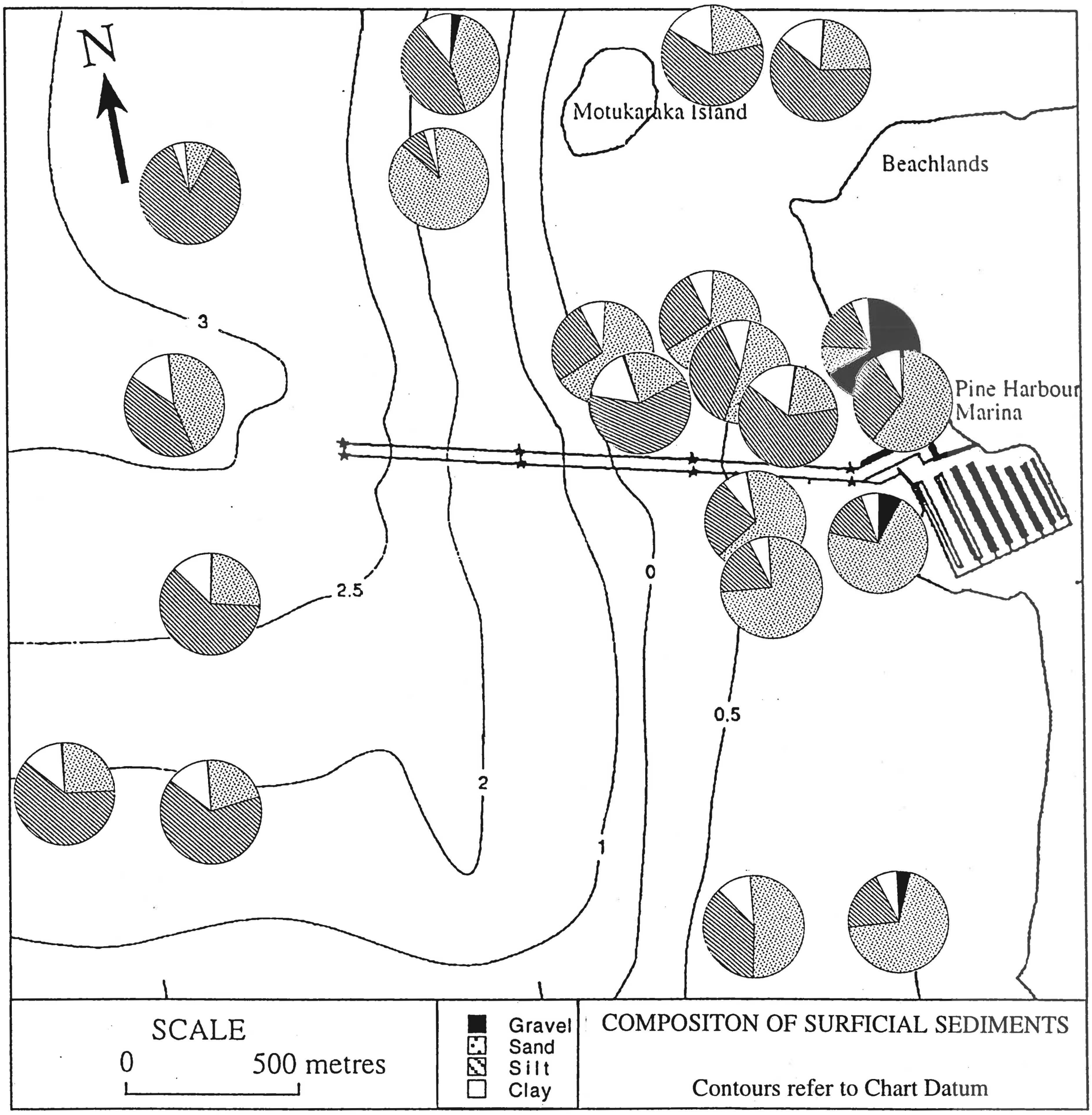

FIGURE 3.5: Ratios of sand, clay and silt in selected samples in the subtidal and intertidal regions fronting Pine Harbour Marina.

3.3 Characteristics of dredgings sediment

Dredge spoil from the 1994 dredging operation at Pine Harbour Marina was dumped on the adjacent intertidal flats. The dredgings material has been characterised in terms of texture, bulk density, moisture content, and clay mineralogy which relate the sediment properties to the stability of the sediment. The sediment structure of dredgings material was examined with scanning electron microscopy (SEM). The origin of sediments infilling the approach channel to Pine Harbour Marina was investigated using mineralogical finger-printing, and the possibility of the dredgings sediment as the source of muddy sediment occasionally despoiling Sunkist Bay was also investigated through a comparison of clay mineral suites from samples along the coastline.

3.3.1 Texture of dredgings sediment

Particle size is important to the hydraulic and engineering behaviour of sediment, with the dominant grain size largely determining sediment properties. Dredgings sediment were comprised of approximately 66% silt, 18% clay and 16% fine sand (Figure 3.6). The sediment grain size distribution of dredgings sediment was significantly different from the fine to medium sand characteristic of the broad intertidal flats. A comparison of sediment from the intertidal flats with sediment samples from the dredge mound, subtidal region and within the approach channel to Pine Harbour Marina is presented in Figure 3.7 and clearly demonstrates the difference in composition of sediment from these locations. Sediment from the dredgings, offshore and in the channel have a greater percentage of silt and clay, and less gravel and sand than intertidal flat sediments.

Intermixed with the fine sand and silt sized sediment of the dredgings were gravel to boulder sized fragments of basement shore platform, excavated from the bottom of the channel, and abundant shell material including *Paphies australus* and *Austrovenus stuchburyii* (Plate 3.1). The sediment surface was pitted with bioturbation holes which allowed the expulsion of pore water during consolidation, and there may have been stress failures where flocs of fine sediment were removed from the mound. The presence of small ripples (H = 1 cm and λ = 4 cm) over parts of the dredgings (Plate 3.1) were indicative of active sediment movement of very fine sand from the dredgings mound.

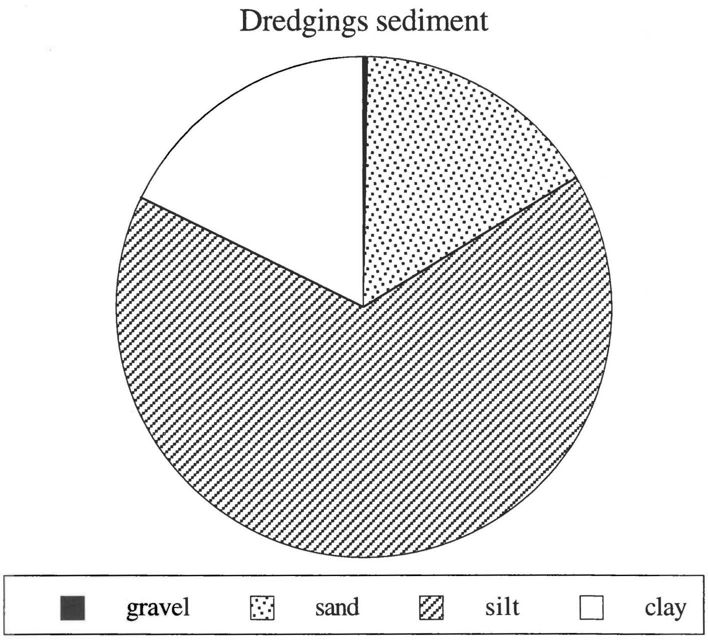

FIGURE 3.6: Textural composition of dredgings sediment.

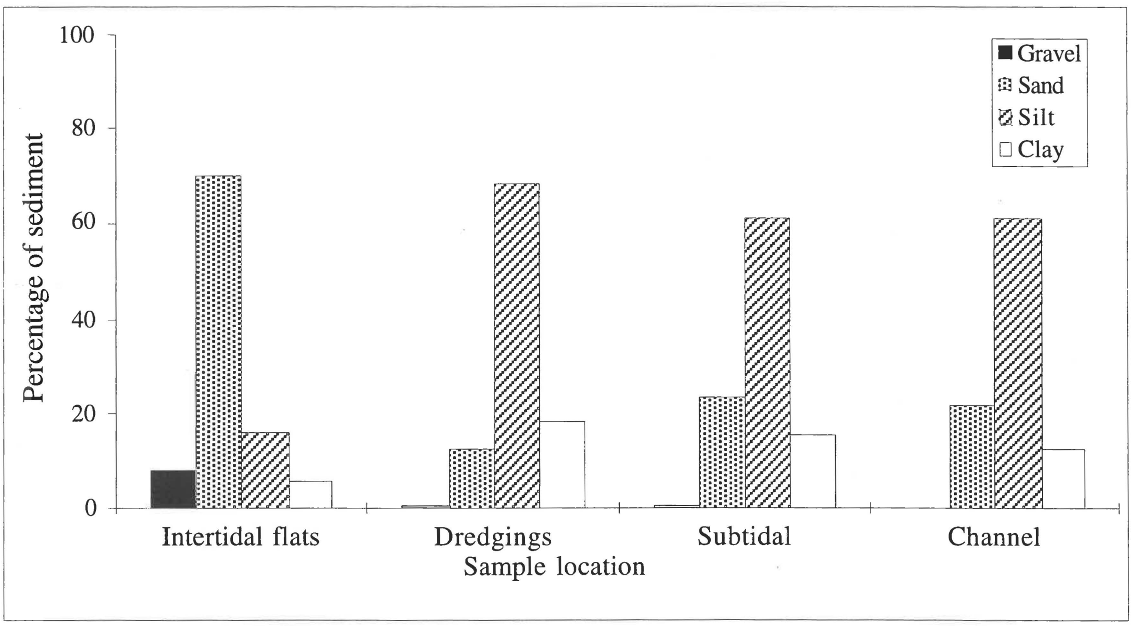

FIGURE 3.7: Comparison of gravel, sand, silt and clay composition of sediment from intertidal flats, dredgings material, the approach channel and subtidal region.

PLATE 3.1: a) Dredgings mound in November 1994 showing some boulders amongst the fine silt sized sediment. b) Bioturbated sediment surface of dredgings mound illustrating abundance of gravel sized fragments of shore platform, broken shells and development of rippled surface in sandier sediment (marker pen for scale).

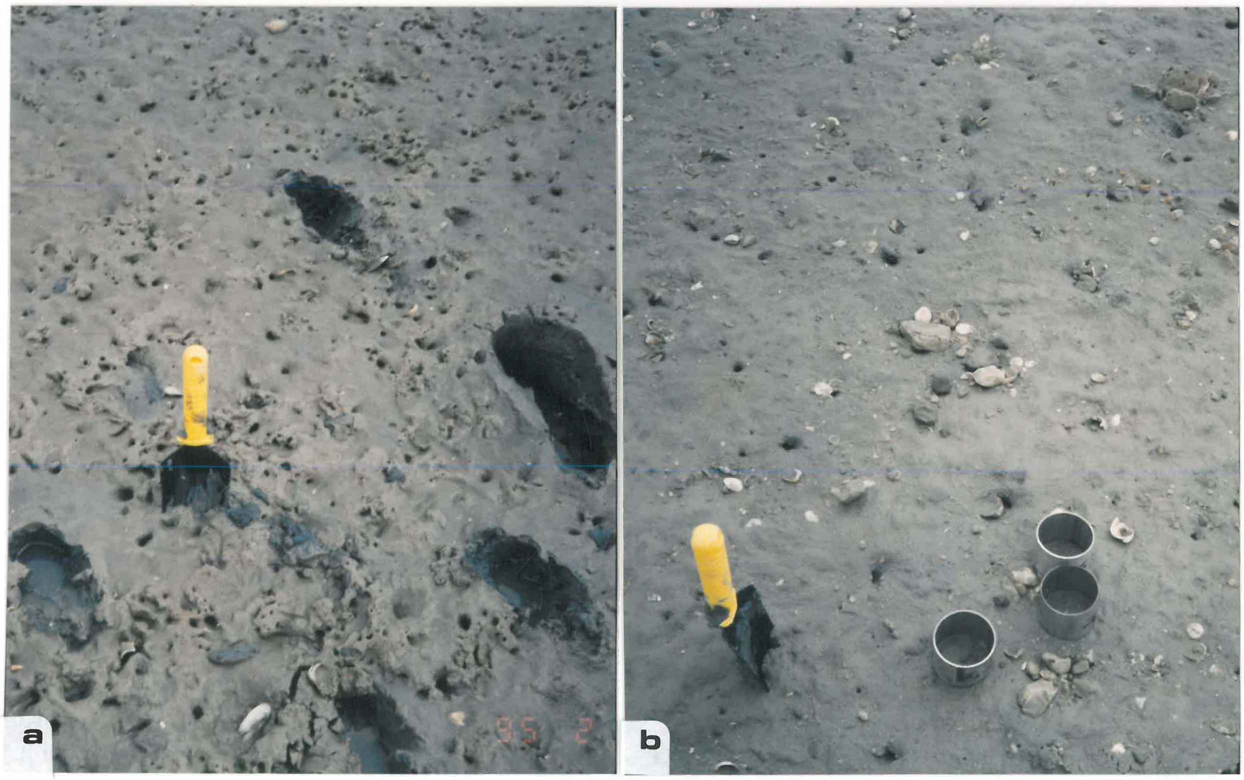

PLATE 3.2: a) Dredge mound sediment with low bulk density and high moisture content was characteristically pitted with bioturbation holes, with greater pore space, and comprised of fine sediment. b) Dredgings sediment which appears partially consolidated and has higher bulk density and lower moisture content than (a).

3.3.2 Bulk density and moisture content

The bulk density and moisture content of dredgings and intertidal flat sediments were compared. Sample cores (6 cm diameter, 4.4 cm height) were taken in the dredgings and on the intertidal flats (Figure 3.1), and the bulk density of sediment determined by the wet sediment weight over the volume of the core (density = mass/volume). Average bulk density of the dredgings sediment cores were between 1.52 and 1.80 g/cm^3 (Figure 3.8). The average bulk density of the natural intertidal flat sediments were slightly higher ranging from 1.89 to 1.92 g/cm^3. This reflects the difference in sediment composition and consolidation of the two sediment bodies. The mass of sediment per unit volume is related to the specific gravity of the soil, volume of pore spaces, and whether the spaces are filled with fluid or gas.

The moisture content of sediment was determined by drying bulk density cores in an oven at 105°C for 2 hours. The weight of water in the sediment is expressed as a proportion of the oven dry weight of the sediment in Figure 3.8. Moisture content was about 25% for intertidal flat sediments, and about 45% in dredgings sediment owing to the greater amount of pore space in the dredgings material which increases the capacity for pore water storage. As bulk density increases moisture content decreases as grains are repacked during consolidation.

The dredgings sediment was very fine and had greater porosity and was less dense than natural sediment. The bulk density changes as a result of repacking. Cores taken from areas in the dredge mound that were visibly different had different bulk densities. Fine dredgings sediment that were bioturbated and appeared pitted had a lower bulk density than cores taken from areas of the dredge mound that were visibly sandier and appeared to be more compact (Plate 3.2). The bioturbated dredgings sediment was assumed to have undergone less consolidation and grain repacking than dredgings sediment that had higher bulk density.

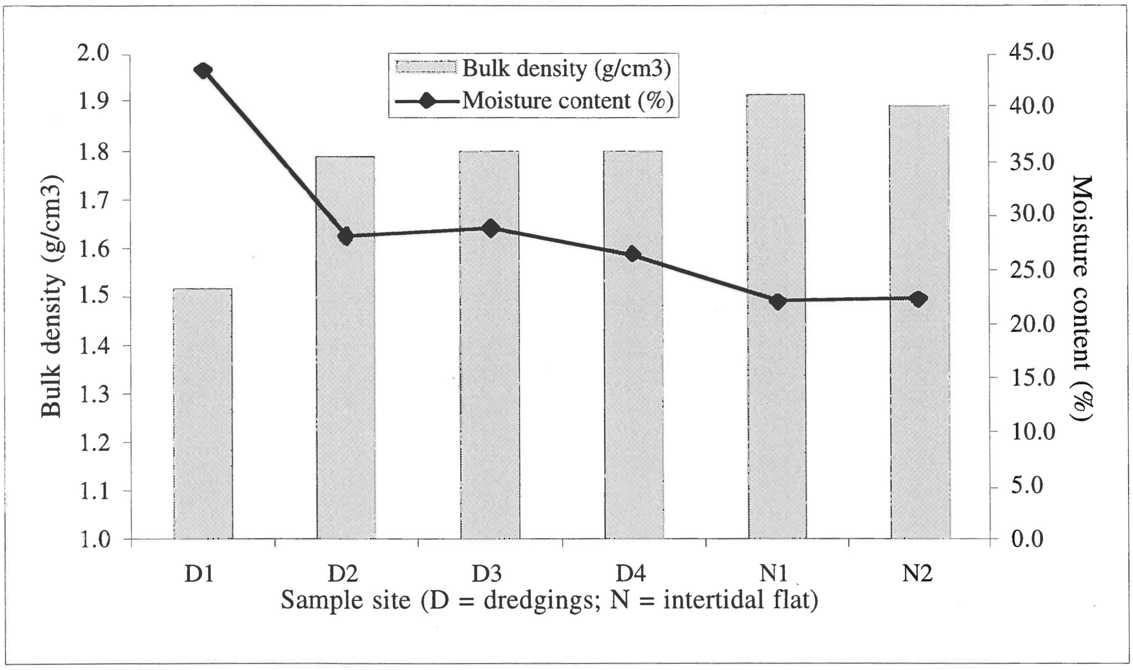

FIGURE 3.8: Comparison of bulk density and moisture content of sediment cores from dredgings sediment (D) and from the natural intertidal flat sediment (N). Core locations are indicated in Figure 3.1b.

3.3.3 Clay mineralogy of dredgings sediment

The clay mineralogy of dredgings sediment was determined with XRD analysis to further investigate the composition of the dredge spoil, and the source of fine sediment infilling the approach channel by comparing clay mineral assemblages of sediments from possible sources along the coastline (Figure 3.9). This mineralogical finger-printing also addresses the separate issue of the source of mud occasionally despoiling nearby Sunkist Bay and investigates the possibility of the dredgings material as the source.

3.3.3.1 Methodology and results

Preparation of samples for XRD clay mineral analysis was undertaken following the Standard Methodology of the NZ Soil Bureau (Whitton & Churchman, 1987) and Hume & Nelson (1982). Slides were made of the clay solutions by using the dropper on glass slide technique in which an eye dropper is used to transfer as much clay suspension as can be held on the slide when resting level. The slide was left to dry in air, and underwent XRD analysis. For positive identification of clay mineral species the untreated slides were also glycolated; heated to 550 °C; and boiled in 10% HCl (Hume & Nelson, 1982).

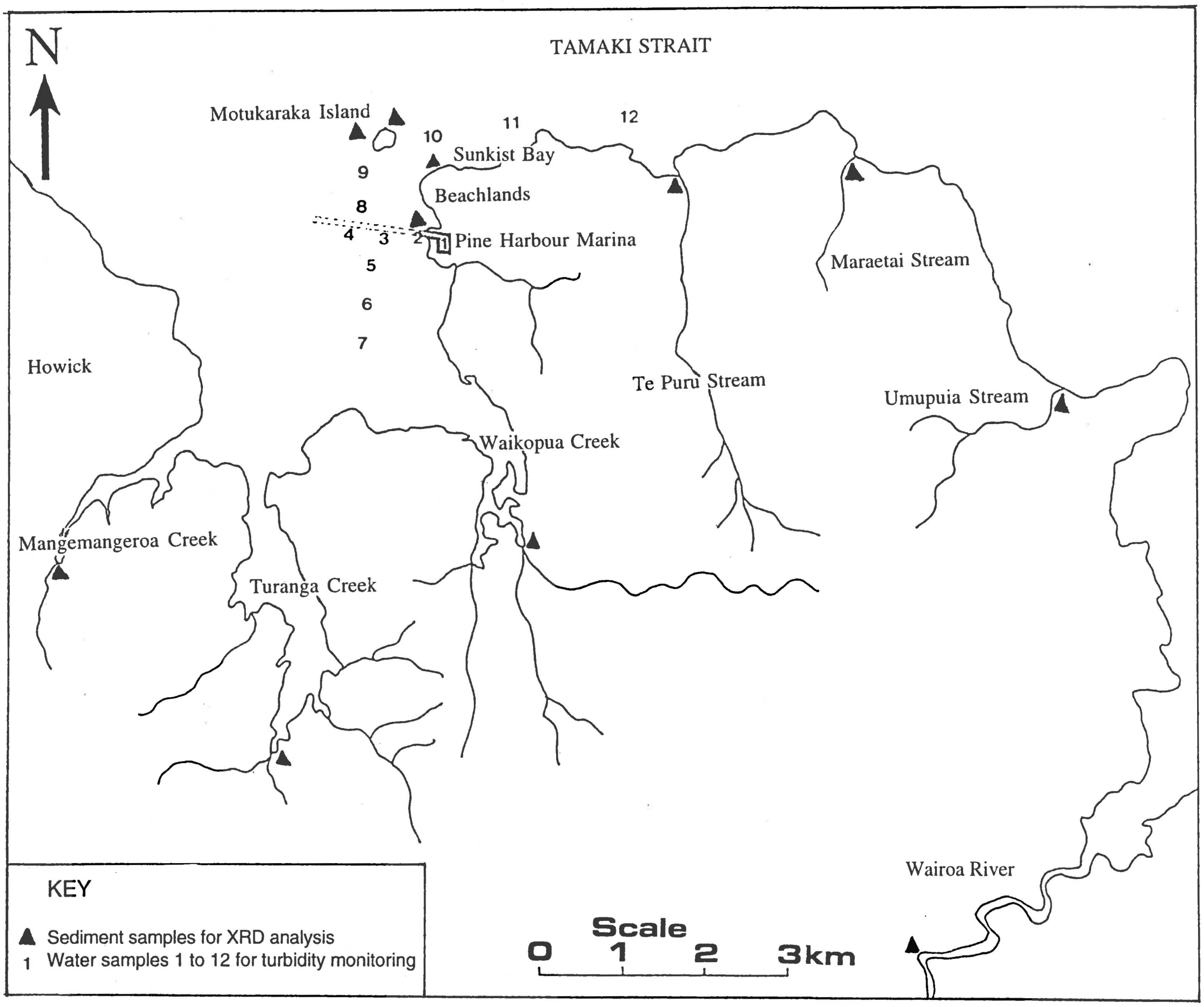

FIGURE 3.9: Location of sediment sampling sites for analysis of clay mineral assemblages with XRD (indicated by triangles), and numbered sites 1 to 12 refer to water sampling sites for turbidity monitoring.

Similar clay minerals were present in all samples. Major basal reflections (001) occurred at 13-15 Å (smectite or undifferentiated mixed layer clays), 10 Å (illite or illite-smectite mixed layer clay), 7.25 Å (kaolinite), 4.27Å (gypsum), 3.65Å (quartz). Calculations of relative amounts of clay minerals can be made from peak intensity measurements on x-ray diffractograms. These are normally carried out by measuring peak height or peak area, however for poorly crystalline clays in which the diffractogram curve is often poorly defined only the peak height can in practice be reasonably determined (Hume & Nelson, 1982). The positions of 001 reflections and relative heights of clay mineral peaks used in the semi-quantification of clay minerals are presented in Table 3.1.

TABLE 3.1: Clay mineral assemblages of samples along Beachlands coastline and relative abundances. Peak heights are measured in millimetres (mm). (S = smectite; MLC = undifferentiated mixed layer clays; I = illite; I-S = illite-smectite mixed layer clay; K = kaolinite).

Sample	S	MLC	I	I-S	K	Semi-quantification
Wairoa R	13 mm		10 mm		12 mm	S~K~I
Umupuia Stream	75 mm	25 mm			30 mm	S>>K~MLC
Maraetai Stream				20 mm	83 mm	K>>I-S
Te Puru Stream		5 mm			10 mm	K>MLC
Sunkist Bay 1	28 mm	10 mm			16 mm	S>K>MLC
Sunkist Bay 2	30 mm	15 mm			17 mm	S>K~MLC
Offshore Sunkist Bay	10 mm	12 mm			12 mm	MLC~K~S
Offshore Motukaraka Is	13 mm	10 mm			10 mm	S>K~MLC
Dredgings	22 mm	11 mm			12 mm	S>K~MLC
Dredgings core 1	17 mm	13 mm			12 mm	S>K~MLC
Dredgings core 2	44 mm	33 mm			10 mm	S>MLC>K
Waikopua Creek	8 mm				11 mm	K~S
Turanga Creek	30 mm			20 mm	15 mm	S>I-S>K
Mangemangeroa Creek	31 mm	15 mm			18 mm	S>K~MLC

3.3.3.2 Interpretation

All samples contained poorly crystalline clays including smectite, undifferentiated mixed layer clays and kaolinite and occasionally illite-smectite mixed layer clays. All samples contained gypsum from marine water, and quartz. Semi-quantification of the clay minerals by measuring peak intensity (height) from XRD diffractograms indicates that smectite is the most abundant clay mineral. Poorly crystalline kaolinite and mixed layer clays were also common and occurred in approximately the same proportions.

The similarity of clay mineral assemblages from samples is not unexpected as the local geology is similar. Waitemata Formation sea cliffs and shore platforms are exposed extensively along the Beachlands coastline and underlies the catchments of Waikopua Creek, Turanga Creek, and Mangemangeroa Creek (Figure 2.1). Basement greywacke rocks underlie Te Puru Stream catchment in the east, and is exposed in upper Waikopua Creek catchment. All sediment was sampled from areas where sediment has relatively short residence times which do not allow for the diagenetic alteration of clay minerals.

Smectite was abundant in all samples along the Beachlands coast, except from Maraetai and Te Puru Streams which drain catchments of greywacke basement rocks that do not weather to smectite clays (Naish, 1990). Naish (1990) describes the transformation of volcanic glass to smectite under conditions of high salinity. Smectite originates from the alteration of volcanic rock fragments which are weathered from Waitemata Formation flysch sequences (C. Nelson, pers. comm.). The abundance of smectite reflects the contribution of weathered shore platform and sea cliffs to the coastal sediment budget.

Similarly Waitemata Basin sediments are also rich in smectite clay minerals derived from the Waitemata Formation (Gregory & Thompson, 1973).

Other clay minerals identified by XRD were poorly crystalline. Poorly crystalline kaolinite originates from weathered soils, compared to highly crystalline kaolinite which originates directly from source rocks. Abundances of highly crystalline illite and kaolinite reflect greywacke source lithology (Naish, 1990) which were rare in the samples with illite only found in Wairoa River samples and highly crystalline kaolinite from Maraetai Stream. Undifferentiated mixed layer clays were poorly crystalline indicating they are weathered from soils in the local catchments.

Clay mineral assemblages in sediment from the dredgings were similar to sediment sampled from Waikopua, Turanga and Mangemangeroa Creeks with greater proportions of smectite and approximate equal proportions of mixed layer clays and kaolinite. Slightly lower abundances of smectite clay minerals were present in sediment from Waikopua Creek, this may be attributed to greywacke source rocks in the upper catchment which do not weather to smectite. Similar proportions of clay minerals, reflecting the abundance of smectite, were detected in subtidal samples and samples from Sunkist Bay. No illite or highly crystalline clay minerals were present in dredgings sediment.

The implications of the mineral finger-printing of samples from along the Beachlands - Maraetai coastline are that sediments infilling the approach channel to Pine Harbour Marina originate from north bound turbid plumes transporting fine sediment from Waikopua, Turanga and Mangemangeroa Creeks in the south. Mineralogical evidence indicates that sediment infilling the approach channel does not originate from streams and catchments to the north by the absence of illite and highly crystalline clay minerals which would be present in sediments weathered from greywacke source rocks.

3.3.4 Structure of dredgings sediment

Coring of the dredge mound was undertaken in April 1995. The core was split lengthwise and the sediment structure described (Figure 3.10). A layer of fine black predominantly silt-sized dredgings sediment was evident overlying natural sandier sediment of the intertidal flats. Sediment was removed from the core for textural and clay mineralogy analysis, and the structure of dredgings sediment from the core examined using scanning electron microscopy (SEM). Sediment removed for SEM was mounted on stubs and freeze dried in liquid nitrogen. Stubs were then coated with a layer of gold palladium in a vacuum with inert gas, to make the sample conducting thus avoid the build up of negatively charged areas when in the SEM.

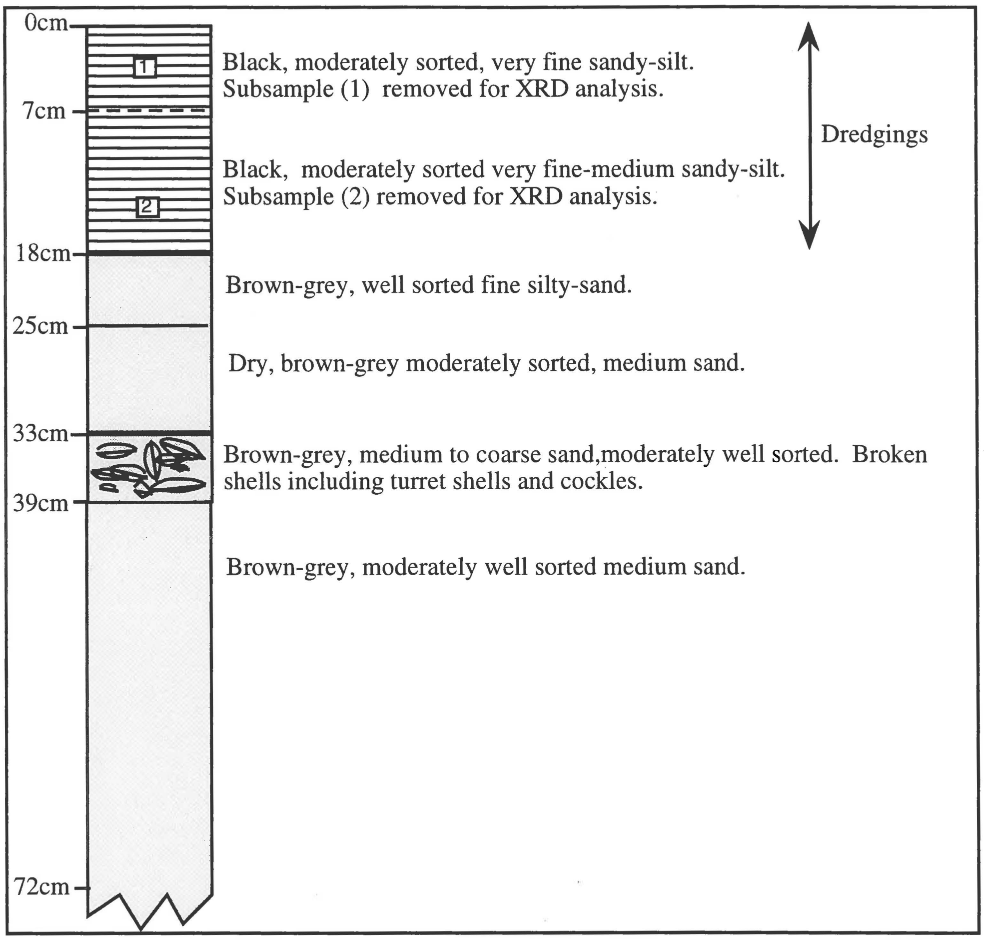

FIGURE 3.10: Sediment textures and observations of core through dredgings sediment deposited on intertidal sand flats adjacent to the approach channel to Pine Harbour Marina.

A variety of clay mineral structures, depending on the mineral type, size and shape of the particles and whether these are aggregated or fully dispersed have been formed and recognised using SEM (Smart & Tovey, 1981). SEM examination of dredgings sediment from the core at Pine Harbour Marina revealed the sediment structure is largely controlled by clay minerals and fine silts which mask the sediment grain surfaces. Plate 3.3 shows a series of SEM micrograms of dredgings sediment. Different clay minerals have different structures which can be used to positively identify the clay minerals from SEM micrograms. Clean crystal faces are rare as most grains are covered by a clay skin type layer. Although the clay skin on many grains is the most obvious feature, from XRD analysis these clay minerals are most likely to consist of kaolinite, smectite and undifferentiated mixed layer clays. Kaolinite occurs in plate-like minerals which are often stacked and curled sheets of clay minerals may be smectite (Hume, 1978). The clay skin coatings on grains affect the behaviour of the sediment primarily by increasing sediment thresholds.

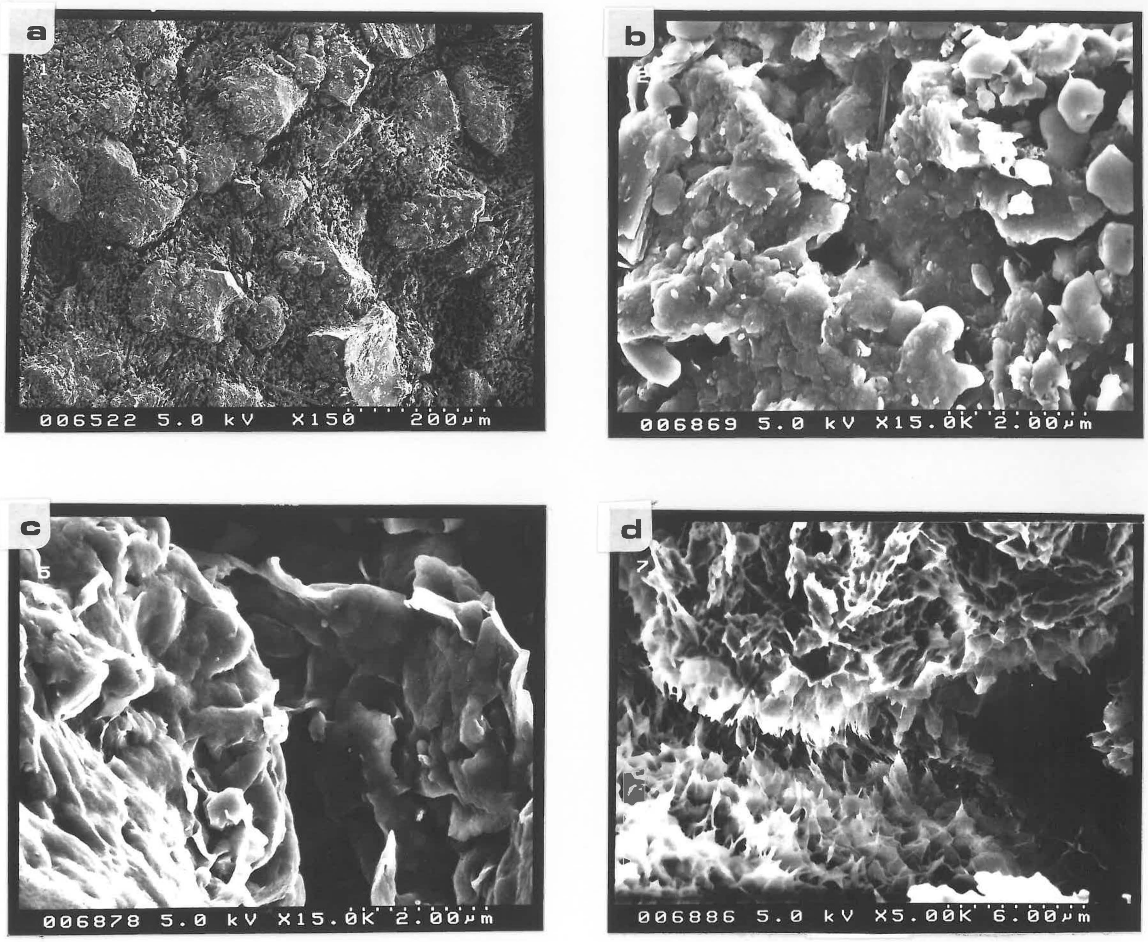

PLATE 3.3: a) Sediment from dredge mound showing cohesive nature of sediment grains which are coated with fine silt and clay minerals; b) Plate like stacks of kaolinite clay minerals mask sediment grains; c) "Wax-like" clay skin masking sediment grains; d) Curled sheets of smectite clay minerals.

3.3.5 Discussion

3.3.5.1 Stability of dredged sediment

Dispersion of dredge spoil from the mound is dependent on properties of the dredged sediment, as resuspension is sensitive to the mechanical properties of sediment. Cohesive coastal and estuarine sediments are generally referred to as "mud", and are a complex mix of materials including water, cohesive sediments consisting of many different clay minerals, organic matter, and small amounts of sand and silt (Dyer, 1986). In cohesive sediments the particles are considered to be flocculated (Mehta & Lee, 1994), and they behave differently to non-cohesive sediments such as sand. Each grain is held by cohesive forces which bond the grain to its neighbours at discrete points of contact (Mehta & Lee, 1994). Thus because of the nature of the grains, cohesive sediments have greater threshold velocities for entrainment of particles into suspension than cohesionless sediments.

The behaviour of cohesive and non-cohesive sediments is different after deposition. Cohesive sediments undergo consolidation as pore water is progressively removed from the sediment. Consolidation is associated with a collapse of sediment structure resulting in an increase in bulk density and shear strength as the weight of overlying flocs causes buried aggregates of particles to condense under the weight. Once the deposit is more than a few flocs thick the squashing begins and causes a slow expulsion of pore water and a gain in shear strength of the mud (Dyer, 1986). As such characteristics of the sediment vary with time and depth. Cohesive sediment becomes harder to erode the more it consolidates and the shear stress of sediment increases.

3.3.5.2 Source of fine sediment occasionally deposited on Sunkist Bay

Mineralogical finger-printing of sediment along the Beachlands - Maraetai coastline implies that it is likely that occasions of muddy sediment despoiling Sunkist Bay occur after wind and wave conditions induce onshore movement of high suspended load waters from wave stirring of sediments deposited offshore of Sunkist Bay and Motukaraka Island. These subtidal sediments originate from erosion of the local catchment dominated by weathering of Waitemata Formation coastal cliffs and shore platforms, and subtidal deposition of fine sediment transported north by turbid plumes from streams to the south. Sediment offshore from Sunkist Bay and near Motukaraka Island is dominated by silt and fine sand. Shore parallel bedforms were observed by SCUBA divers on 20/12/95 (Appendix 1.2) with lighter coloured muddy sediment in troughs suggesting movement of fine sediment onshore, exacerbated by north-east to north-westerly wind conditions.

In a similar investigation into the mud siltation problem at Maraetai undertaken by Ballance (1994), XRD scans of samples from offshore Maraetai, Maraetai boat harbour, Te Puru Stream and Whitford Forest were compared to identify the source of the mud sized sediment. The conclusion of this report was that the mud accumulating in the sea at Maraetai was nothing other than locally derived mud being delivered to the coast by the local streams. However, since all streams draining the Hunua Ranges and surrounding areas would be delivering similar material to the coast, it was not possible to say how far the marine mud at Maraetai had been transported (Ballance, 1994).

3.4 Suspended sediments

3.4.1 Turbidity

Perceived water quality depends largely on appearance. The traditional approach to assessing water quality is by measuring the level of light scattering in water using nephelometric turbidity measurements (NTU) as a relative index of light scattering. Different nephelometers, even though standardised identically give different turbidity values on the same sample, that is, the measurement is instrument-specific. The most commonly used nephelometer in water management is the laboratory based Hach 2100A model which has become the industry standard.

The portable Hach 16800 model was used to determine the turbidity of water samples surrounding Pine Harbour Marina. The Hach 16800 is calibrated to standard NTU sample vials which are purchased with the instrument, however the effects of transporting the Hach 16800 into the field may cause some contamination of the light sensors in the instrument and the results are therefore not absolute indicators of turbidity levels. The Hach 16800 used in this study was calibrated to NIWA Ecosystems Hach 2100A model using 10 water samples collected during long term turbidity monitoring along the Beachlands coast on 26/4/95. The data resulting from water samples analysed with the Hach 2100A model indicated turbidity values 1.8051 times larger than the Hach 16800 NTU values (Figure 3.11). Accordingly, Hach 16800 NTU levels were multiplied by 1.8051 to adjust to equivalent Hach 2100A NTU.

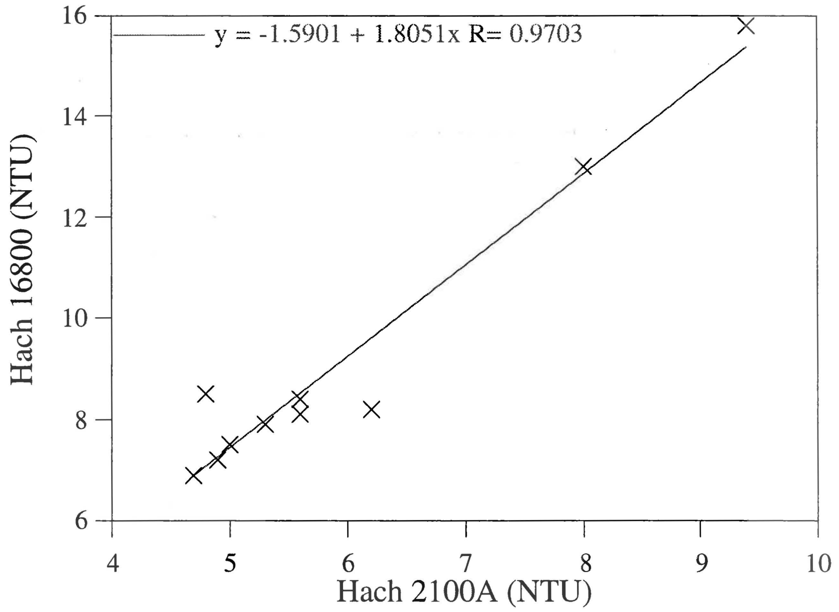

FIGURE 3.11: Comparison of Hach 16800 with Hach 2100A (NTU) based on comparison of 10 water samples collected from along the Beachlands coastline on 26/4/95.

3.4.2 Suspended solids

Suspended particles in water can include a range of materials including grains of rock-forming minerals such as quartz, clay mineral particles, detrital organic matter, virus particles and living cells of bacteria and algae (Davies-Colley, 1994). Suspended solids of water samples were determined using standard APHA (1992) water monitoring methods. The suspended solids measurement measures the mass of suspended particles that can be captured from a measured volume of water by filtration onto a filter made of glass fibres. This measurement does not distinguish between particles of different composition and grain size and different optical behaviour (Davies-Colley, 1994).

For samples collected in this study, suspended solids are related to turbidity in that they generally increase in linear proportion to each other (Figure 3.12).

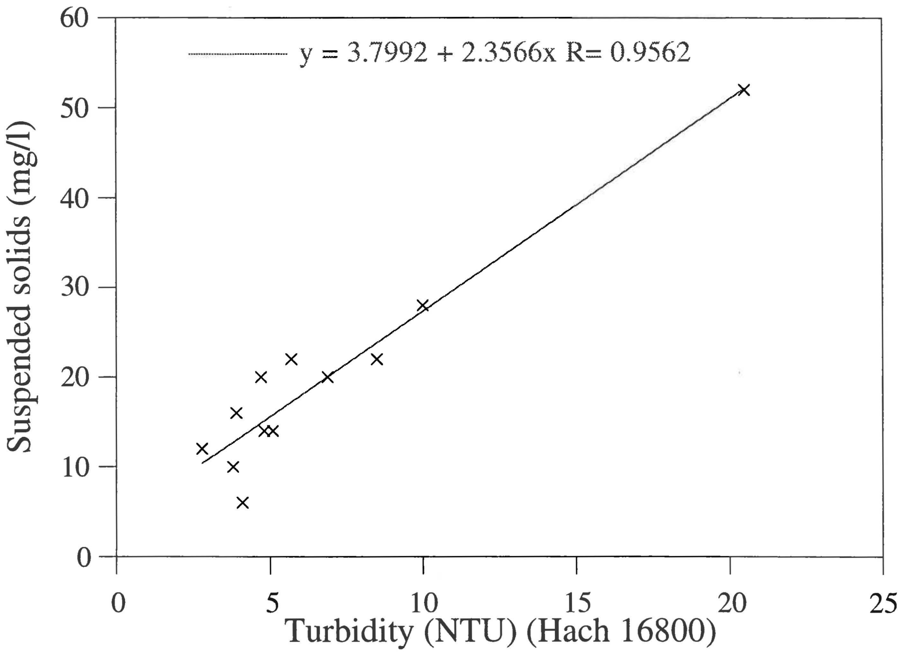

FIGURE 3.12: Comparison of turbidity and suspended solid levels from 12 samples collected along the Beachlands coastline on 17/1/95.

3.4.3 Monitoring of water clarity

During the 1994 dredging operation at Pine Harbour Marina intensive turbidity monitoring was undertaken involving the analysis of water samples collected at a central point in the approach channel approximately 1300 m from the marina entrance, 1-2 m above the bed of the channel. Under permit H/9205 for dredging of the approach channel to Pine Harbour Marina, "trigger" levels imposed by the Auckland Regional Council were 35 NTU for turbidity and for suspended solids concentration 100 mg/l. If levels in excess of trigger levels were recorded during dredging a review of the dredging operation was required. This situation did not arise. During the course of this study the long term variation in turbidity and suspended solids levels in the littoral zone along the Beachlands coastline were investigated, and these natural background turbidity levels have been compared with the levels of suspended sediment during the dredging operation. Water samples for turbidity and suspended solids analysis were collected 1-2 m above the bed at various sampling sites along the Beachlands coastline from Waikopua Creek to Te Puru Stream (Figure 3.9).

3.4.3.1 Turbidity during dredging

A period of intensive turbidity monitoring was undertaken over the course of a tidal cycle and at weekly intervals during the dredging operation to assess the immediate impacts of dredging on water clarity in the region. Samples were taken at the 1300 m marker in the channel (Site 3) and at similar water depths 200 m to the south of the channel (Site 5) (Figure 3.9).

Results of monitoring throughout the dredging are compiled in Appendix 2.1. During the dredging operation turbidity levels at the designated site were between 5 and 26 NTU on 15/6/94, and 9 and 25 NTU on 22/6/94. Turbid plumes beside the dredge barge were visible as sediment was excavated and deposited, the finer sediment remaining suspended for longer periods of time and created a turbid cloud in the vicinity of the works (Plate 3.4). Plumes of suspended sediment beside the dredge had turbidity levels from 25 to 70 NTU recorded on different occasions.

PLATE 3.4 Turbid plume surrounding dredging works as sediment is stirred into suspension with excavation and deposition through water column.

Turbidity levels also increased due to natural processes not attributable to the dredging at the time of the dredging operation. Under 20-30 knot winds and after a period of rainfall on 25/6/94 a turbid zone extending around Sunkist Bay and Motukaraka Island was sampled and measured turbidity ranged from 50-67 NTU (Hach 16800) and suspended solids 169-307 mg/l.

3.4.3.2 Natural background turbidity and suspended solids levels

Water clarity varied in the long term and was influenced by the amount of rainfall and catchment runoff delivering sediment to the marine environment, wave heights entraining sediment, wind speed and direction causing surficial currents along the shoreline, and tidal currents which move turbid plumes along the coast. Long term turbidity and suspended solid levels were investigated at sampling sites along the Beachlands coastline (Figure 3.9) to examine the natural fluctuations in these levels. Raw data from long term turbidity monitoring, and graphs of relative turbidity and suspended solid levels recorded at 3 monthly intervals from October 1994 to November 1995 are presented in Appendix 2.2.

Average turbidity along the Beachlands coastline was less than 10 NTU from October 1994 to November 1995 (Figure 3.13). Greatest variation in turbidity was from water samples collected in the marina approach channel and basin and near Waikopua Creek. Turbidity at these sites increased up to 40-45 NTU on occasion due to a combination of factors including periods of rainfall, high wind speed and large waves, and stage of tidal current. High turbidity inside the marina basin is attributed to turbid plumes travelling along the coast becoming trapped inside the breakwaters. In comparison intensive turbidity monitoring indicates that turbidity levels generated by the dredging works were between 9 and 25 NTU in the marina approach channel. This is slightly higher than natural background turbidity levels in the same location of 9 NTU ± 6 NTU, but was not in exceedance of "trigger" levels.

Average suspended solid concentrations along the littoral zone from Waikopua Creek to Te Puru Stream were between 15 and 50 mg/l from October 1994 to November 1995 (Figure 3.14). Suspended solids concentrations increased up to 100 and 200 mg/l on 18/7/95 along Sunkist Bay to Te Puru Stream. Variation in suspended solids concentrations of most samples was in the order of 10-20 mg/l, however the greatest fluctuations in suspended sediment concentrations were detected near Waikopua and Te Puru Streams, and in the marina basin which possibly reflects the component of organic content eroded from the catchment which varies with the amount of rainfall in the catchment and volume of freshwater delivered to the marine environment.

Overall turbidity is dependent on weather conditions and tide. Local wind generated waves entrain sediment in the shallow water depths along the coastline and the embayment. The turbid plumes are in turn transported along the coastline by the net current which is related to tide and wind driven circulation patterns.

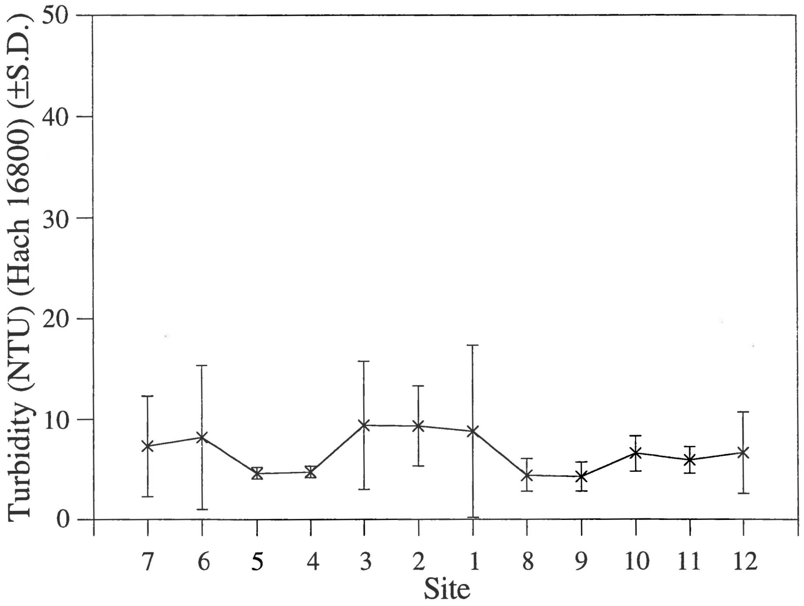

FIGURE 3.13: Mean natural background turbidity (NTU) levels of water samples collected from the littoral zone from south to north along the Beachlands coastline and in the marina approach channel. Sites 5, 6 & 7 are located near Waikopua Creek, sites 1-4 in the vicinity of Pine Harbour Marina, and sites 8-12 north of Pine Harbour Marina along Sunkist Bay to Shelly Bay.

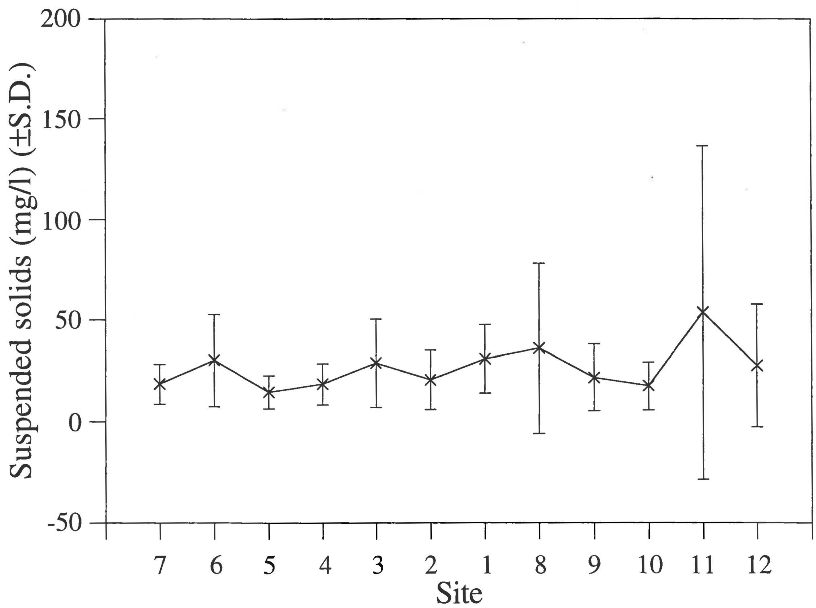

FIGURE 3.14: Mean natural background suspended solid levels (mg/l) of water samples collected from the littoral zone from south to north along the Beachlands coastline and in the marina approach channel. Sites 5, 6 & 7 are located near Waikopua Creek, sites 1-4 in the vicinity of Pine Harbour Marina, and sites 8-12 north of Pine Harbour Marina along Sunkist Bay to Shelly Bay.

3.5 Beach surveys

3.5.1 Methodology

Beach surveys were undertaken by Greenfield Surveyors Ltd along 6 shore normal transects across the intertidal flats fronting Pine Harbour Marina (Figure 3.15). Transects were surveyed at six monthly intervals. The elevation of the tidal flat was surveyed relative to Port of Auckland chart datum (CD) which is the lowest astronomical tide (LAT). The extent of shore platform exposed along the profile and surficial sediment lithology was also recorded during surveying.

Surveys were undertaken before dredging commenced in June 1994, and in December 1994 at the conclusion of the dredging operation. Further beach surveys were undertaken in June 1995 and December 1995 to monitor any subsequent beach changes due to the deposition of dredgings material onto the intertidal flats along the northern side of the approach channel. Accretion or erosion over the intertidal beach sections can also be used to give an approximation of any volumetric beach changes.

The beach sections were also probed to determine the thickness of sediment veneering the shore platforms. The tidal flats were probed along the survey transects approximately every 25 m, this was adjusted if the shore platform abruptly changed gradient, to about 300 m offshore or until probing became difficult. Probing was undertaken using steel rods in 1 m sections, with additional lengths added as the depth of sediment veneer increased.

3.5.2 Results

Ascii files of survey data were input into TECHBASE for analysis and construction of section profiles. The elevation of the intertidal flats above CD for beach sections 1 to 6 are presented in Figures 3.16 to 3.21, along with the lithology of surficial sediments.

Greatest changes in elevation were recorded on the northern intertidal flat, with maximum accretion occurring along Section 1 where 0.5 m of sediment was deposited over the chenier shell ridge, and between 0 and 0.1 m of sediment deposited over the remaining length of section excluding the shore platform, in June 1995. Most accretion occurred in the mid tidal flat area, this was also evident along Sections 2 and 3 although net sediment accretion was between 0.02 and 0.03 m.

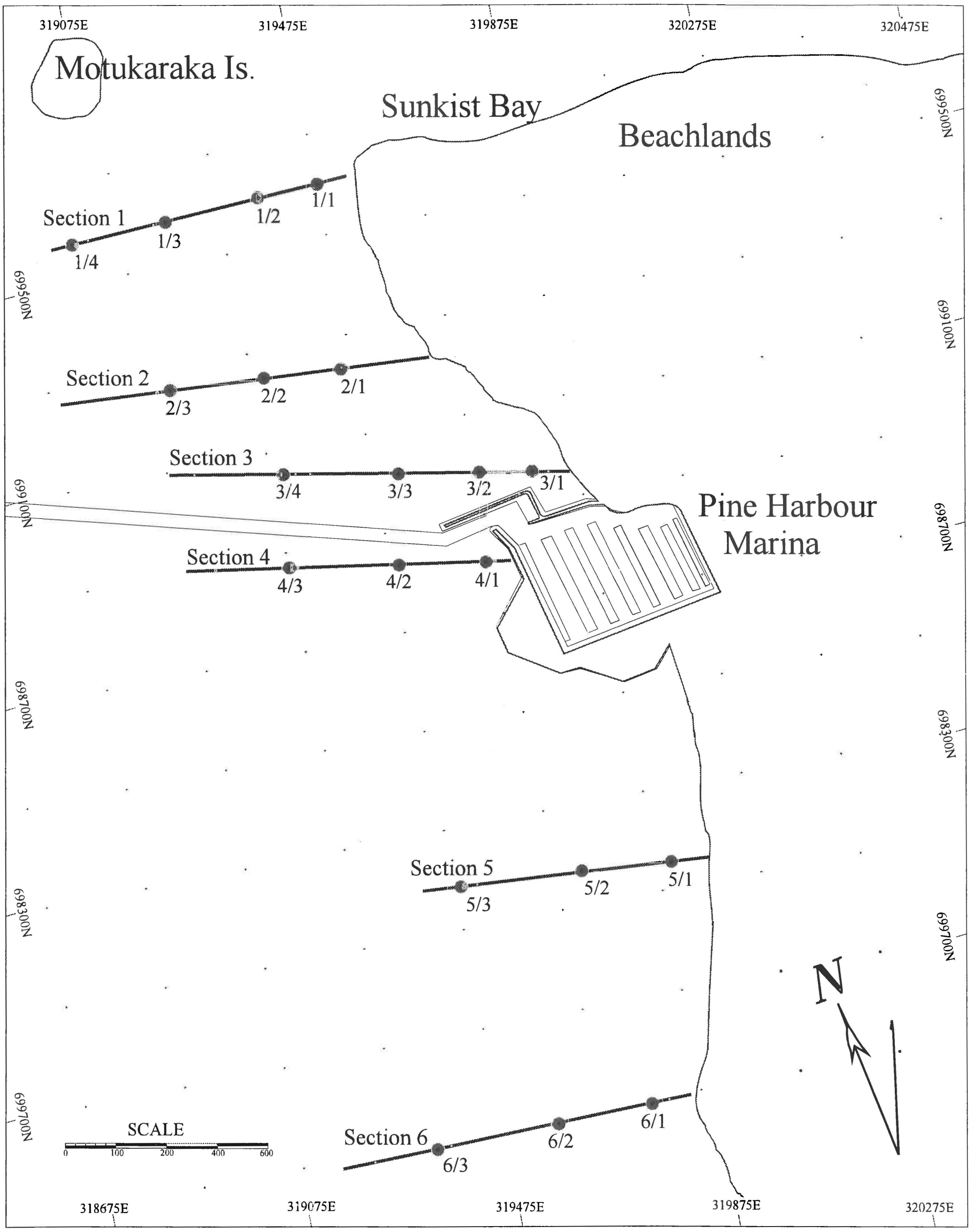

FIGURE 3.15: Location of beach sections 1 to 6 over intertidal flats fronting Pine Harbour Marina surveyed at 6 monthly intervals by Greenfield Surveyors Ltd. Sedimentation rod locations are indicated by dots along the sections.

Along the southern intertidal flat changes in sediment elevation was negligible. Sediment elevation remained constant, fluctuating in the order of a few centimetres. Section 4 shows a dramatic decrease in elevation near the high tide mark where the boat ramp feeder channel was dredged. After dredging survey points along the edges of the channel increase, reflecting the gradual infilling of the boat ramp channel.

The extent of shore platform exposed along each section remained constant with no long term change in sediment veneering shore platforms. Pockets of sandy sediment were occasionally recorded over the shore platform on the northern intertidal flat but were subsequently transported away. Likewise shore platform on the southern intertidal flat did not experience an increase in sediment veneer. Accretion of silty sand was observed along all sections on June 1995, possibly settling from turbid plumes along the coastline or from the onshore movement of fine sediment. The shell ridge which links Motukaraka Island with Beachlands coastline along Section 1 appears the most dynamic and was observed to vary in thickness as shells accreted along the southern side of the shell ridge (Plate 3.5). Parts of the chenier shell ridge were overlain by sandy sediment in subsequent surveys.

PLATE 3.5: Series of shell ridges on the northern intertidal flats. The shell ridge in the background extends from Beachlands coastline to Motukaraka Island (just out of frame on the left). Accretion of shells is evident on the southern side of the shell ridges.

Figures 3.22 & 3.23 illustrate the depth of sediment veneering shore platforms extending from Beachlands coastline. The shore platform extends between 100 and 150 m from the beach face at a gentle angle veneered with up to 0.5 m of sediment, before abruptly changing gradient and dipping more steeply offshore to reach a maximum thickness of sediment veneer between 200 and 350 m from the beach face. Maximum sediment veneer is greatest over shore platform on the southern intertidal flats towards Waikopua Creek. Sections 5 and 6 have between 2.0 and 3.25 m of sediment veneering the shore platform.

Along the northern intertidal flats sediment depth of veneering the shore platform is generally less than in the south, greatest veneer is 2.0 m on Section 2.

3.5.3 Discussion

A trend of greater sediment accretion along the northern intertidal flat than the southern intertidal flat is evident. This accretion maybe due to the addition of sediment into the littoral system, particularly the deposition of dredgings from the Pine Harbour Marina approach channel along the northern intertidal flats. The release of this sediment trapped in the channel into the downdrift side of the littoral transport system is an addition to the sediment budget along the northern intertidal flats. The channel interrupts the passage of sediment along the coastline from south to north, and restricts the amount of sediment moving onto the northern intertidal flats and in consequence reduces the amount of sediment transported downdrift to Beachlands Point and Sunkist Bay.

The accretion of approximately 2.5 cm of sediment in the mid tide region along the northern intertidal flats since deposition of the dredgings indicates that the dredgings have dispersed across the intertidal flats. Sediment accretion is less along the lower intertidal flats and over the shore platform. Sediment accretion was greatest along Section 1. This is mostly due to accretion of shells along the southern side of the shell ridge, and may also be attributed sediment accretion as a result of opposing currents which form the shell ridge and variations in wave energy over the changing chenier shell ridge. Two smaller shell ridges were observed to be accreting along the lower tide regions on Section 2 and 3. Shell ridges experience regular ridge formation by alternating erosion and accretion (King, 1972). During storms minor ridges can be built up and once they are initiated further material can be added. Longshore movement can cause the elongation of the chenier ridges.

An estimate of the volume of sediment accreted over the northern intertidal flats, assuming an average accretion of 2.5 cm (0.025 m) of sediment over the mid tide region, approximates to a total volume increase over the region of:

Volume change = 0.025 m x 100 m (length of profile) x 700 m (northern intertidal flats)
= 2,100 m^3

Accretion of 2,100 m^3 of sediment is about 45% of the dredgings material deposited adjacent to the approach channel on the northern intertidal flat. The remainder of the dredgings material has either been transported offshore, carried in suspension from the intertidal system, or more likely been washed back into the approach channel.

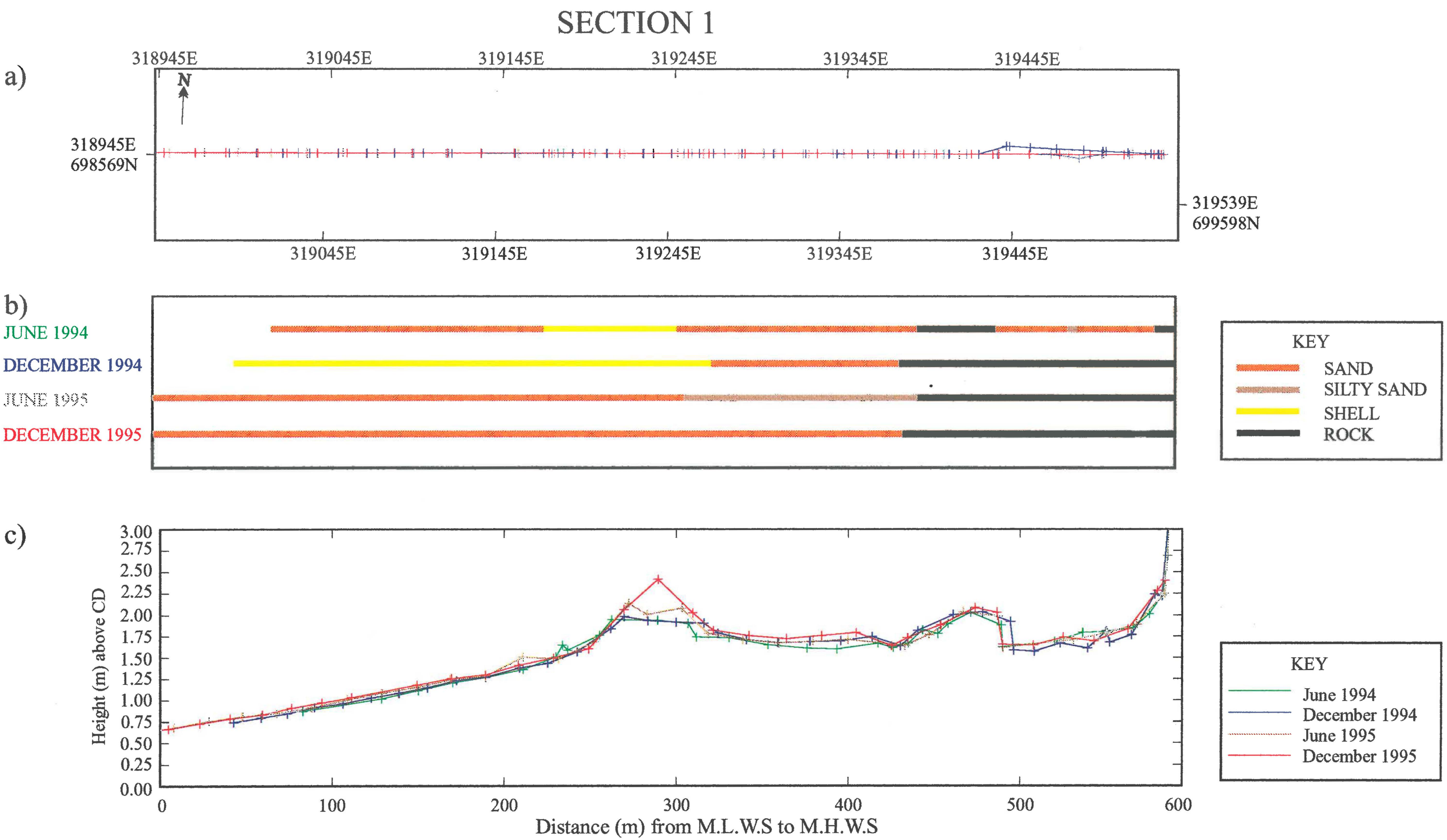

Figure 3.16: SECTION 1: a) Plan view and location of survey points; b) Lithology of surficial sediments; c) Elevation of intertidal flat. VE =50.

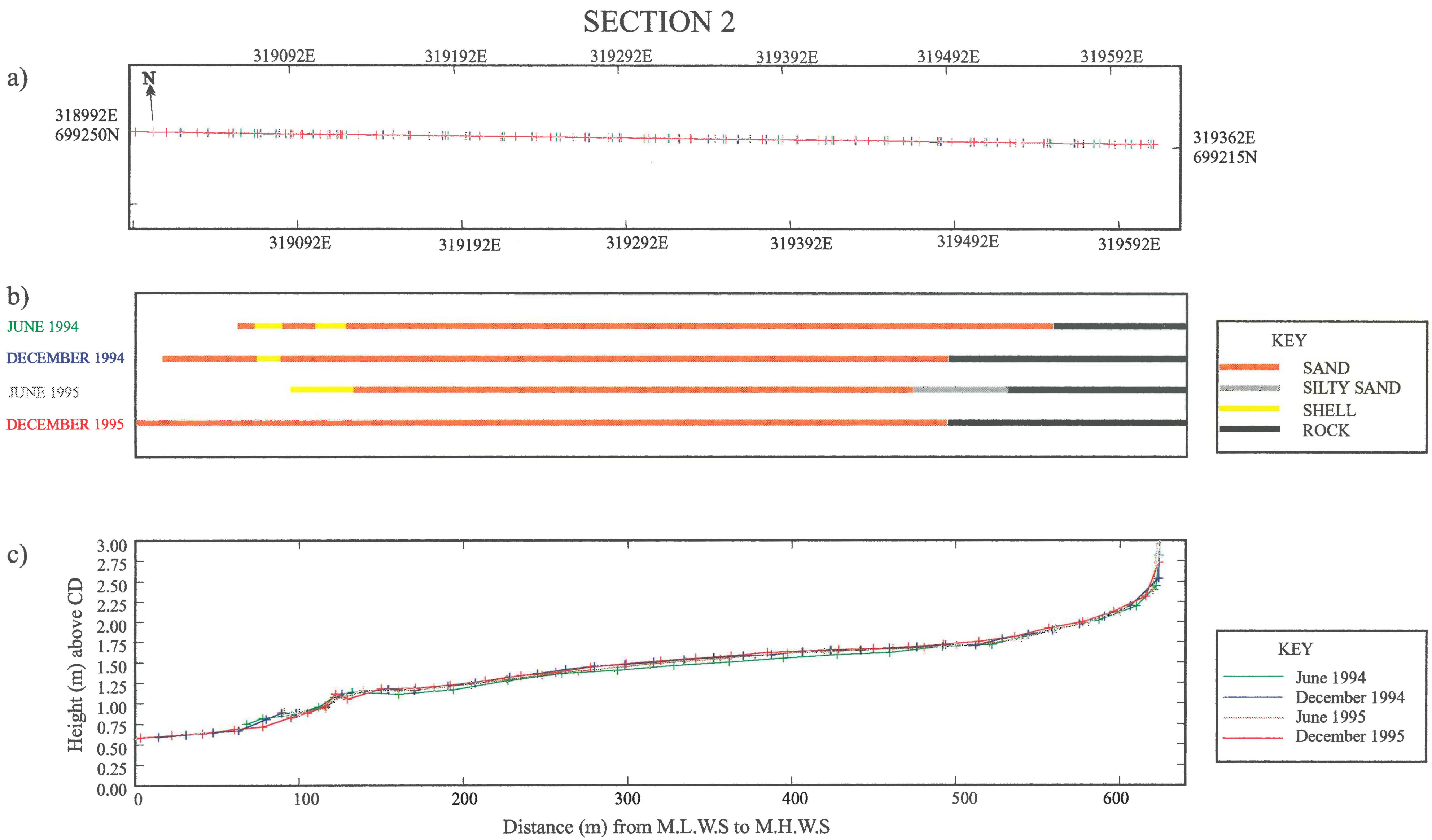

Figure 3.17: SECTION 2: a) Plan view and location of survey points; b) Lithology of surficial sediments; c) Elevation of intertidal flat. VE = 50.

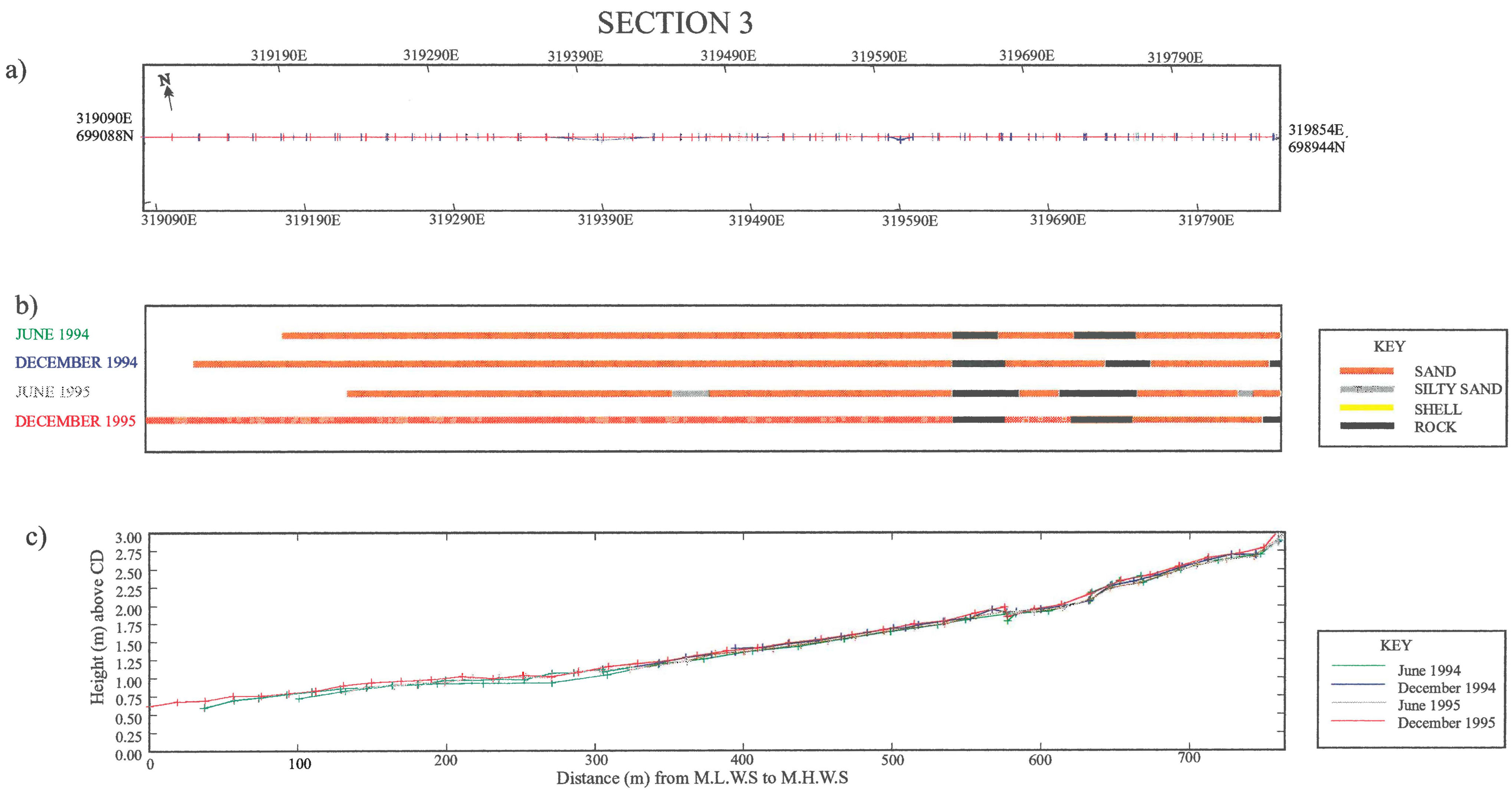

Figure 3.18: SECTION 3: a) Plan view and location of survey points; b) Lithology of surficial sediments; c) Elevation of intertidal flat. VE = 50.

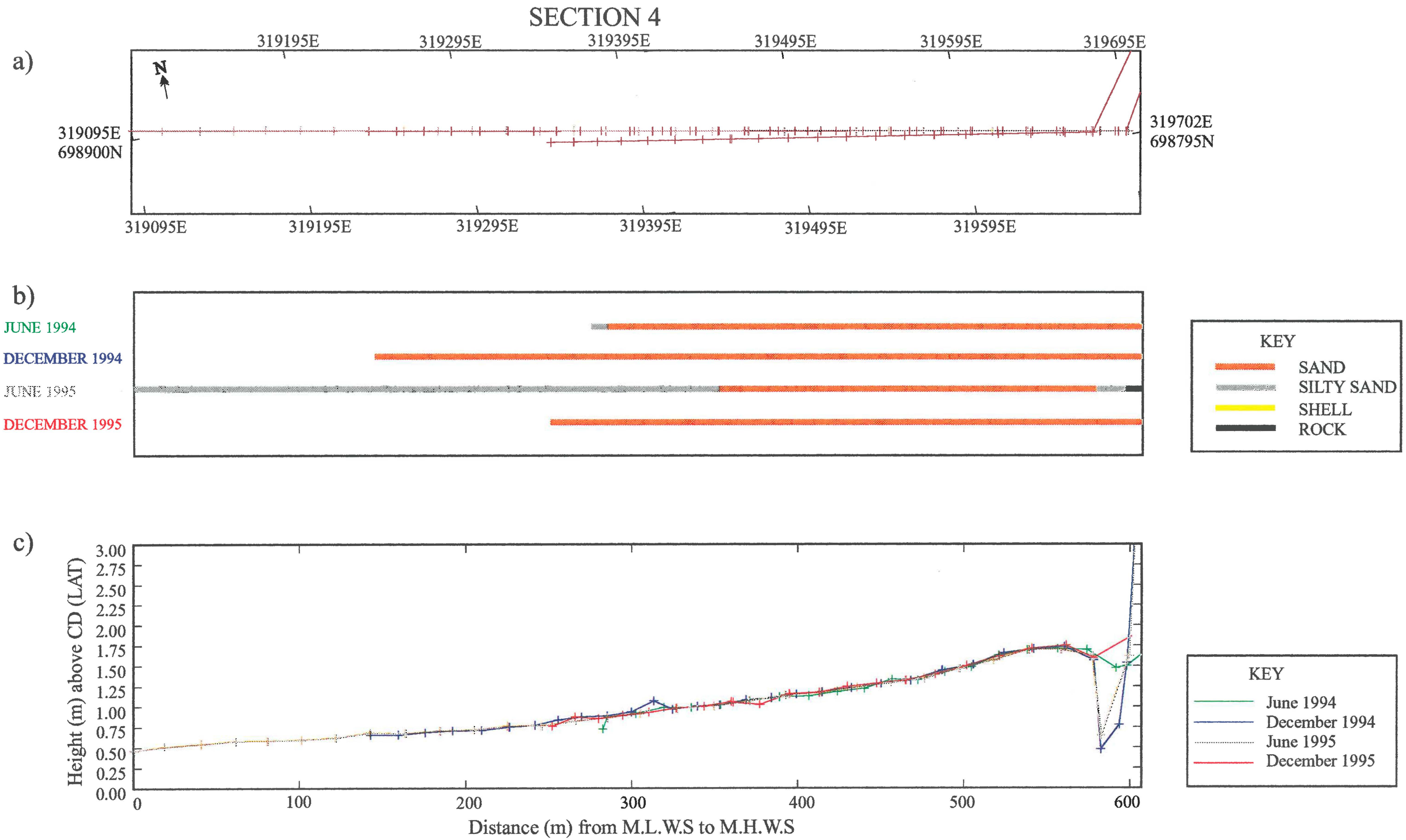

Figure 3.19: SECTION 4: a) Plan view and location of survey points; b) Lithology of surficial sediments; c) Elevation of intertidal flat. V.E. = 50.

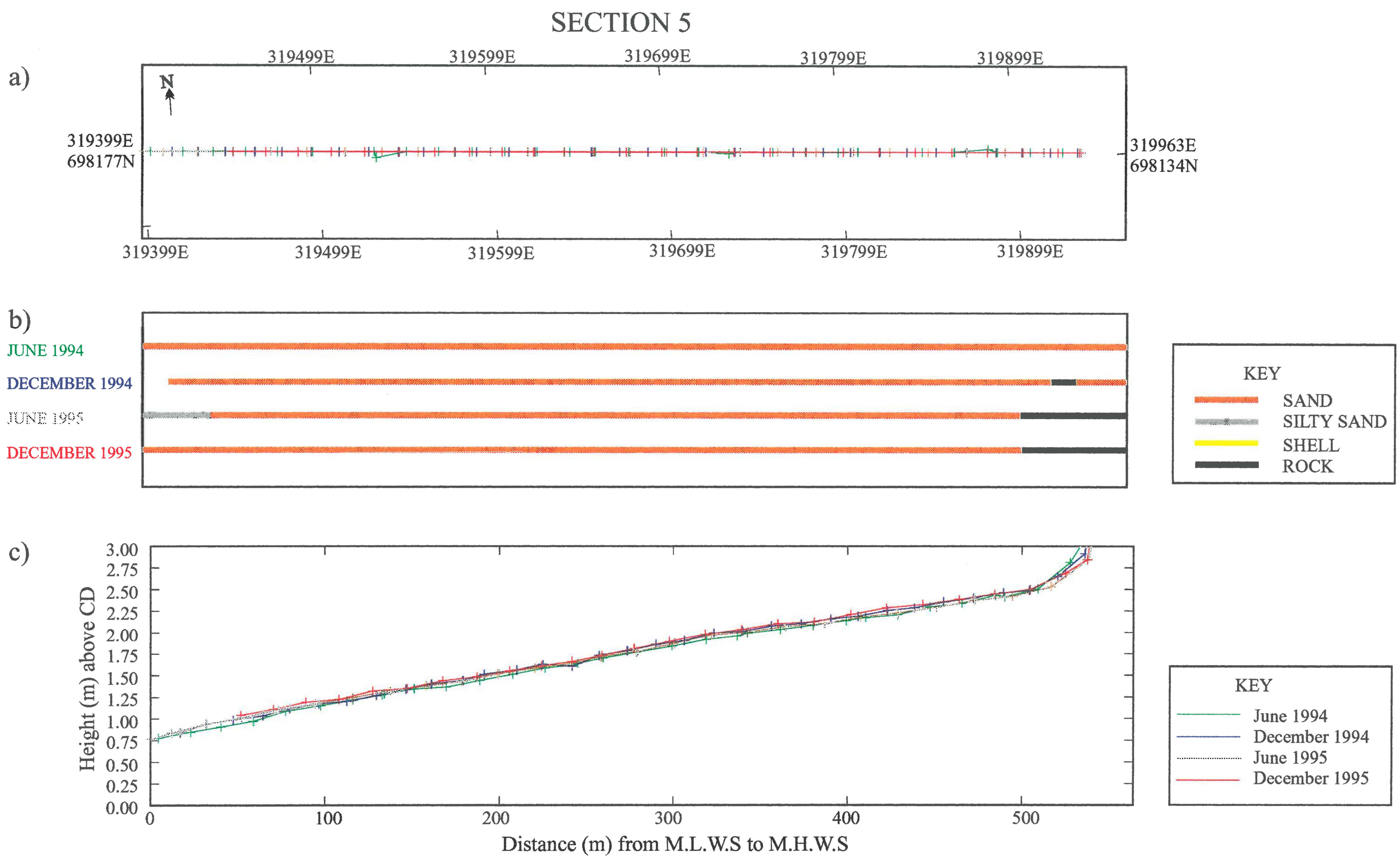

Figure 3.20: SECTION 5: a) Plan view and location of survey points; b) Lithology of surficial sediments; c) Elevation of intertidal flat. V.E. = 50.

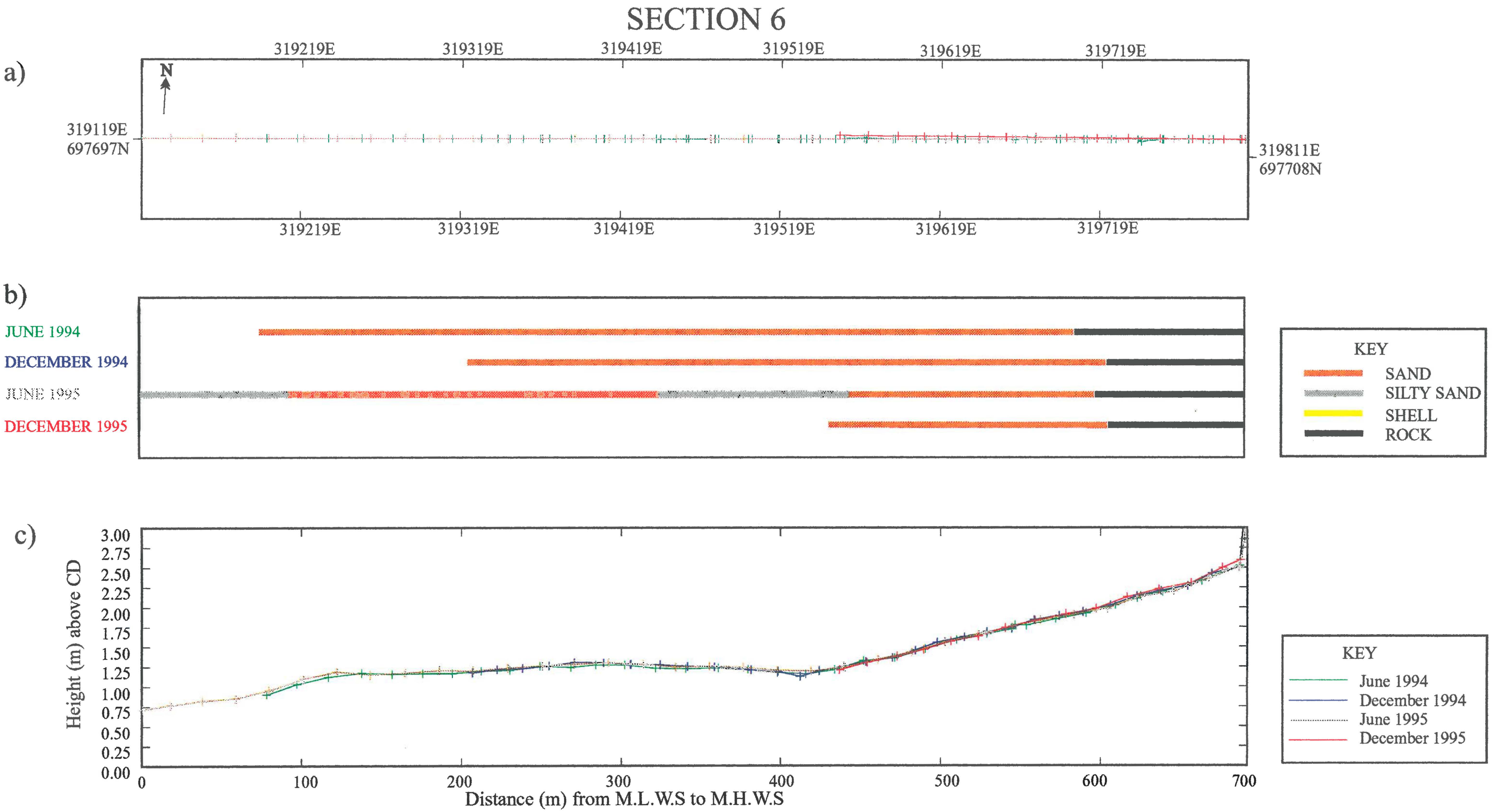

Figure 3.21: SECTION 6: a) Plan view and location of survey points; b) Lithology of surficial sediments; c) Elevation of intertidal flat. V.E. = 50.

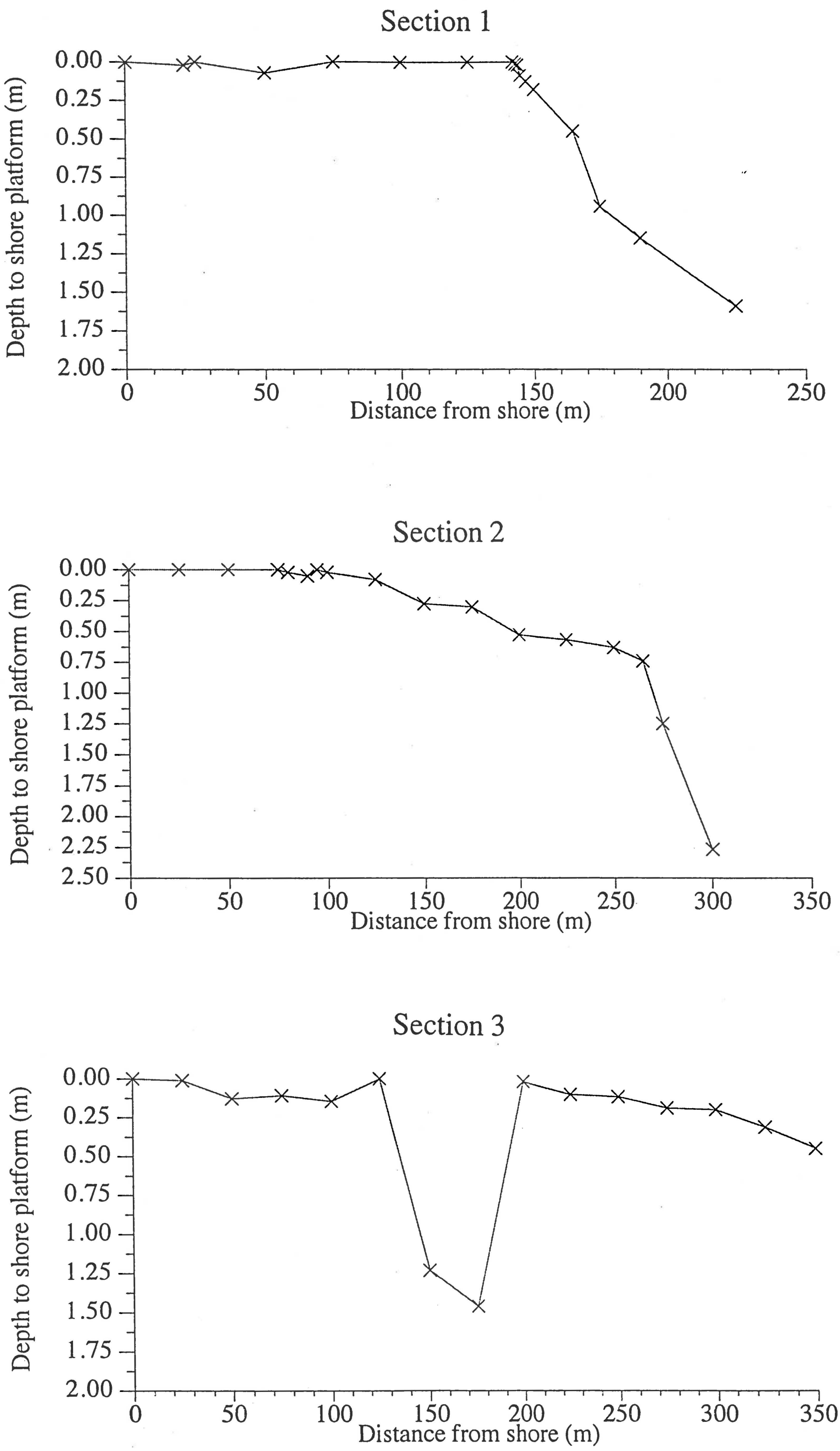

FIGURE 3.22: Depth of sediment veneering Waitemata Formation shore platform along Sections 1, 2 and 3 north of the approach channel to Pine Harbour Marina.

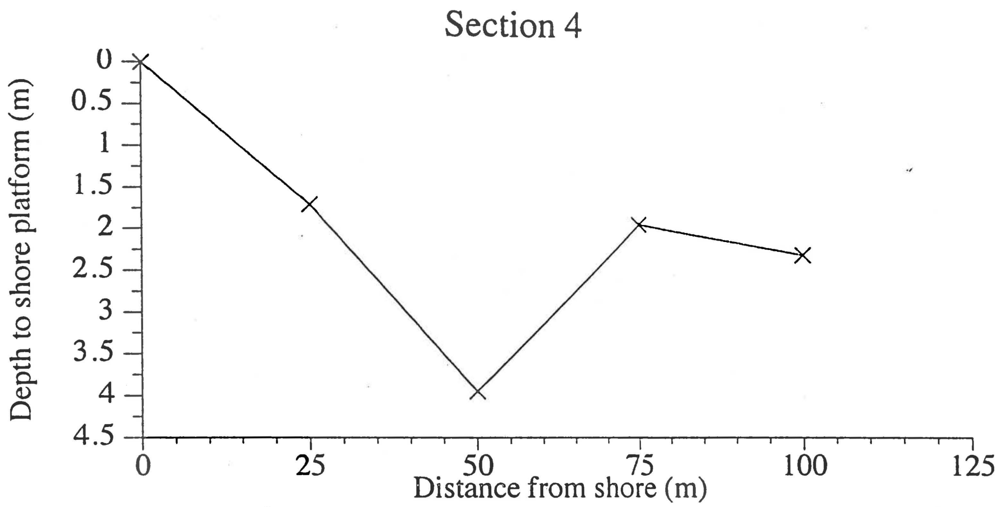

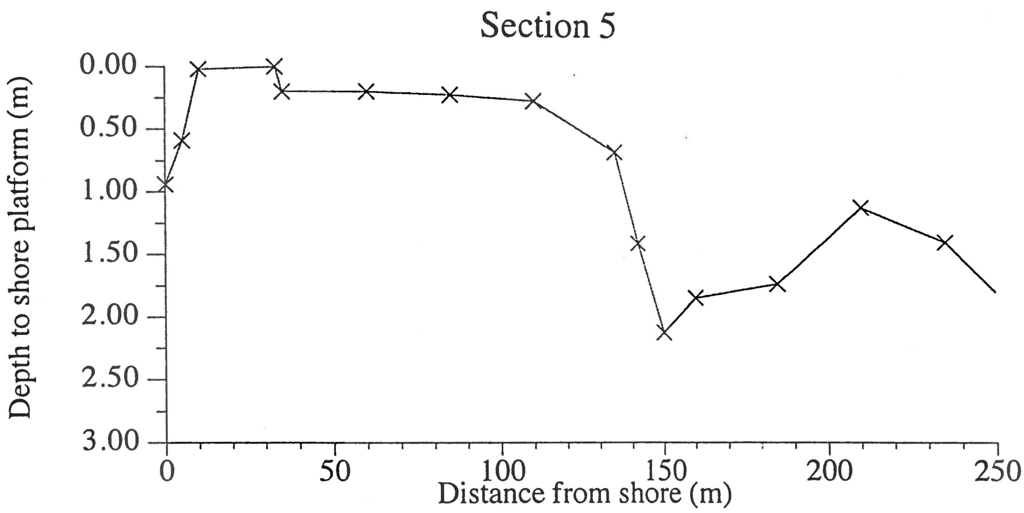

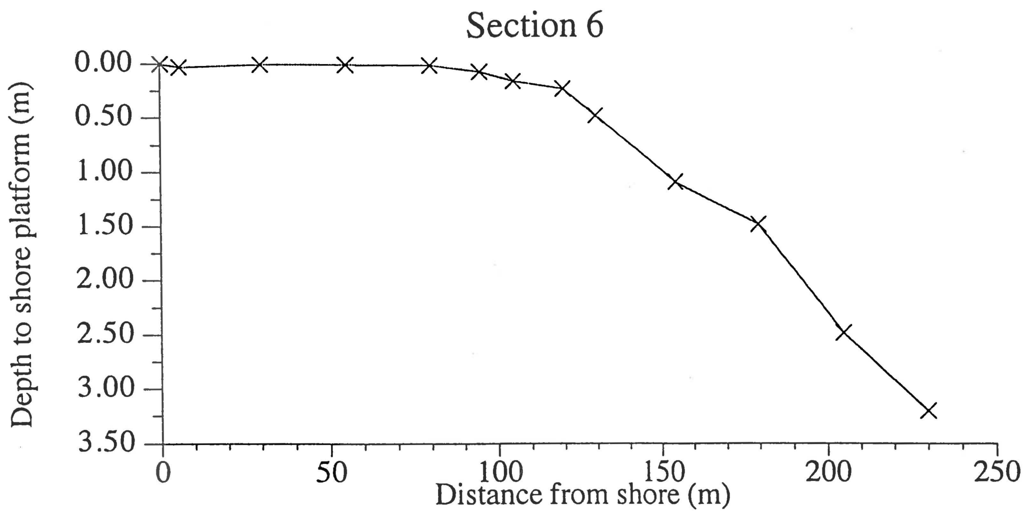

FIGURE 3.23: Depth of sediment veneering Waitemata Formation shore platform along Sections 4, 5 and 6 south of the approach channel to Pine Harbour Marina.

3.6 Sedimentation rods

3.6.1 Introduction

Sedimentation rods record the depth of sediment disturbance and any net change in sediment level relative to the top of the sedimentation rod. Sediment mixing depth is generally accepted as representing the thickness of the nearshore sediment transport layer (Sunamura and Kraus, 1985). It is a result of the reworking of the surficial layer due to sediment transport by waves and currents.

Several methods have been developed to measure the thickness of the active layer. Komar and Inman (1970) used the burial of sediment tracers to define the thickness of the layer of motion. Greenwood (1987) describes the use of depth of activity rods and washers to measure local bed elevation responses to storms in a fetch limited tideless environment. This method was also developed and used by Dolphin (1992) to measure patterns of scour and accretion on intertidal flats in fetch limited environment. The purpose of depth of disturbance rods is to indicate the depth to which sediments are disturbed or mixed and the thickness of sediment that is entrained (lifted) into suspension.

3.6.2 Methodology

Sedimentation rods were established between 1/6/94 and 3/6/94, along the six shore normal beach survey sections (Figure 3.15). The sedimentation rods were installed to monitor any net changes in the surface of the intertidal flats as a result of the addition of sediment from the dredgings. A further six rods were installed from Sunkist Bay to Maraetai to record any periods of muddy deposition reported by local residents in order to investigate the relationship of these events with dredge spoil dispersal. In addition to these 12 rods were installed in the dredgings mound on 12/7/94 to monitor the erosion of the dredgings mound. However most of these additional sedimentation rods suffered from human interference and washout, and no records were obtained from them.

The sedimentation rods consisted of an aluminium or steel rod, 0.5 cm in diameter and up to 1.0 m long. At the designated sites, the aluminium rods were driven into the sediment (steel rods were used in the bare rock) until they were stable, usually about 0.5 m. A length of hollow plastic pipe was fitted over each rod to make the rods more visible. A loose fitting washer was then placed over each rod. When sediments are re-worked and carried into suspension the washer falls to the new surface level and is buried as sediments are deposited. Depth of disturbance rods measure the occurrence and magnitude of these processes.

The sedimentation rods were measured and photographed at monthly intervals. At each visit the distance from the top of the rod to the surface was measured, indicating elevation changes, and the distance to the washer was also measured (Figure 3.24). The rod was also photographed to keep a record of surrounding bedforms (Plate 3.6). Following each recording the washer was returned to the new surface level.

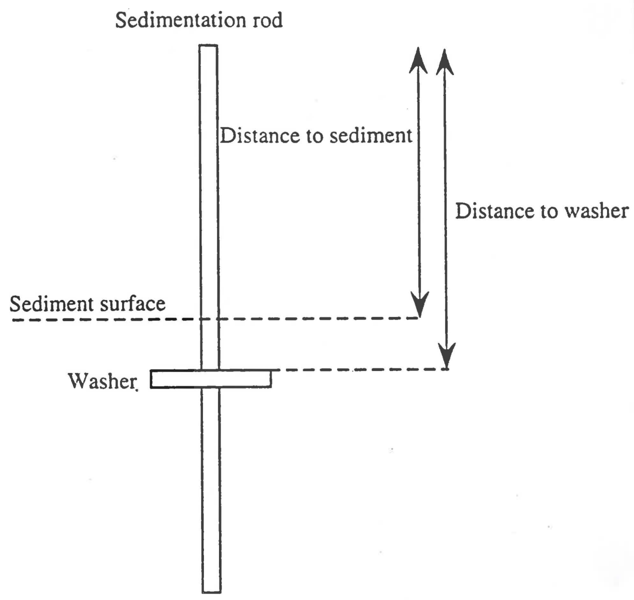

FIGURE 3.24: Schematic diagram of sedimentation rod illustrating the distances measured from the top of the rod to the sediment level, and from the top of the rod to the washer. The washer is returned to the sediment level after measuring.

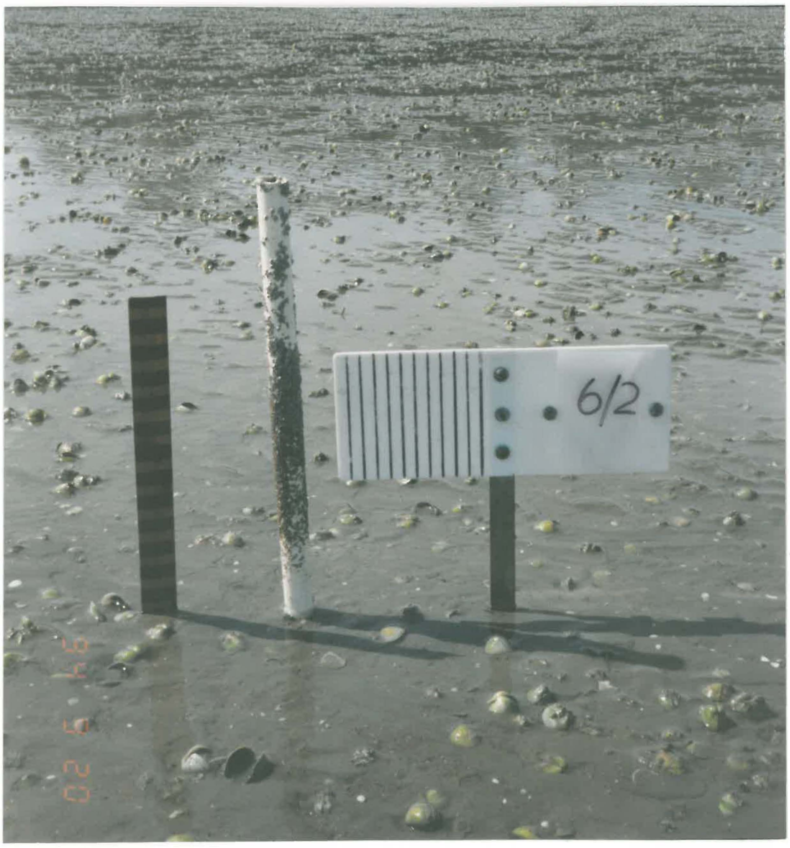

PLATE 3.6: Illustration of sedimentation rod used to measure the depth of sediment disturbance on intertidal flats fronting Pine Harbour Marina.

3.6.3 Results

Raw data of the monitoring of the sedimentation rods around Pine Harbour Marina are listed in Appendix 3.1. The measurements taken from the top of the rod to the sand, and the top of the rod to the washer were used to calculate the depth of sediment disturbance that occurred since the last measurement was taken. Depth of disturbance is calculated by subtracting the distance to the sand from the distance to the washer.

For much of the study period depth of disturbance was less than 1.5 cm. This shallow disturbance is due to small wave ripple (h = 1.0-1.5 cm) movement over the intertidal flats. Depth sediment of disturbance over the northern intertidal flats increased to between 2.0-3.0 cm on occasion, and the deepest depth of disturbance was 6.2 cm on 17/10/94. This corresponds to a period of high winds recorded in Auckland City over late September/October which would have generated larger waves and stronger orbital velocities to mix sediment to greater depths (Figure 3.25). In general depth of disturbance was highest for rods furthest offshore (Figure 3.26).

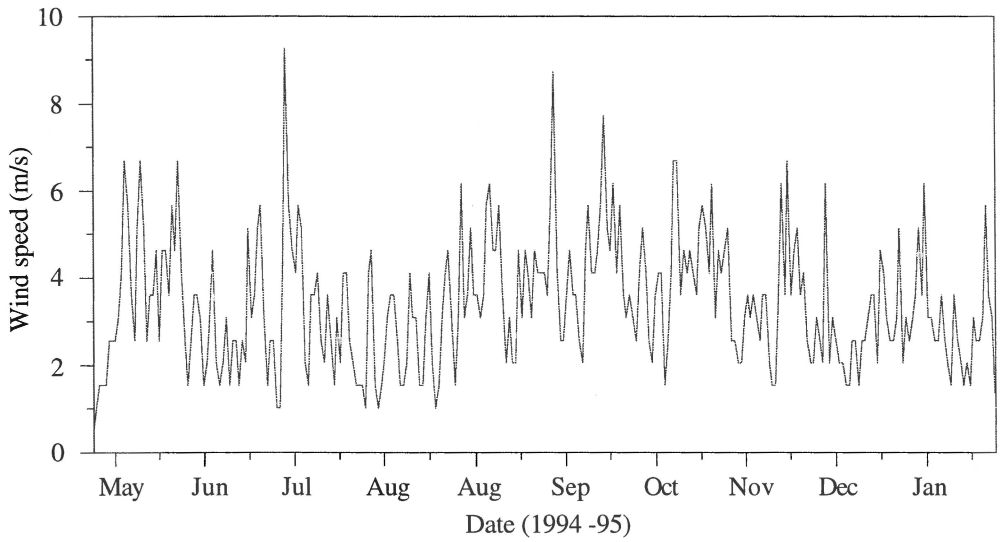

FIGURE 3.25: Average daily wind speeds (m/s) recorded at Auckland City, May 1994 to March 1995 (National Institute of Water and Atmospheric Research, Wellington).

Figure 3.27 shows the relative changes in sediment level at each rod. Greatest accretion of 4.0 cm was recorded in the mid tide region on Section 2 on 29/11/94, however this was subsequently eroded and sediment level returned to the previous level. Sedimentation rods along the northern intertidal flats recorded a small amount of accretion less than 1.0 cm, while along the southern intertidal flats there is a very small net erosion. These small changes in sediment level are insignificant as the sediment level fluctuated in the order of ± 2.0 cm in the long term. The sediment rods were observed on some occasions to have a local scour effect on the sediment at the base of the rod. This scouring may have reduced the amount of accretion recorded on the northern intertidal flats, and increased the amount of erosion around rods along the southern intertidal flats.

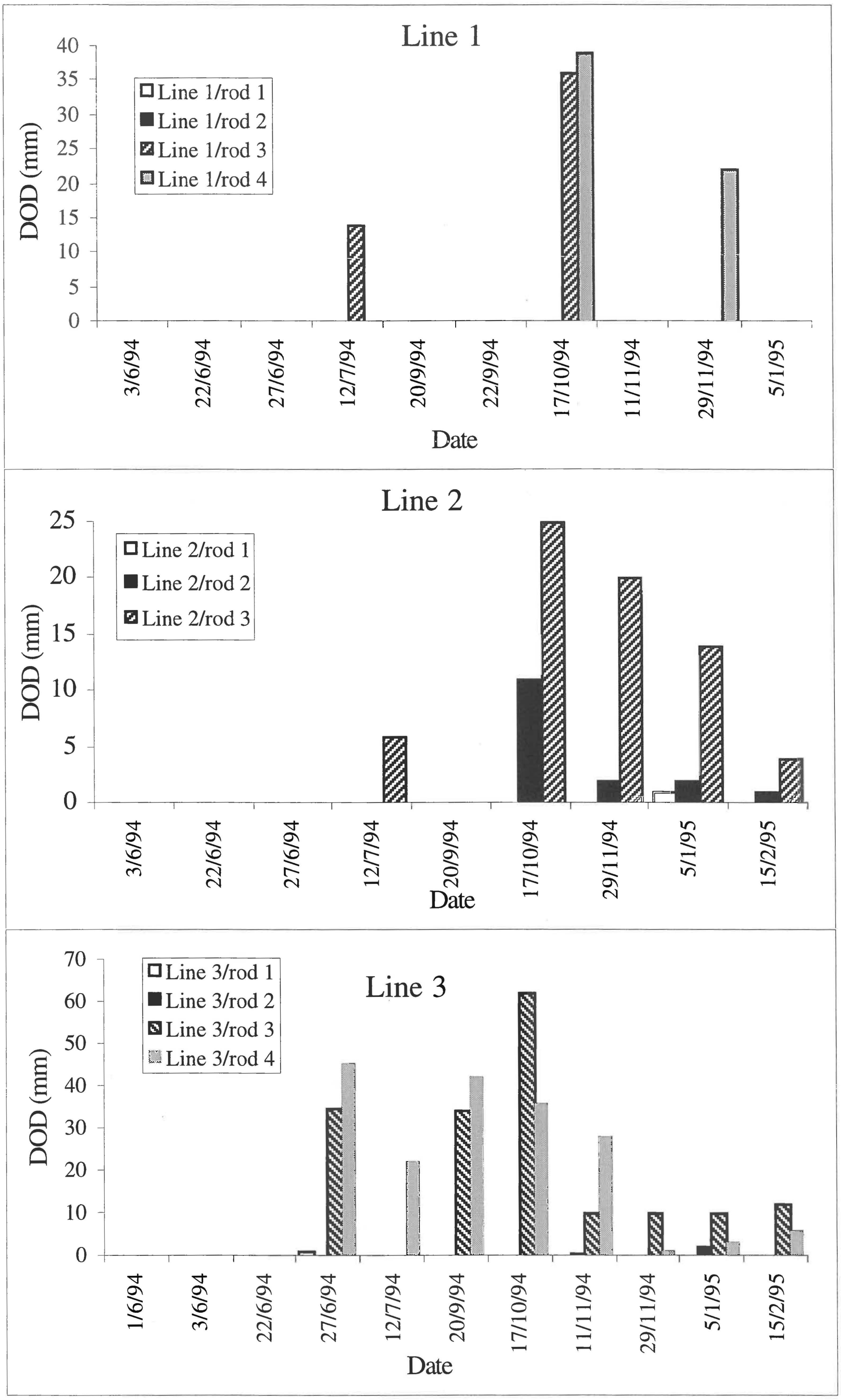

FIGURE 3.26: Depth of sediment disturbance as recorded by sedimentation rods located along beach survey section lines 1, 2 and 3 north of the approach channel to Pine Harbour Marina.

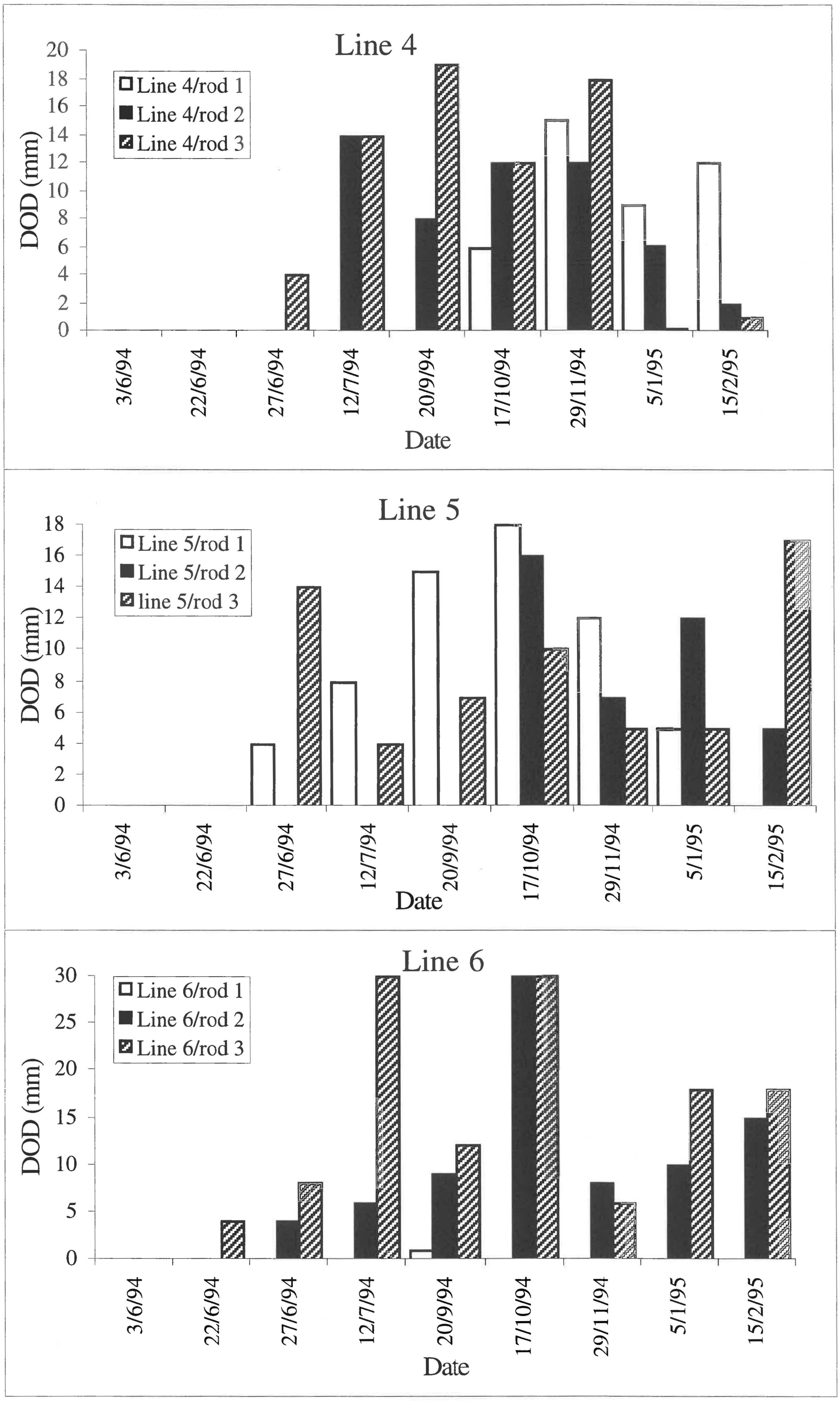

FIGURE 3.26 continued: Depth of sediment disturbance as recorded by sedimentation rods located along beach survey section lines 4, 5 and 6 south of the approach channel to Pine Harbour Marina.

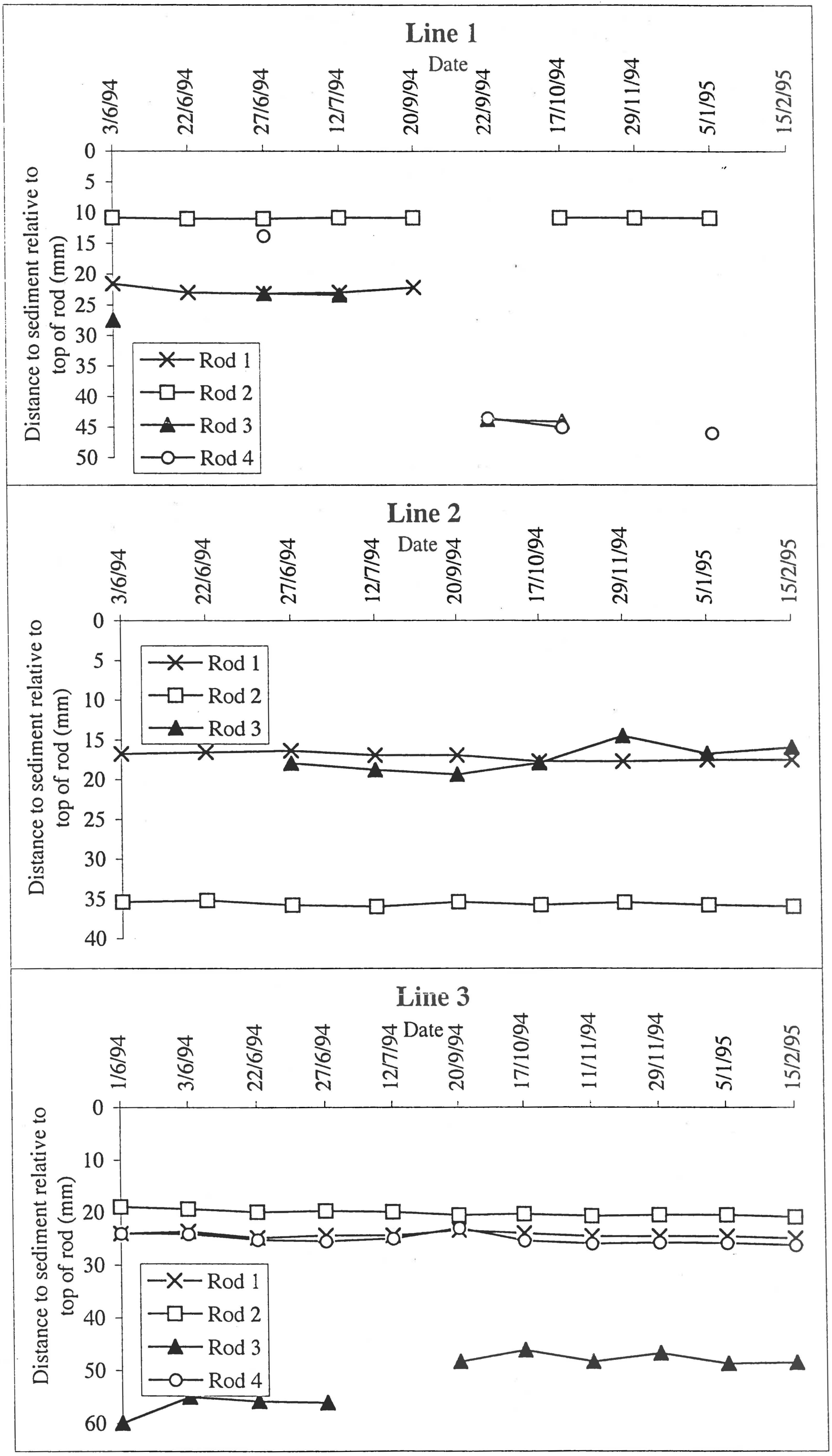

FIGURE 3.27: Variation in sediment levels relative to top of sedimentation rods along beach survey lines 1, 2 and 3 north of the approach channel to Pine Harbour Marina.

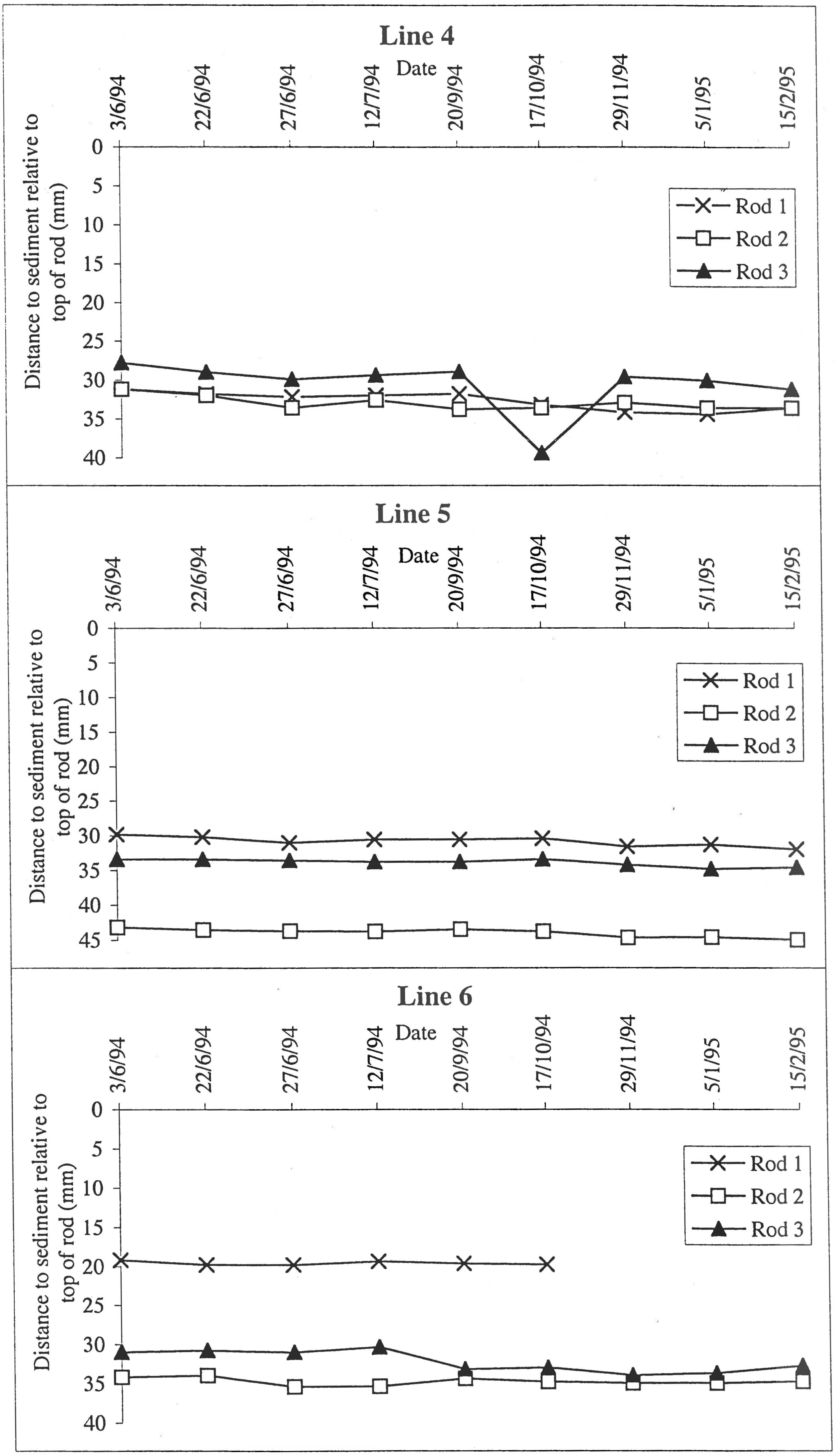

FIGURE 3.27 continued: Variation in sediment levels relative to top of sedimentation rods along beach survey lines 4, 5 and 6 south of the approach channel to Pine Harbour Marina.

3.6.4 Discussion

Sedimentation rods are used to indicate the depth to which sediments are disturbed or mixed and the thickness of sediment that is entrained into suspension. Fluctuations in the sediment elevation on the intertidal flat are also recorded by the sedimentation rods. The detection of greater depth of disturbance measurements relates to increases in available energy and activation of sediment. The depth of disturbance refers to sediment reworking caused by beach processes and is usually assessed over periods associated with tidal cycles or storm events, and therefore depends on the weather patterns and processes operating over the region (Sherman *et al.* 1994).

The sedimentation rods have an associated error value which is determined by surface wave ripples (Dolphin, 1992). A change in washer position may be the result of the washer being on a ripple crest, or in a ripple trough. Local scour effects were observed around the sedimentation rods where the washer was observed to be resting in a hollow at the base of the rod, and sediment that would have presumably been deposited on the washer eroded. Effects of scour by the sediment rod could be eliminated by replacing the rod with floating string tied to a weight buried under the sediment surface. A float attached to the end of the string buoys the string with the tide and does not interfere with sediment accretion and erosion processes. The relative level of the sediment could then be determined by measuring the length of the string exposed above the sediment surface (K. Black, pers. comm.).

Measurements of the amount of variation in the natural sediment surface are made relative to the top of the sediment rod. Erosion or accretion are assessed relative to the top of the sedimentation rod. Uninterrupted data sets are required in order to monitor sediment levels over time. Unfortunately at a number of sites interference with the rods, and subsequent replacements, disrupted in these measurements. The results of monthly monitoring of sedimentation rods at Pine Harbour Marina from June 1994 to March 1995 indicate that in the long term sediment levels fluctuate in the order of ±2.0 cm. The addition of sediment into the system does not account for increased depths of disturbance as there was no net change in sediment level. Although sediment is mixed vertically, net sediment erosion and accretion is much less than DOD. Sediment accretion was less than 0.5 cm on line 3/rod 3 on 17/10/94 although the DOD recorded was 6.2 cm. Overall there was minimal accretion at rods along the northern intertidal flats of approximately 1.0 cm, with less change at rods along southern intertidal flats where net change was slightly erosive.

Sedimentation rods located along northern intertidal flats recorded deeper depths of disturbance (up to 4.0-6.0 cm) than rods located along the southern intertidal flats (up to 3.0 cm). This suggests that wave processes acting over the intertidal flats are varied, and that the northern side of the approach channel is more exposed to large infrequent wave from the north-west, which have the potential to disturb sediment to greater depths. Differences in depth of disturbance may also be due to the type of substrate where the sedimentation rods are located. A rod located in an area of predominantly bare rock, with a relatively thin veneer of sediment, will have less sediment available to be activated by wave processes than areas of sand. Depth of disturbance varied along the survey lines, and reactivation of sediment was greatest at sedimentation rods which were further offshore. In all cases the outer rods on each survey line display the greatest sediment activity due to their longer exposure to wave processes allowing greater sediment activation, and in deeper water wave heights are greater.

Sherman *et al.* (1994) used fluorescent-tracer sands to determine the mixing depth in a low-energy reflective environment similar to conditions at Pine Harbour Marina (H_s = 0.09-0.13 m and T_s = 2.1-2.2 s). They found that the average mixing depth for this environment during their experiment (wind speeds 5.3-11.7 m/s) were about 22% of the significant wave height. A similar relationship between mixing depth and wave energy is recorded by sedimentation rods on the intertidal flats fronting Pine Harbour Marina where prevailing south-westerly winds generate waves 0.1-0.2 m and sediment mixing depths are 1.0-1.5 cm for most of the time. Sediment depth of disturbance measurements on the intertidal flats fronting Pine Harbour Marina are similar to DOD recorded by Dolphin *et al.* (1995), who defined different scales of mixing on sand flats in a similar fetch limited environment. In their study depth of disturbance in the order of 1.0-1.5 cm was attributed to the movement of small wave ripples which occur frequently over the intertidal flats and produce no net sediment transport. Depths of disturbance of 2.0-3.0 cm are attributed to increased wind and wave action during storm events which mix sediments to greater depths and cause net sediment transport (Dolphin *et al.* 1995). At Pine Harbour Marina sediment depth of disturbance increased up to 2.0-3.0 cm on occasion and a maximum depth of mixing of 6.2 cm were recorded, although minimal net sediment transport was detected by the change in sediment elevation relative to the top of the sedimentation rods. These periods of increased surficial sediment mixing and net sediment transport occur under storm conditions. For most of the measurement period sediment mixing was shallow (1.0-1.5 cm) and was attributed to ripple movement.

3.7 Hydrographic surveys

3.7.1 Methodology

Hydrographic surveys of the approach channel to Pine Harbour Marina were undertaken on four occasions using a Furuno Echosounder, measuring depths to ±10 cm accuracy. HYDRO software was used to interface with NAVTRAC differential GPS for position fixing (accurate to ±1.5 m) and the depth sounding. Surveys were undertaken on: 15/06/94; 03/11/94; 03/05/95; and 18/07/95, over 9 runlines spaced 12.5 m apart which were oriented east to west along the length of the channel, providing full channel coverage plus 50 m either side. Depth and position data were logged every 10 m. Adequate coverage of survey points over the channel area of interest was important in order to model the channel surface accurately. Some small areas without data resulted in interpolated surfaces. Because the approach channel is long and thin, it was important to get data points inside the channel on the pre-determined runlines to ensure coverage of the 25 m width of channel. However, during the surveying, sailing precisely along the runlines was difficult due to the effects of currents, waves and wind.

A differential GPS base station was set up for each survey. On 15/06/94 the GPS base station was located at the top of the marina administration building, however masts in the marina basin caused some interference to the GPS signal. This problem was rectified in subsequent surveys by relocating the base station to the surveyors peg on the mound on the outer breakwater.

Data was tide corrected in HYDRO relative to Pine Harbour Marina stageboard, which was surveyed in to the lowest astronomical tide (LAT), from which regular readings of tidal height were taken throughout the survey. Tide corrected data was loaded into TECHBASE for modelling.

Raw data was shallower than expected for the survey from 03/11/95. The data was modified, using the reasonable assumption that the elevation of the intertidal flats remained static, by correcting data to independent beach profiles of the dredgings. This involved adding 0.4 m to survey data which had the effect of deepening the channel and reduced the intertidal flats to the same level as the previous survey indicated. Inadequate coverage of the channel area close to the marina entrance on 3/11/94 caused inaccurate representation of the bathymetry when modelled. This problem was overcome by introducing data points into the survey, assuming the depths would be similar to depths measured in the following survey on 03/05/95. Data from all other surveys were verified from corresponding areas against survey points of the beach profile sections undertaken by Greenfield Surveyors Ltd.

Data was modelled in 10 m by 5 m grid cells, contoured every 0.5 m with depths relative to CD which is the lowest astronomical tide. Volume changes were calculated between surveys to estimate the amount of infilling or erosion occurring in the channel. Cross sections through the channel indicate the relative levels of erosion and accretion occurring in the channel between surveys.

3.7.2 Results

3.7.2.1 Bathymetry

In June 1994 depths in the Pine Harbour Marina approach channel landward of the 1300 m marker were less than 2.0 m below CD. Several shallow "problem areas" were evident in the landward section of the channel, where depths were 0.5 m below CD at the entrance and near the second unlit channel marker, and 1.0 m below CD near the 800 m marker (Figure 3.28).

Between June and October 1994 dredging deepened the channel, increasing depths to 2.0 m below CD at the marina entrance and seaward of the 800 m markers. Depths along most of the channel were increased by approximately 1.0 m, excluding an area around the second unlit marker which was missed in the dredging operation (Figure 3.29). Depths in the landward section of approach channel were increased to between 1.0 and 1.5 m below CD, the channel was generally deeper along the northern side of the channel (Figure 3.30).

In the 7 months following dredging to 3/5/95, the landward section of the approach channel suffered sediment accretion and infilled by up to 0.5 m, reducing channel depths to 1.5 m at the entrance and near the 800 m markers. However, an area of sediment loss was evident between the second and third unlit markers, where depths increased by 0.5 m due to approximately 500 m^3 (100 m x 10 m x 0.5 m) of sediment being removed from a shallow area missed during the main dredging operation (Figure 3.31). Depths in the remainder of the channel were between 1.0 and 1.5 m below CD, with channel depths less than 2.0 m below CD in the landward 1450 m of channel (Figure 3.32).

The last survey undertaken on 18/7/95, 9 months after the completion of the dredging works, indicates channel depths less than 2.0 m below CD landward of the 1300 m markers. The landward section of the approach channel suffered significant infilling, the entrance having accreted by 1.0 m, reducing depths to between 0 and 0.5 m below CD, while between the second and third unlit markers some 0.5 m of accretion occurred (Figure 3.33). Another shallow area was near the 800 m marker where depths reduced to between 1.0 and 1.5 m below CD. A deep narrow channel, 1.5 m below CD, was evident down the centre of the channel (Figure 3.34).

3.7.2.2 Volume changes

Volume changes were calculated in TECHBASE between different survey dates over the entire channel area (approximately 200,000 m^3), and over the smaller landward end of the approach channel (approximately 45,000 m^3) (Figure 3.36). Volume changes expressed in cubic metres are listed in Table 3.2. Volume change calculations have a combined error of ±20cm, comprised of ±10cm accuracy of each survey. This height error, multiplied by the area the volume change is calculated over, gives the total possible error for assessing the volume change. However the likely error is much smaller, somewhere in the order of 2.0-3.0 cm, but difficult to gauge.

TABLE 3.2: Approximate sediment volume changes over defined channel areas (-ve = erosion; +ve = accretion) and total possible error.

Survey dates	Small area volume changes (±9,000 m^3)	Large area volume changes (±40,000 m^3)
15/06/94 to 03/11/94	-4,700 m^3	-3,800 m^3
03/11/94 to 03/05/95	+7,800 m^3	+25,200 m^3
03/05/95 to 18/07/95	-1,600 m^3	-13,200 m^3
03/11/94 to 18/07/95	+6,200 m^3	+12,000 m^3

The most dynamic area of the channel is the landward 1200 m section, with insignificant changes occurring elsewhere in the channel. Between 15/06/94 and 03/11/94 these changes were mainly erosive, due to the combined action of the dredging and natural processes, and approximately 3,800 m^3 of sediment was lost from the total channel area. Channel depths were increased by 1.5 m at the entrance and by 0.5 to 1.0 m along the landward 1100 m during the 1994 dredging operation.

For the period from 03/11/94 to 18/07/95, in the 9 months since dredging most changes occur in the landward 1100 m (Figure 3.35). Most accretion occurred at the entrance (1.0 to 1.5 m) and between the 800 and 1100 m section where sediment accreted up to 1.0 m. The channel infilled along the northern channel edge by approximately 0.5 m over the 700 m section from the marina entrance. This infilling may be from the slumping of the dredged material back into the channel from the adjacent intertidal flats.

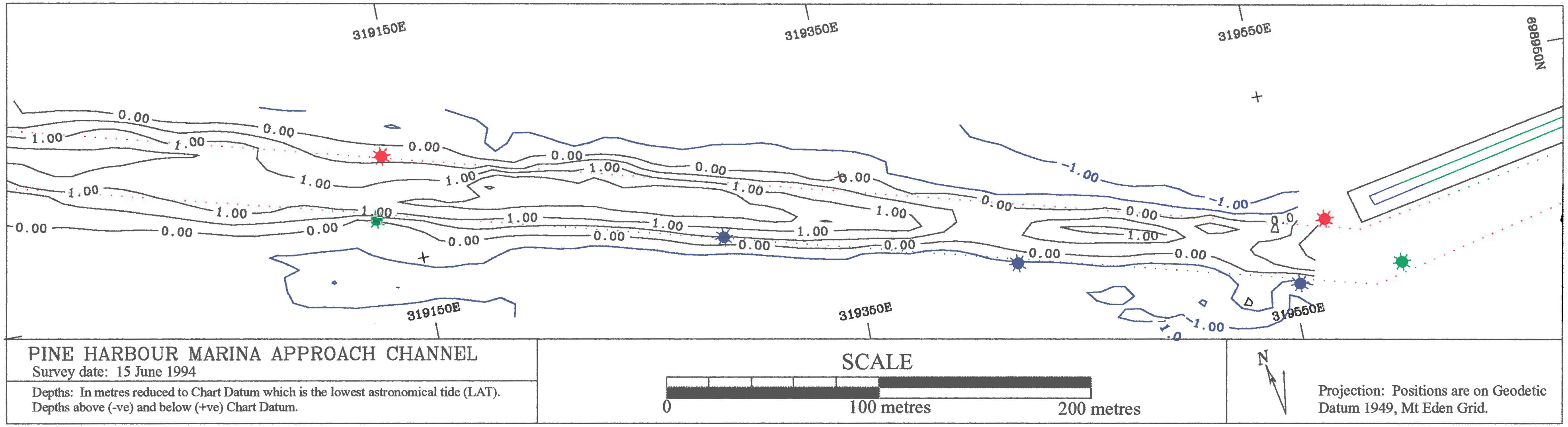

Figure 3.28: Bathymetry of the landward section of the approach channel to Pine Harbour Marina on 15/6/94. Depths in metres relative to CD.

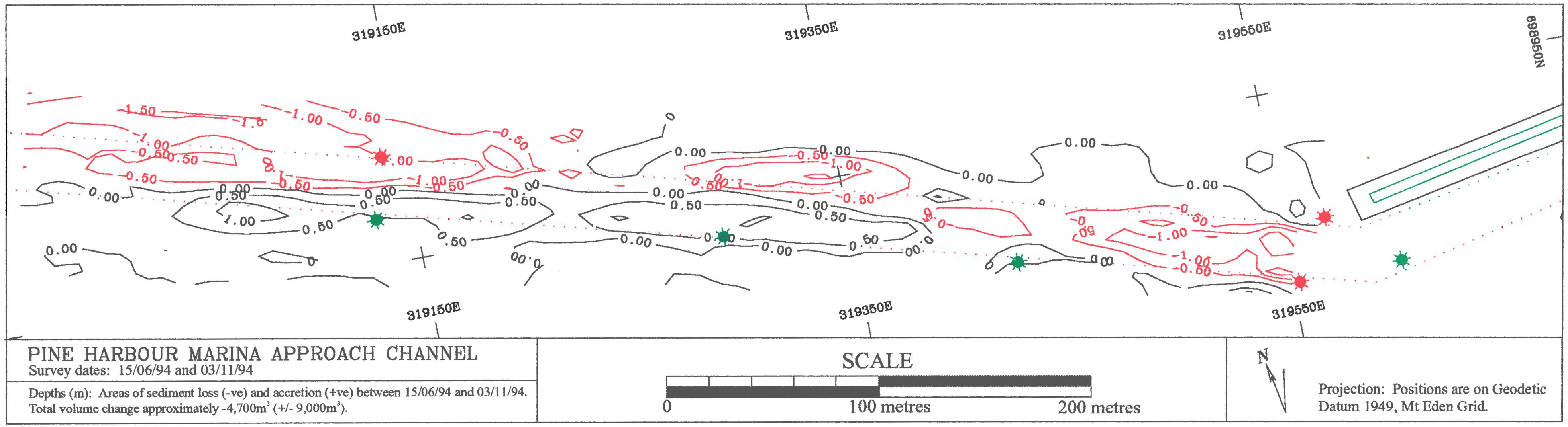

Figure 3.29: Areas of sediment loss (-ve) and accretion (+ve) in depths (m) in the approach channel to Pine Harbour Marina between 15/6/94 and 3/11/94.

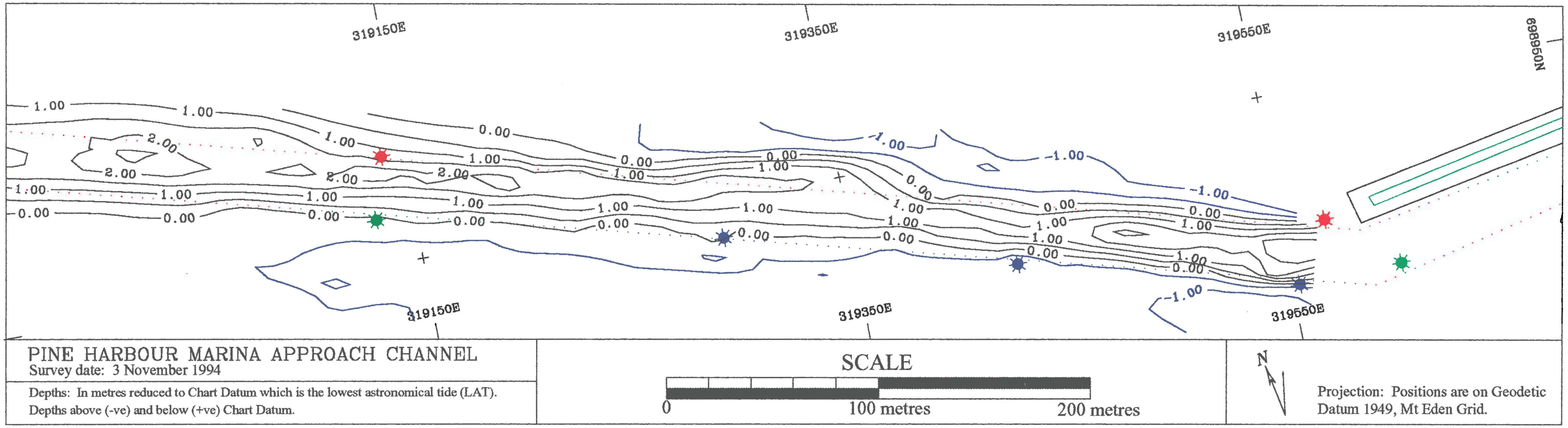

Figure 3.30: Bathymetry of the landward section of the approach channel to Pine Harbour Marina on 3/11/94. Depths in metres relative to CD.

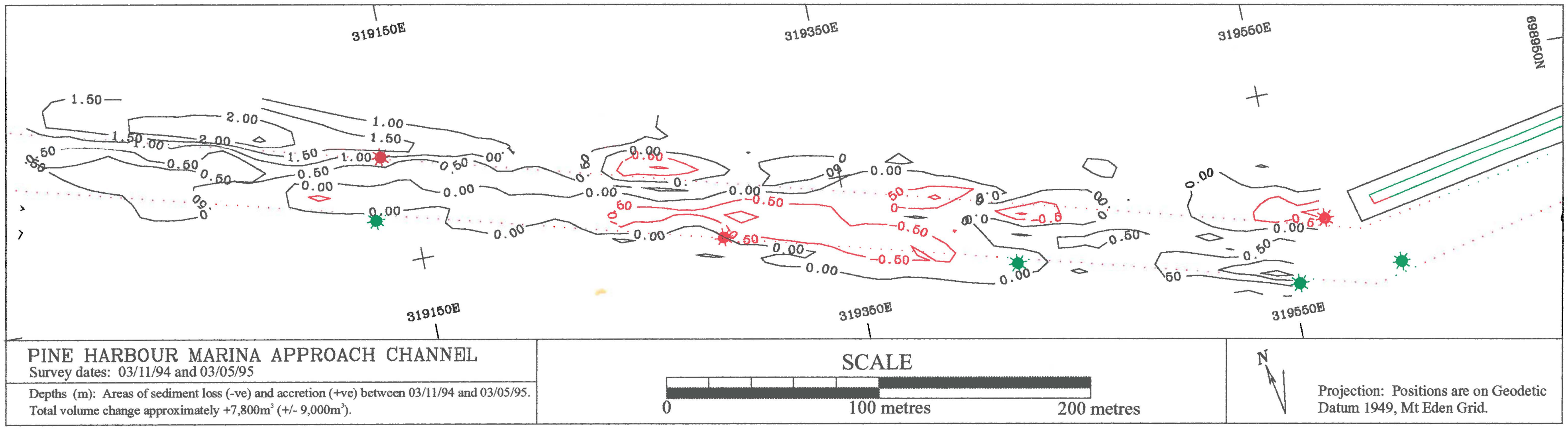

Figure 3.31: Areas of sediment loss (-ve) and accretion(+ve) in depths (m) in the approach channel to Pine Harbour Marina between 3/11/95 and 3/5/95.

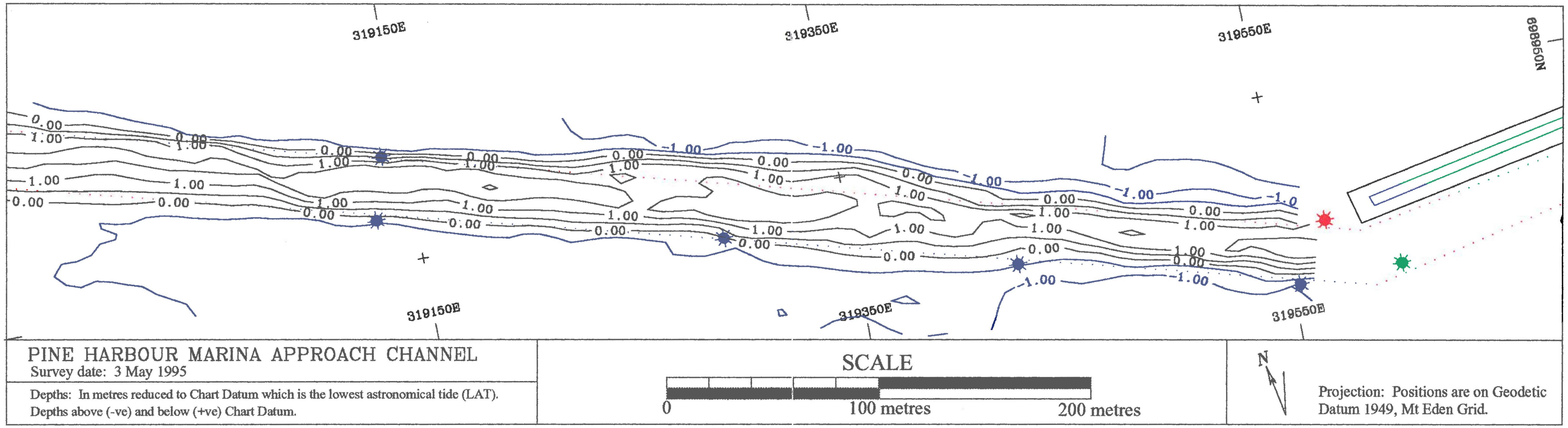

Figure 3.32: Bathymetry of the landward section of the approach channel to Pine Harbour Marina, 3/5/95. Depths in metres relative to CD.

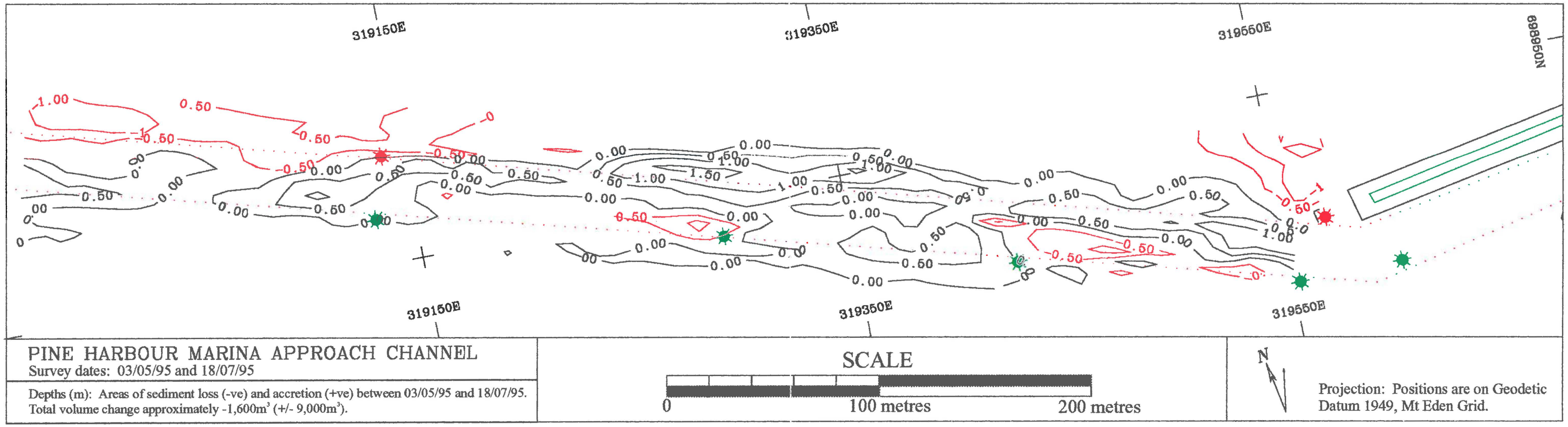

Figure 3.33: Areas of sediment loss (-ve) and accretion (+ve) in depths (m) in the approach channel to Pine Harbour Marina between 3/5/95 and 18/7/95.

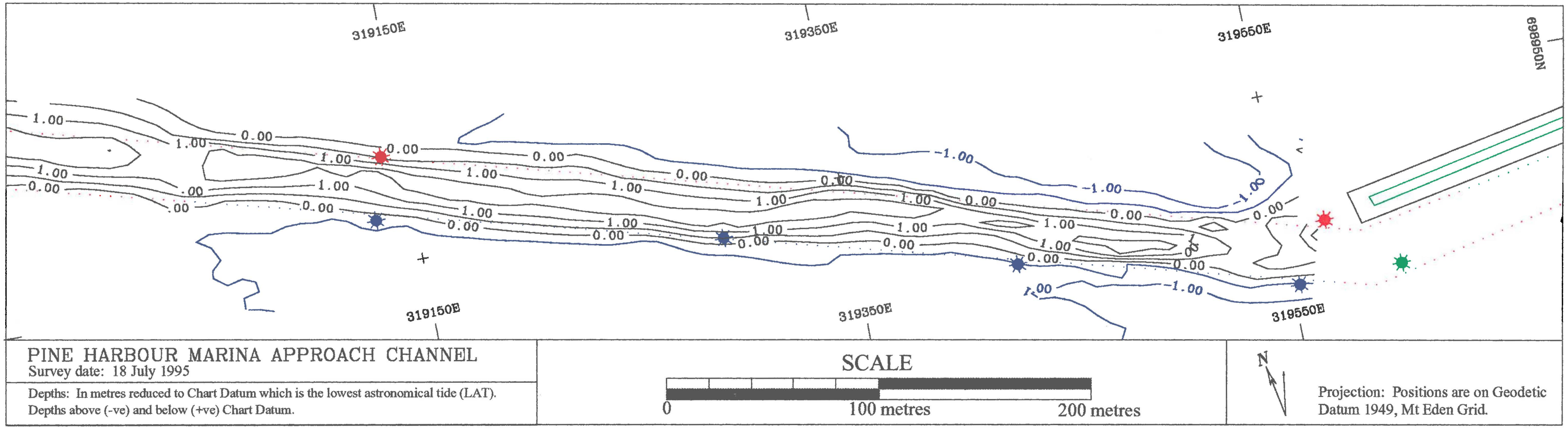

Figure 3.34: Bathymetry of the landward section of the approach channel to Pine Harbour Marina on 18/7/95. Depths in metres relative to CD.

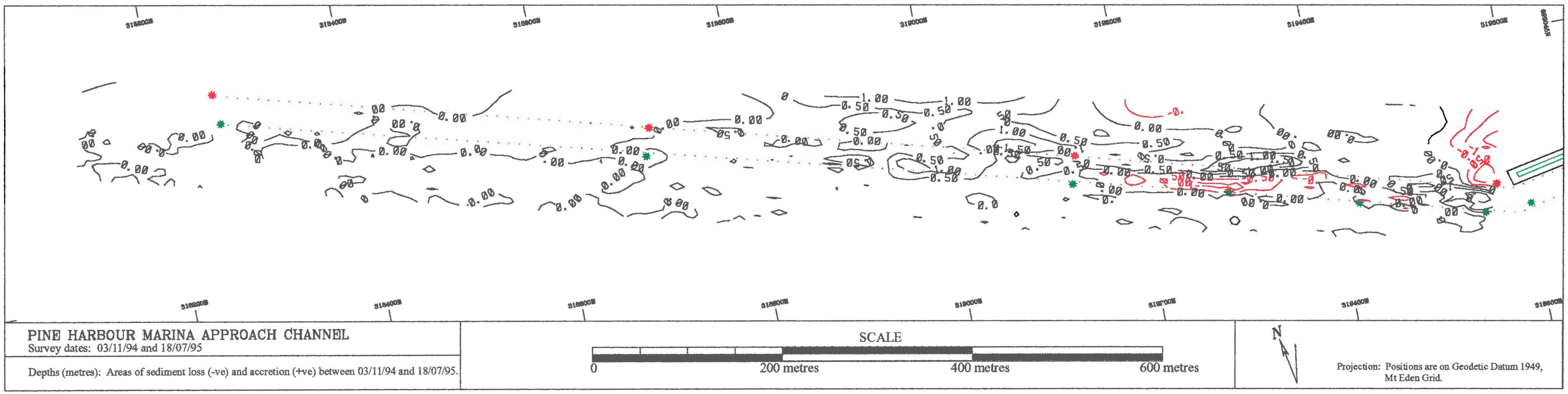

Figure 3.35: Areas of sediment loss (-ve) and accretion (+ve) in depths (m) in the approach channel to Pine Harbour Marina between 3/11/94 and 18/7/95.

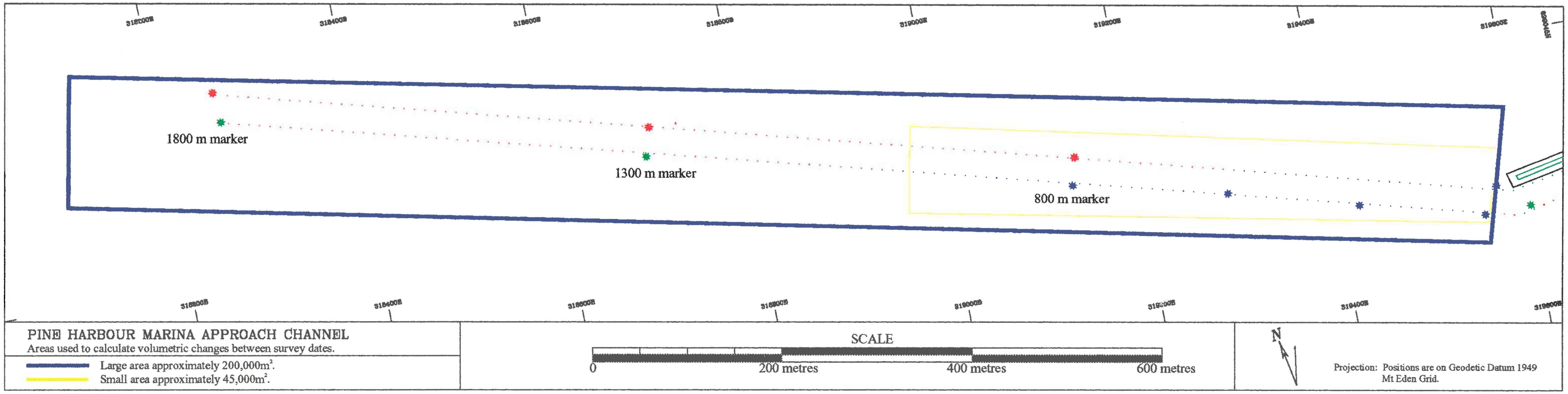

Figure 3.36: Location of areas over approach channel to Pine Harbour Marina for which volume changes were calculated between hydrographic surveys.

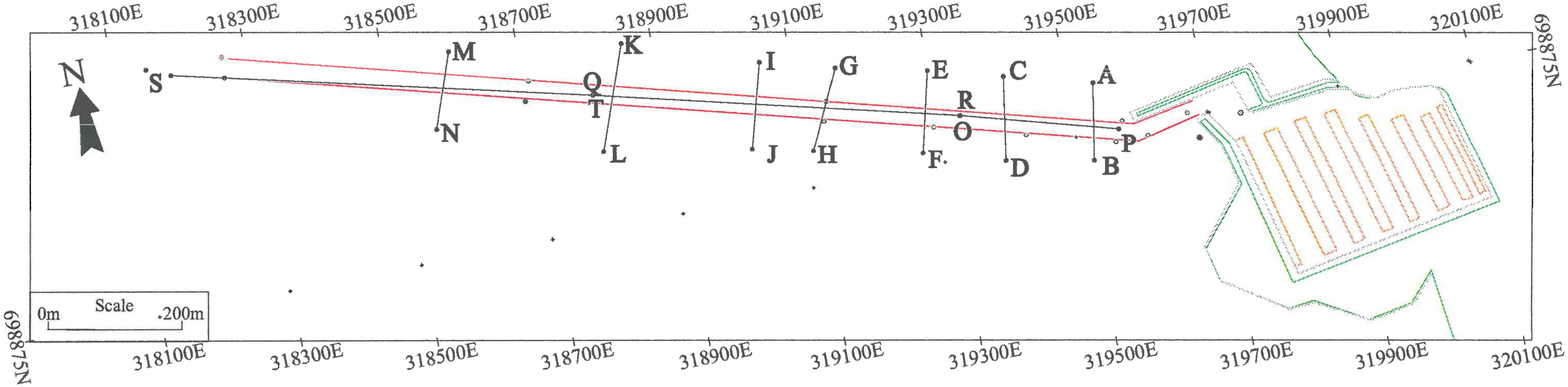

Figure 3.37: Location of cross sections through the approach channel to Pine Harbour Marina.

3.7.2.3 Cross sections

Figure 3.37 shows the location of cross sections through the approach channel to Pine Harbour Marina. Cross sections are modelled on survey data, indicated by crosses, where data points 2.5 m either side of the survey line are projected onto the profile. The vertical exaggeration (V.E.) of cross sections was between 5 and 10 times.

Profile AB (Figure 3.38) illustrates that the entrance to the marina basin was 0.5 m below CD before dredging and increased to 1.75 m below CD with dredging. Within 7 months of dredging the channel infilled with sediment, reducing depths along the southern side to 1.25 m below CD, possibly where sediment infilling the boatramp overflowed into the channel. Further sediment accretion occurred in the following 2 months reducing channel depth at the entrance to 0.5 m below CD. Channel width varied over the period of surveying from 22 m to 30 m to 25 m.

Channel depth across Profile CD was increased from 0.5 m below CD to 1.5 m below CD after dredging (Figure 3.39). The channel was scoured and width increased between subsequent surveys until 18/7/95 when the channel infilled on the north and south sides by approximately 0.5 m. However the channel depth remained approximately 1.5 m below CD in the centre of the channel.

Profile EF, illustrated in Figure 3.40, shows that channel depths have remained around 1.5 to 2.0 m below CD through the centre of the channel. Dredging widened the channel on the northern side by approximately 5 m. Since dredging the channel has infilled along the sides, with sediment accretion of 0.5 m on the south side since 3/11/94, which was subsequently eroded and the northern side accreted by up to 1.0 m on 18/7/95.

Profiles GH and IJ (Figure 3.41 & 3.42 respectively) were dredged to 2.0 m below CD. Since dredging both have experienced gradual infilling of 0.5 m to 1.0 m of sediment, reducing depths to 1.0 m below CD. The subtidal Profiles KL and MN (Figures 3.43 & 3.44) are the most stable with insignificant fluctuations in sea bed elevation. The channel form is barely distinguishable, losing shape and experiencing less change with increasing distance from shore.

Cross sections through the middle of the channel confirm that most change occurred in the landward section of the channel. Profile OP (Figure 3.45) through the centre of the landward 250 m of approach channel indicates that sediment levels accreted by 1.5 m in some areas since dredging, reducing the channel to pre-dredging depths at the marina entrance 0.5 m below CD. The landward 150 m is less than 1.0 m below CD, infilling between 0.5 and 1.0 m since dredging. Further seaward, between 150 and 250 m from the entrance, there has been 0.5 m of sediment loss since dredging. This is a small area of "touch up" dredging, in the area missed during the main dredging operation.

Profile QR (Figure 3.46) was reduced to 2.0 m below CD with dredging which removed "problem" shallow area 1.0 m below CD near the 800 m marker. Sediment accreted since dredging by up to 0.5 m, reducing channel depths to 1.5 m below CD along most of the section on 3/5/95. The survey of 18/7/95 indicated that since dredging a total of 1.0 m of accretion occurred in some areas. Areas greatest affected by infilling were located between the second unlit marker, approximately 300 m from the marina entrance, and mid way between the 800 m and 1300 m markers where channel depths reduced to 1.0 and 1.5 m below CD. The seaward end of the channel beyond 1100 m shows little to no change as demonstrated in Profile ST (Figure 3.47). Channel depths grade from approximately 2.0 m below CD to 2.5 m below CD at the 1800 m markers.

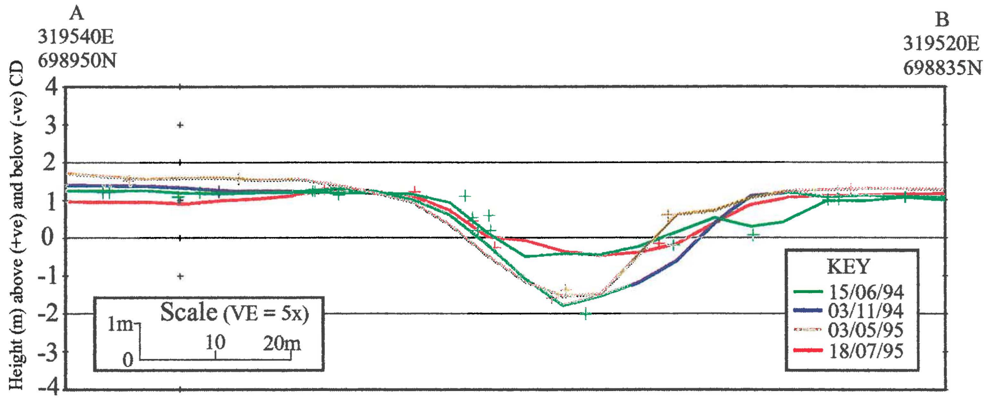

Figure 3.38: Modelled cross section from A to B through the approach channel to Pine Harbour Marina, near the entrance to the marina basin.

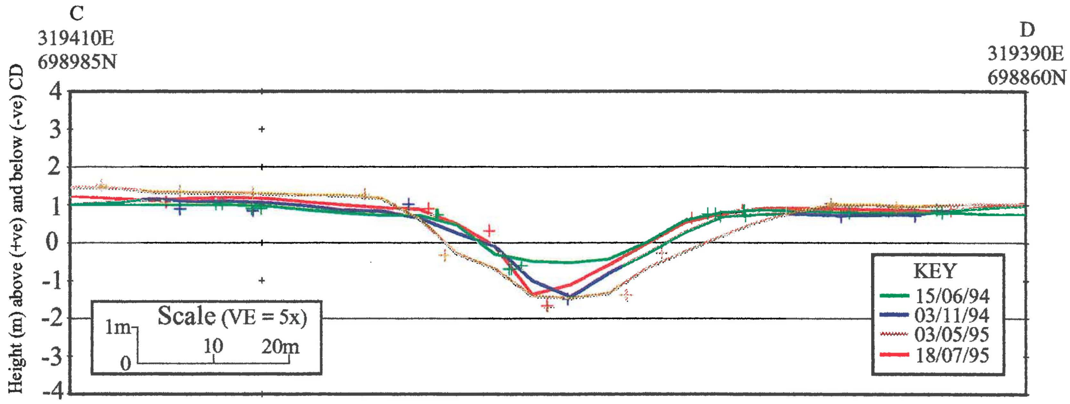

Figure 3.39: Modelled cross section from C to D through the approach channel to Pine Harbour Marina, 175 m from the entrance to the marina basin.

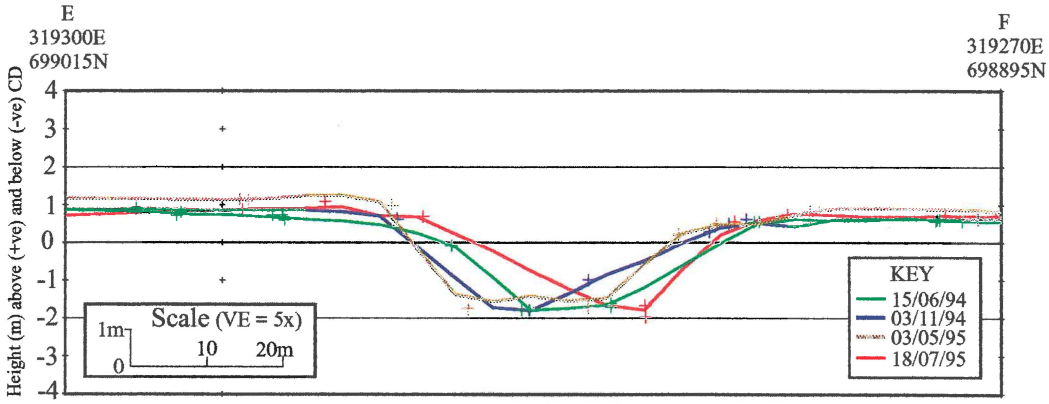

Figure 3.40: Modelled cross section from E to F through the approach channel to Pine Harbour Marina, 300 m from the entrance to the marina basin.

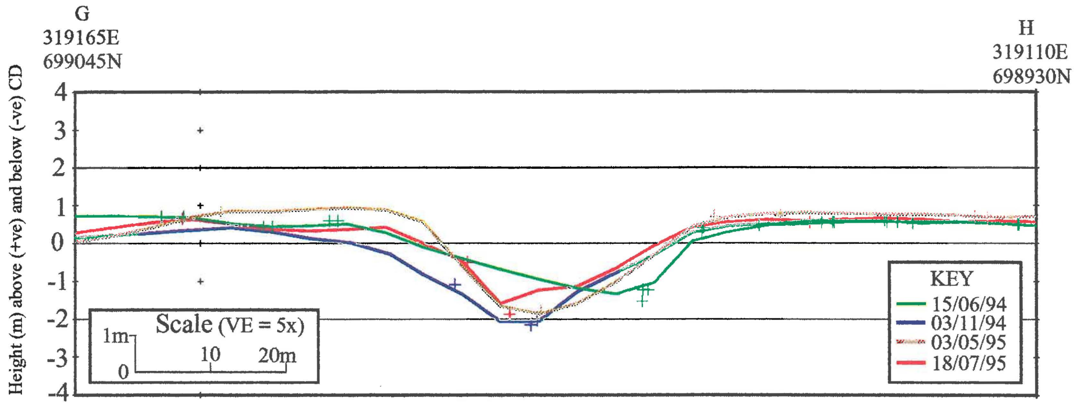

Figure 3.41: Modelled cross section from G to H through the approach channel to Pine Harbour Marina, near the 800 m channel markers.

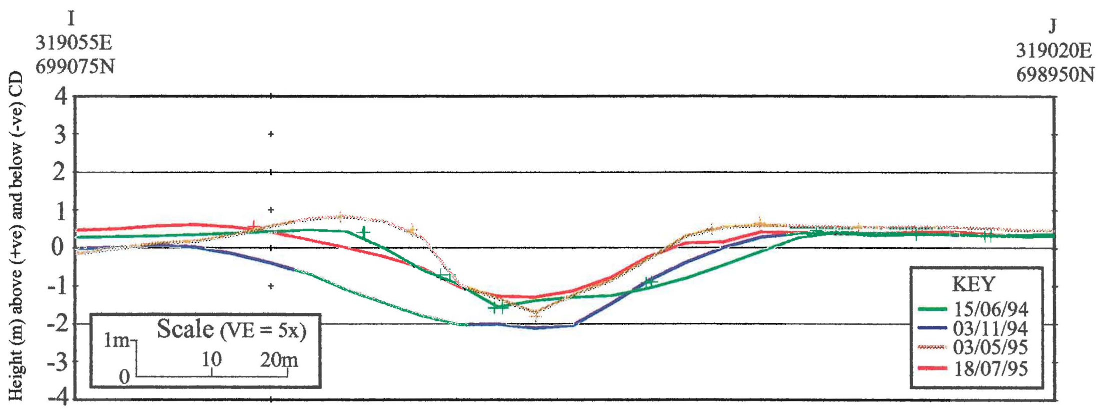

Figure 3.42: Modelled cross section from I to J through the approach channel to Pine Harbour Marina.

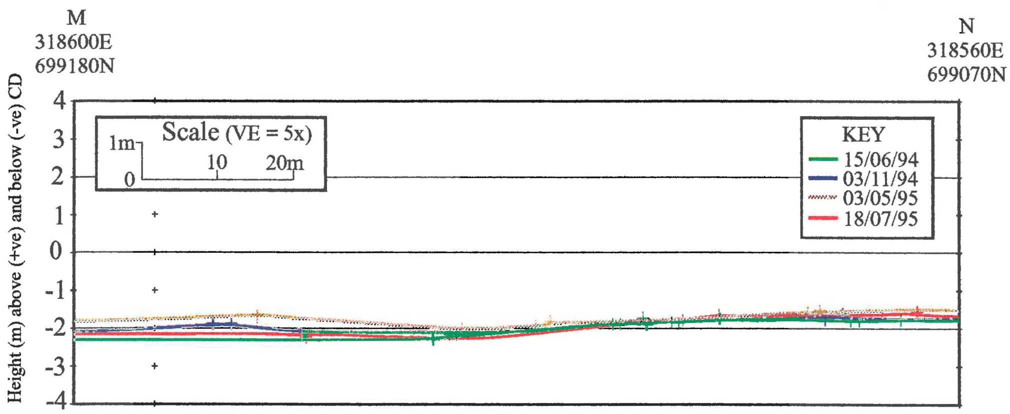

Figure 3.43: Modelled cross section from M to N through the approach channel to Pine Harbour Marina.

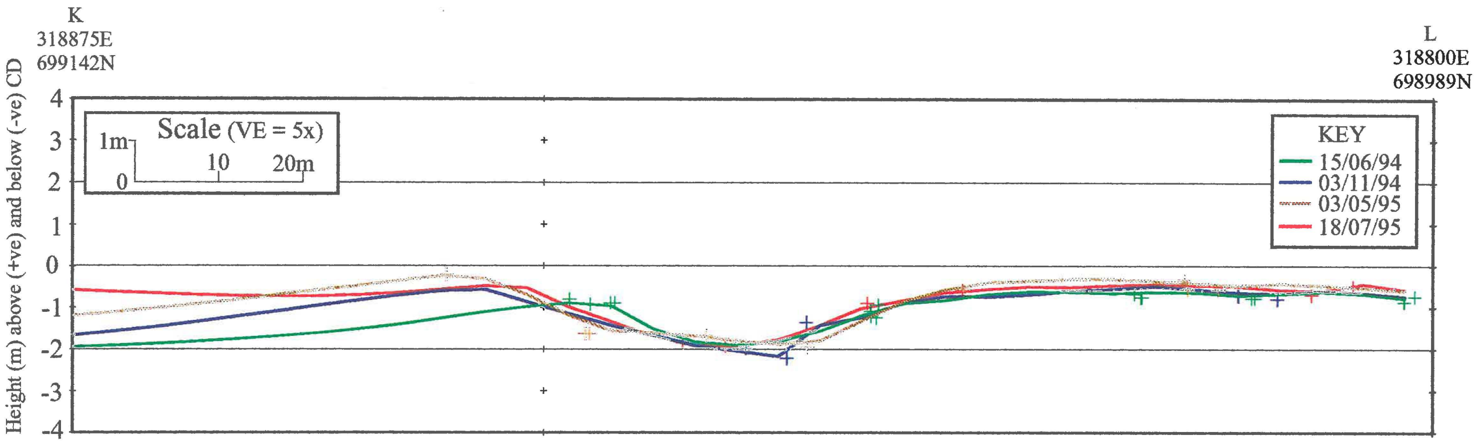

Figure 3.44: Modelled cross section from K to L across the approach channel to Pine Harbour Marina.

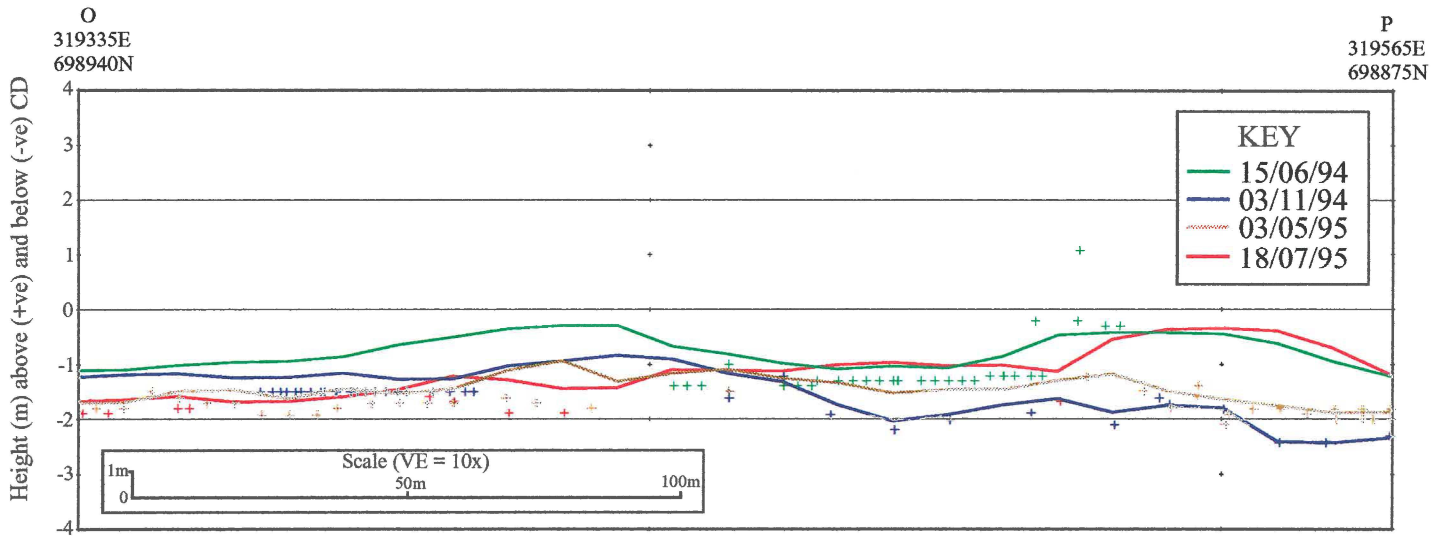

Figure 3.45: Modelled cross section from O to P through the middle of the approach channel to Pine Harbour Marina.

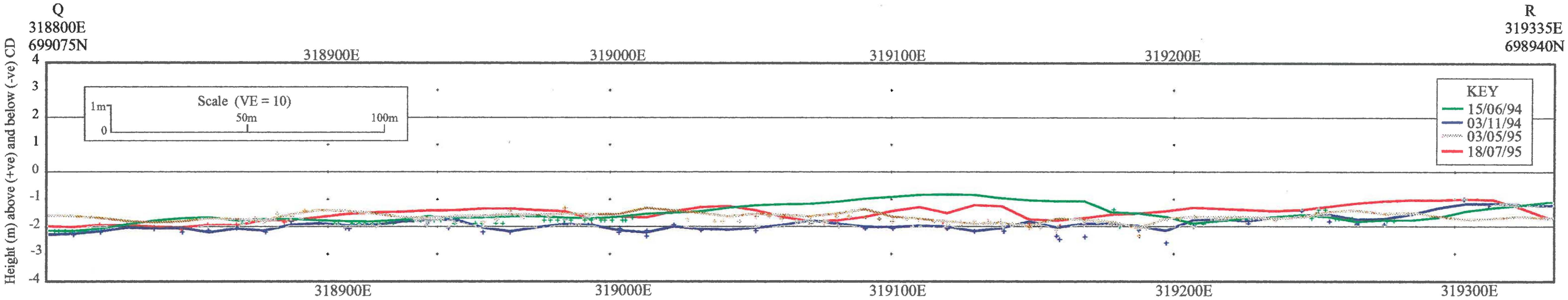

Figure 3.46: Modelled cross section from Q to R through the middle of the approach channel to Pine Harbour Marina.

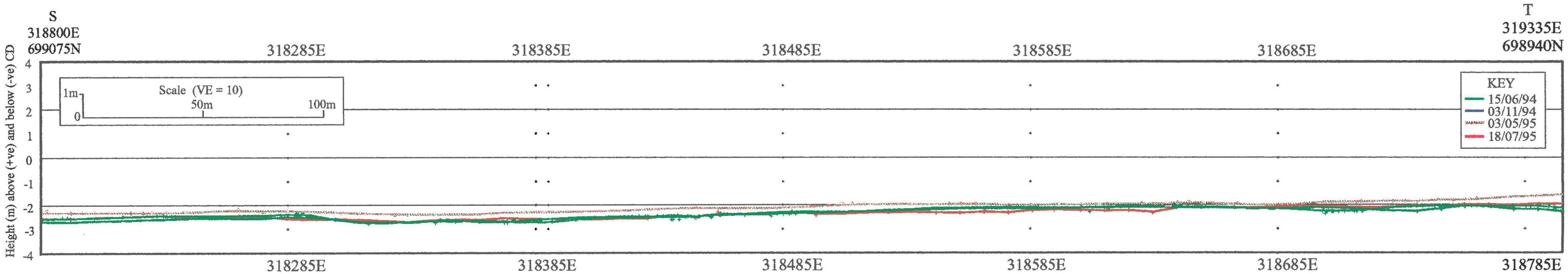

Figure 3.47: Modelled cross section from S to T through the middle of the approach channel to Pine Harbour Marina.

3.7.2.4 Side scan survey & Raytheon hydrographic soundings of channel

The approach channel to Pine Harbour Marina was surveyed with side scan in August 1995. Side scan sonar was undertaken at high tide in water depths around 5 m. Although the channel is not the ideal location to use the side scan sonar it did provide a useful image of the channel shape, depth and sediment substrate.

The side scan sonar trace showed darker reflections encroaching into the channel from the southern side from the entrance to the marina until the first unlit starboard marker. This area is interpreted to be fine sediment infilling the boat ramp feeder channel and spilling into the approach channel. Along the centre of the channel reflectance is stronger until mid way between the 800 and 1300 m starboard markers, indicating that this length of the channel is shallow and sediment on channel floor is highly reflective representing finer silt sized sediment.

Darker reflectance is evident along intertidal flats north of the channel where the dredgings were deposited. Amongst the reflections blocks of the boulder sized dredgings removed from the approach channel amongst the finer sediment could be identified. The northern side of the channel showed darker reflectance fingering into the channel at various locations and an irregular shape to the channel edges. The darker reflectance is interpreted to be fine sediment from the dredgings moving back into the channel. The outer channel has lighter reflectance indicating that the channel is deeper. Between the 1300 and 1800 m markers the channel has a large bend in it and fingers of darker reflections encroach into the channel.

Channel bathymetry was also surveyed with a Raytheon 719B Hydrographic Sounder, producing an analogue trace, in October 1995. Channel depths were at least 1.5 m below CD until midway between the 800 and 1300 m markers. Depths along the northern side of the channel were less than 0.5 m below CD along most the channel until midway between the 800 and 1300 m markers. A number of vessels reported groundings along the channel midway between the 800 and 1300 m markers to Pine Harbour Administration on 12/8/95, 13/8/95, 21/8/95, 26/9/95 and 28/9/95.

3.7.3 Discussion

The approach channel has infilled since dredging. In order to investigate further the interpretation of channel changes recorded by the hydrographic surveys, SCUBA diver observations were made on 27 September 1995 for the purpose of ascertaining the depth of silt deposited on the channel floor (Appendix 1.2). The channel floor was probed with a 1.5 m steel rod before encountering any firm sediment substrate underlying the fine silt.

This confirmed that a significant amount of fine sediment had infilled the approach channel.

The landward 1100 m of the approach channel suffered the most changes and appears to be more dynamic than the seaward half. The comparison of hydrographic survey data along channel cross sections between the four survey dates reveals patterns of channel infill and indicate that sediment infilled up to 1.0 m at the entrance to the marina basin in 9 months following 1994 dredging operation. Areas of infilling occurred along the channel edges, where sediment infilled up to 0.5 m. Specific areas of concern showing maximum infill are located at the marina entrance; between the second and third unlit starboard markers; and just beyond the 800 m marker. In these three locations sediment levels built up to reduce channel depths to levels experienced prior to dredging.

There are three possible sources of sediment infilling the approach channel to Pine Harbour Marina. The first is sediment transported from the south to the north over the intertidal flats by the littoral drift which become trapped in the deeper water of the approach channel. Sediments at the bottom of the channel require greater wave energy to entrain sediment into suspension for sediment transport than on the intertidal flats. Wave orbital velocities which entrain sediment decrease with depth. The effect of greater water depths in the channel means that higher wave orbital velocities at the bed are required to entrain sediment, and these are experienced infrequently over the channel.

The second source of fine sediment infilling the channel is the re-deposition of fine sediment from the dredgings mound back into the channel through resuspension and transport back into the channel or by geomechanical failure of dredgings sediment which may have slumped back down into the channel. Sediment levels on the intertidal flats to the north and south of the marina remained constant, although there was greater fluctuation in sediment levels at the immediate channel edges. The edges of the channel change more as they are affected by wave and current processes in the channel, the fact that they are not straight indicates some erosion and accretion occurs along these edges. Accretion of sediment along the northern edge of the channel was detected in hydrographic surveys.

A third possible source of sediment infilling the channel is silt and clay transported as suspension in the littoral system which are deposited by flocculation processes when fresh water, from marina drainage and local streams, interacts with high suspended load salt water.

Average accretion of 0.5 m of sediment along the northern edge of the channel for the 700 m section from the marina entrance to mid way between the 800 and 1300 m markers, equates to a volume of approximately 5250 m^3 of sediment infilling the channel within 9 months of dredging. This rate of channel accretion equates to 7000 m^3 per year, and is much faster than the rate of 3,000 m^3 estimated by Healy (1994) for this coastal sector. This can largely be attributed to the transport and slumping of dredged material back into the channel soon after deposition on the adjacent northern intertidal flats.

3.8 Monitoring profiles of dumped dredge material

3.8.1 Methodology

A series of north to south trending transects were established adjacent to the approach channel in December 1994. Survey lines 1 to 4 are located on the northern side of the channel, and lines 5 to 8 on the southern side (Figure 3.48). These lines were surveyed at monthly intervals from December 1994 to May 1995 to trace the erosion of the dredgings from the disposal site. Survey line 5 was not surveyed on subsequent surveys as it was often below the low tide level.

Surveys were undertaken using a surveyors level, staff and tripod between reference pegs marking the end points of the survey lines. Marker pegs were surveyed by Greenfield Surveyors Ltd for location relative to Mt Eden grid, and chart datum (CD) which is the lowest astronomical tide (Port of Auckland datum). Profiles show change in tidal flat elevation relative to CD.

3.8.2 Results

Figure 3.49 shows the profiles of dredgings on the northern intertidal flats. Along all profiles the maximum change in sediment levels were recorded at the channel edge, where the dredge mound eroded up to 0.3 m. Change in elevation of intertidal flats decreases with increasing distance from the channel, with accretion in the order of 0.05 to 0.1 m of sediment recorded at a distance 90 m north of the channel.

Figure 3.50 illustrates profiles along the southern intertidal flats which were surveyed to record the natural variation in intertidal flat elevation to compare with changes in sediment level over the dredgings. Like the northern side greatest change in surface level occurs at the channel edge. Profile 8 shows the most change with approximately 0.15 m of erosion at the channel edge where drainage channels have scoured into the intertidal flats. The sediment level fluctuates in the order of 0.05 m along the profiles, however this reduces with increasing distance from the channel and no net change in the elevation was detected along the outer survey lines 75 m from the channel.

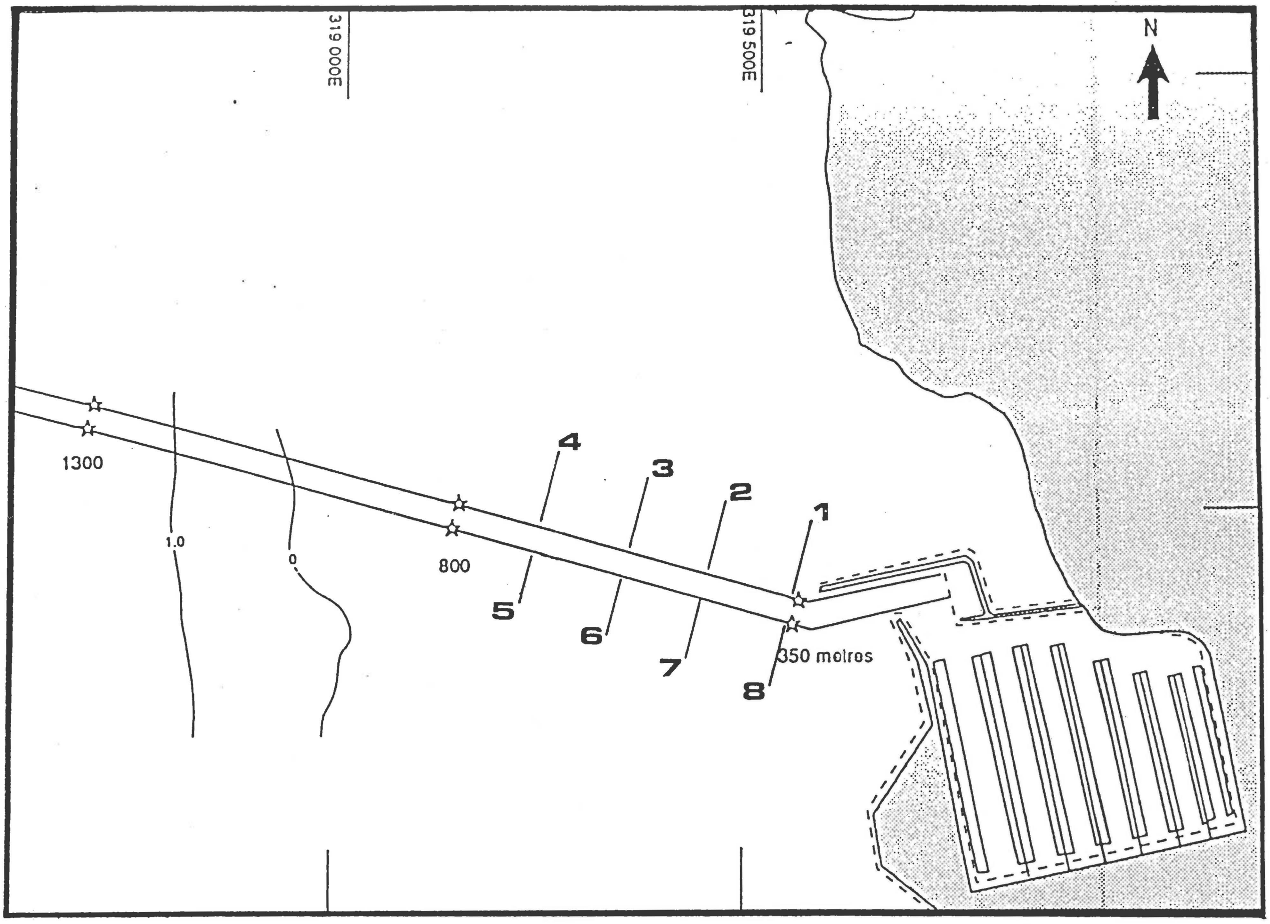

FIGURE 3.48: Location of profiles surveyed monthly, from December 1994 to May 1995, across the dredge mounds on the northern side of the approach channel and across natural intertidal flat sediments south of the marina approach channel.

3.8.3 Discussion

Monthly surveying of dredgings mound from December 1994 to May 1995 demonstrate net erosion of dredgings sediment. On the northern intertidal flat most erosion occurs near the edge of the channel where the dredgings mound was highest. The northern intertidal flats are eroded by up to 0.3 m at the channel edge presumably due to the consolidation and erosion of the dredgings mound. Erosion of dredgings increased with formation of drainage channels scouring the intertidal flats with ebbing tide over time (Plate 3.7). These drainage channels also accommodate rainfall runoff from the intertidal flats at low tide.

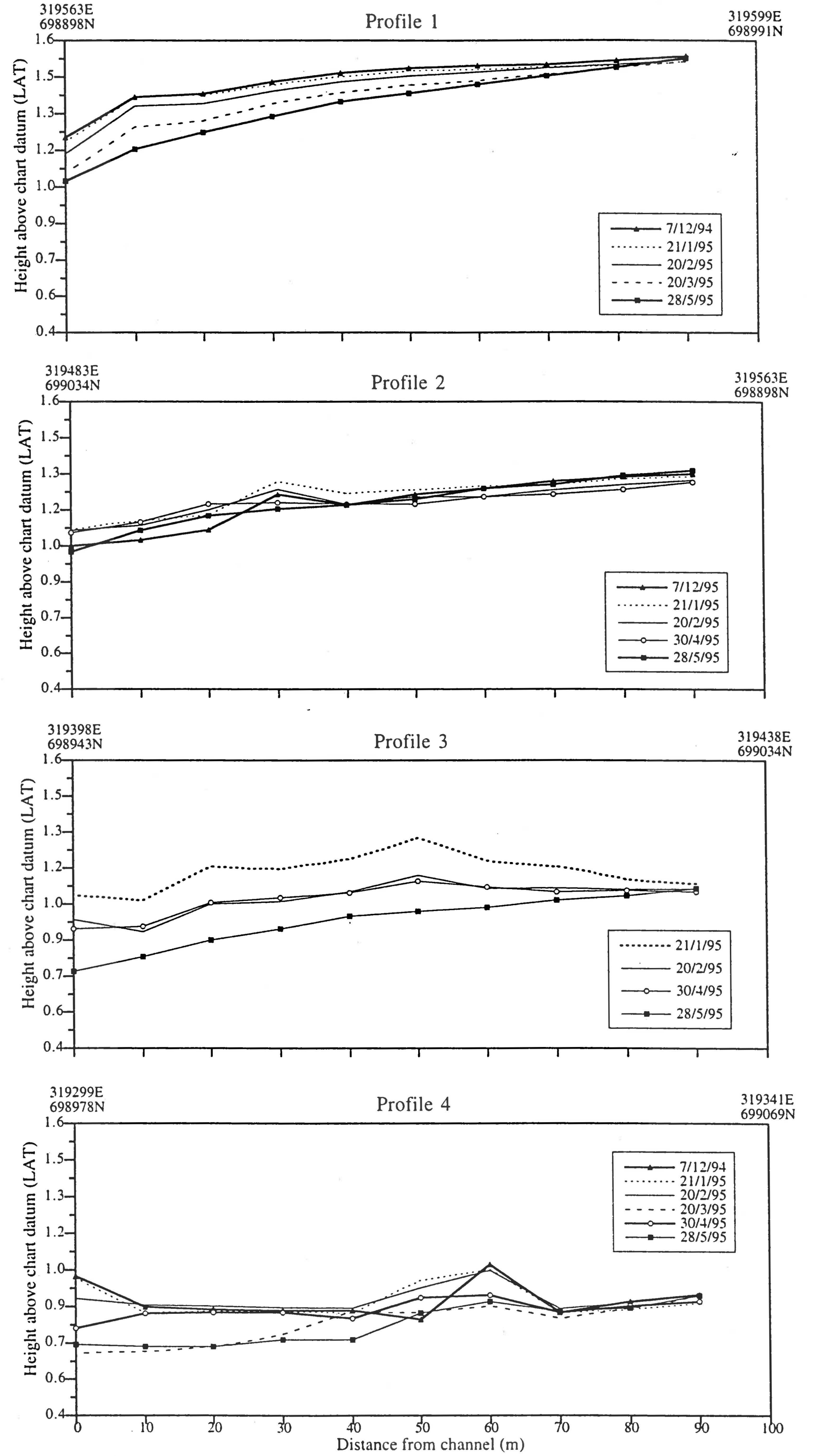

FIGURE 3.49: Profiles over the dumped dredge material on intertidal flats north of the approach channel to Pine Harbour Marina, December 1994 to May 1995.

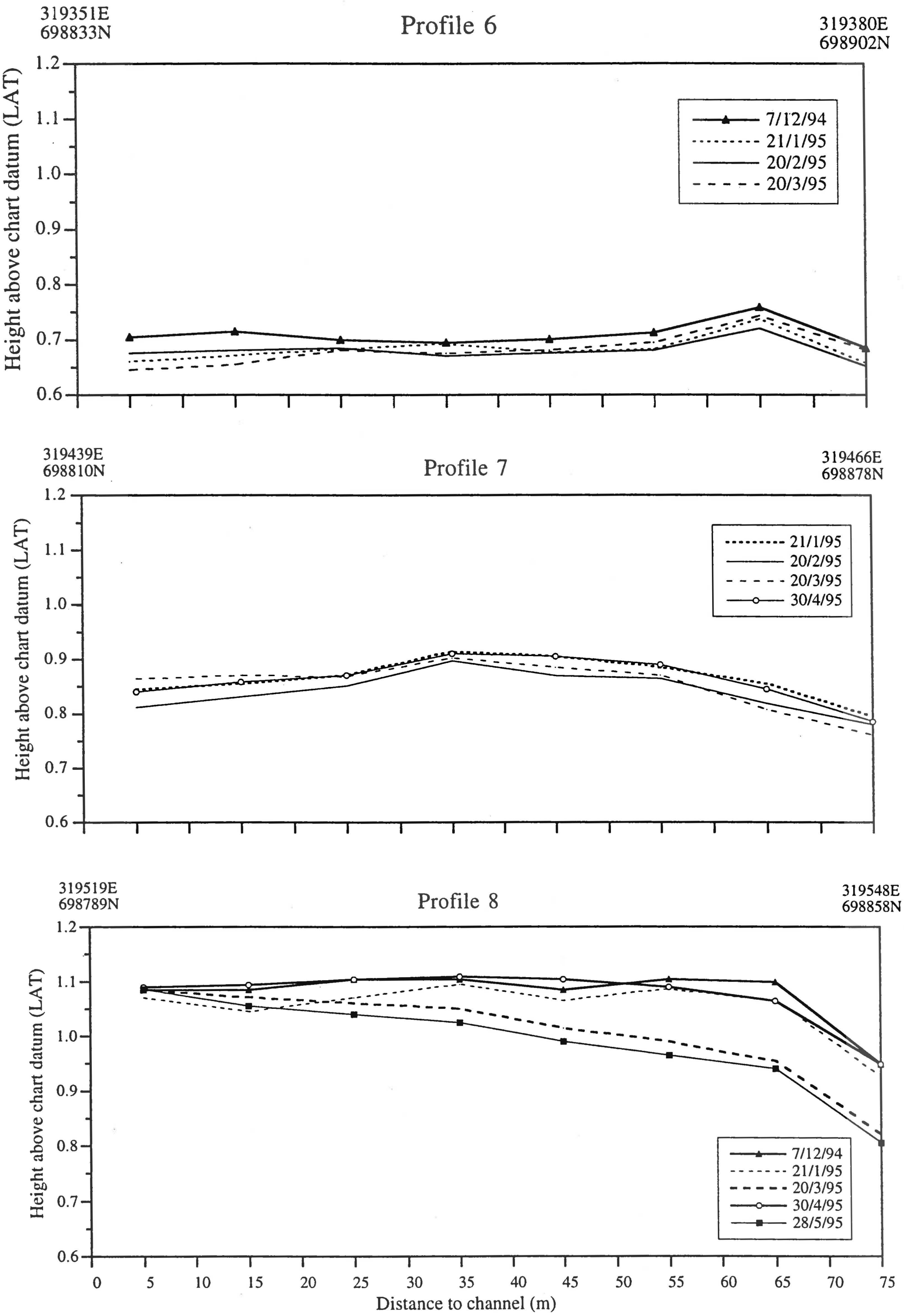

FIGURE 3.50: Surveyed profiles of intertidal flats on south side of the approach channel to Pine Harbour Marina, December 1994 to May 1995.

Plate 3.7: Drainage channels scoured into intertidal flats and dredgings mound on northern side of approach channel.

The dredgings mound dissipated over time but it is difficult to interpret any net migration of the mound. They seem to consolidate and fine material becomes washed out rather than the mound moving across the intertidal flats as a coherent unit. Thus while the data show clearly that the dredgings mound is decreasing in height it is difficult to detect the direction of sediment dispersal. Consolidation of dredgings involves the restructuring and packing of sediment grains in the dredgings and the expulsion of water between grains. Some fine sediment from the dredgings will have been entrained by wave processes and transported with the net current from the dredgings mound. A build up of approximately 0.05 m of sediment north of the dredgings in May 1995 indicates that sediment has dispersed as a veneer over the intertidal flats to the north. Some sediment from the dredgings mound was also transported south, back into the channel. This finding is supported by the observation of greatest erosion occurring at the channel edge, but without corresponding build up of sediment to the north of the mound. Further from the channel, sediment accretion of approximately 0.05 m is recorded at 90 m distance, representing dispersion of some of the dredged material.

3.9 Chapter summary

- Sediment grain size is similar over most of the intertidal flats, with mean grain size of surficial sediment between 2.5 and 3.0 Ø (fine sand). Beach sediments are generally coarser, and finer sediment occurs near the head of the inlet and offshore. Subtidal and channel sediments are comprised of at least 75 % silt and clay. Mean grain size of the dredgings is finer than 3.0 Ø (very fine sand). Across most of the intertidal flats sediment is negatively skewed and most sediment is moderately to moderately well sorted.

- Dredgings sediment was comprised 84 % silt and clay, and 16 % sand with minor amounts gravel fragments. Bulk density of the dredgings sediment was less than the intertidal flat sediments, and moisture content of dredgings was generally higher than sand on the intertidal flat. SEM examination of dredgings sediment revealed the sediment structure is largely controlled by clay minerals and fine silts which mask sediment grain surfaces. The masking of grains with clay minerals increases sediment threshold velocities for entrainment by increasing the cohesiveness of the sediment and encouraging grain to grain binding.

- Clay mineralogy analysis with XRD revealed that sediments from the dredgings and along the Beachlands coast were comprised of similar clay minerals, predominantly poorly crystalline smectite, kaolinite, and undifferentiated mixed layer clays which are derived from the local geology and indicate that sediments originate from weathering of Waitemata Formation. This implies that sediments infilling the approach channel to Pine Harbour Marina originate from northbound turbid plumes, and that sediment infilling the channel does not originate from the north. Likewise muddy sediment occasionally deposited on Sunkist Bay is likely to originate from these turbid plumes, or from onshore movement of fine subtidal sediments under strong northerly winds.

- Suspended sediment levels were increased locally due to the dredging operation at Pine Harbour Marina, however levels did not exceed "trigger" levels imposed by the Auckland Regional Council. During dredging local turbidity levels were between 9-26 NTU, increasing up to 72 NTU in turbid plumes immediately adjacent to the dredge barge. Increased levels of suspended sediment are caused by the fine sediment resuspension during excavation and deposition of dredgings sediment through the water column. During the dredging operation natural processes of wind, waves and tides also agitated bed sediments and increased local turbidity levels, on occasion turbidity at the control site was greater than turbidity generated by the barge.

- In comparison background turbidity levels ranged from 5-45 NTU and were greatest near the marina basin and near streams discharging into the marine environment. Average turbidity along the Beachlands coastline was less than 10 NTU. Greatest variation in turbidity was from water samples collected in the marina approach channel and basin and near Waikopua Creek. Turbidity at these sites increased up to 40-45 NTU on occasion due to a combination of factors including periods of rainfall, high wind speed and large waves, and stage of tidal current.

- Suspended solids ranged from 5-75 mg/l over most of the littoral zone, and were highest near streams reaching up to 100 and 200 mg/l towards Te Puru Stream. Average suspended solid concentrations along the littoral zone from Waikopua Creek to Te Puru Stream were between 15 and 50 mg/l. Variation in suspended solids concentrations of most samples was in the order of 10-20 mg/l, however the greatest fluctuations in suspended sediment concentrations were detected near Waikopua and Te Puru Streams, and in the marina basin which may reflect the component of organic matter eroded from the catchment which varies with the amount of rainfall in the catchment and volume of freshwater delivered to the marine environment.

- Overall turbidity is dependent on weather conditions and tide. Local wind generated waves entrain sediment in the shallow water depths along the coastline and the embayment. The turbid plumes are in turn transported along the coastline by the net current which is related to tide and wind driven circulation patterns.

- Sedimentation rods indicate that sediment depths of disturbance (DOD) or sediment mixing varies over the intertidal flats. For most of the measurement period DOD was less than 1.0-1.5 cm, this shallow depth of mixing is attributed to frequent ripple movement over the intertidal flat surface and is similar to DOD in other fetch limited environments (e.g. Dolphin *et al.* 1995). Depth of disturbance between 2.0-3.0 cm is associated with storm conditions and increased wave energy. Greatest depth of sediment mixing was 6.2 cm after a period of high wind speeds over the region. Sedimentation rods located north of the approach channel had greater DOD than rods located south of the approach channel. This suggests that wave processes acting over the intertidal flats are varied, and that the northern side of the approach channel is more exposed to extreme wave conditions from the north-west, which have the potential to disturb sediment to greater depths. The sedimentation rods located further offshore recorded deeper depth of disturbance due to the longer exposure of the lower tidal region to wave processes and larger wave heights in the deeper water resulting in greater sediment activation.

- Greater depth of disturbance did not correspond to significant changes in net sediment level due to erosion or accretion. Overall there was minimal accretion of approximately 1.0 cm at sedimentation rods along the northern intertidal flats, with less change at sedimentation rods along southern intertidal flats where change in sediment level was slightly erosive. The addition of dredgings sediment into the littoral system may account for the small amount of net accretion on the northern side. However local scour effects are likely to have removed some sediment from the base of the sediment rods along both the northern and southern intertidal flats, and so net changes in sediment level are not an accurate indication of the amount of accretion and erosion occurring on the intertidal flats.

- Intertidal beach surveys indicate that an average of approximately 0.025 m of sediment accreted over the mid tide region on the northern intertidal flats. This equates to 2100 m^3 of sediment which is approximately half of the dredgings material reintroduced to the littoral system downdrift of the approach channel. Thus, approximately half of the dredgings material is assumed to have been dispersed over the northern intertidal flats. The remainder of the dredgings material is assumed to have been carried off in suspension or redeposited back into the approach channel. The latter is the most probable destination of the majority of the dredgings material as hydrographic surveys recorded channel infilling in the 9 months since the 1994 dredging, and diver observation of channel sediments revealed at least 1.5 m of silt sized sediment on the channel floor.

- Monthly surveys of profiles either side of the channel showed greatest change in sediment levels at the edge of the channel. The dredgings mound eroded up to 0.3 m over the 6 month period of surveying at the channel edge. The mound consolidated and some dredgings sediment was entrained into suspension and dispersed over the intertidal flat to the north, resulting in approximately 0.05 m of sediment accretion 90 m from the channel. Not all dredgings material eroded is accounted for by the small amount of accretion to the north of the dredgings mound. Greater sediment erosion a the channel edge is caused by constant exposure to wave energy and additional effects of vessel wake. In addition the formation of small drainage channels from the intertidal flats eroded the dredgings material and transported some sediment back into the approach channel. Therefore it is inferred that most of the dredgings sediment was redeposited into the marina approach channel. Subsequently in 1995 the dredge mound essentially disappeared except for remnant boulders of bedrock remaining at the dumpsite. This feature is discussed in Chapter 5.

- A series of hydrographic surveys of the approach channel to Pine Harbour Marina revealed that the channel infilled with sediment since dredging in 1994. The landward 1100 m of the approach channel suffered the most sediment deposition. Specific areas of concern that infilled the most rapidly are located at the marina entrance, between the second and third unlit starboard markers, and just beyond the 800 m marker. In these three locations sediment levels built up to reduce water depths to that prevailing prior to dredging.

- In the 9 months following dredging an average of at least 0.5 m of sediment accretion occurred along the northern edge of the channel over the 700 m section of channel from the entrance of the marina basin to midway between the 800 and 1300 m markers which is equal to a volume of approximately 5250 m^3 of sediment infilling the channel. This rate of infilling equates to 7,000 m^3 per year which is much higher than expected and can be attributed to 3 possible sources. These include sediment transported by the littoral drift from the south which is trapped in the approach channel as it interrupts the littoral system, or deposition of flocculated particles as freshwater draining from the marina compound and local streams interacts with the high suspended load salt water. The third and most likely source of much of the sediment infilling the approach channel is dredgings sediment which was deposited along the adjacent northern intertidal flats that has been re-suspended and transported back into the channel under north-westerly wind conditions or with drainage off the intertidal flats, or dredgings sediment has slumped back into the channel due to geomechanical failure. The path of sediment dispersion over the intertidal flats is investigated by the sediment tracing experiment discussed in Chapter 5.

CHAPTER FOUR
THE FORCING PROCESSES: TIDES, CURRENTS, WAVES & WINDS

4.1 Introduction

To examine hydrodynamic processes in the embayment between Howick and Beachlands Point affecting the intertidal flats and approach channel fronting Pine Harbour Marina, InterOcean S4, S4DW and S4ADW vector averaging current meters were deployed in the subtidal region adjacent to the channel (Table 4.1 and Figure 4.1). Current meters were moored on a stainless steel rod 1 m above the bed on a bottom mounted concrete block.

TABLE 4.1: Instrument deployments for tide, current, wave and wind data collection.

Deployment period	Instrument	Location	Measured	Cycle
17/6/94-27/7/94	S4DW*	Site 2	X & Y velocity Pressure	0.5 s interval 1 min burst every 10 min.
7/10/94-9/11/94	S4ADW	Site 2	X & Y velocity Pressure	3 min burst every 3 hours
23/11/94-20/12/94	S4ADW	Site 1	X & Y velocity Pressure	3 min burst every 3 hours
17/6/94-27/7/94	S4	Site 1	X & Y velocity Conductivity Temperature	0.5 s interval 1 min burst every 10 min.
11/10/94-9/11/94	S4	Site 1	X & Y velocity Conductivity Temperature	0.5 s interval 1 min burst every 10 min.
20/12/94-29/12/94	S4	Site 1	X & Y velocity	3 min burst every 2 hours
23/11/94-17/1/95	Wind anemometer	Site 3	Wind speed Wind direction	10 min average
10/12/94-20/12/94	Tide gauge	Site 4	Water level	10 min average
Permanent fixture	Stageboard	Site 5	Water level	

* denotes deployments which failed to record data due to memory problems.

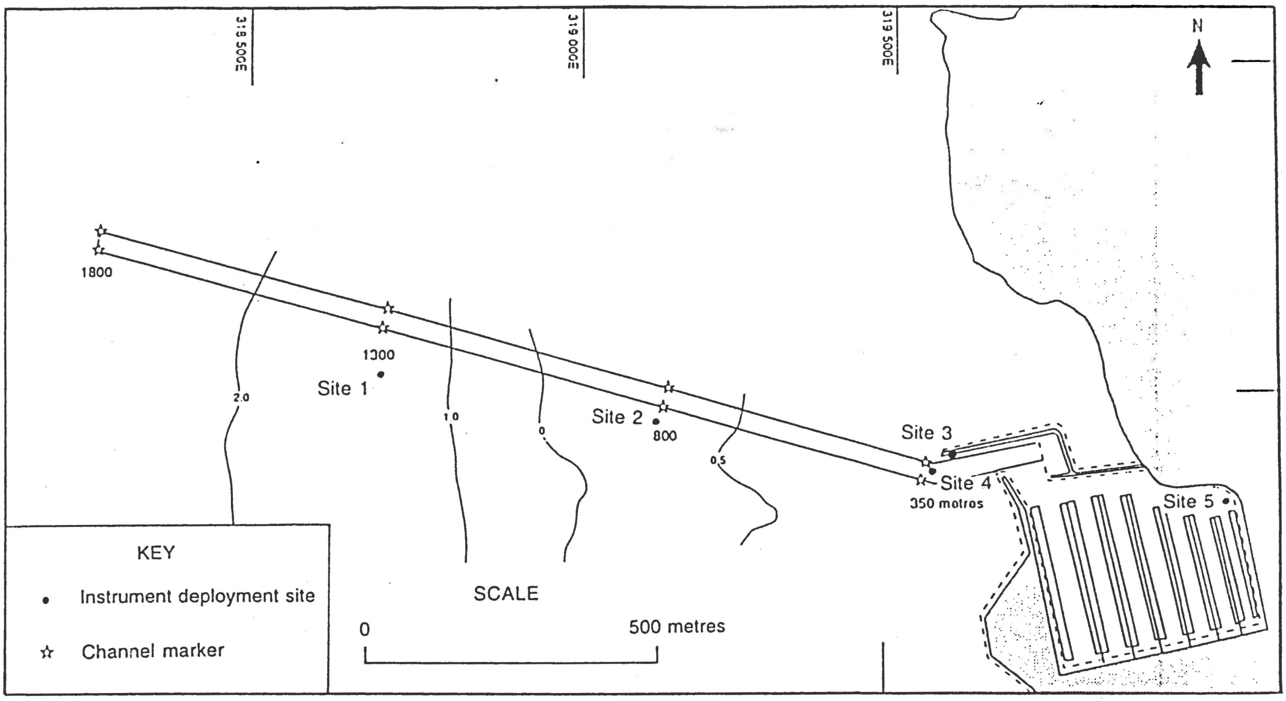

FIGURE 4.1: Location of deployment sites of instruments recording tide, current, wave and wind data at Pine Harbour Marina.

4.2 Tidal regime

A tide gauge recorded pressure every 10 minutes for ten days, from 10/12/94 to 20/12/94, at Site 4 (Figure 4.1). These data were adjusted to chart datum (CD) using the Pine Harbour Marina stageboard (Site 5) which was surveyed relative to Port of Auckland lowest astronomical tide (LAT). There is an error due to the accuracy of the person reading the tide level. The time lag between the tide gauge and stageboard may also affect calibration, but because the two stations are close (500 m) it was assumed that the time lag was negligible. Tide gauge data were reduced by 1.0522 m to CD (Figure 4.2). Mean sea level at Pine Harbour Marina was determined to be 1.762 m above CD.

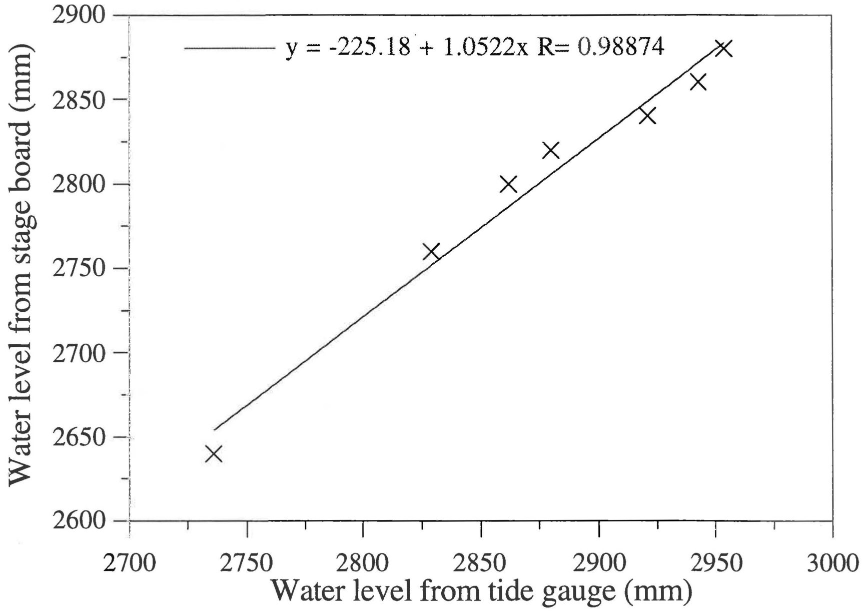

FIGURE 4.2: Calibration of tide gauge to CD with Pine Harbour Marina Stageboard.

4.2.1 Tidal analysis

Tidal amplitudes and phases were extracted with THANAL, a tidal analysis program which takes data files from InterOcean S4 current meter or similar data files, and derives tidal constituents by least squares best fit harmonic analysis (de Lange *et al.,* 1993). Tidal constituents are normally fitted to depth (pressure) and velocity data. THANAL creates an output file which consists of the period, frequency, amplitude and phase of approximately 63 tidal components. Tidal heights were predicted for Pine Harbour Marina by THPRED, a tidal prediction program which takes files of tidal constituents and predicts tidal values for specified time intervals.

Pine Harbour Marina is located in a meso-tidal embayment with maximum spring tidal range of 3.20 m (Figure 4.3). Tides at Pine Harbour Marina are semi-diurnal. Highest tidal elevation (relative to CD) varies from 3.40 m at spring high tide to 2.65 m at neap high tide. Low tide varies from 0.20 m at spring tide to 1.00 m during neap tide.

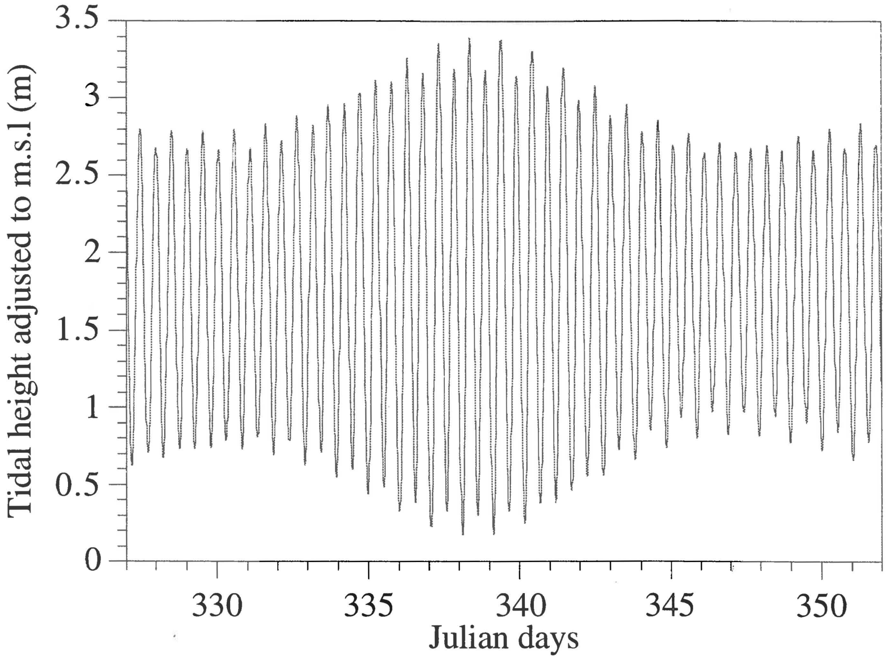

FIGURE 4.3: Tide curve predicted by THPRED at Pine Harbour Marina from 23/11/94 to 20/12/94.

4.3 Currents

4.3.1 Current data analysis

Current data were analysed using S4 Application Software (APP) to retrieve data from the S4 and to convert it to ASCII format. S4REFORM, current meter calibration program, was used to convert S4 data into standard calibrated S4 data file format generated by APP (de Lange *et al.,* 1993). Figure 4.4 illustrates the processing of S4 and S4ADW InterOcean current meter data.

Residual analysis of U and V velocity data is undertaken using THRESI, a tidal residual analysis program which removes the predicted tidal values from the measured data to determine the tidal residuals. Tidal residuals are currents that are not tidally induced, i.e. wind generated, or storm surge etc. (de Lange *et al.,* 1993). THRESI outputs vector data consisting of the speed, direction and x and y velocities for each of the measured, predicted and residual currents.

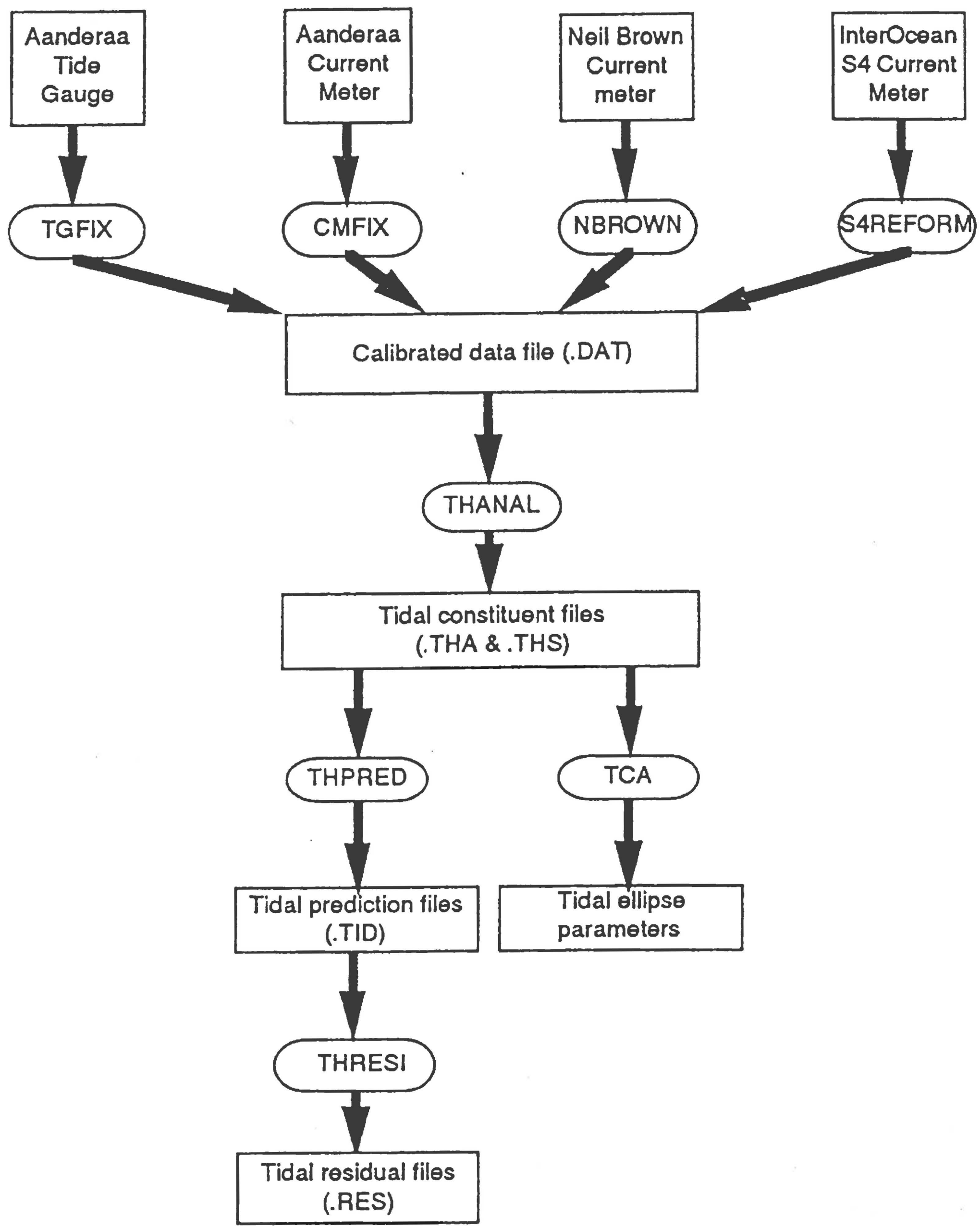

FIGURE 4.4: Flowchart of the programs used for tidal data reduction and analysis (de Lange et al., 1993).

Ideally residual current analysis is undertaken on data records of at least 39 days to remove most tidal constituents. Tidal constituents with a periodicity of more than 39 days are insignificant. The data set for Pine Harbour Marina covered a period of 28 days, and while THRESI has removed most of the tidal components a longer period would have allowed the filtering of more tidal constituents from the residual current. Data and time constraints did not allow for the extension of the initial data file from 28 days, and it was assumed that the improvement to the residual data would have been minor (W. de Lange, pers. comm.).

The U and V current vectors at Site 1 (Figure 4.5) from 23/11/94 to 20/12/94 are skewed in an elliptical shape around the central point (0,0), indicating that the currents at this site are essentially tidal although the skewness indicates that some non-tidal processes also drive currents in the region. These are thought to be local wind driven circulation and wave induced currents. Ocean currents are excluded, as an investigation into the residual circulation in Hauraki Gulf undertaken by Proctor & Greig (1989) concluded circulation from the intrusion of the East Auckland Current and wind generated flows from the shelf into the Gulf does not reach the southern end of Hauraki gulf past northern Waiheke Island.

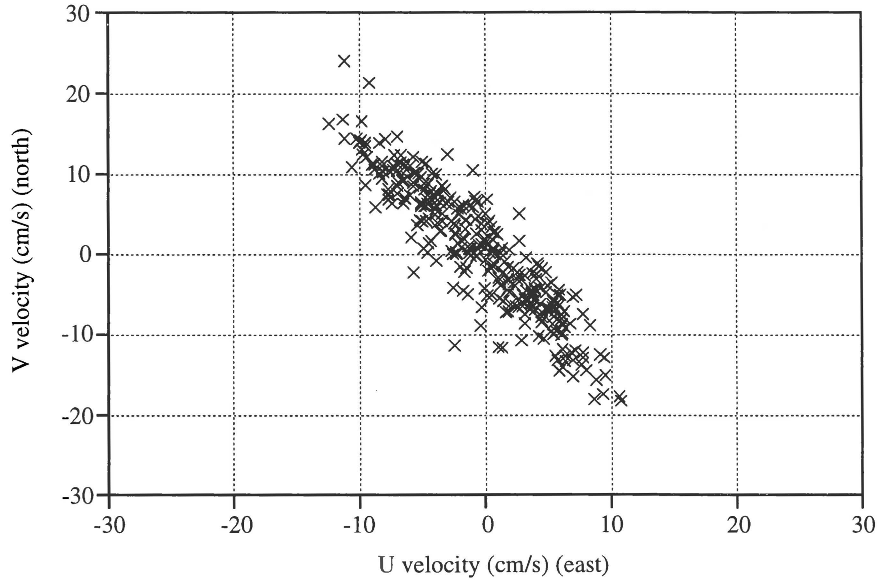

FIGURE 4.5: U and V vector plot of current speeds.

Current speeds, averaged over 3 minute bursts, at Site 1 for the period 20/12/94 to 29/12/94 fluctuate with ebb and flood tidal currents at speeds less than 25 cm/s (Figure 4.6). Current speeds are increased with increased wind speeds. Peak current velocities up to 75 cm/s were measured by the S4 InterOcean current meter on 22/12/94/ These occur at the same time increased wind speeds were measured at Pine Harbour Marina (Figure 4.7).

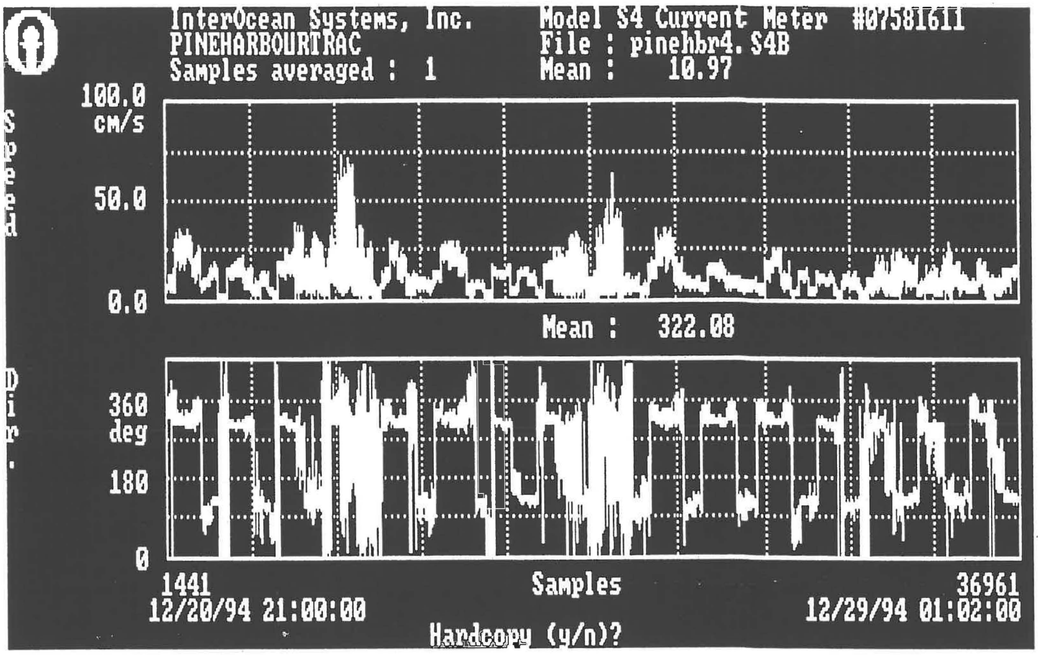

FIGURE 4.6: Three minute burst averages of current speeds at Site 1 from 20/12/94 to 29/12/94.

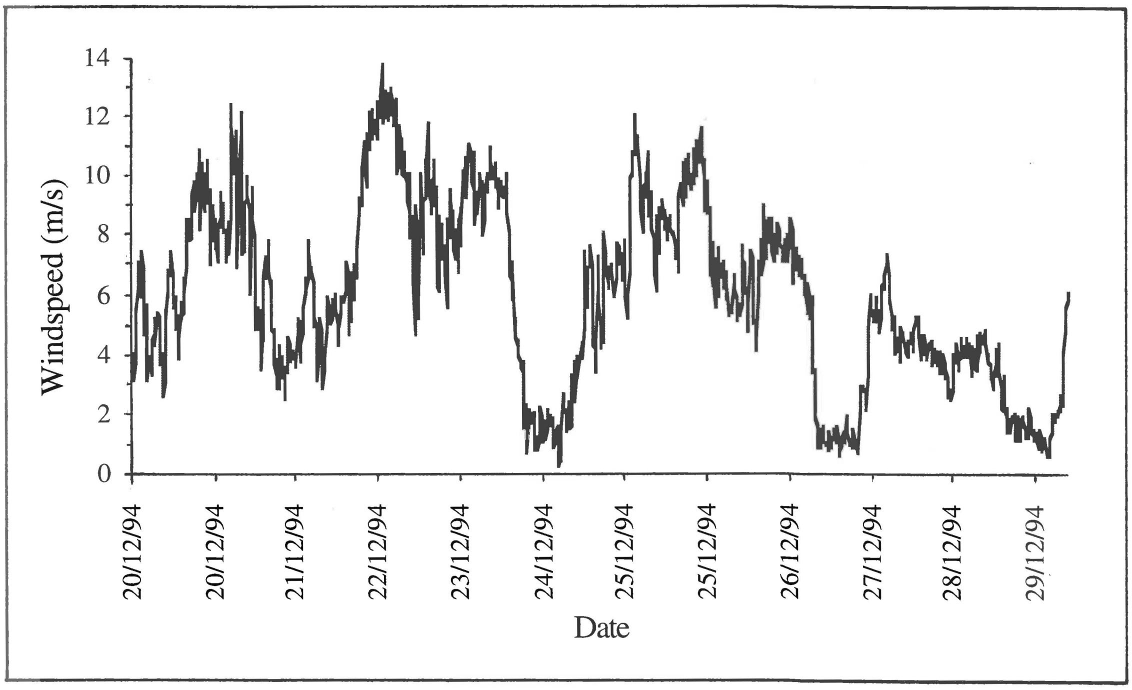

FIGURE 4.7: Wind speeds recorded at Pine Harbour Marina from 20/12/94 to 29/12/94.

4.3.2 Tidal currents

Measured, predicted and residual current speeds at Site 1 for the period from 23/11/94 to 20/12/94 indicate that predicted tidal currents are weak, generally less than 15 cm/s (Figure 4.8). Residual (non-tidal) currents, due to onshore and offshore winds, also have low velocities generally less than 10 cm/s, but occasionally reach up to 15 cm/s.

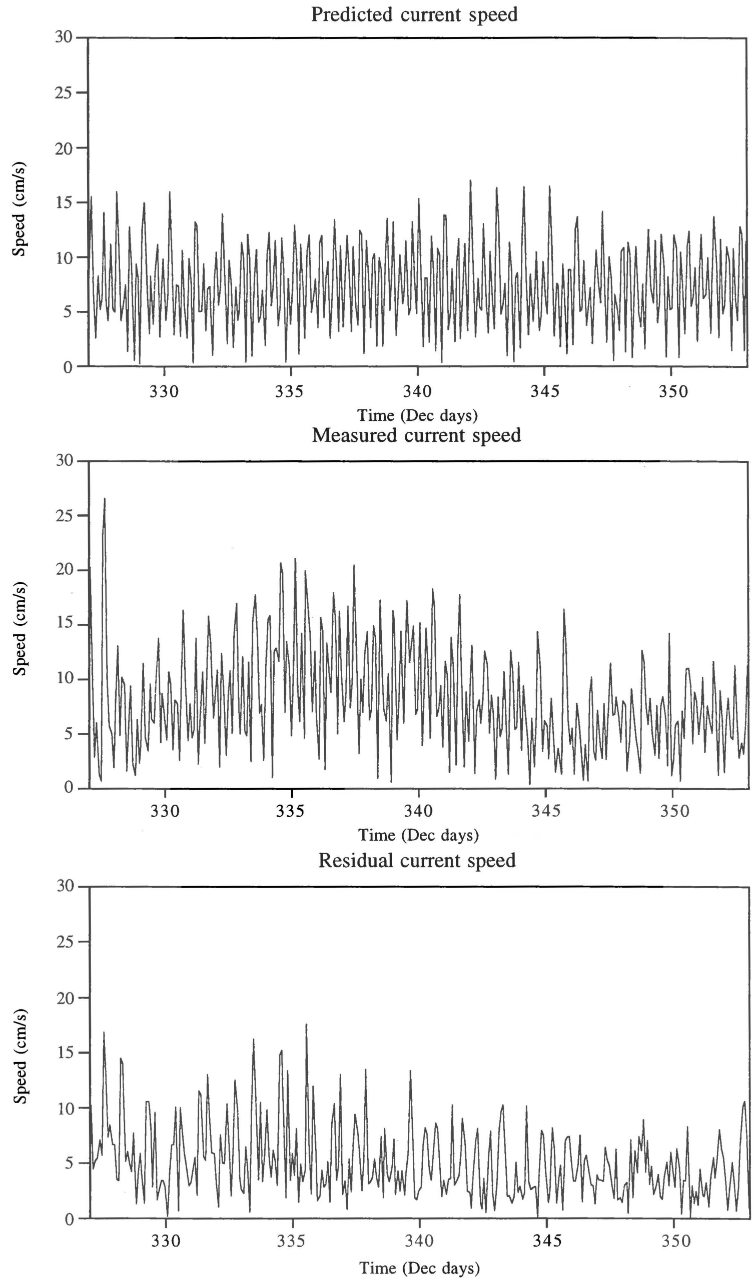

FIGURE 4.8: Predicted, measured and residual current speeds at Site 1 from 23/11/94 to 20/12/94.

Analysis of predicted currents over a tidal cycle indicate that highest tidal current velocities occur at mid tide (Figure 4.9). Current measurements at Site 1 indicate that flood tidal currents are directed towards the south and south-east, while the ebb tide flows out of the embayment towards the north-west (Figure 4.10). North-westerly directed currents are stronger than south-easterly currents, reaching a maximum velocity of 17 cm/s between 23/11/94 to 20/12/94.

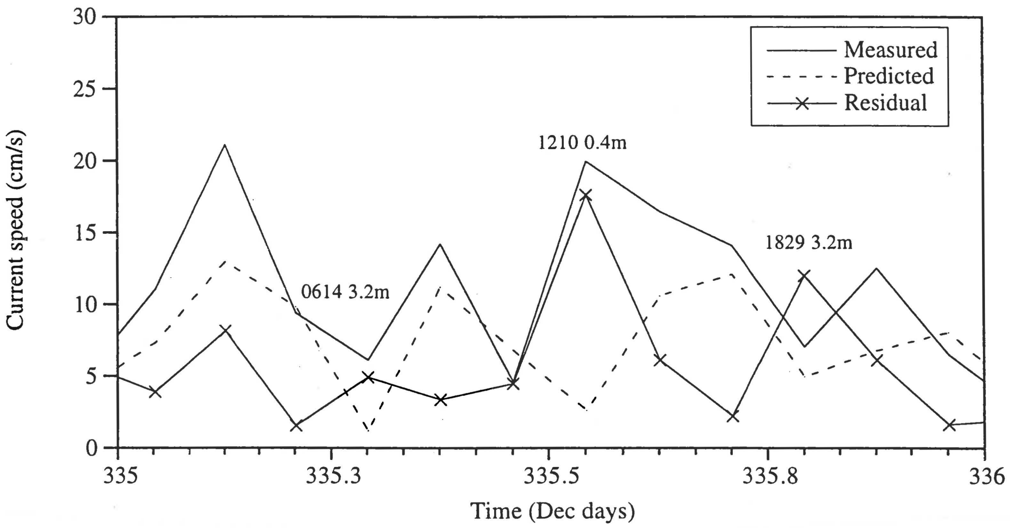

FIGURE 4.9: Measured, predicted and residual current velocities for 2/12/94.

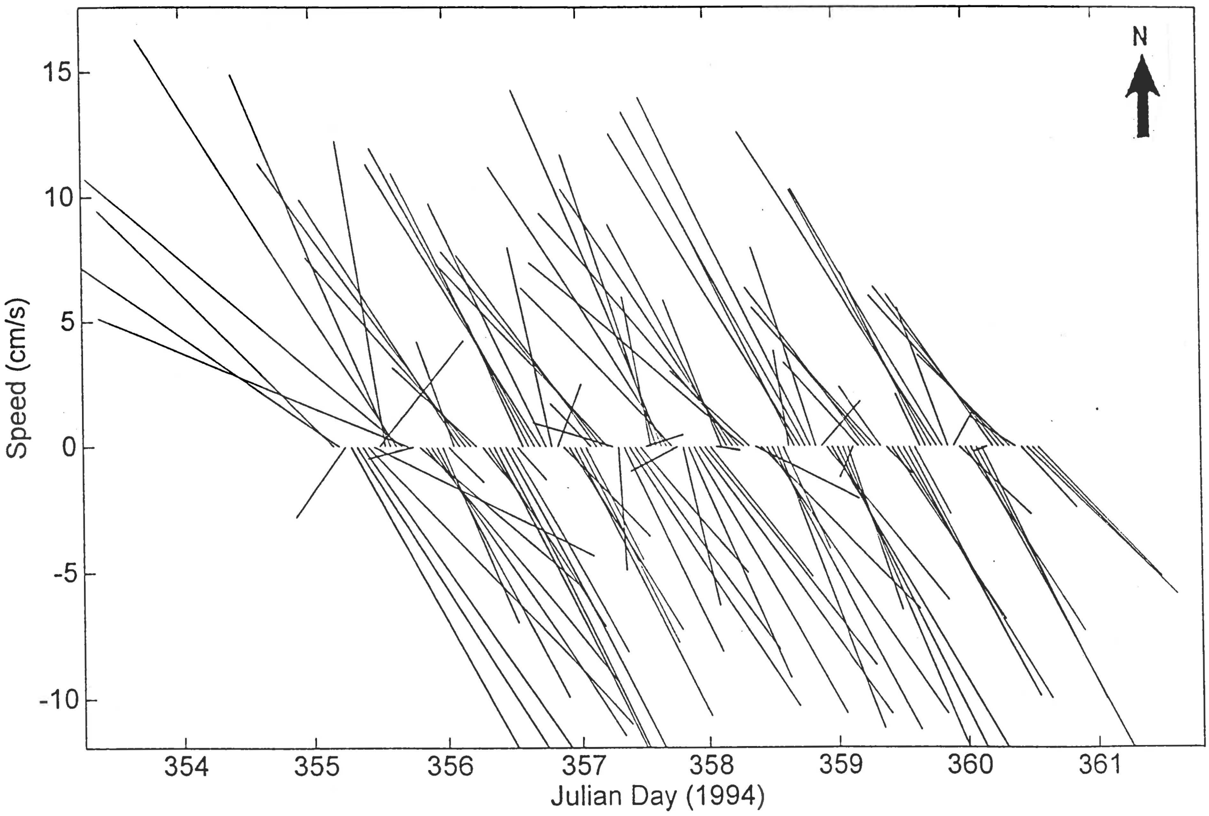

FIGURE 4.10: Vector plot of tidal current from 23/11/94 to 20/12/94.

No current measurements were made on the intertidal flats because of the risk associated with the exposure of the current meter on the intertidal flat at low tide and risk of interference with the instrument. As such, generalisations of current activity over the intertidal flats can only be proposed. Current velocities and directions over the intertidal flats will be different from those recorded at Site 1 as different processes are important over the shallower sandflats. Currents over the intertidal flats are assumed to be weak and dominated by tidal forces due to the low wave energy in the environment (Figure 4.19). From observations over the intertidal flats it appeared as though there was a progressive turning of flow as water rises and falls over the intertidal flats due to the effect of the channel and the coastline. The flood tide is directed onshore towards the east onto the intertidal flats after entering the embayment from the north-west. The ebb tide drains from the intertidal flats towards the west, and there was some evidence of drainage from the northern intertidal flats towards the south-west into the channel, by the scouring of small drainage channels alongside the channel. Tidal currents are inferred to be stronger over the mid to low tide intertidal flat than in the near shore where tidal currents are small and short lived due to the limited duration of coverage by the tide.

Currents measurements were not made in the approach channel to Pine Harbour Marina. It is assumed that channel currents are dominated by the tide and flow east and west with the flood and ebb tidal cycle. At low tide current direction is determined by channel orientation which is aligned east to west through the intertidal flats. During the early stages of the flood tide currents will be directed onshore towards the marina basin. At later stages in the flood tide the direction may be directed alongshore towards the south-east as water depths increase over the adjacent intertidal flats. The opposite situation is thought to occur during the ebbing tide, until in the later stages of the ebb tide currents are directed offshore. Greatest current velocities are presumed to occur at mid tide. However these currents in the channel are assumed to be weak, and insufficient to entrain silt sized sediment (0.03 mm) at the bottom of the channel. Thus sediment which settles in the approach channel is rarely entrained into suspension and remains trapped in the deeper water.

4.3.3 Wave induced currents

Residual currents at Site 1, from 23/11/94 to 20/12/94, fluctuate with some periodicity which indicates that tidal constituents have not been completely filtered from measured currents (Figure 4.9). This periodicity may be produced by a longer period tidal component affecting the region that was not filtered from the 28 days of data input into THRESI. Residual currents are inferred to be local wave induced currents driven by wind stress, and are therefore episodic fluctuating after a slight lag period following changing wind speeds. Figure 4.11 presents the residual current velocities and wind speeds from 23/11/94 to 20/12/94. At some high wind speeds residual currents are not as high as would be expected, this may be due to restricted fetch at low tide reducing the coverage of the intertidal flats thereby limiting wave heights, or tidal currents flowing in the opposite direction may reduce wave heights and retard residual currents.

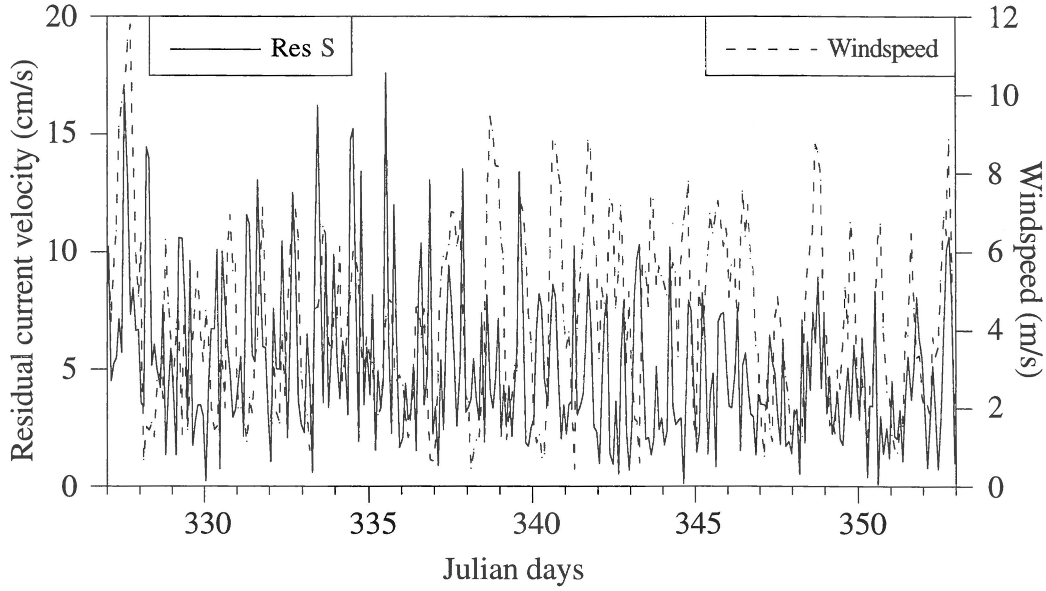

FIGURE 4.11: Residual current velocities measured at Site 1 and wind speed from 23/11/94 to 20/12/94.

4.3.4 Wind driven circulation

In relatively shallow depths, the water responds rapidly to wind stress and there is a strong tendency for the surface currents to be aligned with the wind direction (Nierododa & Swift, 1991). Proctor & Greig (1989) showed that wind stress is an important mechanism for generation of longshore currents in the Hauraki Gulf, and that surface currents are mainly in the direction of the wind but are modified by topographic features.

At Pine Harbour Marina wind from the south-west creates wind stress in the embayment and over the intertidal flats fronting Pine Harbour Marina, producing a longshore current towards the north. In contrast wind from the west produces onshore currents that are turned towards the south by Motukaraka Island and the chenier shell ridge which extends across the northern intertidal flats.

4.4 Wave regime

Waves are said to be fetch limited if the land limits the full development of the wave field or if the distance over which the wind blows controls the maximum development of the waves (Komar, 1976). The formation of waves in fetch limited environments is dependent on wind speeds, fetch lengths and the duration of wind speeds. Fetch length varies with wind direction and stage of the tidal cycle. The prevailing south-westerly wind direction at Pine Harbour Marina has a restricted fetch of approximately 4 km which is reduced at low tide when there is less horizontal coverage of water over the region (Figure 4.12). Maximum fetch of approximately 10 km is towards the north-west. Largest waves are generated when high wind speeds and increased wave energy coincide with high tide when fetch is greatest.

Throughout the tidal cycle fetch length is continually changing. At high tide fetch from the south is 4 km which is reduced to 2 km at low tide. Conditions for generation of large waves (height) are most favourable during spring tides when water depth is significantly greater than during neap tides. Tide plays a major role in regulating water depth on the intertidal flats where water depths vary from 0 to 2.5 m. Water depths at high tide may remain at elevated levels for longer periods due to a number of processes. During storms wind wave set up and decreased atmospheric pressure further increase water depth and duration near high tides. Across the shallow slope of intertidal flats, any decreases in atmospheric pressure and corresponding increases in water elevation result in a far greater horizontal coverage of the intertidal flats.

4.4.1 Shallow water wave effects

4.4.1.1 Bottom friction

Waves lose energy through bottom friction and turbulence as water under waves interacts with bed sediment, and there is some frictional drag at the water and sediment interface which slows the flow of water over the bed. The boundary layer influenced by the friction extends upwards towards the surface of the water. In shallow water the boundary layer can occupy the whole water depth (Neilsen, 1992). Increased bottom friction slows the wave and can hasten wave attenuation (Mei, 1989).

Waves propagate from Tamaki Strait into the embayment enclosed by Howick and Beachlands Points. Waves begin to feel the frictional effects of the seabed in shallower water depths, however the subtidal region is dominated by silt sized sediment so bottom friction is minimal. The effects of bottom friction may increase as waves travel over the relatively coarser sediment on the intertidal flats (Figure 3.2 in Chapter 3).

4.4.1.2 Wave shoaling and breaking

As waves approach shallow water some frictional drag at the sea bed causes waves to become steeper, and wave heights to increase until at a certain location the wave breaks due to it becoming unstable in shallow water depths. The wave-breaking will typically take place when the wave height is about 0.8 times the local water depth (Fredsoe & Deigaard, 1992). The forward wave orbital velocity at the crest becomes large, and the crest topples because it is unstable. The wave shoaling process is characterised by a very small energy loss but the wave expends a large amount of energy upon breaking. Wave energy is dissipated in the turbulence at the surf zone, and wave heights decrease towards the shore in the surf zone (Fredsoe & Deigaard, 1992).

At Pine Harbour Marina waves from Tamaki Strait begin to shoal as they encounter the shallow water depths in the embayment. Most waves will have broken and reformed by the time they reach the intertidal flats. Water depths over the intertidal flats vary at different stages of the tide, and with this variation the region where wave shoaling occurs also changes as wave height is a function of water depth. As waves break and reform to break again, they dissipate decreasing amounts of energy across the intertidal flat. The location of breaking waves will vary as water depth changes with tides. Entrainment of sediment will be significant under the larger breaking waves.

4.4.1.3 Wave reflection

As a wave breaks, the energy it received from the wind is dissipated. Some energy is reflected back out to sea, the amount depending upon the slope of the beach, the shallower the angle of the beach slope, the less energy is reflected (Wright & Short, 1983). Waves are also reflected when they encounter vertical barriers such as seawalls, jetties, or other similar structures and are reflected with little energy loss.

The northern and western breakwaters protecting Pine Harbour Marina basin are constructed from basalt rock which reflect some wave energy across the intertidal flats at high tide. The breakwaters are constructed of large boulders which allow the percolation of water and dissipation of wave energy into the barrier while reflecting some energy back onto the intertidal flats. Oscillatory currents of reflected waves will increase turbulence and enhance entrainment of particles for a limited period of time. Waves only encounter the northern and western breakwaters at high tide, and reflection of wave energy would occur for a short and insignificant period of time.

Effects of wave reflection around Pine Harbour Marina are assumed to be negligible because of the shallow gradient of the intertidal flats (Figure 3.18 in Chapter 3). Reflection of low energy waves, which dominate the wave climate (Figure 4.19), is assumed to be insignificant and large infrequent storm waves will only be reflected from breakwaters at high tide.

4.4.1.4 Wave refraction

Depth changes effect wave energy and height such that the direction of wave propagation is influenced by changes in water depth and wave crests parallel depth contours. Changes in bottom topography, or obstacles the wave train encounters, cause wave rays to bend around obstructions towards shallow water (Komar, 1976). Refraction causes convergence and divergence of wave rays. Convergence of wave rays concentrates wave energy. Areas of convergence, such as at headlands are exposed to greater wave heights, while areas of wave ray divergence, or spreading out of energy, occurs in bays (Dyer, 1986).

Waves approaching the embayment between Howick and Beachlands Points from Tamaki Strait are likely to be refracted around the coastline as water depths reduce. Wave crests bend towards the shoreline concentrating wave energy around Motukaraka Island. Evidence of wave convergence can be seen on the northern side of Motukaraka Island where the shore platform is exposed and no beach has developed. The embayment and intertidal flats have a uniformly shallow gradient and it is therefore assumed that wave refraction over the area is negligible.

4.4.2 Wave analysis

An S4ADW InterOcean current meter was deployed at Site 1 (Figure 4.1) in 3.4 m of water. The instrument was moored on a steel rod at 1m above the bed and was secured to a concrete block. To convert bursts of pressure data recorded by the S4ADW current meter (which are a function of water depth) to real wave data a wave attenuation correction factor must be applied to transform the data to the surface. Long period low frequency waves have a greater effect at depth on the current meter, than high frequency waves (small amplitude short period waves) which have little to no effect on the current meter at depth due to attenuation. High frequency are over estimated when orbital velocities at the instrument depth are transformed to the surface due to the exponential relationship predicted by linear theory.

At Pine Harbour Marina the area has limited fetch and shallow water depths, so wave periods are typically small. Standard wave analysis could not be performed on the current meter pressure data because of the nature of these small short period waves, due to the pressure correction discussed above, and because they are difficult to discern from turbulence and other noise in the pressure record. This makes it difficult to define a cut off point for high frequency waves to eliminate noise without removing real wave data.

As no recorded wave data was derived from the S4 current meter deployments, a wave climate for the embayment surrounding Pine Harbour Marina was predicted using WGEN3DD, a wave generation model for estuaries developed by Black & Rosenberg (1992). The numerical model (WGEN3DD, Black & Rosenberg, 1992) has been successfully applied previously to Port Phillip Bay, in south-eastern Australia (K. Black, pers. comm.). At that site however, fetches were much longer than those at Pine Harbour. This study aims to assess the wave prediction formulae in very short fetches and to examine the effectiveness of linear theory for short-period waves. Also investigated were the formulae used to calculate significant wave heights - JONSWAP and SMB. Wave predictions were made at Pine Harbour Marina with relation to sediment transport issues and implications for dredge spoil dispersion over intertidal flats.

4.4.3 Wave model WGEN3DD

4.4.3.1 Background

In the sea there is seldom a single frequency of surface waves present. Generally there will be a spectrum of waves with frequency and amplitude varying with time. The longer the measurement time, the wider the spectrum, as it encompasses the larger waves in the storms as well as calm periods (Dyer, 1986). Wave spectrum forecast methods describe the generated waves in terms of the complete spectrum of periods and energies, not just in terms of a single significant wave height and period. The spectrum methods are preferred because they arrive at a far closer realisation to the wave conditions, however spectrum methods are more complex in application and in some instances for this reason the significant wave method is utilized (Komar, 1976).

4.4.3.2 Sverdrup, Munk and Bretschneider (SMB)

As cited in Black & Healy (1981), Sverdrup and Munk (1947) produced the first widely used wave prediction system based on a series of predictive curves which were later modified by Bretschneider in 1958, using additional empirical data. At the time SMB was developed spectral analysis techniques had not been applied to sea waves, and SMB used significant wave parameters to describe sea wave motions (Komar, 1976). The SMB prediction curves have also been converted to a series of equations which predict the spectral wave height (which is less than the significant height) and the peak spectral period (Coastal Engineering Center, 1984). These equations have been adjusted for specific conditions such an infinite fetch in deep water or a short fetch in shallow water. SMB inputs are wind speed and fetch, from which it predicts significant wave heights and periods, incorporating bottom friction (Black & Healy, 1981). The SMB method is often used for shallow water and fetch limited cases. The wave height is given by,

$$\frac{gH}{U^2} = 0.283 \tanh\left[0.578\left(\frac{gd}{U^2}\right)^{0.75}\right] \tanh\left[\frac{0.0125\left(\frac{gF}{U^2}\right)^{0.42}}{\tanh\left[0.578\left(\frac{gd}{U^2}\right)^{0.75}\right]}\right] \qquad (4.1)$$

Where; g is the gravitational acceleration, H is wave height, T is wave period, U is wind speed, d is water depth, and f is wind fetch. These equations are for the shallow water case and reduce to the deep water equations when d is large.

4.4.3.3 JONSWAP

In 1968 and 1969 scientists from four countries cooperated in an experiment called the Joint North Sea Project (JONSWAP) to measure wave growth (Black & Healy, 1981). The JONSWAP experiment derived a spectral form for a fetch limited sea, which was later extended to a duration limited sea. From the data the JONSWAP spectrum was calculated for deep water fetch limited ($\leq$160 km) conditions and maximum wind speeds between 15 and 20 m/s (Hasselman *et al.*, 1976). The JONSWAP spectrum has been used widely for a range of conditions resulting in a number of revised constants for particular situations (de Lange, 1988). It is applicable to fetch limited waves in deep water and has been extended to allow for duration limited conditions (de Lange, 1988). Inputs into the JONSWAP spectrum are the wave fetch and wind speed (Black & Healy, 1981).

The JONSWAP spectrum is,

$$S(f) = \frac{\alpha g^2}{(2\pi)^4} f^{-5} \exp \frac{-5}{4}\left(\frac{f}{f_p}\right)^{14}\left[\gamma^{\exp}\left[\frac{-(f-f_p)^2}{2\sigma^2 f_p{}^2}\right]\right] \qquad (4.2)$$

where

$$\alpha = 0.076x^{-0.22}$$

and x, the non-dimensional fetch is

$$x = \frac{Fg}{U_{10}^2} \qquad (4.3)$$

$\sigma = \sigma_a = 0.07$ for $f<f_p$

$\sigma = \sigma_b = 0.09$ for $f>f_p$

4.4.3.4 Wave generation model

The model WGEN3DD for fetch-limited seas takes a gridded bathymetry to determine the effective fetch in estuaries or semi-enclosed water bodies and calculates wave height and wave period as well as the bottom horizontal orbital velocity (Black, 1995). The JONSWAP method was applied to hindcast wave height and period. The SMB method was also tested and compared to the results from JONSWAP.

Since the JONSWAP equation was developed for deep water conditions it does not explicitly consider shoaling, friction and wave breaking, these factors have been included into the numerical model WGEN3DD (K. Black, pers. comm.). The model adopts linear theory for the shoaling and friction, and a depth limitation for the wave breaking. The JONSWAP method significant wave height (H_s) is proportional only to the fetch and wind speed and not the water depth.

In order to obtain wave orbital motions at depth, the model takes the theoretical sea surface spectrum and, by breaking the spectrum into frequency bands, the orbital currents are calculated for each band using linear wave theory as a transfer function. The spectrum of orbital motion is then reconstructed at the selected depth. The spectral components for the surface elevation and for the orbital motion at depth are separately summed to recreate time series of sea surface elevation and orbital velocity. These time series are then analysed for significant heights, orbital motion and for period statistics.

In essence, for each wind condition modelled, the process occurs in 4 stages (Black, 1995). In stage 1, the theoretical spectrum is divided into frequency bands and the component amplitude is calculated where,

$$S(f) = \frac{a^2}{2\Delta F} \qquad (4.4)$$

where S(f) is the spectral energy density, a the component amplitude and ΔF the bandwidth.

In stage 2, each spectral component is converted to an orbital motion at the selected depth where,

$$u = \frac{\pi H}{T} \frac{\cosh[k(z+h)]}{\sinh(kh)} \cos(kx - \sigma t) \qquad (4.5)$$

where H is the wave height, T the wave period, k the wave number, z the vertical co-ordinate (positive upwards), h the water depth, σ the radian frequency, x the horizontal co-ordinate and t the time.

In stage 3, the spectrum of orbital motion is reconstructed and time series of sea surface elevations and orbital motion are generated by linear summation of components. In stage 4, a zero up-crossing analysis is applied to calculate height, period and orbital motion statistics.

Wave shoaling was added by a multiplicative factor applied to each frequency band, where

$E.C_g$ = constant for each frequency (4.6)

and $E=0.125\rho gH^2$ where H is wave height, ρ is water density (normally 1025 kg.m^{-3}) and

$$C_g = n.c \qquad (4.7)$$

where

$$c = \frac{gT}{2\pi}\tanh\frac{2\pi h}{L} \qquad (4.8)$$

and

$$n = \frac{1}{2}\left[1 + \frac{2kh}{\sinh(2kh)}\right] \qquad (4.9)$$

Wave breaking is imposed using a simple similarity assumption, i.e. the wave height is truncated to the depth limited value given by

$$H_b = \gamma h \qquad (4.10)$$

where H_b is the breaking wave height and γ is taken as a commonly adopted value of 0.8.

The friction is calculated by adopting the method of Bretschneider and Reid (1958) and applied by Black and Rosenberg (1992). The dissipation term is

$$F_D = \frac{\rho C_f}{6\pi}\left[\frac{H\sigma}{\sinh(kh)}\right]^3 \qquad (4.11)$$

where C_f is the friction coefficient (set by calibration).

The model acts by subdividing the fetch into short lengths of order 100 m. In each segment, the model checks for the breaking depth limitation and truncates the height if necessary after incorporating shoaling. It calculates the frictional loss over the segment and the effect of these factors is accumulated over the full fetch to produce the hindcast wave height at the measurement location. This technique makes it possible to incorporate inter-tidal sand banks. By having a gridded bathymetry (relative to CD) over the full model region and by entering the tidal sea levels above datum as input data, the model determines total water depth in each cell. For each wind condition modelled, the fetch and water depth in each segment is then calculated from the tidally-corrected gridded depth data.

The total energy in the spectrum is calculated using the wind fetch F and wind speed U, the wave heights statistics can then be calculated.

$$E_{tot} = 1.6 * 10^{-7}\left(\frac{U^2 F}{g}\right) \qquad (4.12)$$

Significant wave height, average of the highest 1/3 of waves, is calculated from the total energy derived above from the wind speed (U) and fetch (F).

$$H_{1/3} = 4\sqrt{E_{tot}} \qquad (4.13)$$

The horizontal orbital velocity at z metres down from the water surface was then calculated:

$$u = \frac{\pi H}{T} e^{kz} \qquad (4.14)$$

where z is the water depth (-ve), and

$$k = \frac{2\pi}{L} \qquad \text{and} \qquad L = \frac{gT^2}{2\pi} \qquad (4.15)$$

Unlike the SMB equations, the JONSWAP significant wave height is proportional only to the fetch and wind speed, and not the water depth. The shoaling is calculated separately by adding a multiplicative factor which was applied to each frequency band (eqn 4.6). Using gridded bathymetry with known orientation, the model calculates the effective fetch for each simulated wind direction and employs either the JONSWAP or SMB wave generation formulae.

4.4.4 Application of WGEN3DD at Pine Harbour Marina

An area encompassing the shallow tidal embayment in which Pine Harbour Marina is located and extending north across Tamaki Strait to the shores of Rangitoto and Waiheke Islands was gridded with bathymetric data. Grid sizes were 320 x 320 m which provided sufficient resolution for the modelling (Figure 4.12). The resolution was primarily determined by the scale of the morphological features of the region. The corresponding depths at the mid-point of each cell were then manually interpolated. The bathymetry file was input to WGEN3DD along with wind data recorded on site at 5 m above mean sea level, and tidal data taken from the nearby Port of Auckland. A wind correction factor of 1.17 was applied to wind speeds to adjust data to the standard elevation of 10 m above the water surface.

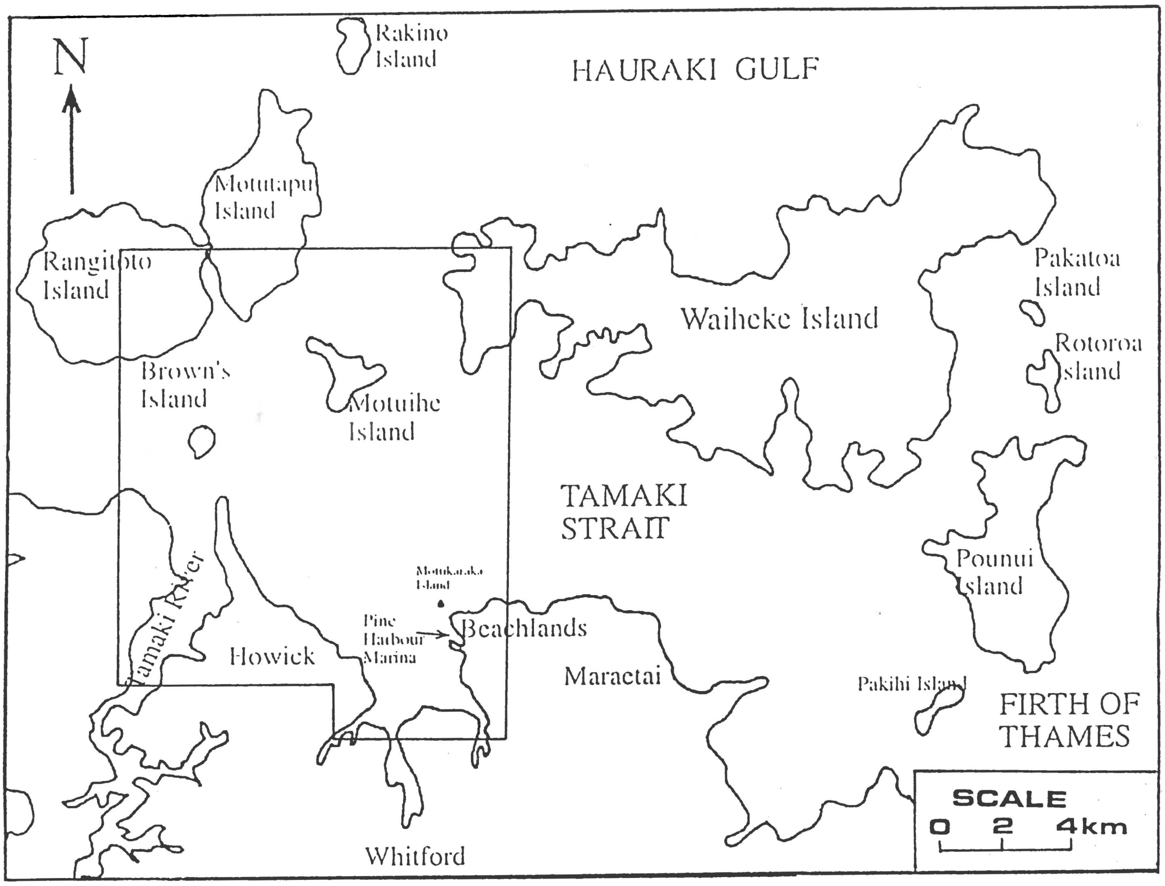

FIGURE 4.12: Location of area gridded with bathymetry data (inside frame) input into WGEN3DD for wave prediction at Pine Harbour Marina.

WGEN3DD was set up to generate wave data for the site and time period corresponding to S4 electromagnetic current meter measurements of two orthogonal current vectors at Site 1. The instrument recorded instantaneous wave orbital motion at 0.5 s intervals in bursts of 3 minutes every 2 hours. Each S4 burst was analysed for significant and mean orbital velocity statistics. For comparison with these measurements, numerically-generated wave heights were converted to orbital velocities at the depth of the instrument using linear wave theory, in order to verify model predictions. Two semi-empirical wave height generation formulae, JONSWAP and SMB, were also investigated.

Comparisons were made between the standard deviation of the orbital velocity (U_{BSD}) predicted by WGEN3DD at 1.0 m above the bed, and the root mean square of orbital velocity (U_{RMS}) from the S4 record measured at the instrument height (1.0 m above the bed). U_{RMS} 1.0 m above the bed was determined from the scatter of the X and Y velocity components of the current for each burst measured by the S4 electromagnetic current meter. Regression analysis of each burst was undertaken to determine the principal direction of the current, and the root mean square of the velocity component calculated for each burst to give the U_{RMS} 1.0 m above the bed (R. Gormon, pers. comm.). U_{BSD} is the standard deviation of the wave orbital velocity, predicted 1.0 m above the bed equivalent to the height of the current meter. U_{BSD} is essentially the same as U_{RMS} if the mean is removed from analysis (K. Black, pers. comm.).

The U_{RMS} from the current meter compared well with predicted U_{BSD} from WGEN3DD using the JONSWAP equation, showing good agreement between the trends of increasing and decreasing orbital velocities (Figure 4.13). The gradient for the regression analysis was 1.40, the intercept was 2.57, and correlation was 0.19 (Figure 4.14). The model tended to under predict wave orbital velocities above 12 cm/s. For comparison with the JONSWAP predictions the model was also run using the SMB equation. There was not a great deal of difference between the two methods after wave shoaling was added to the JONSWAP equation, although the SMB method proved slightly more accurate arriving at a closer prediction to higher orbital velocities. This could be due to the fact than JONSWAP equation was developed for deep water conditions and the SMB equation developed for shallow water conditions. Regression analysis for both equations yielded similar correlation coefficients ($R = 0.19$ and $R = 0.21$ for JONSWAP and SMB respectively).

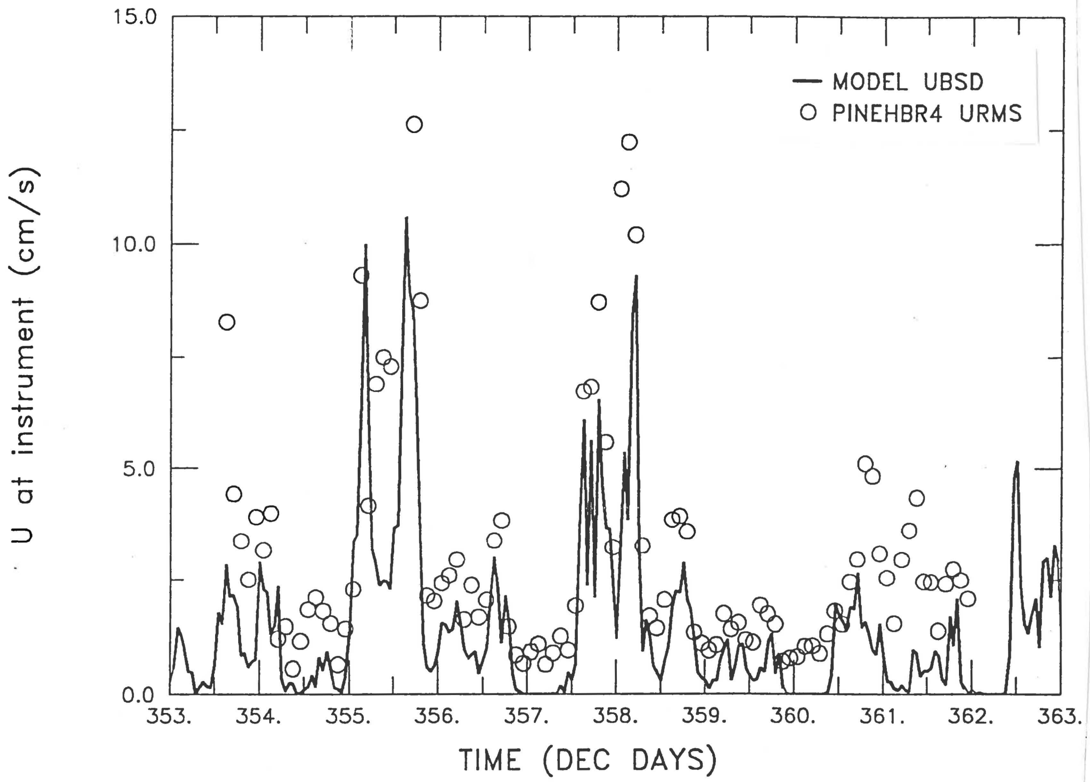

FIGURE 4.13: Standard deviation of wave orbital velocity (U_{BSD}) predicted by WGEN3DD using JONSWAP equation, and root mean square of wave orbital velocity (U_{RMS}) recorded at Site 1. Site depth 1.7 m, instrument height 1.0 m.

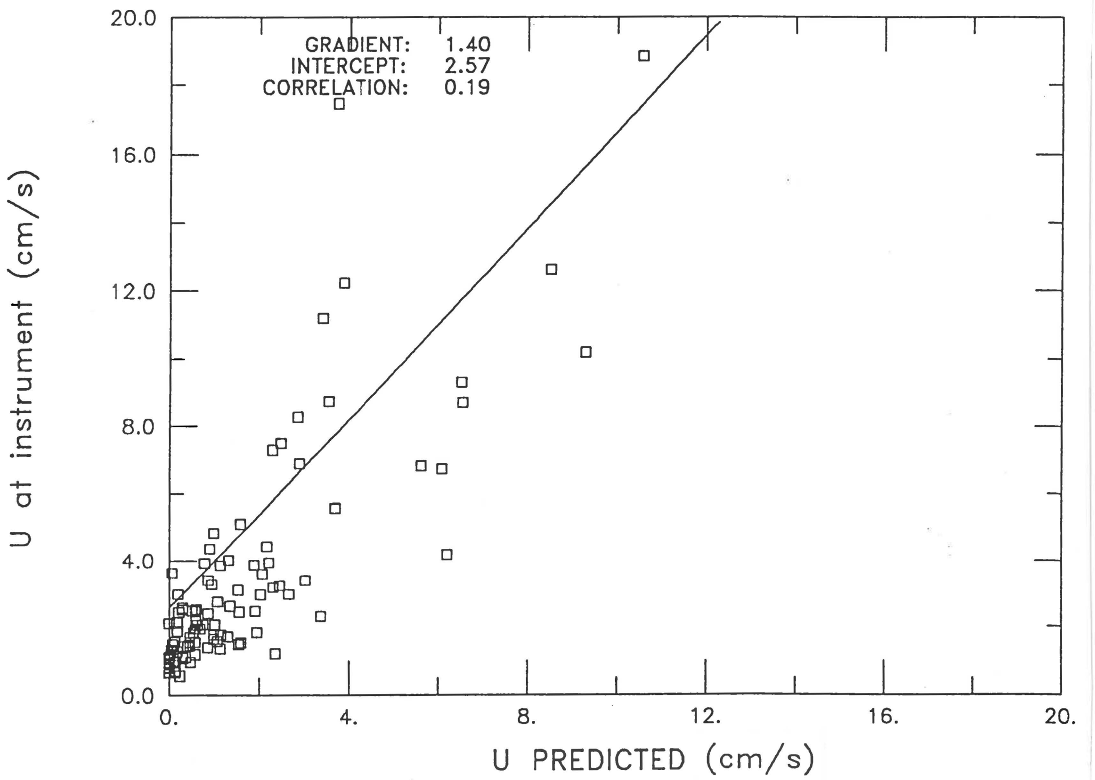

FIGURE 4.14: Regression analysis of JONSWAP of standard deviation of wave orbital velocity and root mean square of wave orbital velocity calculated by S4 current meter at Site 1. Site depth 1.7 m, instrument height 1.0 m.

4.4.4.1 Effective depth

Previous work has suggested that linear theory underestimates the orbital motion at depth for high frequency waves (K. Black, per. comm.). This was investigated. The effective depth is the depth below the water surface where the measured orbital velocities and linear theory results are in agreement. To determine the effective depth, the model was run for a range of instrument depth values to determine the depth below the water surface where measurements and linear theory are in agreement.

The model was run using the JONSWAP equation at depths of 0.5 m, 0.3 m and 0.1 m below the surface, in comparison to the actual depth which was 0.7 m below the surface (Figures 4.15, 4.16 & 4.17). The effective depth is the water depth minus the current meter elevation. Regression analysis indicates that the best agreement between modelled and recorded data was obtained when the height of the instrument in was raised to 0.1 m below the surface (Figure 4.18). This was equivalent to raising the instrument 0.6 m in the water column to 1.6 m above the bed compared to the actual height 1.0 m above the bed. Although there was a fairly good match when the current meter elevation was set to 0.7 m below the surface (the actual height), the best match was obtained when it was set at 0.1 m. At this height, the gradient for the regression analysis is 0.98 (close to the ideal gradient), the intercept is 2.22 (the closest to the ideal so far) and correlation is 0.20. This means that the effective depth of the current meter is 0.1 m (the water depth - current meter elevation).

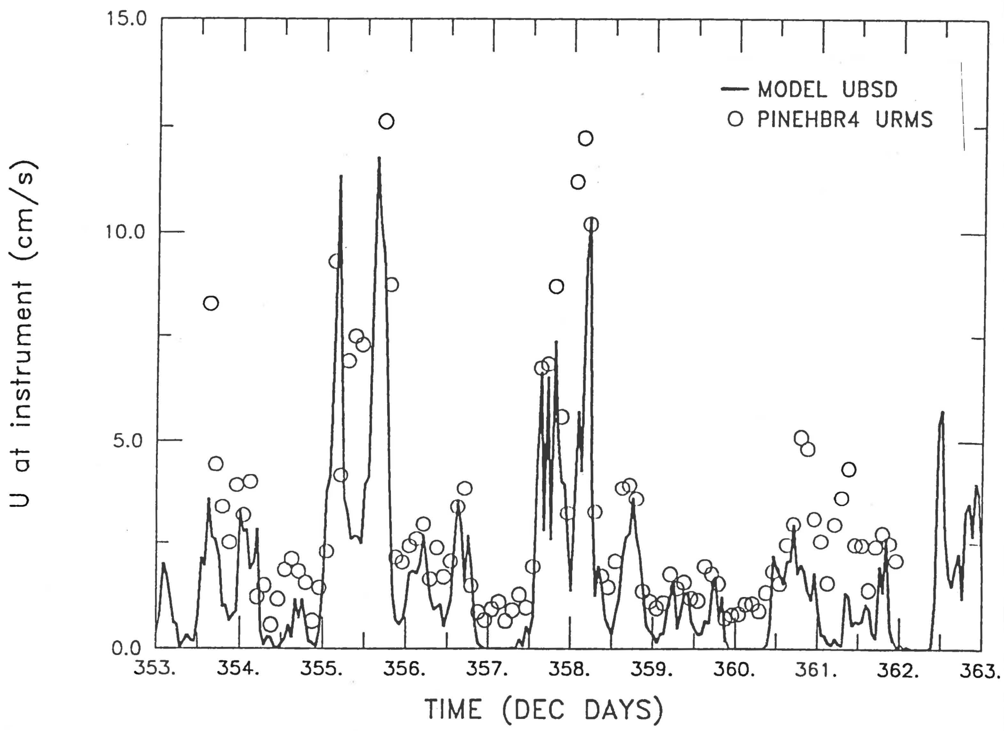

FIGURE 4.15: Predicted U_{BSD} 0.5 m below surface (site depth 1.7 m, instrument height 1.2 m) compared to U_{RMS} calculated 1.0 m above the bed.

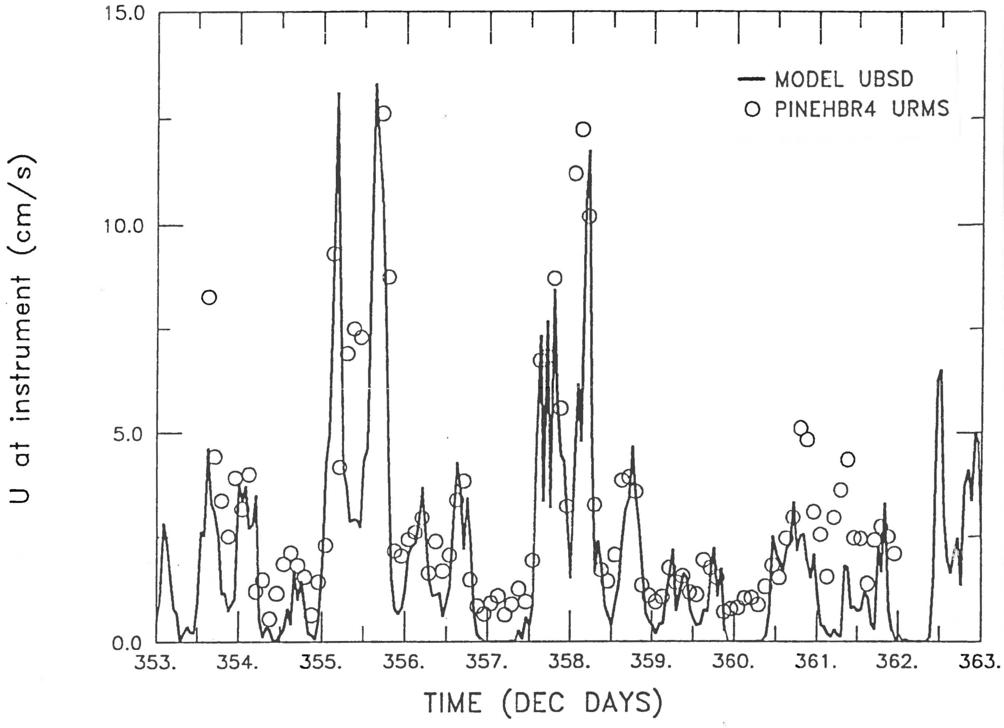

FIGURE 4.16: Predicted U_{BSD} 0.3 m below surface (site depth 1.7 m, instrument height 1.4 m) compared to U_{RMS} calculated 1.0 m above the bed.

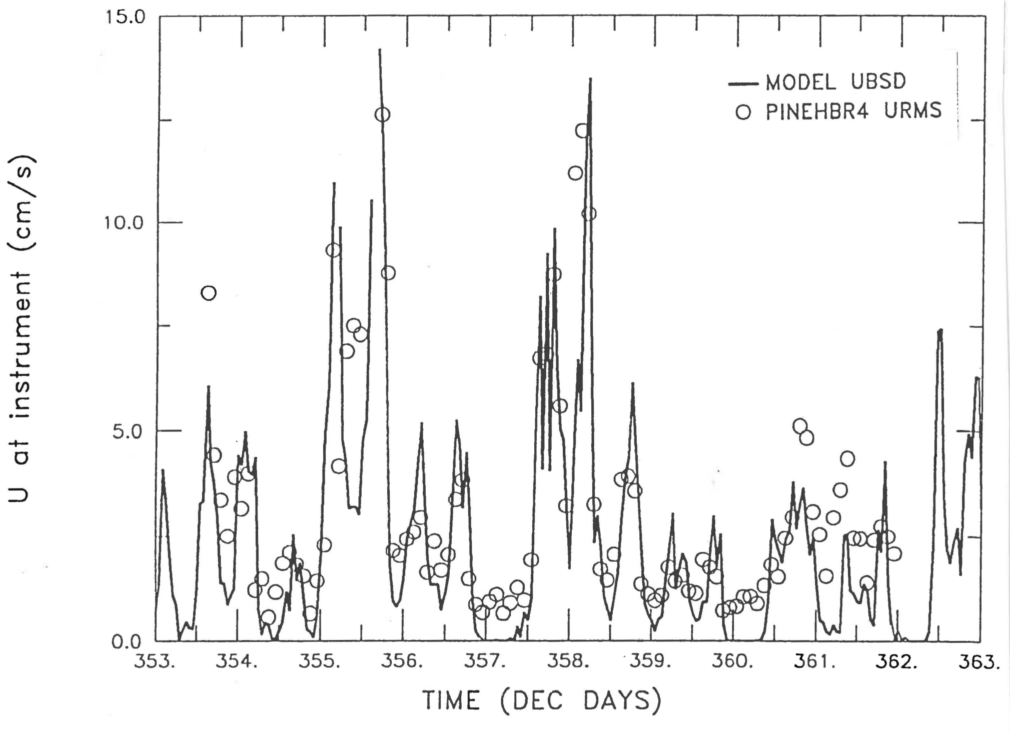

FIGURE 4.17: Predicted U_{BSD} 0.1 m below surface (site depth 1.7 m, instrument height 1.6 m) compared to U_{RMS} calculated 1.0 m above the bed.

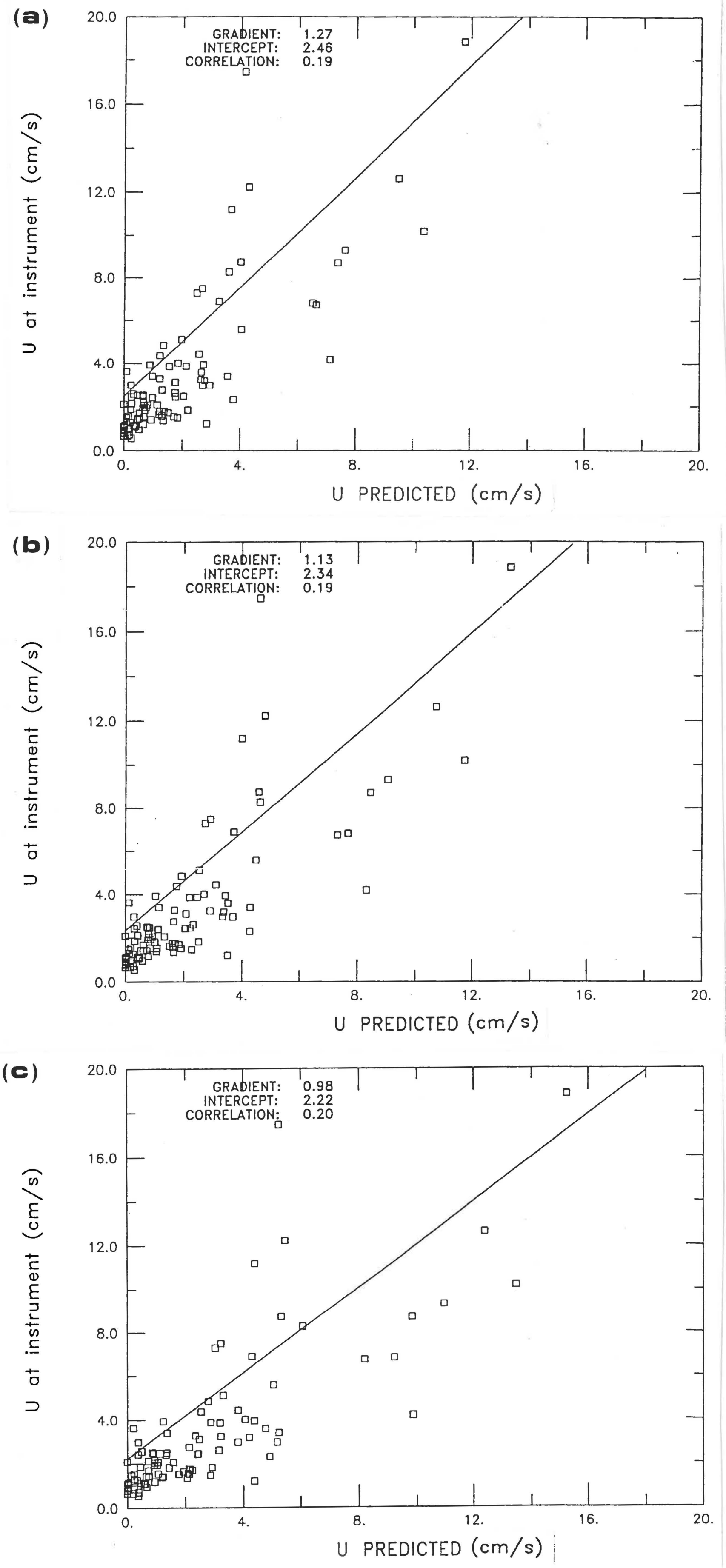

FIGURE 4.18: Regression analysis of WGEN3DD predicted orbital velocities for a) 0.5 m, b) 0.3 m, and c) 0.1 m below the surface compared to the measured orbital velocity at 0.7 m below the surface.

4.4.4.2 Wave hindcasting at Pine Harbour Marina

The model WGEN3DD was used, once it was calibrated, for the generation of a wave rose and for establishing a long-term time series of wave heights at Pine Harbour Marina. A wind rose of wind speeds recorded at 10 minute intervals at Pine Harbour Marina for the period from 23/11/94 to 17/1/95 was input into WGEN3DD and the corresponding wave heights and periods generated by wind speeds from each quadrant calculated. The probability of occurrence of wind speeds and directions over this period is tabulated in Table 4.2.

TABLE 4.2: Pine Harbour Marina wind data recorded at 10 minute intervals from 23/11/94 to 17/1/95.

Direction	Wind speed (m/s)						
	0-1	1-3	3-6	6-10	10-16	16-21	Prob. of occurrence
NNE	0.03	0.82	1.99	0.18	0.00	0.00	3.01
NE	0.23	1.01	3.74	1.15	0.00	0.00	6.14
ENE	0.22	2.42	3.50	0.46	0.00	0.00	6.59
E	0.39	4.60	1.02	0.05	0.00	0.00	6.07
ESE	0.42	2.83	0.20	0.00	0.00	0.00	3.45
SE	0.24	5.55	1.49	0.00	0.00	0.00	7.29
SSE	0.11	2.05	4.12	0.86	0.00	0.00	7.15
S	0.15	0.80	4.01	5.20	0.90	0.05	11.11
SSW	0.05	0.44	2.34	11.06	4.48	0.18	18.55
SW	0.08	0.40	1.39	1.85	0.72	0.00	4.44
WSW	0.08	0.46	0.99	0.65	0.30	0.00	2.47
W	0.04	0.47	0.97	0.59	1.00	0.01	3.09
WNW	0.01	0.35	0.94	1.24	0.23	0.00	2.77
NW	0.01	0.40	1.76	1.19	0.01	0.00	3.38
NNW	0.01	0.90	5.34	4.67	0.15	0.00	11.07
N	0.05	0.94	2.39	0.06	0.00	0.00	3.44
Probability of occurrence	2.11	24.45	36.20	29.20	7.79	0.24	100.00

4.4.4.3 Offshore wave climate

WGEN3DD predicted significant wave heights for 3.4 m water depths at Site 1 (Figure 4.1). Wave conditions were hindcast with wind rose data from Table 4.2, and the probability of occurrence corresponds to the significant wave heights (H_s) and significant wave periods (T_s). Raw data is compiled in Appendix 4.1.

Significant wave height

Significant wave heights (H_s) are generally less than 0.2 m but reach up to 0.5 m under high wind speeds which transfer more energy to waves generating larger wave heights. Daily variations in significant wave height are caused by changes in fetch length in the embayment due to tidal fluctuations which decrease the area of coverage of water over the embayment and thus limit the effective fetch (Figure 4.19). The concept of effective fetch was introduced to reduce the fetch length to account for the narrowness of the fetch (Coastal Engineering Center, 1984). The adjustment provided improved wave estimates.

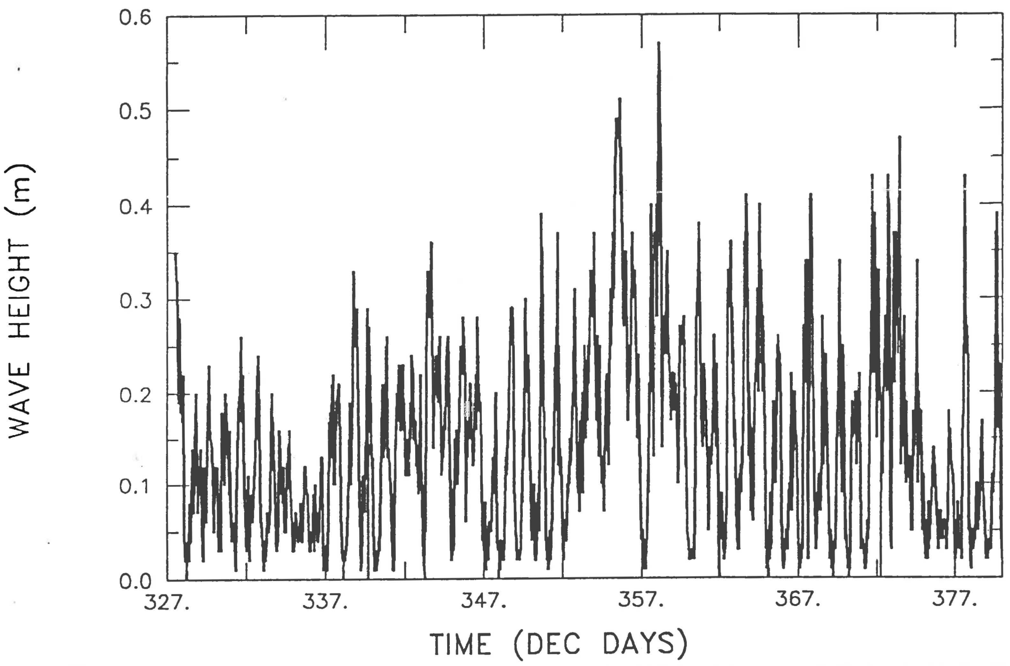

FIGURE 4.19: Significant wave heights (H_s) in metres predicted by WGEN3DD for Site 1 from wind data recorded at Pine Harbour Marina from 23/11/94 to 17/1/95.

The long term wave climate at Pine Harbour Marina is dominated by low energy events owing to the restricted fetch and shallow water in the embayment. Under windy conditions small short period sea waves, colloquially known as wave or wind 'chop', are generated. For 62.76% of the measurement period wind speeds were less than 6 m/s and predicted significant wave heights were less than 0.25 m (Figure 4.20). For one third of this time wind speeds are less than 3 m/s and significant wave heights less than 0.1 m. Wind rose data (Table 4.2) show that southerly winds are most common over the region, occurring approximately 50% of the measurement period, and that greatest wind speeds exceeding 10 m/s were recorded from the south and west. For 11% of the time SSW wind speeds were between 6-10 m/s, generating significant wave heights up to 0.26 m. Greatest effective fetch is to the north-west, however winds from this quadrant blow only 3.38% of the time and wind speeds reached 10 m/s less than 1% of the measurement period.

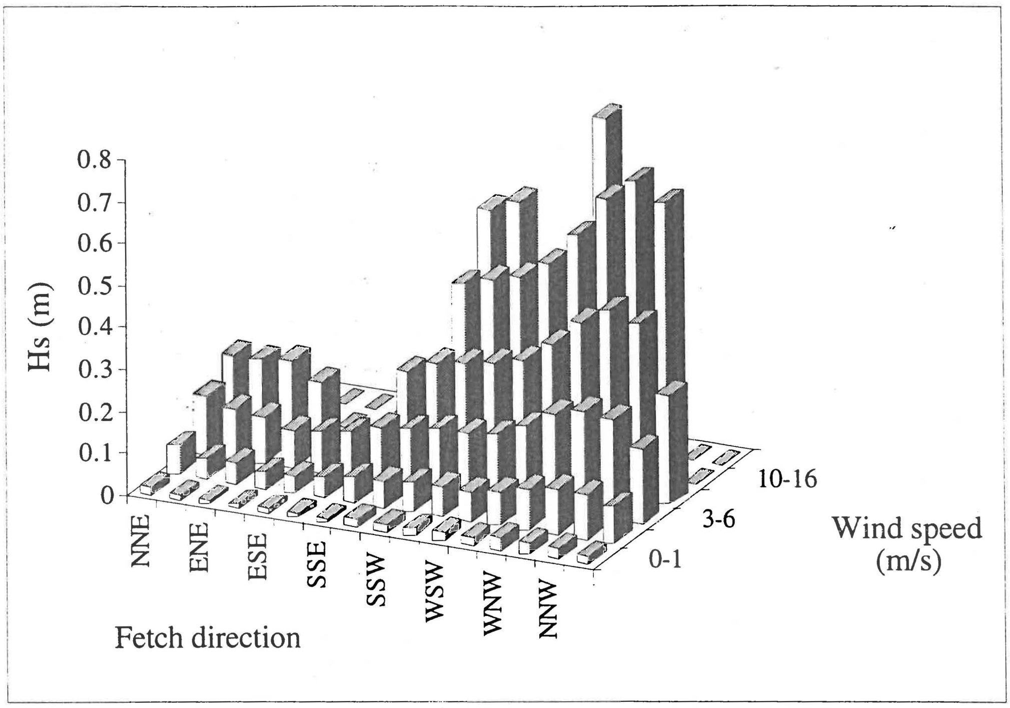

FIGURE 4.20: WGEN3DD predicted significant wave heights (Hs) for wind speed and fetch directions at Site 1 Pine Harbour Marina.

Wave heights (H_s) over 0.4 m are generated by wind speeds exceeding 6 m/s from the NNW, NW and WNW, and by wind speeds greater than 10 m/s from the southerly quadrant to compensate for the shorter fetch. Significant wave heights greater than 0.5 m are generated by high wind speeds greater than 10 m/s from the WSW, W and WNW and occur approximately 1% of the measurement period. Winds from NE to SE do not generate waves other than small wave chop or surface ripples because the effective fetch is less than 1 km and the north-south orientation of the coastline shelters the embayment from winds from this direction.

Significant wave period

WGEN3DD predictions of wave periods (T_s) over the tidal embayment are between 1.0 and 2.5 s (Figure 4.21). Short wave periods are typical of shallow water depths and limited fetch environments. Wave heights will be smaller and wave periods shorter if generation takes place in transitional or shallow water, and wave climate will frequently be dominated by locally generated wind waves (Coastal Engineering Center, 1984). At Pine Harbour wave periods increase up to 2.5 s when winds generate waves from the north-west.

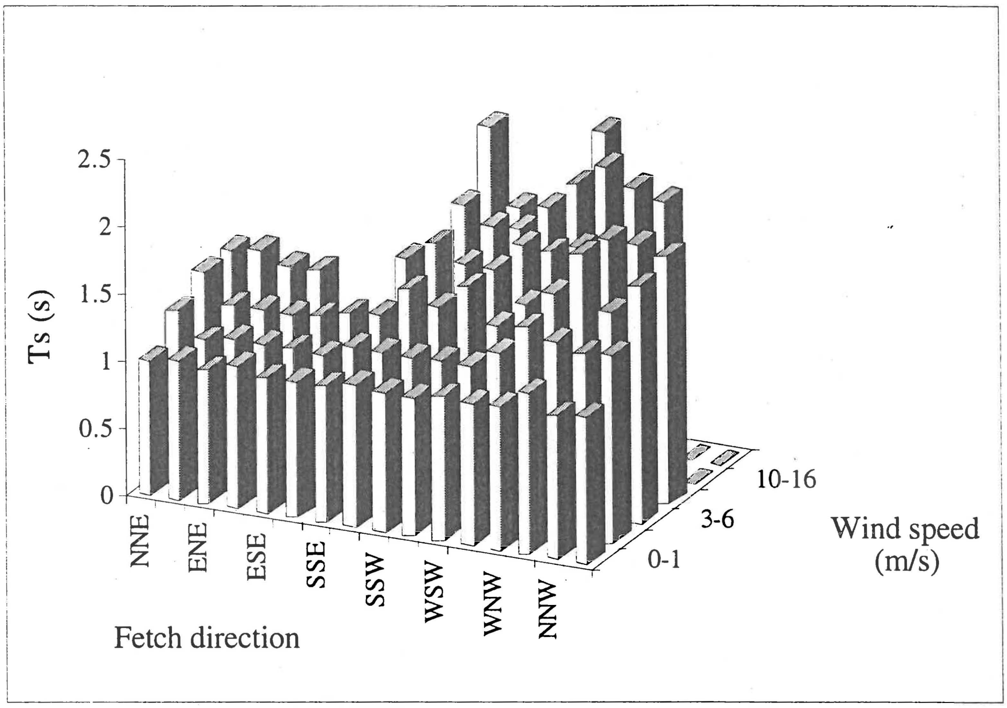

FIGURE 4.21: WGEN3DD predicted significant wave periods (Ts) for wind speed and fetch directions at Site 1, Pine Harbour Marina.

4.4.4.4 Waves over the intertidal flats

WGEN3DD was also used to predict wave conditions for a site located 1.5 m above CD on the intertidal flats fronting Pine Harbour Marina. Wave conditions were hindcast with wind rose data from Table 4.2 and corresponds to the significant wave heights and significant wave periods compiled in Appendix 4.2. Wave conditions for this site were predicted to relate to sediment transport patterns observed and discussed with the fluorescent tracer experiment in the following chapter.

<u>Significant wave height</u>

The intertidal flats fronting Pine Harbour Marina undergo alternate wetting and drying with the tidal cycle which restricts the frequency and height of waves over the region by controlling water depth. Waves over the upper intertidal flat are limited by the shallow water depth. Significant wave heights fluctuate with the tide, reaching maximum height at high tide when water depths over the intertidal flat are deepest (approximately 1.9 m) and fetch is greatest (Figure 4.22).

Significant wave heights (H_s) on the intertidal flats are less than 0.1 m for approximately 25% of the measurement period. Locally generated sea waves were dominated by frequent (30% of measurement period) southerly winds (from 135° to 225°) (Table 4.2). Wave heights are small and exceed 0.3 m less than 10% of the measurement period from 23/11/94 to 17/1/95. For winds of similar speeds, H_s is greatest when winds are from the west and northwest (250° to 340°) because fetch is greatest in this direction and fetch is limited in the south (Figure 4.23). Wind speeds associated with the maximum predicted waves (H_s) 0.81 m were in the order of 16-21 m/s from the west (250° to 290°).

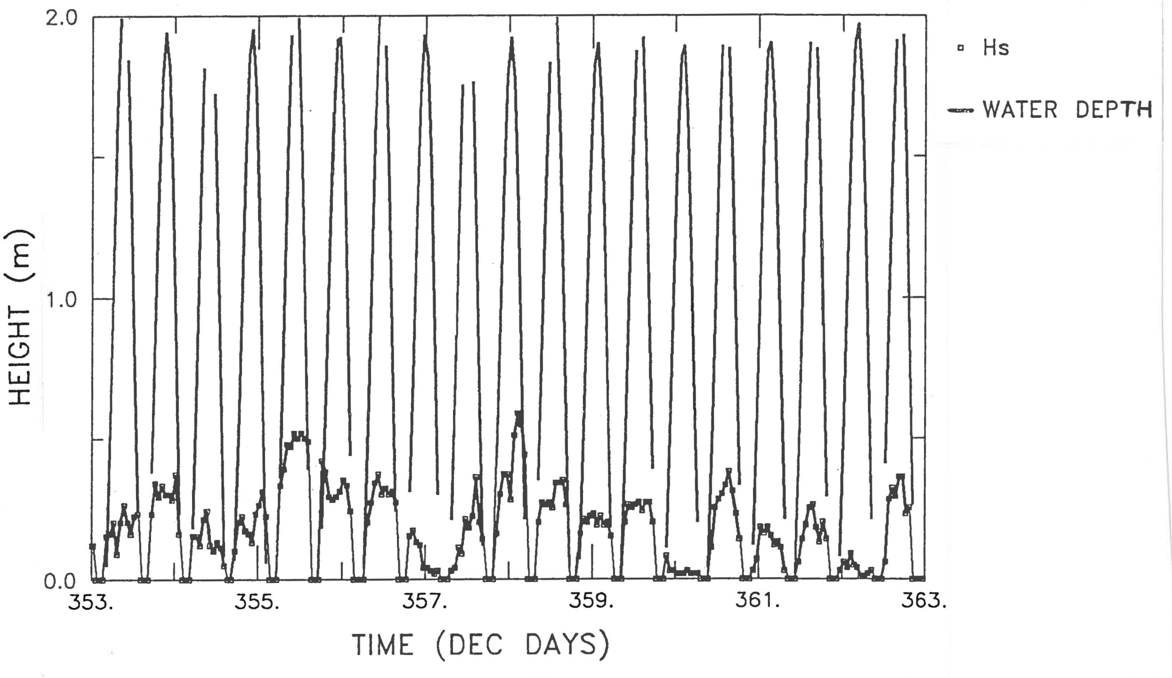

FIGURE 4.22: Significant wave height and water level at tracer site from 23/11/94 to 17/1/95.

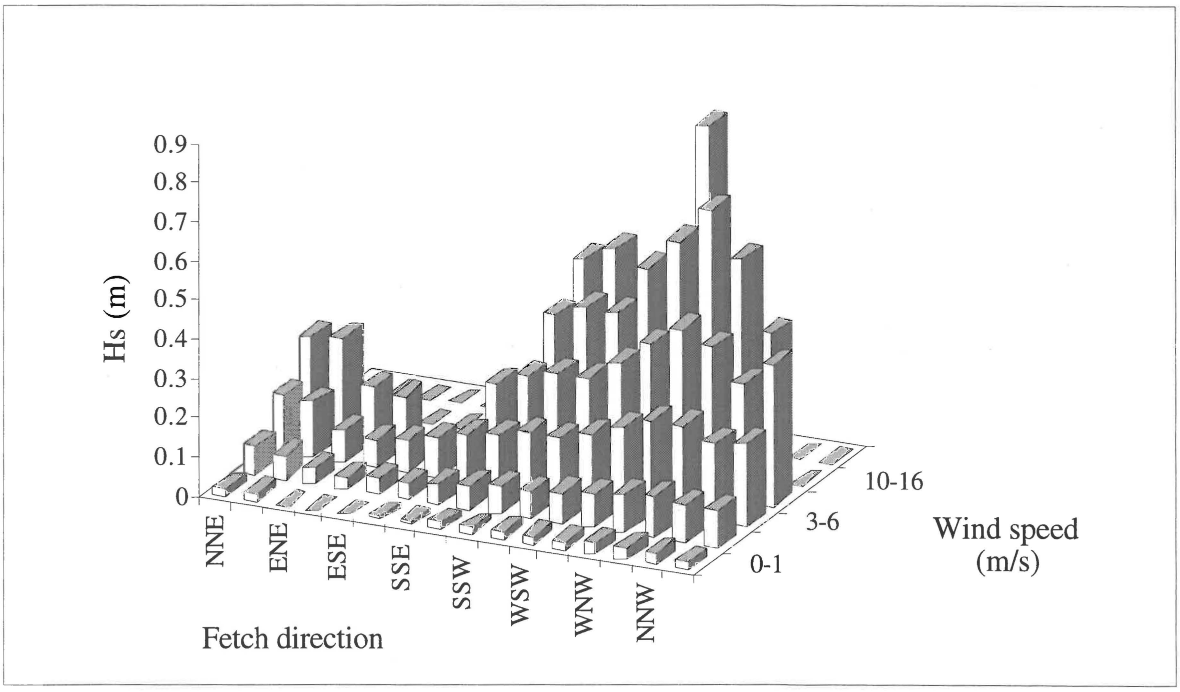

FIGURE 4.23: Significant wave height (H_s) predicted by WGEN3DD over intertidal flats from wind data recorded at Pine Harbour Marina from 23/11/94 to 17/1/95.

The maximum predicted wave height of 0.81 m requires minimum water depth of 1.0 m over the intertidal flats to support the wave prior to breaking. This was determined using breaker ratio ($\gamma_b = H_b/h_b$) for planar beaches of 0.8 (Komar, 1976). Waves of this height

(H_s) require the coincidence of high wind speeds from the northwest and a tidal height of at least 2.5 m.

Significant wave period

Waves predicted by WGEN3DD are short period spilling type sea waves which can shoal, break and reform many times as they move across the low gradient intertidal flat. Significant wave periods (T_s) predicted for waves over the intertidal flats are between 1.5 and 3.5 s (Figure 4.24).

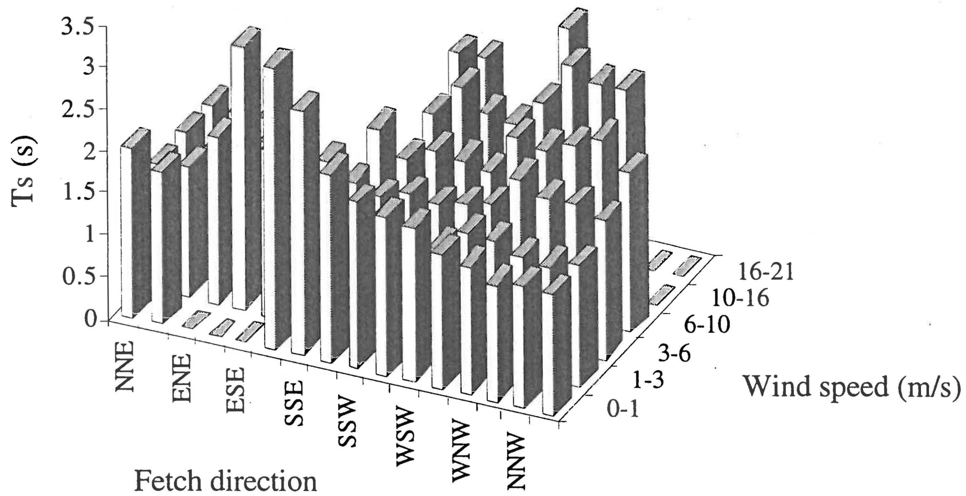

FIGURE 4.24: Significant wave period (T_s) predicted by WGEN3DD over intertidal flats from wind rose.

4.4.4.5 Wave power resultant

Wave energy in at Pine Harbour Marina is low due to the restricted fetches and shallow water depths in the embayment. Limited fetch restricts the transfer of energy from the wind to the water surface thereby restricting wave heights (H_s). The wave climate at Pine Harbour Marina is dominated by local wind generated waves from the south and southwest under the prevailing southwesterly wind which blows for 31.3% of the time (Figure 2.4). Waves (H_s) are of small to moderate height, limited by the short fetch across the embayment in the south. The energy of the prevailing south-westerly wind creates wind driven circulation towards the north and generates high frequency waves from the south. These conditions have the greatest impact on the Beachlands coastline and drive sediment transport in the littoral system north from Waikopua Creek to Motukaraka Island. Less frequent winds from the west (14.3%) and northwest (5.7%) generate large waves across the greater fetch which can entrain significant volumes of sediment. Westerly winds create an onshore current which transports suspended sediment towards the south as the current is modified by the local topography.

4.5 Discussion

Waves are the dominant entrainment mechanism for sediment, producing oscillatory and rapidly varying currents. Surface waves produce an oscillatory motion in the water, the water particles following circular paths if the water is deep, and elliptical paths in the case of waves in intermediate and shallow water. Near the bottom, the elliptical motion is reduced to a to-and-fro horizontal motion (Komar, 1976). The wave's orbital motion mobilizes sediment when the fluid flowing over sediment grains reaches a critical shear stress or flow velocity greater than the force holding the grain in place, sufficient to cause them to move from the bed into the flow and be transported (Komar & Miller, 1973). This velocity equals the critical or threshold velocity.

Sediment entrainment and deposition represents the balance between bed shear stress trying to move sediment and gravity trying to keep grains in place. There is a relationship between grain size and shear velocity, with smaller particles having a greater chance of becoming suspended than large particles due to larger grains having a higher critical shear stress (Nielsen, 1992). Once sediment grains are entrained in the water column they can be transported by the net current. Miller *et al.* (1977) developed a modified Shields-type threshold diagram in which the velocity required to initiate sediment transport 100 cm above the sediment bed can be determined for two grain size classes. The threshold orbital velocities 100 cm above the bed, necessary for sediment entrainment under waves, were determined for different sediment grain sizes distributed around Pine Harbour Marina using the equations proposed by Miller *et al.* (1977) for two sediment grain size classes (D) (Table 4.3).

$$U_{100} = 122.6D^{0.29} \text{ for D} < 0.2 \text{ cm} \qquad (4.16)$$

$$U_{100} = 160.0D^{0.45} \text{ for D} > 0.2 \text{ cm} \qquad (4.17)$$

TABLE 4.3: Critical sediment entrainment velocities 1 m above the bed, calculated using Miller et al. (1977).

Sediment location	Average sediment diameter phi	mm	U_{100} (cm/s)
Beach face & shell ridge	-1.5	0.2800	90
Intertidal flats	2.5	0.0177	38
Dredgings	4.0	0.0063	28
Offshore & channel	5.0	0.0030	23

Komar & Miller (1973, 1975) reviewed data and analyses of previous work on the threshold of sediment movement under oscillatory waves, and have shown that for grain sizes less than 0.5 mm (medium sands and finer) the boundary layer was still laminar and the threshold of motion could be represented by a critical value ψ_c of the mobility number,

$$\psi_c = 0.21\left(\frac{d_0}{D}\right)^{1/2} \qquad (4.18)$$

where,

$$d_0 = \frac{U_{max}T}{\pi} \qquad (4.19)$$

$$U_{max} = \frac{\pi H}{T\sinh\left(\frac{2\pi d}{L}\right)} \qquad (4.20)$$

and, T is wave period, H is wave height, d is water depth, L is wave length, and D is grain diameter.

For grains coarser than 0.5 mm, within turbulent boundary layers, the relation becomes,

$$\psi_c = 0.46\pi\left(\frac{d_0}{D}\right)^{1/4} \qquad (4.21)$$

Komar & Miller (1975) simplified the approach for determining the threshold velocity since the threshold for a given grain size and density can be specified by a single combination of wave period T and orbital velocity u_m (Figure 4.25). The higher the wave period the greater the orbital velocity required to reach the threshold velocity. There is some difficulty in joining the curves in the region at low periods where sediment grains are equal to 0.5 mm. Komar & Miller (1975) joined these curves by dashed lines indicating a compromise in the results.

Komar & Miller (1975) predictive curves in Figure 4.25 show the threshold near bed orbital velocities and wave periods required for movement of sediment grain sizes. In order for waves with periods of 1.0 s, similar to the 1.0-2.0 s wave periods (T_s) at Pine Harbour Marina, to move medium sand with grain diameter of 0.2 mm, a near bed orbital velocity of 8.0 cm/s is required Fine sand and silt, less than 0.1 mm diameter, require near bed orbital velocities of approximately 5.0-6.0 cm/s for a 1.0 s wave (T_s).

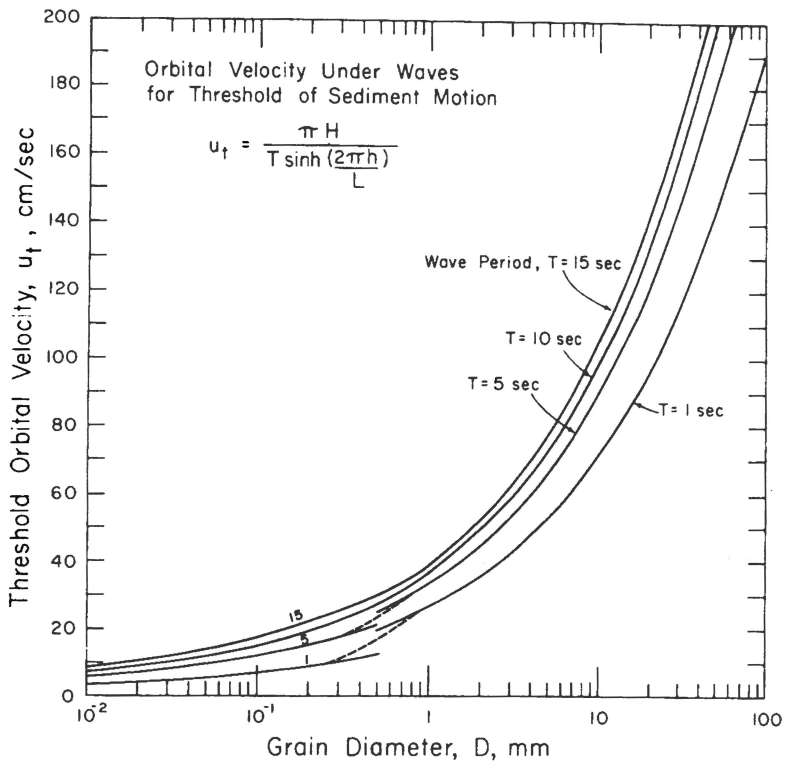

FIGURE 4.25: Near bottom orbital velocity u_m for sediment threshold under waves (Komar & Miller, 1975).

Orbital velocities associated with offshore wave climate at Pine Harbour Marina were calculated in order to determine whether sediment entrainment velocities of different grain sizes were exceeded under different wave heights. Linear theory is inappropriate in the shallow water environment at Pine Harbour Marina, necessitating the use of Stoke's second order theory. In Stoke's second order approximation, as given in Komar (1976), wave orbits are not closed which leads to a non-periodic drift or mass transport in the direction of wave advance.

$$\overline{U} = \frac{1}{2}\left(\frac{\pi H}{L}\right)^2 C \frac{\cosh[2k(z+h)]}{[\sinh(kh)]^2} \qquad (4.22)$$

Wave heights (H_s) predicted by model WGEN3DD were used to calculate orbital wave velocities 100 cm above the bed for comparison with entrainment velocities of grain sizes calculated using Miller et al. (1977). Critical near bed orbital velocities predicted from Komar & Miller (1975) are also presented in Table 4.4.

TABLE 4.4: Wave orbital velocities calculated by Stoke's theory for wave climate offshore Pine Harbour Marina.

Water depth (m)	Wave period (s)	Wave height (m)	Orbital velocity (cm/s) U_{100}	Bed
3.5	1.5	0.1	0.25	0.08
2.0	1.5	0.1	3.60	1.20
1.5	1.5	0.1	8.80	2.90
1.0	1.5	0.1	22.0	6.70
3.5	1.5	0.2	0.56	0.19
1.5	1.5	0.2	18.0	6.00
3.5	1.5	0.3	0.97	0.35
1.5	1.5	0.3	28.0	9.90
3.5	1.5	0.4	1.50	0.58
1.5	1.5	0.4	38.0	14.0
3.5	1.5	0.5	2.60	0.91
3.5	2.5	0.5	16.0	13.0

Typical waves experienced offshore at Pine Harbour Marina, H_s = 0.1-0.4 m, T_s = 1.0-2.5 s, are insufficient to entrain sediment in 3.5 m water depth. Infrequent high energy waves H_s = 0.5 m, T_s = 2.5 s are capable of entraining sediment finer than 0.02 mm (coarse silt) as the near bed orbital velocity exceeds the threshold limit of Komar & Miller (1975). At water depths in the embayment of 1.5 m, orbital velocities waves greater than 0.2 m are capable of exceeding sediment threshold velocities for silt sized sediment grains, less than 0.02 mm in diameter. However silt sized sediments are deposited in deeper water in the marina approach channel and offshore in the subtidal region where water depths are greater than 1.5 m, and so entrainment of sediment under these wave conditions offshore is rare.

The threshold of sediment motion will be exceeded more frequently in the shallower water depths on the intertidal flats than in the subtidal region offshore Pine Harbour Marina. At early stages of the tide the orbital motion at the bed due to wave breaking and turbulence in the shallow water depth may maximise sediment transport at this time rather than at high tide when water depth and wave heights are greatest. Sediment transport over the intertidal flats is discussed with reference to a fluorescent tracer experiment in Chapter 5.

4.6 Chapter summary

- Maximum tidal range at Pine Harbour Marina is 3.20 m. Highest spring tidal elevation relative to CD is 3.40 m and at neap tide 2.65 m. The tidal cycle is important in determining the duration, coverage, and depth of water over the intertidal flats, thereby limiting waves and currents in the area. At low tide fetch to the south is reduced from 4 km to 2 km. Maximum fetch of 10 km is to the north-west.

- Currents over the embayment are predominantly tidal. Stronger ebb tidal currents flow towards the northwest, and flood tidal currents flow in the reverse direction towards the south-east creating tidal asymmetry which produces a net current towards the north-west in the direction of the ebb tide. These current velocities are not capable of entraining sediment, but may transport sediment suspended in the water column to the north-west or south-east.

- Currents over the intertidal flats vary from those offshore due to the shape of the coastline and time over which the intertidal flats are inundated with water. Tidal currents appear to flow onto the intertidal flats towards the east, and drain off to the west with some water draining towards the channel with the ebbing tide. Tidal currents are weak over the intertidal flats but may be sufficient to transport sediment suspended in the water column by breaking waves. Wind driven circulation is important over the intertidal flats, creating a longshore current with prevailing south-westerly winds and an onshore surface current with westerly winds. The direction of the onshore current is changed by the local geomorphology. The chenier shell ridge extending across the northern intertidal flats from the Beachlands coastline to Motukaraka Island causes the onshore current to turn towards the south and flow longshore towards the marina approach channel.

- Calibration of the wave model WGEN3DD illustrated that linear theory equations for orbital motion under-estimate the actual measured orbital motion using intermediate and deep water waves, particularly at high frequency. An "effective depth" of 0.1 m was determined, which is the depth below the water surface where measurements and linear theory are in agreement. This effective depth is usually closer to the surface than the actual depth of the instrument. In this study it was found that the effective depth was 0.6 m higher in the water column than the instrument. This correction is similar to previous results for similar conditions (K. Black, pers. comm.).

- Sediment entrainment capabilities of waves vary with wave height, sediment grain size, water depth and sediment density. As wave orbital velocities are attenuated to the bed they decrease, and small wave heights have less impact upon the sediment than larger waves. Wave heights (H_s) between 0.1 and 0.5 m with wave period (T_s) of 1.5 s are insufficient to entrain sediment in 3.5 m water depth. As such sediment is rarely entrained by waves in the approach channel and subtidal region of the embayment. However, at shallower water depths of 1.5 m wave orbital velocities exceed threshold velocities of fine sediment less than 0.02 mm. Fine silt sized sediment in the subtidal region and in the marina approach channel may be entrained into suspension during low tide when water depths are shallower. Sediment entrainment is greatest on the intertidal flats. At early stages of the tide orbital motion due to wave breaking and turbulence has a greater effect on sediment grains on the bed due to the shallow water depths and may maximise sediment transport at this time.

- The wave climate at Pine Harbour Marina is controlled by a combination of wind speed and direction, and various controls exerted by the tidal height which determines fetch. As a result large waves occur infrequently. The wave climate offshore Pine Harbour Marina is characterised by waves with H_s = 0.1-0.2 m, and T_s 1.0-2.5 s. Large wave events are rare, but waves (H_s) up to 0.5 m and wave periods (T_s) of 2.5 s are generated by wind speeds (>10 m/s) from the northwest where fetch is greatest.

- Over the shallow water depths on the intertidal flats processes of wave shoaling and breaking are more important than they are offshore in the embayment. Significant wave heights (H_s) between 0.1 and 0.3 m and wave periods (T_s) between 1.5 and 3.5 s were predicted by WGEN3DD over the intertidal flats. Greatest waves (H_s) up to 0.81 m were generated by high wind speeds from the west and north-west. However wave heights are restricted by the water depth over the intertidal flats which is controlled by the tidal cycle. Greatest near bed orbital velocities and turbulence due to breaking waves occurs at early stages of the tide, maximising sediment transport at this time rather than when water depths over the intertidal flats are deepest at high tide. Greater sediment transport occurs over the intertidal region than the subtidal region because sediment threshold velocities are more frequently exceeded in the shallower water depths. Thus sediment deposited in the approach channel to Pine Harbour Marina is infrequently entrained as wave orbital velocities are attenuated before they reach the bed in deep water.

- Total wave power is directed alongshore towards the north by the prevailing southerly winds which occur for approximately 50% of the time (Table 4.2). Southerly winds generate waves (H_s) from the south and south-west between 0.1 and 0.3 m. During less frequent north-westerly winds, the greater effective fetch permits the generation of larger waves for similar wind speeds. The energy of the prevailing south-westerly wind creates wind driven circulation towards the north and generates high frequency waves from the south. These conditions have the greatest day to day impact on the Beachlands coastline and drive sediment transport in the littoral system north from Waikopua Creek to Motukaraka Island. However large infrequent storms from the north may produce a significant amount of net sediment transport towards the south over shorter time periods.

CHAPTER FIVE: SEDIMENT MIXING AND TRANSPORT: TRACER STUDIES & PROCESSES

5.1 *Introduction*

In order to anticipate impacts of nearshore structures which interrupt littoral transport it is desirable for coastal engineers and geomorphologists to be able to quantitatively predict sediment transport rates and pathways as a function of wave and current conditions. Sediment tracing is a useful technique in following the transport pathway of sand grains. This chapter describes an experiment in which sediment tracers are used to determine the patterns of sediment transport on the intertidal flats fronting Pine Harbour Marina. The patterns of sediment transport have direct implications for the dispersal of dredgings sediment dumped on the intertidal flats adjacent to the approach channel to Pine Harbour Marina during the 1994 dredging works.

5.2 *Fluorescent tracer experiment*

5.2.1 Background

Successful sediment tracing began in the mid 1950's with the advent of radioactive and fluorescent marking techniques. Prior to these techniques, the investigation of sand grain motion was possible only by mathematical model, or in laboratory flumes and wave basins where investigations were hampered by problems of scale and realism (Ingle, 1966). Beginning in the 1960's, sand tracers came into use to determine "instantaneous" littoral transport rates that could be related to relatively constant conditions of waves and currents (Komar, 1990). The use of radioactive tracers (e.g. Heathershaw & Carr, 1977) became unpopular with the public, and fell from favour in the 1960's. Komar and Inman (1970) used sand grains tagged with fluorescent dye to measure littoral sand transport rates quantitatively related to wave and current measurements. Since then most quantitative type experiments of longshore sediment transport rates in surf zones have involved sand marked with fluorescent colours (Kraus *et al.*, 1982; Inman *et al.*, 1980; Knoth & Nummedal, 1977).

The successful use of tracer sand to determine sediment transport rates relies on the two basic premises that the tracer behaves exactly in the same way as the native sand, and that the motion of the tracer centroid can be determined. The centroid velocity provides an estimate of the transport velocity, which when multiplied by the thickness of the moving sand, yields the transport rate (White and Inman, 1989). An assumption made in the tracer experiment is that the tracers do not change the characteristics of the transport system and that the tracers behave in the transport system as the native material whose transport rate is to be determined (Madsen, 1989).

Fluorescent tracer particles were used at Pine Harbour Marina in an attempt to mimic the sediment transport patterns of very fine sediment similar to dredgings material deposited on the intertidal flats adjacent to the approach channel during the dredging program from June to October 1994. The fluorescent tracer particles are manufactured from an artificial plastic substance by Environmental Tracing Systems in the United Kingdom. This particular tracer has not previously been used for tracer experiments in a New Zealand study. The tracer consists of environmentally benign artificial plastic particles, which are safe to humans and animals, that fluoresce bright orange under ultra-violet light.

During standard analysis, samples are returned for laboratory analysis using laser technology including an Analytical Flow Cytometer (AFC) which measures the number of non-fluorescent and fluorescent particles and the particle size. AFC offers high detectability and gives the concentration of tracer particles per unit area or volume. The tracer is highly durable because the properties that are used to detect the tracer are not just a coating on the outside of the grain, as with conventional tracers such as sediment grains tagged with fluorescent colour.

Properties of the artificial fluorescent tracer can be varied to suit the conditions being monitored. The tracer used at Pine Harbour Marina consisted of very fine sand and silt sized particles ranging in size from 3.0 to 6.0 phi (0.1-0.01 mm). The mean grain size of tracer particles was 3.6 phi (0.085 mm) and was similar to the dredge spoil deposited on the intertidal flats which had mean grain size of 4.0 phi (0.063 mm). The tracer particles and dredge spoil sediment were finer than the natural sediment on the intertidal flat which had a mean grain size of 2.5 phi (0.177 mm). Fluorescent particles used in the experiment trace the transport direction, and rate of transport of fine sand and coarse silt sized sediment over the intertidal flats which are used to infer the direction and rate of dredgings sediment dispersion on the intertidal flats.

5.3 Methodology

Test releases, using 1 kg of fluorescent tracer, were undertaken in order to determine the best method to release the tracer on to the intertidal flats, and to give an indication of the amount of movement of tracer that could be expected to help in the design of a sampling system. The test release took place in a few centimetres of water. Some tracer remained dry, floating on the surface of the water moving onshore with the prevailing south-westerly wind. Tracer particles that settled in the test release was observed to move with the bedload towards the south-west. The tracer moved, in both directions, up to 50 m from the test release site.

On 20/12/94, a tracer release site was selected approximately 100 m to the north of the dredgings on the northern side of the approach channel to Pine Harbour Marina (Figure 5.1). 6.5 kg of fluorescent tracer (0.1-0.01 mm) was mixed with approximately an equal volume of natural sediment and a generous amount of detergent, to act as a wetting agent, in water until thoroughly mixed (Plate 5.1). The tracer and natural sediment mixture was then spread approximately 1-3 cm thick, within a 5 m radius of a central stake. A surface sample of the top 2-3 cm was taken to determine the initial concentration of tracer.

PLATE 5.1: Release site of fluorescent tracer particles mixed with natural sediment and spread up to 3.0 cm over surface of the intertidal flats around a central stake. Finer tracer particles can be seen floating on water ponded between ripples.

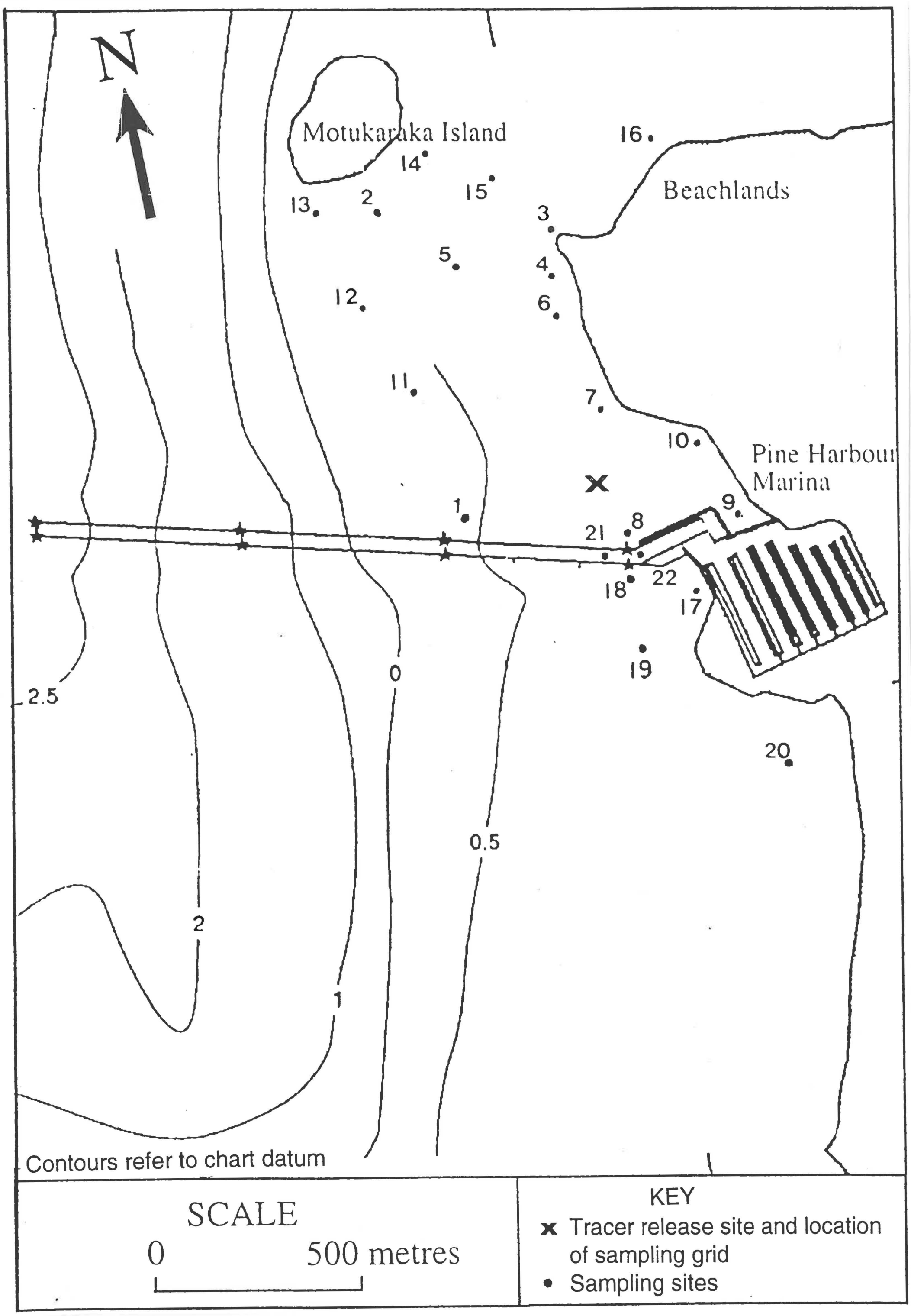

FIGURE 5.1: Location of tracer release site (indicated by X) on the sandflats to the north of the approach channel to Pine Harbour Marina. Intensive sampling grid is located around the release site (refer to Figure 5.2) and further ranging sampling sites are numbered 1 to 22.

A sampling system, in which 17 samples were collected, was set up based on the observations of how far the tracer moved in test releases (Figure 5.2). Spot samples 1 to 10, were taken at further ranging sites. These were increased towards the end of the experiment in a far ranging search for fluorescent tracer (samples 11 to 20). Samples were collected on the 21/12/94 am, 21/12/94 pm, 22/12/94, 23/12/94, 27/12/94, and 10/1/95. Two channel samples were collected on 17/1/95 (samples 21 and 22). Further to this, the sampling of the grid and spot samples was repeated on 27/2/95.

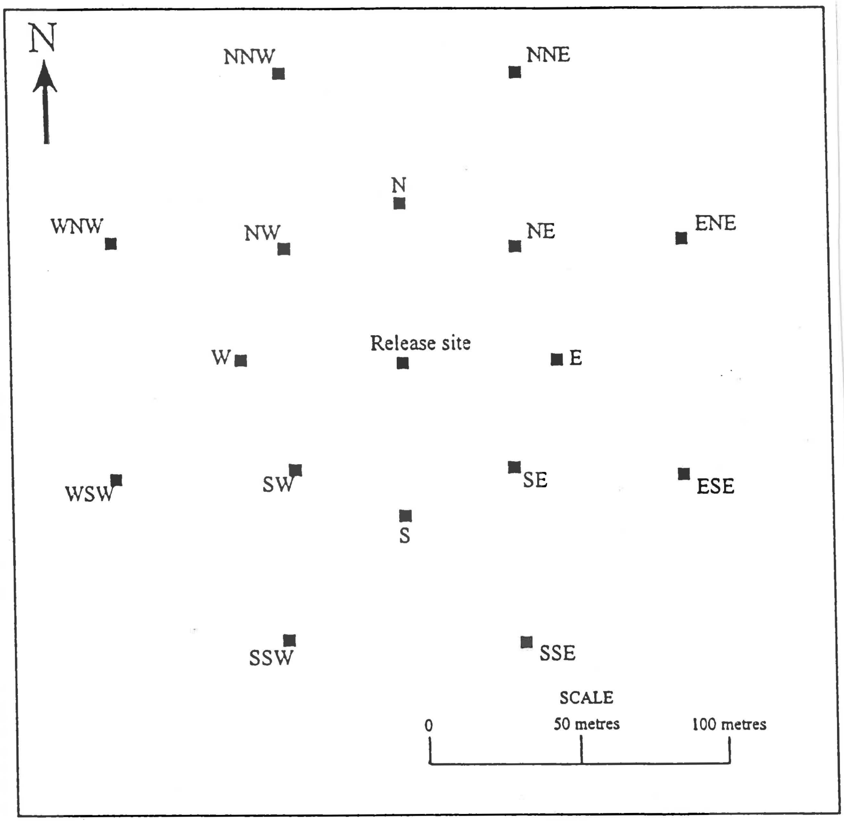

FIGURE 5.2: Sampling grid for collection of tracer samples centred around tracer release site. Samples taken at every 22.5° around the compass, at alternating distances 50 m and 100 m from the release site indicated by small boxes.

Approximately 500 g of sediment was collected from the top 2.0-3.0 cm of sediment, encompassing the aerobic layer which was assumed to be the depth of the mobile layer or depth to which tracer is mixed by bedforms under wave action. Sedimentation rods (discussed previously in Chapter 3) indicated that sediment was disturbed to depths of about 2.0 cm. Sediment cores, 10 cm diameter and 20 cm long, were taken at the release site on each sampling. Cores were frozen, to prevent disturbance during transport to the laboratory for determination of maximum mixing depths of tracer.

Samples were washed through a 2 mm mesh sieve with freshwater to remove salt crystals, and all sand and mud collected in a tray below. The gravel sized particles and shells were disposed of after being thoroughly rinsed and examined under the UV light to ensure no fluorescent tracer remained on them. Excess water was decanted off the samples, which were then dried for at least 24 hours in an oven at 45-60 °C. Dry samples were sieved through a 2 mm mesh sieve to disaggregate particles. The sample was mixed uniformly, and a 100-200 g subsample was taken. The standard method for determining the concentration of fluorescent tracer particles contained in each sample is to analyse the sediment in an analytical flow cytometer (AFC). However AFC analytical equipment was unavailable for the processing of sediment samples from this tracer experiment, necessitating a revised method for determining fluorescent tracer concentrations, in which a sediment sub-sample was spread in a thin layer under ultra violet (UV) light, and the number of fluorescent particles per sample counted. Where tracer concentrations were extremely high a smaller subsample was taken to reduce the error in counting a large number of grains. Concentration were expressed as the number of fluorescent grains per kilogram.

5.3.1 Accuracy of determining tracer concentrations

To compare the accuracy of the UV light method to standard AFC analysis, 20 samples were sent to the manufacturers of the fluorescent tracer (Environmental Tracing Systems, United Kingdom) for comparison of results. Regression analysis of the results obtained via the two different methods indicated that there was no correlation between the methods, and that UV light analysis did not accurately detect tracer particles (Figure 5.3).

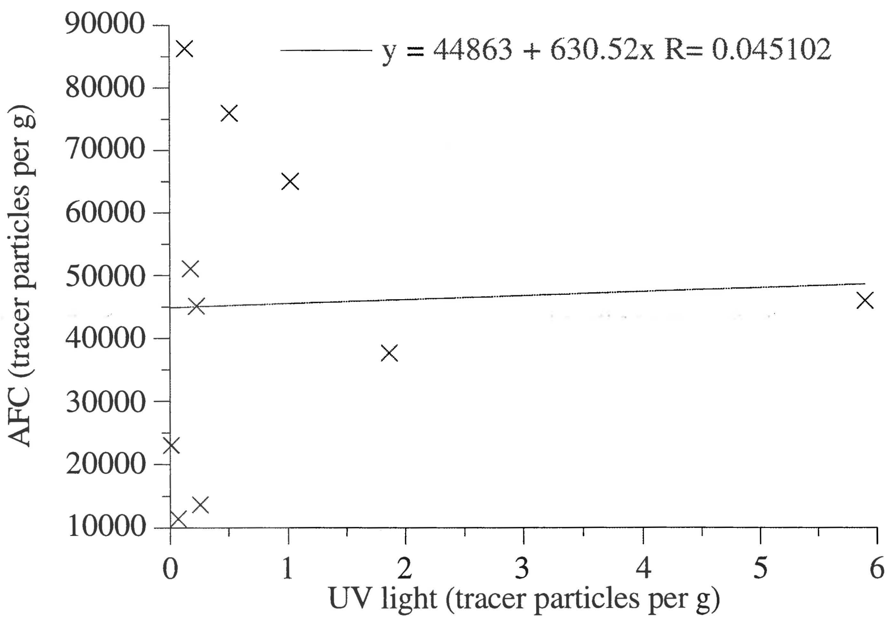

FIGURE 5.3: Regression analysis of tracer particle concentrations (particles per g) detected through UV light method and AFC analysis.

AFC grain size distribution of tracer particles in sediment samples revealed that the majority of tracer particles were very fine (<0.05 mm) and undetectable with the naked eye (Appendix 5.1). Concentration of tracer particles were determined per grain size class under UV light, after 20 samples were sieved into half phi size classes from 1.0 to 4.0 phi (0.5-0.06 mm). The majority of the tracer particles were finer than 4 phi (0.06 mm) (Figure 5.4). Higher concentrations of tracer particles were detected with UV analysis when samples were divided into grain size classes, highlighting discrepancies in the reproducibility of the UV light method. This may be a factor of fine tracer particles in the bulk sample being masked by the larger sediment grains and the difficulty in seeing particles smaller than 4.0 phi (0.06 mm). Coarser tracer particles were most easily seen by the eye and it is assumed that results from the bulk UV light method reflect transport patterns of coarser tracer particles.

The comparison of analysis techniques indicated that results obtained through the UV light method were not representative of the total tracer concentration. However these results were considered to be an approximation of the coarse grained tracer concentrations, based on the assumption that fine tracer particles were undetectable by the naked eye, and the results where used to give an indication of the direction of coarse sediment grain transport but could not be used in the calculation of the transport rate of tracer. Calculation of mass transport rates requires accurate tracer particle concentrations from AFC analysis. Therefore a further 50 samples were selected for AFC analysis in the UK to yield time series concentrations of tracer particles for a number of sites and better grid coverage to map tracer dispersion from the release site.

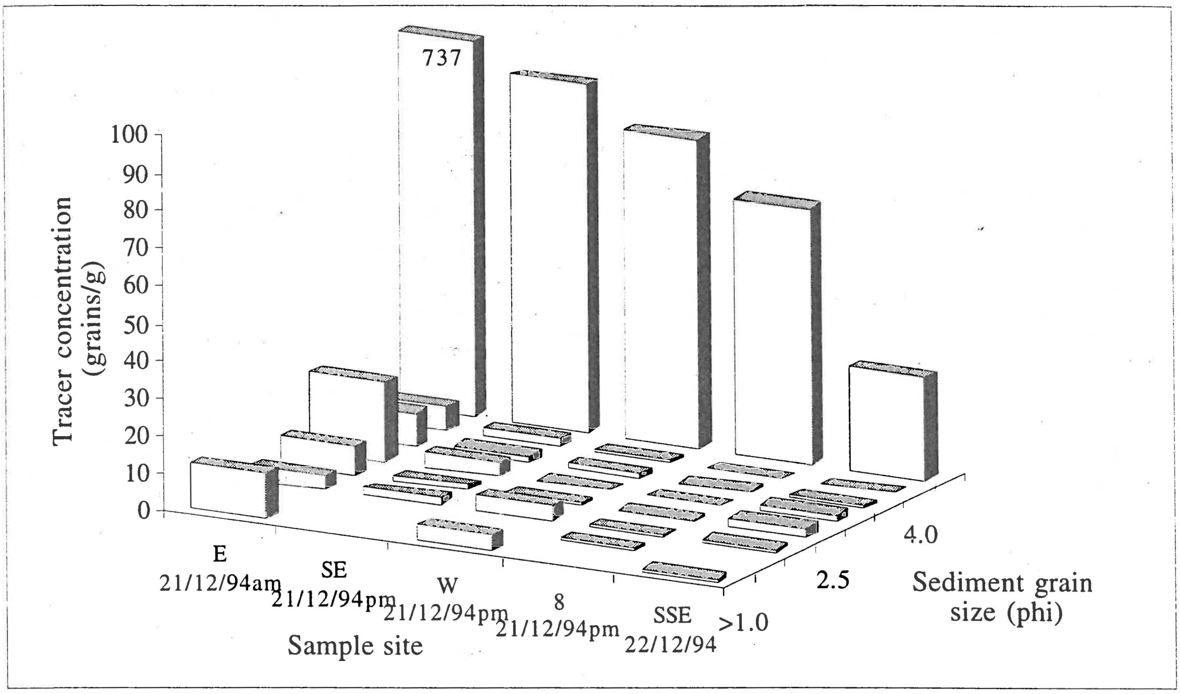

FIGURE 5.4: Concentration of tracer particles (grains per gram) detected in grain size divisions under UV light.

5.4 Sediment mixing depths

Two sets of experiments were undertaken to determine the mixing depths of sediment on the intertidal flats. These investigations included determining the vertical mixing of fluorescent tracer particles, and a mixing depth experiment using plugs of dyed sediment inserted into the intertidal flats.

5.4.1 Vertical mixing of fluorescent tracer particles

Sediment cores (10 cm diameter and 20 cm in length) were taken at the tracer release site coincident with sampling for fluorescent tracer over the intertidal flats. Cores were transported back to the laboratory where they were split lengthways and examined under UV light to determine the maximum depth to which tracer was mixed.

A further four cores were taken on 21/8/95, at distances 0, 50, 100, and 150 m south-east of the release site to determine vertical concentrations of tracer particles over a longer time period. Cores were split into 2 cm segments and analysed under UV light to determine the concentration of tracer particles in each segment. AFC analysis was also undertaken by Environmental Tracing Systems on 1 core from the release site on 21/8/95.

5.4.2 Depth of mixing of dyed sediment

An experiment to investigate the depth of sediment mixing on the intertidal flats was undertaken in March 1995. Sediment from the intertidal flats was dyed pink according to the methodology of Kench (1990). Plugs of the dyed sediment were inserted into the intertidal flats at various distances (50, 100, 150 and 200 m) offshore from the western breakwater on the southern intertidal flats. This was accomplished by driving a plastic core (10 cm diameter and 20 cm long) into the intertidal flat and removing the natural sediment from inside the core. The core was then refilled with the pink dyed sediment, and the plastic core encasing the sediment was removed leaving the dyed plug of sediment flush with the natural sediment surface on the intertidal flats.

Plugs were sampled on subsequent days to record the depth of sediment mixing. This was determined from the amount of natural sediment overlying the pink dyed sediment. Sampling involved coring the plugs of dyed sediment with a clear plastic syringe (1.5 cm diameter, 10 cm in length). The amount natural sediment overlying the pink sediment was clearly evident through the clear plastic of the syringe and represented the depth of sediment mixing. The thickness of natural sediment over the pink dyed sediment was measured.

5.4.3 Results

Similar depths of mixing were measured in the two sets of mixing depth experiments. The depth of tracer mixing determined with UV light increased with time after fluorescent tracer release, reaching maximum vertical mixing depth of 2.5 cm on 27/2/95 (Figure 5.5). The dyed sand mixing depth experiment also recorded a maximum depth of sediment mixing of 2.5 cm (Figure 5.6). Sediment mixing depth was greater closer to shore. This may be due to the increased turbulent energy in the breaking wave zone at high tide.

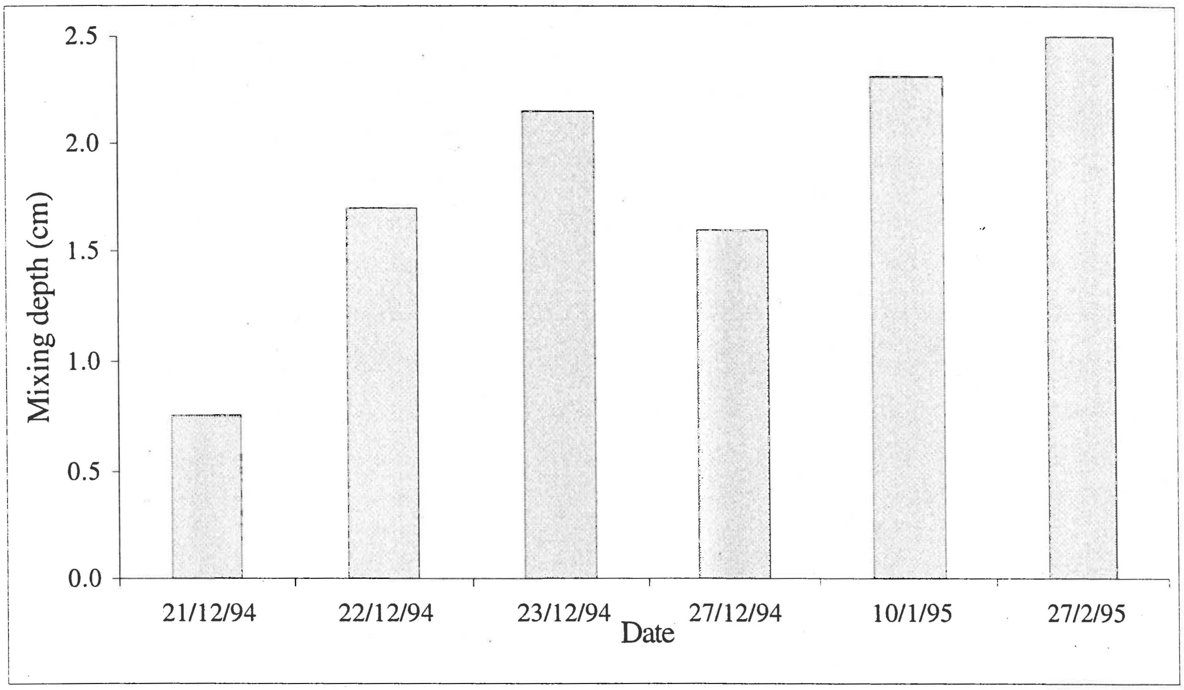

FIGURE 5.5: Depth of vertical mixing of tracer particles at release site from 21/12/94 to 27/2/95.

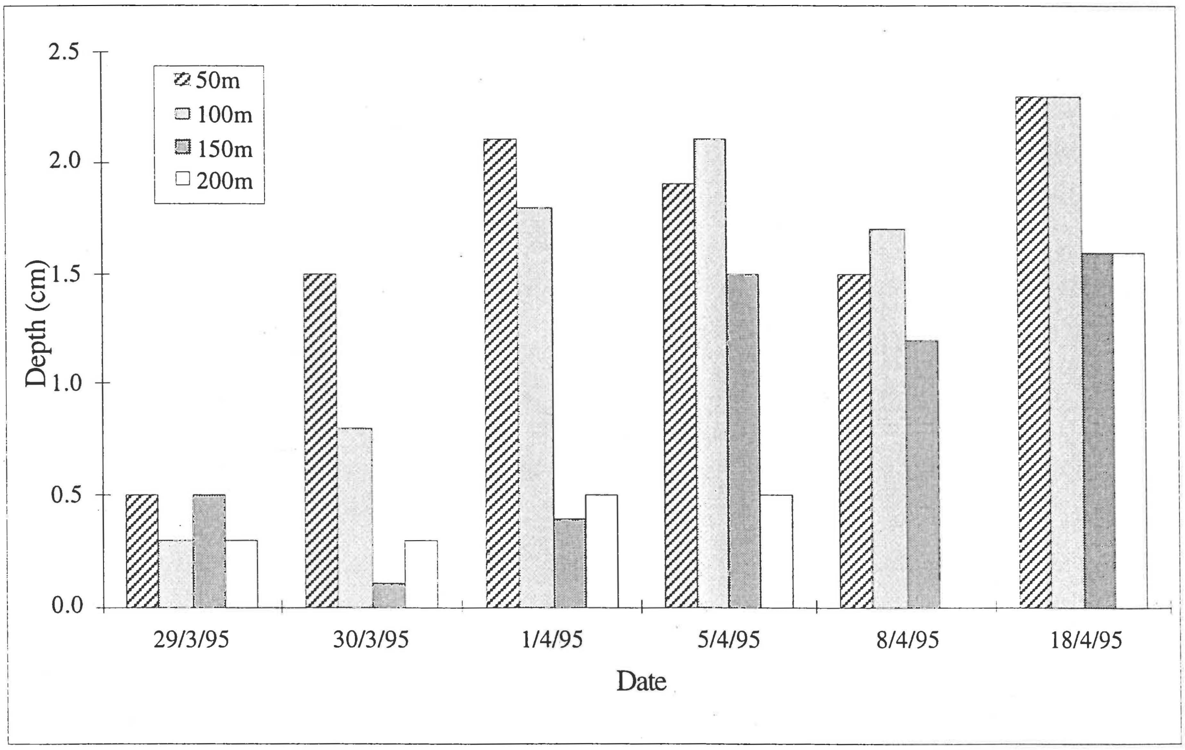

FIGURE 5.6: Cross shore variations in sediment mixing depth determined from plugs of dyed sediment from 29/3/95 to 18/4/95.

Cores taken at progressive distances from the release site were analysed with UV light and indicated that highest concentrations of tracer particles were found in the upper 2-4 cm of the core at the release point and tracer particles were detected to a maximum depth of 12 cm at this site (Figure 5.7). Vertical mixing of fluorescent tracer decreased with distance from the release site.

Tracer particles detected using UV light method are assumed to be representative of the coarse tracer grains only. Analysis of the release site core with AFC revealed tracer mixing to greater depths and in higher concentrations. Using AFC detection, greatest concentration of tracer particles occurred between 13 and 17 cm depth at the release site on 21/8/95 (Figure 5.8). Most of the tracer particles detected with AFC at depths greater than 10 cm are assumed to be very fine particles as they were not detected in UV analysis.

Sediment mixing depths in the order of 2.5 cm are similar to mixing depths recorded by sedimentation rods installed along the intertidal flats (Figure 3.26). Mixing depths were generally less than 1.5 cm due to shallow disturbance created by ripple movement (h = 1.0-1.5 cm). Depth of sediment disturbance at sedimentation rods increased to between 2.0 and 3.0 cm associated with storm periods. The maximum sediment mixing depth recorded by sedimentation rods was 6.2 cm on the northern intertidal flats which is exposed to higher wave energy from infrequent north-westerly storms.

Sediment moves both horizontally and vertically under the combined influence of physical and biological processes on the intertidal flats. Bedforms observed on the intertidal flats have an average height of 1.0-1.5 cm and 3.0-6.0 cm wavelengths (Appendix 1.1). These bedforms do not account for the maximum mixing depth of tracer particles of 17 cm measured at the release site. Likewise sediment mixing depths recorded by sedimentation rods were between 1.0-6.2 cm, indicating that mixing to depths of 17 cm cannot be attributed to wave action, and it is assumed that biological activity is responsible for the majority of deeper vertical mixing of sediment at the release site and over the entire intertidal sand flats. The 2.0-3.0 cm light coloured aerobic layer of sediment is the most obvious indicator of the activities of bioturbators and benthic feeding organisms ingesting and reworking sediment. Short term mixing is dominated primarily by wave action and bedform migration mixing in the top few centimetres. Biological organisms are the dominant mechanism of sediment mixing in the long term mixing tracer to greater depths by reworking the sediment. Coarse grains may be more inactive biologically with fine grains preferentially ingested by bioturbators reworking the sediment, and fine particles may be preferentially ingested by infauna.

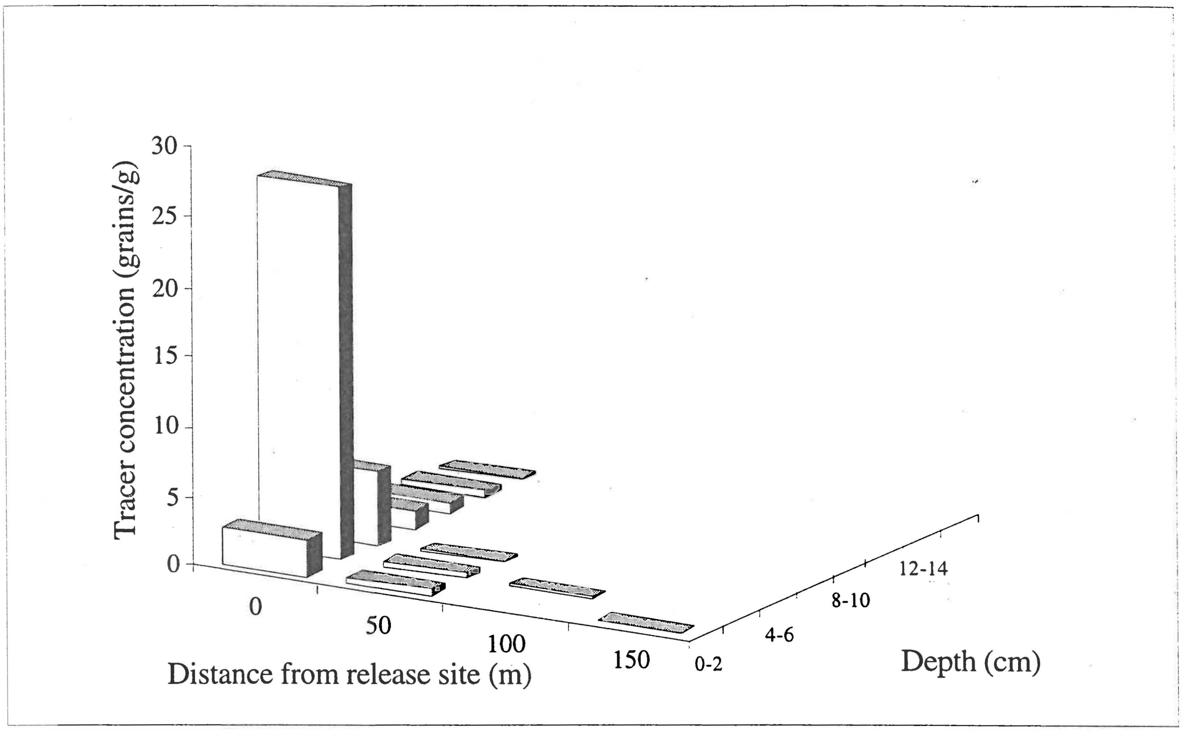

FIGURE 5.7: Depth of vertical mixing of tracer particles, determined with UV light, in cores taken at distances 0, 50, 100 and 150 m along a transect south-east of the tracer release site, 21/8/95.

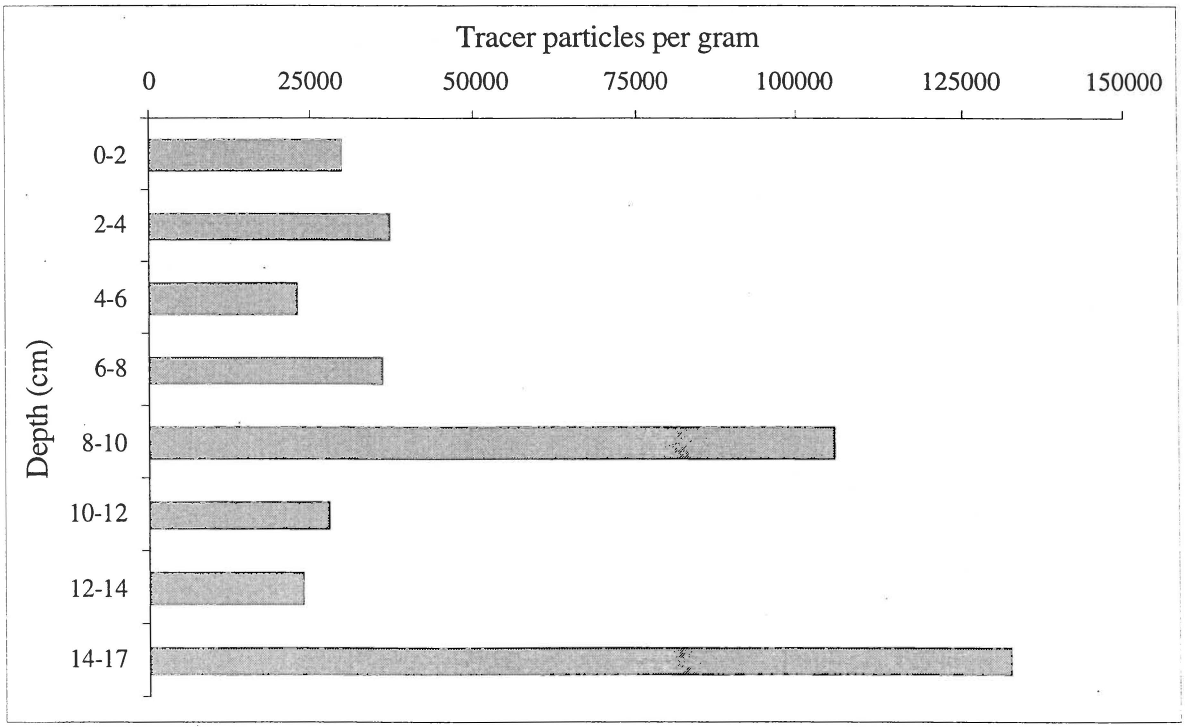

FIGURE 5.8: Depth of vertical mixing of tracer particles at release site 21/8/95, determined by AFC.

5.5 Wind, waves and currents during the tracer experiment

To monitor wave and current conditions for the duration of the tracer experiment, a S4ADW InterOcean current meter was deployed in 3.4 m water depth at Site 1 (Figure 4.1). The current meter deployment site was selected to ensure the operation of the instrument. S4 current meter measurements were not made on the intertidal flats because exposure of the current meter at low tide increased the risk of interference. An S4ADW InterOcean current meter was deployed from 23 November 1994 to 20 December 1994, and was replaced with an S4 InterOcean current meter in the same location from 20 December 1995 to 29 December 1995. With the data for confirmation the wave generation model WGEN3DD (Black & Rosenberg, 1992) was used predict the wave conditions at the tracer site for the duration of the experiment on the intertidal zone.

5.5.1 Wave conditions

Wave heights predicted for the tracer site on the intertidal flats exceed 0.3 m less than 10 % of the measurement period from 23/11/94 to 17/1/95. Significant wave heights (H_s) at the tracer site are less than 0.1 m for approximately 25 % of the measurement period. For nearly 75% of the measurement period waves were less than 0.25 m, generated by wind speeds less than 6 m/s. During this period, locally generated sea waves were dominated by frequent (30% of measurement period) southerly winds (from 135° to 225°) (Table 4.2). Significant wave periods (T_s) predicted for waves over the intertidal flats are between 1.5 and 3.5 s.

Prevailing winds for the duration of the sediment tracer experiment were from the west and south-west (200° to 290°), with wind speeds up to 15 m/s recorded from the west as two storm events passed over the region on 22/12/94 and 25/12/94 (Figure 5.9 & 5.10). Time series of significant wave heights predicted at the tracer site for the corresponding 10 day period indicate that periods of high wind speeds from the west (250° to 290°) increased significant wave heights up to 0.6 m at the tracer site (Figure 5.11).

During the period of high westerly winds on 22/12/94 and 23/12/94 wave orbital velocities, which are a function of wave height, also increased to between 30 cm/s and 55 cm/s (Figure 5.12). Near bed orbital velocities predicted by WGEN3DD for the period between 20/12/94 and 17/1/95 (Julian days 354 to 379) were between 10 cm/s and 20 cm/s for the majority of the measurement period (Figure 5.12). At early stages of the tide the orbital motion at the bed and turbulence due to breaking waves in the shallow depth may maximise sediment transport at this time rather than at high tide when the water depth is greatest. In a review of the distribution of longshore sediment transport across the surf zone Bodge (1989) also identified that greater sediment transport is often associated with shallower depths.

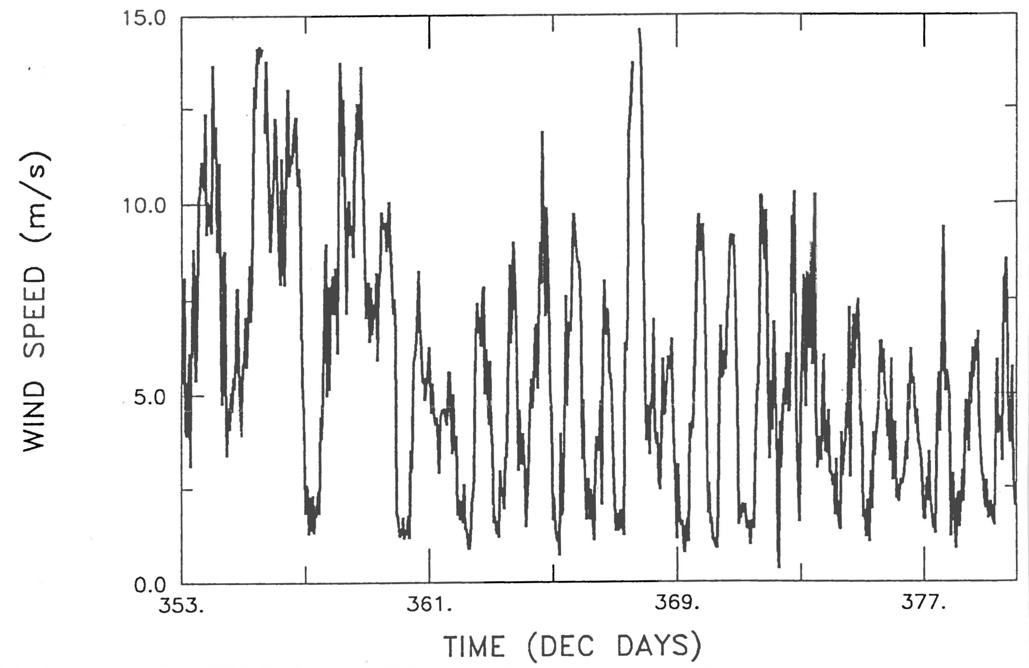

FIGURE 5.9: Time series of wind speed recorded at Pine Harbour Marina from 20/12/94 to 29/12/94, indicating the passing of two storm events with wind speeds up to 15 m/s.

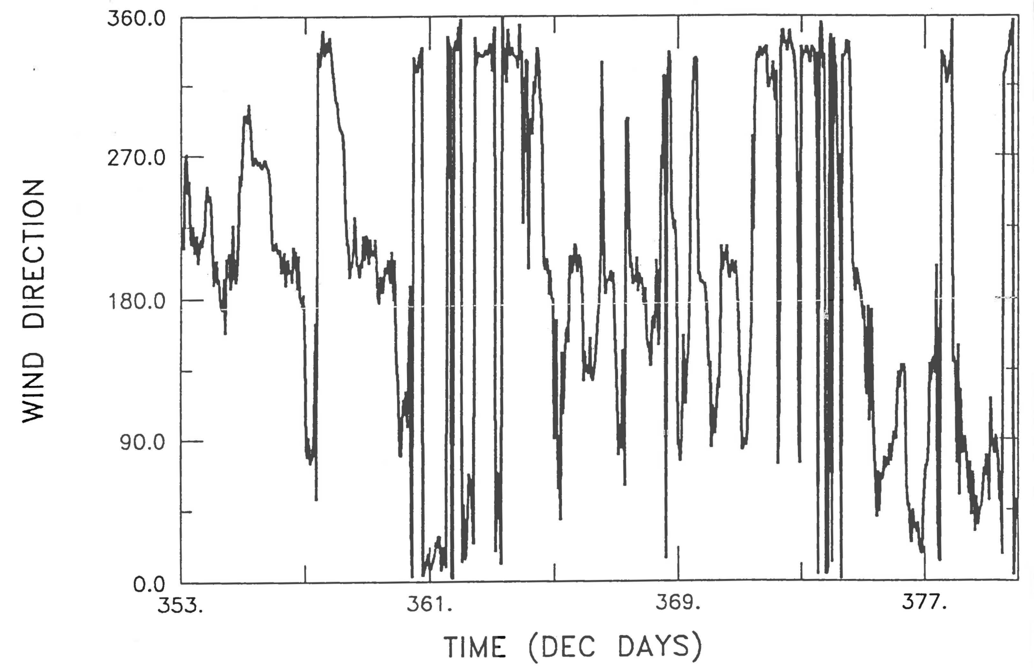

FIGURE 5.10: Time series of wind direction recorded at Pine Harbour Marina, 20/12/94 to 29/12/94 indicating high wind speeds correspond to winds from the west.

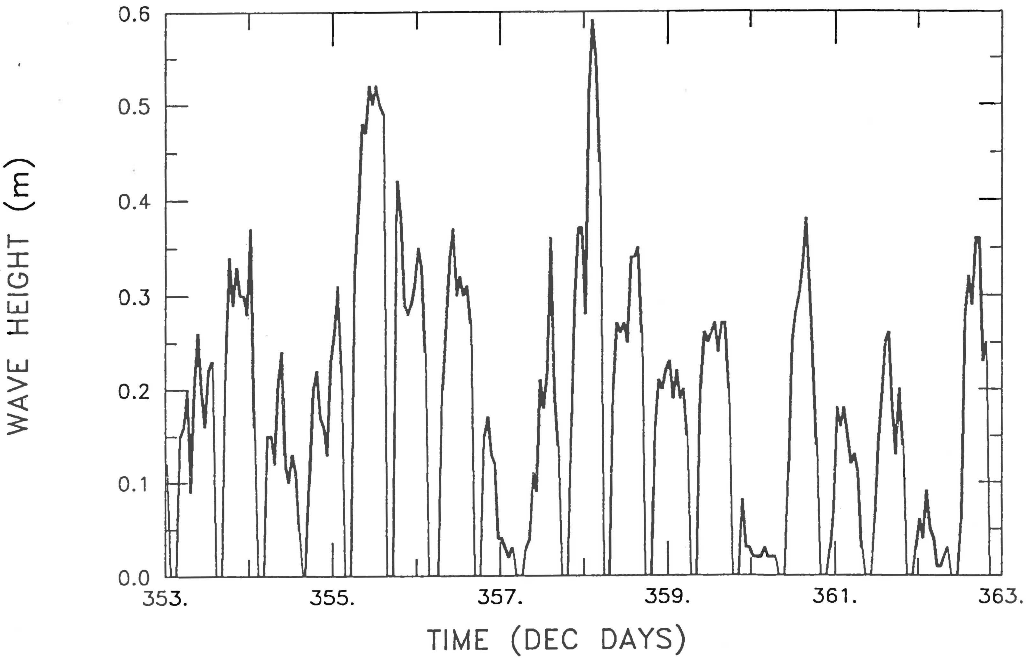

FIGURE 5.11: Significant wave heights predicted by WGEN3DD on the intertidal flats fronting Pine Harbour Marina from 20/12/94 to 29/12/94.

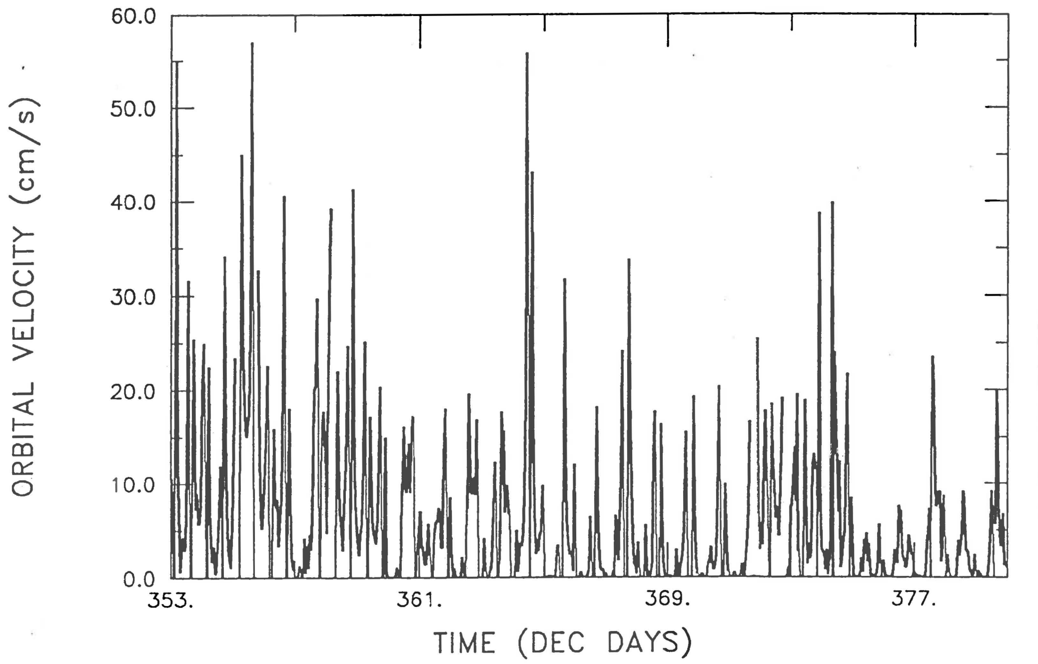

FIGURE 5.12: Near bed wave orbital velocities predicted by WGEN3DD for waves predicted at tracer site on intertidal flats fronting Pine Harbour Marina from 20/12/94 to 17/1/95 (Julian day 353 to 379).

Komar & Miller (1975) developed a curve to predict the threshold velocities of sediment grain sizes under conditions defined by wave period and orbital velocity (Figure 4.25). Threshold velocities of fine sand and coarse silt are not addressed in detail in these predictive curves, however it is interpreted that the mean tracer particle size of 0.085 mm has a near bed threshold velocity of around 10 cm/s. In comparison the threshold velocity of sediment from the intertidal flats with a mean grain size of 0.2 mm is 18 cm/s.

The threshold velocity for entrainment of tracer particles was exceeded for approximately 75% of the period for which WGEN3DD predicted wave conditions at the tracer site on the intertidal flats fronting Pine Harbour Marina. In comparison the threshold velocity sand on the intertidal flat was exceeded for about 45% of the measurement period. Thus, the tracer would have been entrained more often than natural sand.

5.5.2 Currents

The vector plot of S4 current measurements offshore at Site 1 in Figure 5.13 indicates alternating current directions, aligned 135°-315°, controlled by the tidal cycle. Generally ebb tidal currents flowing longshore towards the north-west are faster than flood tidal currents towards the south-east. However in the period coinciding with high wind speeds, on 22/12/94 and 23/12/94 (Julian days 355 and 356) and 26/12/94 (Julian day 359), currents directed towards the south and south-east increased and the longshore north-west current reduced. This may due to wind driven circulation in the embayment.

Current measurements recorded offshore cannot be directly translated onto the intertidal flats, but they can be used as an approximation of the direction of current flow over the intertidal flat region and speeds are likely to be less. With no direct current measurements on the intertidal flats it is presumed that wind from the west creates an onshore current which is turned towards the south by the curved chenier shell ridge extending across the intertidal flats from Beachlands coastline to Motukaraka Island restricting the flow of water north. The effect of the westerly wind driven circulation enhances currents flowing towards the south-east at early stages of the tide and opposes the longshore north-western current created as the tide ebbs, as recorded at the current meter site.

At Pine Harbour Marina the outgoing tide drains off the northern intertidal flats into the approach channel and may transport suspended sediment south with this flow. Wind driven circulation in the embayment and over the intertidal flats is an important mechanism by which entrained sediment is transported. Sediment is transported longshore towards the north-west under prevailing south-westerly winds, and in the opposite direction when west and north-westerly winds create an onshore current which is altered by the local topography to flow south towards the approach channel to Pine Harbour Marina.

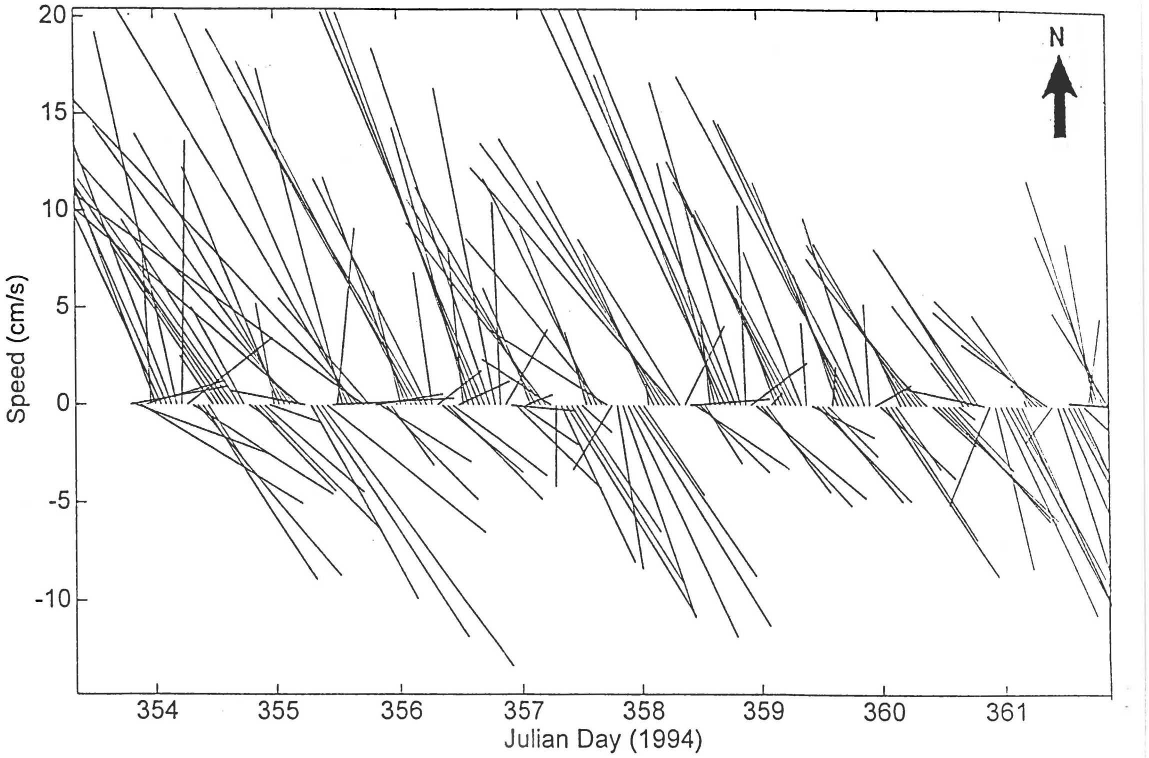

FIGURE 5.13: Vector plot of total currents measured by S4 electromagnetic current meter at Site 1, Pine Harbour Marina from 21/12/94 to 29/12/94 (Julian day 354 to 361).

5.6 Results

5.6.1 UV light analysis

The net direction of coarse tracer particle movement was determined by plotting the spatial distribution of tracer particle concentrations, detected through bulk UV light analysis, onto a grid centred about the release site. Contouring of the concentrations of tracer revealed the dominant direction of coarse tracer particle transport during the experiment was towards the south and south-east (Figure 5.14). At later stages in the tracer experiment coarse tracer particles began to show dispersion towards the north.

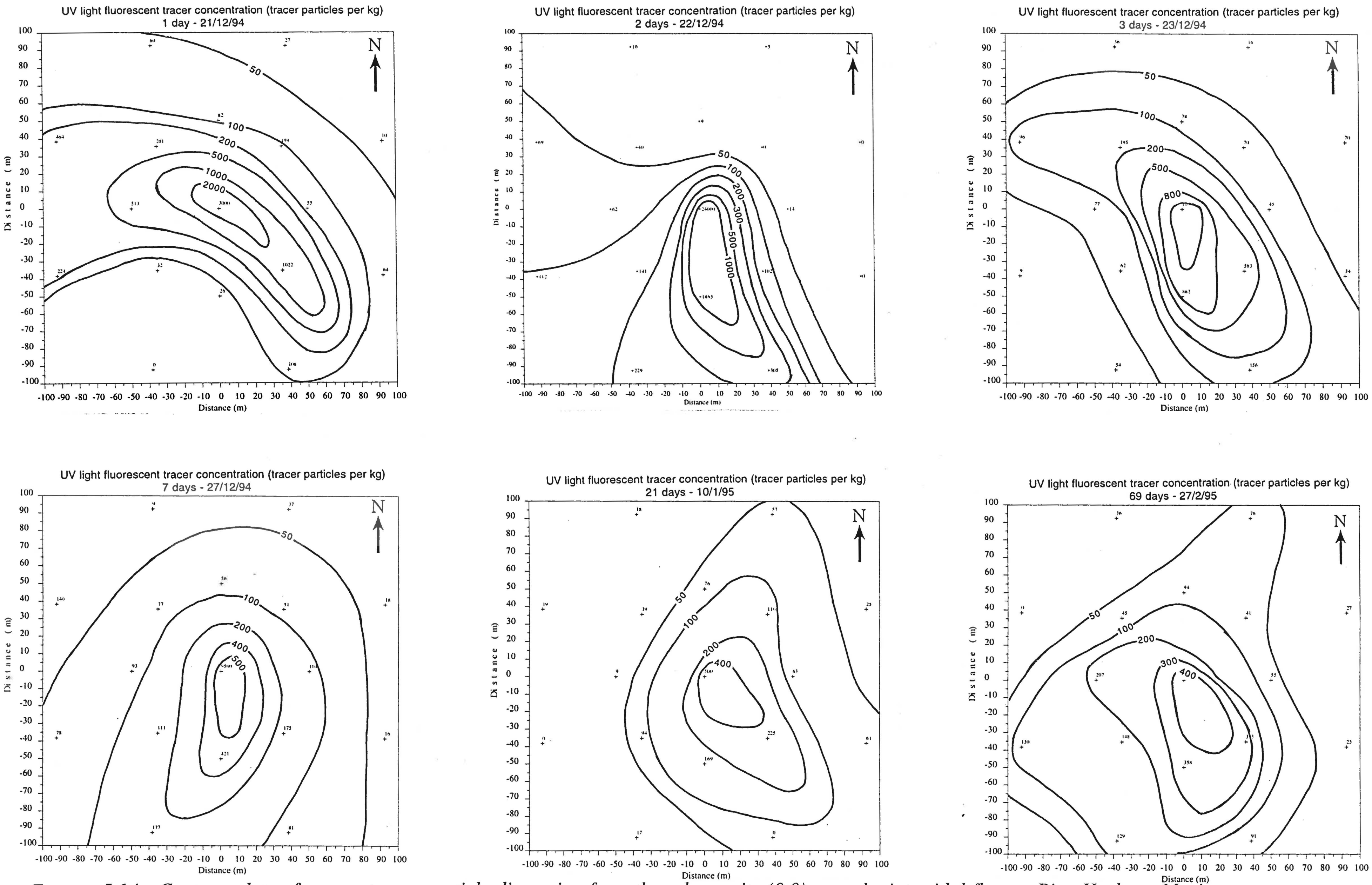

FIGURE 5.14: Contour plots of coarse tracer particle dispersion from the release site (0,0) over the intertidal flats at Pine Harbour Marina from 21/12/94 to 27/2/95.

5.6.2 AFC analysis

AFC analysis results are representative of the entire tracer particle size range and are preferred over the bulk UV analysis results which detect only coarse tracer particles. The UV light system may be indicative of the transport of natural sands which are coarser than the tracer particles. AFC analysis was undertaken on 60 samples to give the exact quantity of fluorescent and non-fluorescent particles in each sample, expressed as a concentration of tracer particles per gram. Results of UV light and AFC analysis are compiled as Appendix 5.2.

Tracer particle dispersion patterns from AFC results for 23/12/94 are illustrated in Figure 5.15 and indicate that the tracer centroid moved at least 100 m to the south-southeast within 3 days of injection. On 27/2/95 the tracer centroid was detected to have migrated towards the south-west, and tracer particle concentrations in the north began to increase (Figure 5.16). A simple statistical diffusion coefficient was calculated for each spatial sampling day which assumed that there was no spatial bias in the movement of tracer (eqn. 5.1). In the calculation each grain is considered as an occurrence, therefore the total number of occurrences was obtained by summing over all tracer grains. The diffusion coefficient is non directional and was calculated from the standard deviation of the sampling site relative to the release point, weighted by the number of tracer particles at the site, and divided by the time since tracer release. The diffusion coefficient is an indication of the rate of tracer dispersion. Thus,

$$D_{x,y} = \frac{\sum_{i=1}^{N} M\left(\mathrm{x}_{\mathrm{i}} - \overline{\mathrm{x}}\right)^2}{2\Delta t.\sum_{i=1}^{N} M} \qquad (5.1)$$

where M is the number of tracer particles (grains); $(\mathrm{x}_\mathrm{i} - \overline{\mathrm{x}})$ is the distance (m) from the tracer injection site; and t is the time lapse since tracer injection (days).

A diffusion coefficient was obtained for spatial data from 23/12/94 and 27/2/95. Diffusion coefficient was equal to 1270.43 $\mathrm{m^2 day^{-1}}$ three days after tracer release, and decreased to 76.49 $\mathrm{m^2 day^{-1}}$ after 69 days. The diffusion coefficients indicate that tracer dispersed rapidly soon after release as tracer was primarily dispersed horizontally across the sediment surface. During later stages, the reduced diffusion coefficient means that tracer movement slowed after reaching an equilibrium level of widespread dispersion after which there was minimal net sediment transport.

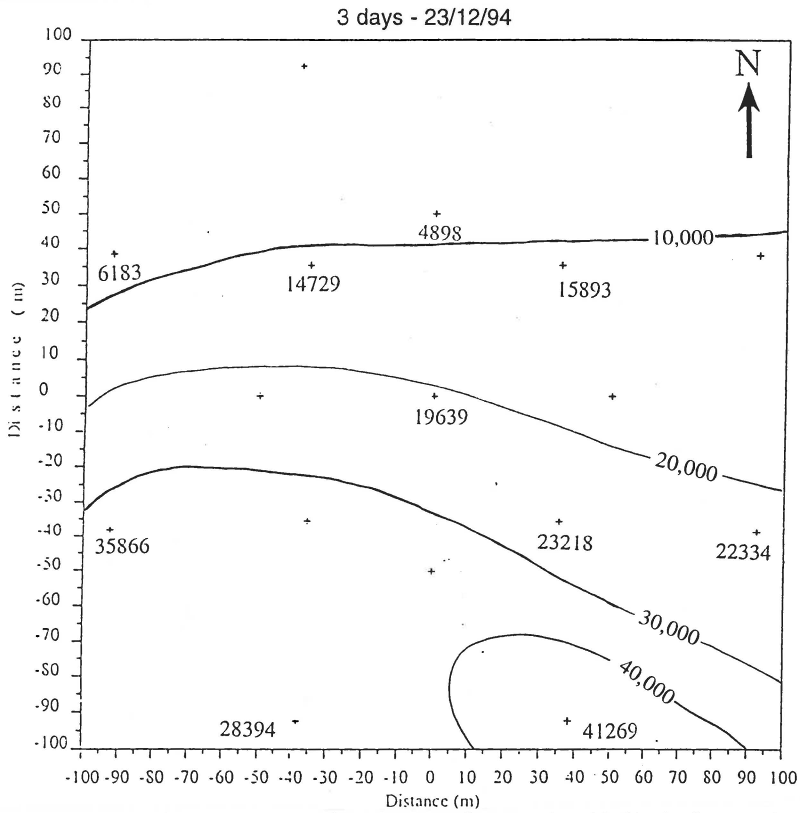

FIGURE 5.15: Dispersion of tracer particles from release site (0,0) 3 days after tracer injection on intertidal flats at Pine Harbour Marina on 23/12/94.

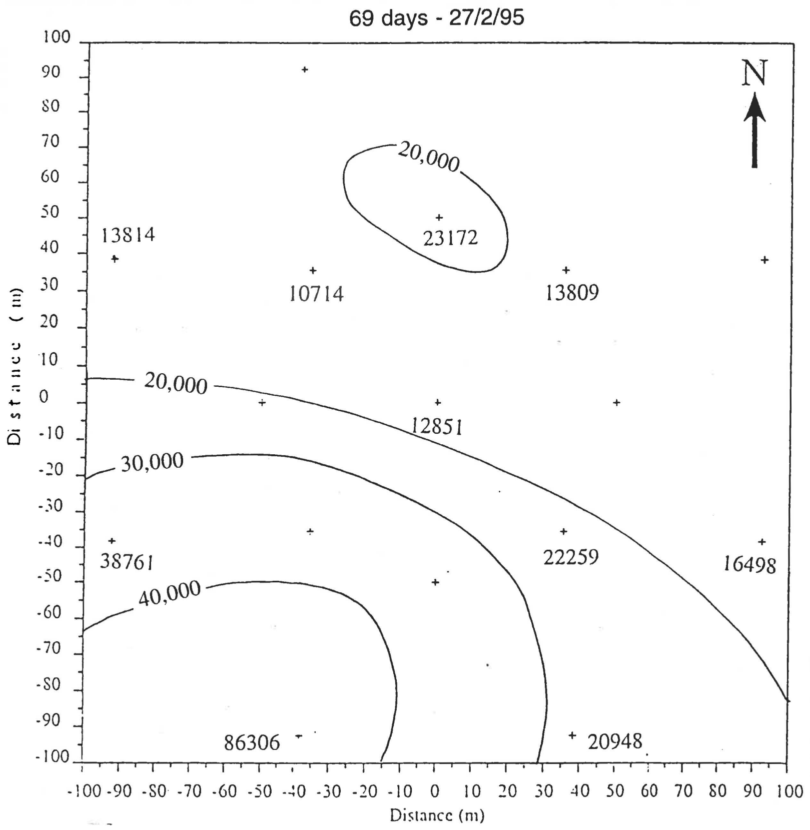

FIGURE 5.16: Dispersion of tracer particles from release site (0,0) 69 days after tracer injection on intertidal flats at Pine Harbour Marina on 27/2/95.

Time series of AFC tracer concentrations at 3 sites sampled over the duration of the tracer experiment are presented in Figure 5.17. The number of tracer particles at the release site (0,0) decreased rapidly in a short time after release. The rate of dispersion of tracer particles from the release site slowed with time as relative changes in concentration became less. This was also indicated by the decrease in diffusion coefficient from 1270.43 m^2day^{-1} to 76.49 m^2day^{-1} from 23/12/94 to 27/2/95. Tracer concentrations fluctuate at sampling sites located 50 m north and 100 m south-southwest of the release site, exhibiting a series of peaks in tracer concentration rather than a uniform change through time. This may represent the transportation of sand tracer in pulses along the intertidal flats associated with bursts of energy associated with increases in wave activity.

The fluctuating pattern of tracer accretion and loss at sampling sites suggests that there was little net sediment transport over the intertidal flats once the tracer particles initially dispersed and reached an equilibrium distribution over the area. Tracer concentration at the release site one year after tracer injection on 20/12/95 was similar to the concentration of tracer grains recorded 10 months earlier on 27/2/95, suggesting negligible net sediment transport from the site in the long term.

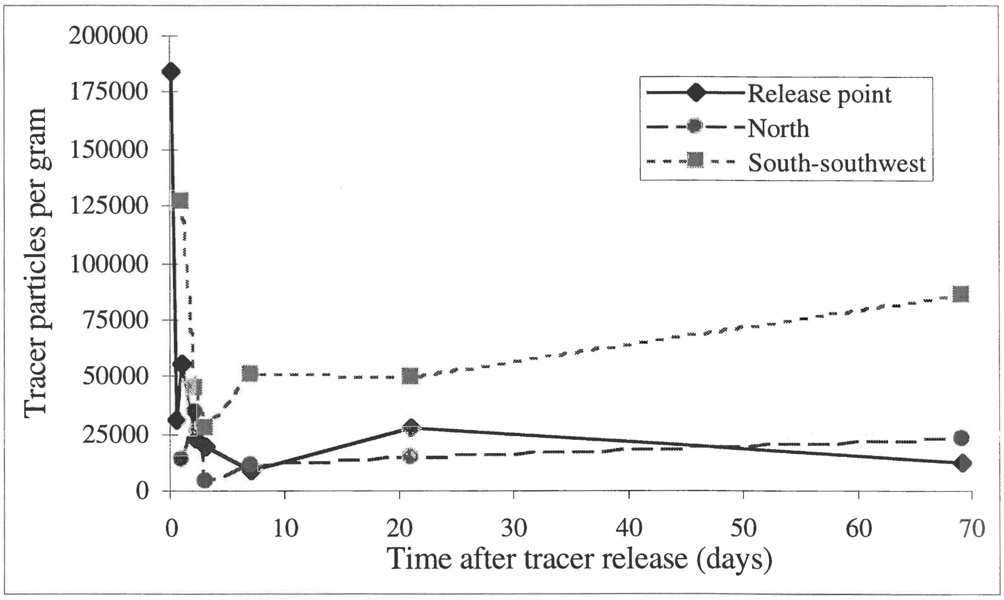

FIGURE 5.17: Time series of varying concentrations of tracer particles (grains per gram) at 3 sites: release site, north 50 m, and south-southwest 100 m.

5.7 Direction of sediment movement

The direction of tracer transport is indicated on contour plots of tracer dispersion from 23/12/94 and 27/2/95 by the location of the tracer centroid relative to the release site. Tracer particles were observed to move south-east at the beginning of the tracer experiment on 23/12/94 (Figure 5.15). The highest concentrations of tracer particles were found in channel samples on 17/1/95 (847,516 and 727,569 grains/g at Sites 21 and 22 respectively). This indicates there was significant movement of the tracer particles south and accumulation of fine sediment from the intertidal flats in the approach channel. Two months after tracer release the highest concentration of tracer particles on the intertidal flats was in the south-west (Figure 5.16). This suggests that sediment transport was directed towards the south for a significant period of time. Some tracer particles transported south bypassed the channel and were deposited on the southern side of the channel in concentrations up to 12,497 grains per gram at Site 19 on 27/2/95. It is assumed that these tracer particles represent the finer fraction of the tracer material as they were not observed by eye under UV light. An increase in the concentration of tracer particles north of the release site on 27/2/95 may also indicate some transport north during later stages of the experiment, as might be expected in an alternating littoral drift system.

A vector plot of total currents, derived from the S4 deployed during the tracer experiment at Site 1, indicates that north-west longshore current speeds were reduced when opposing winds from the west and north-west were strong (Figure 5.9 & Figure 5.13). These winds generated a longshore current which transported suspended sediment towards the south during the period when westerly winds, up to 15 m/s, were recorded at Pine Harbour Marina on 22/12/94 and 23/12/94. This accounts for the detection of the greatest concentrations of tracer particles south of the release site and the accumulation of fine sediment in the approach channel to the marina.

5.8 Tracer transport rates

The AFC results for tracer concentration are expressed in terms of the number of tracer grains per sample weight. This unit misrepresents tracer concentration when there is a range of tracer grain sizes by placing greater emphasis on the fine grain sizes. This weakness could be overcome if the results from the AFC were output as the mass of tracer particles per sample weight. The grain sizes of tracer particles used at Pine Harbour Marina ranged between

0.10 mm and 0.01 mm. Highest concentrations of tracer particles may be comprised of very fine tracer grains which have less mass than coarser tracer particles.

Calculation of sediment transport rates is made difficult by the limited number of samples analysed with the AFC. In addition the estimated transport rate is the upper limit of sand transport expected over the intertidal flats because the transport of natural sand sized grains would actually be less than transport of the finer tracer particles.

The mass balance equation for tracer can be treated as being composed of advective and diffusive components so,

$$\frac{\partial M}{\partial t} = U\frac{\partial M}{\partial x} + V\frac{\partial M}{\partial y} + W\frac{\partial M}{\partial z} + \frac{\partial}{\partial x}\left(\Sigma x\frac{\partial M}{\partial x}\right) + \frac{\partial}{\partial y}\left(\Sigma y\frac{\partial M}{\partial y}\right) + \frac{\partial}{\partial z}\left(\Sigma z\frac{\partial M}{\partial z}\right) \qquad (5.2)$$

where, M is the number of tracer particles (grains); U, V, and W are the advective velocities in the crosshore (x), longshore (y) and vertical directions (z) respectively.

If we assume that the vertical movement is purely diffusive then the vertical advection is zero. Also, after several weeks the spatial gradients in the tracer over the measurement region are also close to zero. Thus, at this time

$$\partial M = \frac{\partial}{\partial z}\left(\Sigma z\frac{\partial M}{\partial z}\right) \qquad (5.3)$$

that is, the process is primarily driven by the bioturbation of sediment by infaunal organisms.

Just after tracer release, bioturbation is small and the transport is mostly advective, driven by currents. Thus,

$$\frac{\partial M}{\partial t} = U\frac{\partial M}{\partial x} + V\frac{\partial M}{\partial y} \qquad (5.4)$$

If U and V are of order 0.1 m/s

and $\frac{\partial M}{\partial x} = \frac{\partial M}{\partial y} = \frac{\text{12,552 tracer grains/gram}}{\text{100 metres}}$ (Figure 5.15)

then $\frac{\partial M}{\partial t}$ is of order 12.5 tracer grains/gram/second.

Figure 5.17 shows a decay of tracer at the release site of order 152,588 grains/gram over 12 hours which is 35 tracer grains/gram/second which has the right order of magnitude. Assuming consistency of the advection process in the early stage of tracer dispersion, the order of magnitude compares well with the rate of movement predicted by the mass balance equation.

In the absence of accurate spatial tracer gradients, tracer size distributions, current measurements, and depth of disturbance and speed of tracer penetration into the sediments, calculation of the sediment transport rate over the intertidal flats is restricted. Without detailed numerical modelling of these processes an estimate of sediment transport rates is not possible beyond the diffusion coefficients already presented. The numerical modelling is beyond the scope of this thesis.

Tracer transport rates were obtained by multiplying the change in the number of tracer grains by the mass of each tracer particle, which was then converted to kg per hour by dividing by the time between sampling (Table 5.1). Tracer particle movement was greatest at the start of the tracer experiment with 1.08×10^{-5} $kg.hr^{-1}$ of tracer removed from the release site. This may be due to a combination of factors including the rapid dispersion of tracer particles in the early stages of the experiment, and the high energy levels which increased tracer particle entrainment and transport rates on the intertidal flats soon after tracer release (Figure 5.17). Transport of tracer particles was greatest towards the south. At sampling site 100 m SSW of the release site average tracer transport was 4.07×10^{-7} $kg.hr^{-1}$, while at sampling site 50 m N of release site average tracer transport rate was 4.1×10^{-8} $kg.hr^{1}$. Overall movement of tracer particles was greatest towards the approach channel south of the release site, with average tracer transport rate of $4.5 \times 10^{-7} kg.hr^{-1}$ calculated at Site 8 near the edge of the approach channel to Pine Harbour Marina. Tracer movement onshore at Site 9 was greater than tracer transport rates offshore at Site 1 (Table 5.1). Average tracer transport over the intertidal flats was 1.64×10^{-7} $kghr^{-1}$. This rate of tracer transport is assumed to be similar to the rate of dispersion of fine sediment similar to the dredgings sediment deposited on the intertidal flats at Pine Harbour Marina.

TABLE 5.1: Concentration of tracer particles (grains/g) per sediment sample and movement of tracer particles between sampling occurrences (-ve = erosion, +ve = accretion).

Days since release	Conc. tracer (grains/g)	Time between sampling (hours)	Change in tracer conc. between sampling (grains/g)	Tracer transport rate kg per hour
Sample location: Release site				
0	184240	0	0	0
0.5	31652	12	-152588	-1.084×10^{-5}
1	55650	12	23998	1.704×10^{-6}
2	23029	24	-32621	-1.158×10^{-6}
3	19639	24	-3390	-1.204×10^{-7}
7	8901	96	-10738	-9.531×10^{-8}
21	28389	336	19488	4.942×10^{-8}
69	12851	1152	-15538	-1.149×10^{-8}
365	12435	7104	-416	-4.990×10^{-11}
Average tracer movement from release site				-1.310×10^{-6}
Sample location: 50 m N				
0	0	0	0	0
1	13800	24	13800	4.900×10^{-7}
2	35077	24	21277	7.554×10^{-7}
3	4898	24	-30179	-1.072×10^{-6}
7	11489	96	6591	5.850×10^{-8}
21	14629	336	3140	7.963×10^{-9}
69	23172	1152	8543	6.319×10^{-9}
Average rate of tracer transport 50 m N				4.100×10^{-8}
Sample location: 100 m SSW				
0	0	0	0	0
1	127066	24	127066	9.023×10^{-6}
2	45089	24	-81977	-5.821×10^{-6}
3	28394	24	-16695	-1.186×10^{-6}
7	51111	96	22717	4.033×10^{-7}
21	50420	336	-691	-1.752×10^{-9}
69	86306	1152	35886	2.609×10^{-8}
Average rate of tracer transport 100 m SSW				4.070×10^{-7}
Sample location: Site 1				
0	0	0	0	0
3	13609	72	13609	1.611×10^{-7}
69	7882	1584	-5727	-3.081×10^{-9}
Average rate of tracer transport at Site 1				7.900×10^{-8}
Sample location: Site 2				
0	0	0	0	0
3	8408	72	8408	9.951×10^{-8}
69	9807	1584	1399	7.526×10^{-10}
Average rate of tracer transport at Site 2				5.010×10^{-8}

TABLE 5.1 continued: Concentration of tracer particles (grains/g) per sediment sample and movement of tracer particles between sampling occurrences (-ve = erosion, +ve = accretion).

Days since release	Conc. tracer (grains/g)	Time between sampling (hours)	Change in tracer conc. between sampling (grains/g)	Tracer transport rate kg per hour
Sample location: Site 6				
0	0	0	0	0
3	8470	72	8470	1.002×10^{-7}
21	85759	432	77289	1.525×10^{-7}
69	25314	48	-60445	-4.471×10^{-8}
Average rate of tracer transport at Site 6				6.930×10^{-8}
Sample location: Site 9				
0	0	0	0	0
3	47188	72	47188	5.585×10^{-7}
69	30085	1584	-17103	-9.201×10^{-9}
Average rate of tracer transport at Site 9				2.750×10^{-7}
Sample location: Site 8				
0	0	0	0	0
1	23003	24	23003	8.167×10^{-7}
69	183951	1632	160948	8.404×10^{-8}
Average rate of tracer transport at Site 8				4.500×10^{-7}
Sample location: 100m SSE				
0	0	0	0	0
3	41269	72	41269	4.884×10^{-7}
21	24657	432	-16612	-3.277×10^{-8}
Average rate of tracer transport 100m SSE				2.28×10^{-7}

5.9 Other tracers

The movement of coarse gravel sized brick chip particles (2.0-3.0 cm in diameter) were observed to determine the frequency of movement of similar sized fragments of bed rock and shell material from the dredgings mound. Three plots of brick chips (2.0 m x 2.5 m x 0.003 m) were laid out on the intertidal flats on 28/11/94 (Plate 5.2a). Two plots were located north of the dredgings mound, and a further plot was laid out on the southern side the approach channel (Figure 5.18). The brick chip plots were revisited after 1, 5, 9, 24, 38, 54, 80 days, and the number of brick chips that had moved from the plot counted, and the distance and direction of movement noted (Appendix 5.3).

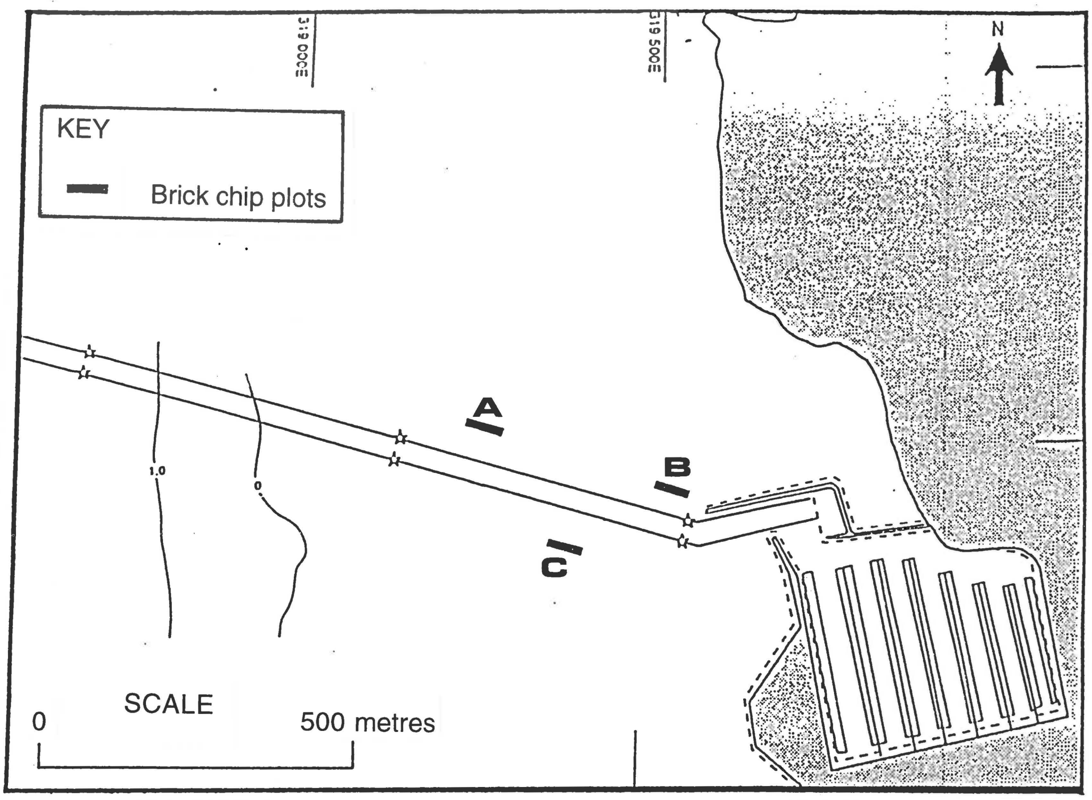

FIGURE 5.18: Location of brick chip plots on intertidal flats fronting Pine Harbour Marina. Brick chip plots represented by bars (not to scale).

Brick chips did not move until 22/12/94 (after 24 days) when a small number of brick chips moved up to 1 m towards the east after a period of strong westerly winds (up to 15 m/s) (Figure 5.9). Further movement of brick chips was observed on 15/2/95 (80 days) when chips moved up to 2 m towards the east. The brick chips acted as a trap for fine sediment. Silt and fine sand were subsequently deposited over the brick chip plots and covered brick chips that had moved from the plots onto the intertidal flats. Bedform ripples (ht = 1.0-1.5 cm, λ = 2.0-5.0 cm) developed around the plots and sediment was observed to accrete along the southern side of the brick chip plots, demonstrating active sediment movement towards the north (Plate 5.2b).

Movement of brick chips at Plot A on the northern side of the approach channel was greater than at Plot B, located near the marina break water, and Plot C located south of the approach channel. This reflects the variation in wave energy over the intertidal flats, and implies that the northern intertidal flats are exposed to higher wave energies. Movement of brick chips from the release plots occurred with large infrequent wind generated waves from the west. However, for the majority of the time the low wave energy (H_s) experienced over the intertidal flats is insufficient to exceed the threshold velocity of the the large brick chip particles (2-3 cm) and no movement of brick chips was recorded. The net movement of brick chips over the measurement period was towards the east associated with high wind speeds blowing from the west.

PLATE 5.2: a) Brick chip plots (2.5 m x 2.0 m x 0.03 m) laid out on the intertidal flats fronting Pine Harbour Marina on 28/11/94; b) Sediment was observed to build up on the south side of the brick chip plots and fine silty sediment accreted on the brick chips on 23/12/94.

5.10 Discussion

5.10.1 Sediment mixing

Sediment on intertidal flats undergoes considerable reworking by burrowing organisms. The vertical mixing of the fluorescent tracer particles and mixing depth experiment using dyed sediment confirms that sediment is mixed to depths of approximately 2.5 cm over the intertidal flats in the short term. Similar sediment mixing depths were recorded by sedimentation rods installed along the intertidal flats, where mixing depths were generally less than 1.5 cm due to shallow disturbance created by ripple movement (h = 1.0-1.5 cm). Sedimentation rod results showed that waves were capable of mixing sediment to greater depths of 2.3-3.0 cm with storm periods. The maximum sediment mixing depth recorded by sedimentation rods attributed to wave action was 6.2 cm. Vertical mixing of fluorescent tracer particles indicate that fine sediment was mixed up to 17 cm over longer time periods which are not attributable to wave processes over the intertidal flats. It is assumed that the majority of the deeper vertical mixing of sediment is the result of biological reworking of sediments.

Bioturbators alter the sediment surface by depositing sediment on the surface, in the form of faeces or in the process of tunnelling, and by transporting sediment above the surface while feeding or while burrowing (Brenchley, 1981; Grant & Daborn, 1994). Johnson (1967) studied the vertical distribution of macroscopic invertebrates within intertidal sands. He cites Holme (1964) in that the majority of benthic animals may be found the top 10 cm of sediment, and that organisms below this depth are often large and are infrequent. The average median depth of all species was 8 cm, and the maximum depth to the uppermost part of an individual ranged from 13 to 25 cm (Johnson, 1967). Similar depths of activity were found by Meadows and Tait (1989) who found that beyond 2-3 cm, ripple laminations are replaced by subtle bioturbate textures created by amphipods and polychaetes. Types of internal structures include dense vertical burrows of spionid worm, small domiciles of bivalves, burrowing activity of numerous amphipods just below the substrate surface, long vertical muddy walled tubes of ghost shrimp, and branched u-shaped burrows and mucous tubes of polychaetes (Howard and Dörjes, 1972) (Figure 5.19).

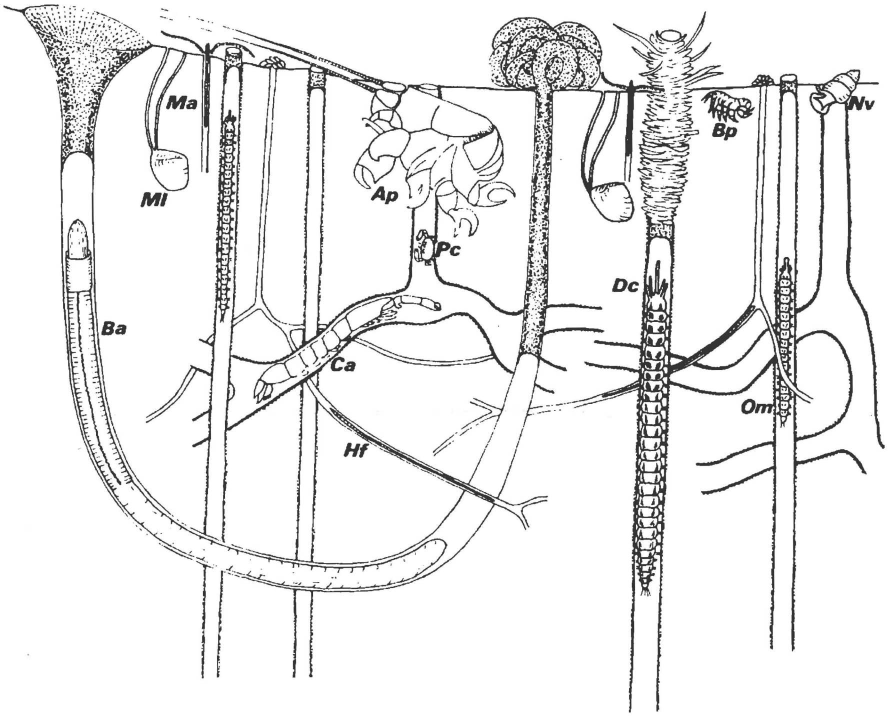

Burrowing characteristics of the most important animals, burrows, and tubes in the muddy sediments of Nannygoat tidal flat. (Ap = *Albunea paretii*, Ba = *Balanoglossus sp.*, Bp = *Bathyporcia sp.*, Ca = *Callianassa sp.*, Hf = *Heteromastus filiformis*, Om = *Onuphis microcephala*, Dc = *Diopatra cuprea*, Ma = *Magelone sp.*, Ml = *Mulinia lateralis*, Nv = *Nassarius vibex*, Pc = *Pinnixa chaetopterana*.)

FIGURE 5.19: Vertical distribution and burrowing structures of intertidal infauna. Vertical scale approximately 10 cm (Howard and Dörjes, 1972).

5.10.2 Sediment transport patterns

Musick Point wind rose (Figure 2.4) indicates that south-westerly winds prevail for 31.3% of the time over the Pine Harbour Marina region, with wind from the west 14.3%, south 9.8% and from the north-west 5.7% of the time. In the long term net sediment transport is determined by the prevailing south-westerly wind which creates longshore current towards the north. Geomorphic evidence of sediment transport in this direction exists in the form of a growing spit on the southern side of the marina, and the barren shore platforms exposed north of the marina because sediment transported towards the north is trapped in the approach channel to the marina cutting off the littoral flow of sediment. Sediment accretion along the southern side of the brick chip plots also suggests a net sediment transport direction to the north.

From the results of the tracer experiment several scenarios of sediment transport direction under different wind and wave conditions affecting the intertidal flats fronting Pine Harbour Marina are summarised below. The north-south oriented coastline shelters the embayment and intertidal flats fronting Pine Harbour Marina from winds from the northern and eastern sectors. In general suspended sediment is transported downdrift of the prevailing wind. However different combinations of waves, entraining varying amounts of sediment, and wind from different directions can produce different patterns and magnitudes of sediment transport.

Small short period waves ($H_s \leq 0.2$, $T_s = 1.5$ s) occur for approximately 30% of the time generated by south-westerly winds less than 10 m/s. These sea waves approach the coastline across limited fetch (high tide = 4 km, low tide = 2 km) from the south-west. Entrained sediment is transported north by the longshore current under the combined influence of the prevailing south-westerly winds and the faster ebb tide which flows towards the north-west. South-westerly winds exceeding 10 m/s generate larger waves (H_s = 0.3-0.4 m, T_s = 1.5 s) which are capable of entraining greater volumes of sediment than smaller waves which is transported north by the longshore current (Figure 5.20).

Winds less than 10 m/s from the west and north-west sectors generate waves up to 0.4 m (H_s) and T_s of 2.0 s from the greatest fetch (up to 10 km in the north-west). These high energy waves activate sediment to greater depths and the associated higher wave orbital velocities exceed entrainment threshold of larger grain sizes. Sediment is then transported by the net current. The residual current at Pine Harbour is directed longshore to the north-west. Under these conditions westerly wind stress changes the circulation pattern over the embayment retarding the longshore current which generally prevails over the region to the north-west. Westerly winds create an onshore current which is turned towards the south under the influence of the local topography. This longshore current transports suspended sediment south towards the approach channel to Pine Harbour Marina (Figure 5.21). On rare occasions large waves approach from the north-west. Wind speeds up to 15 m/s were recorded during the sediment tracer experiment, these winds can generate waves up to 0.6 m when they coincide with high tide over the intertidal flats. This was observed during storm conditions that occurred in the sediment tracer experiment, when significant quantities of tracer particles accumulated in the approach channel to Pine Harbour Marina.

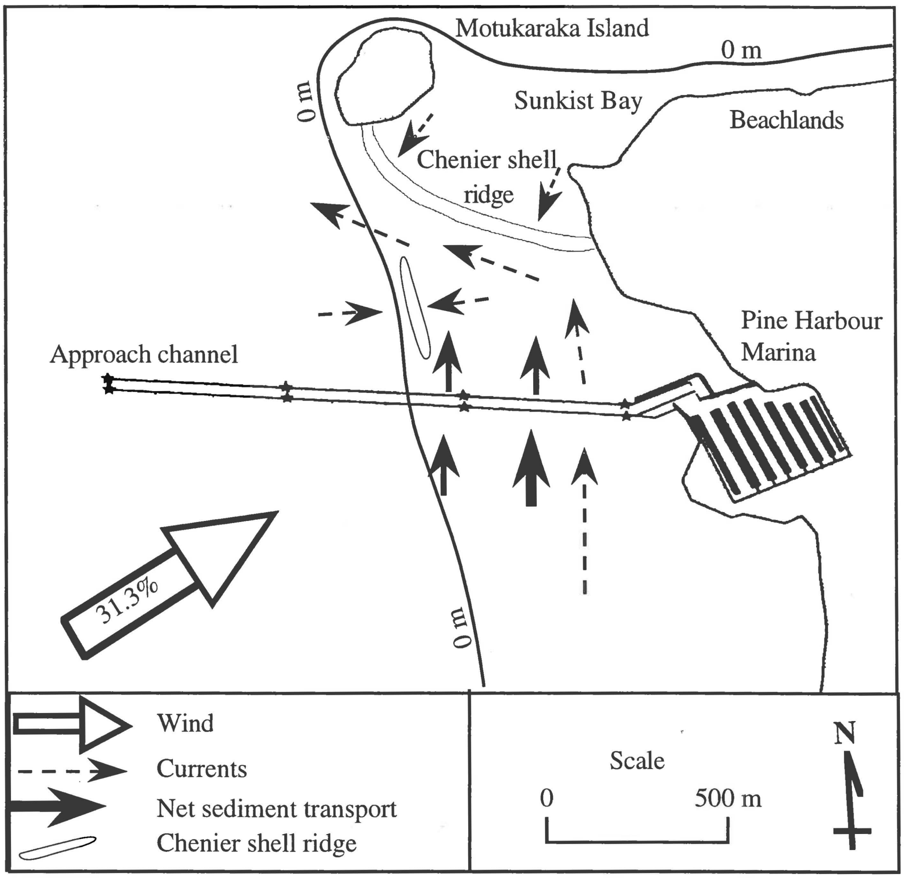

FIGURE 5.20: Direction of longshore current and net sediment transport during prevailing winds from the south-west (31.3%).

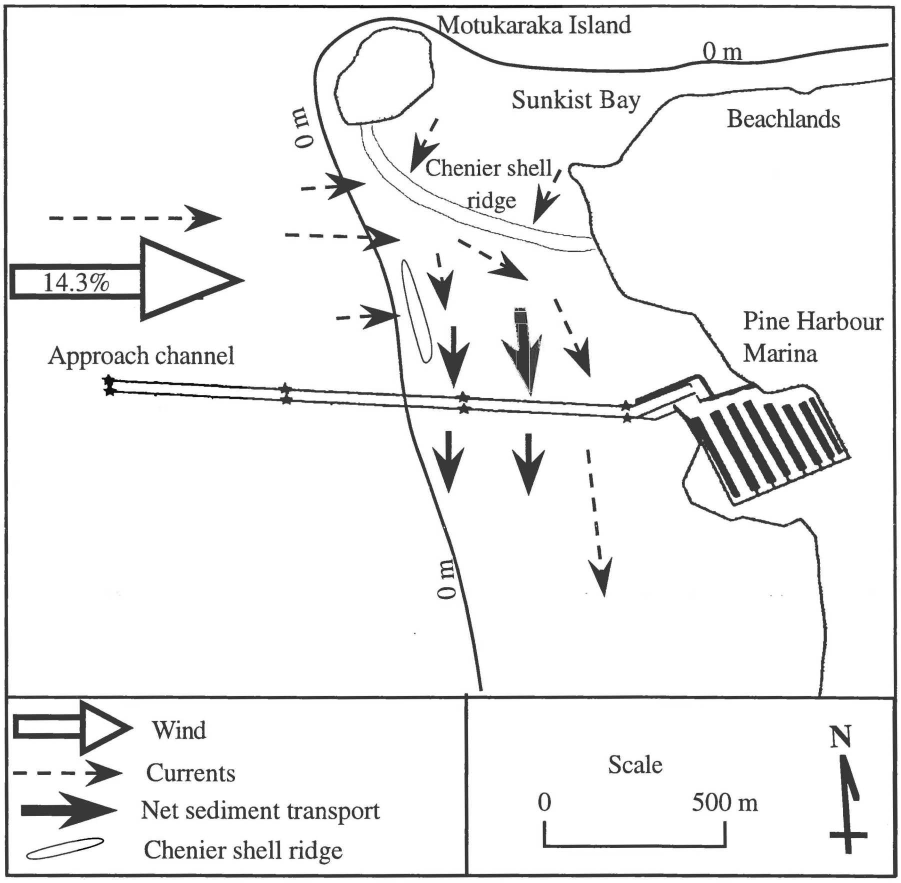

FIGURE 5.21: During less frequent westerly winds an onshore current is generated which is turned towards the south by Beachlands coastline and chenier shell ridge producing net sediment transport towards the south.

5.10.3 Dredge mound dispersion

Sediment excavated from the approach channel to Pine Harbour Marina during maintenance dredging in June to October 1994 were sidecast onto the northern intertidal flats adjacent to the channel upon the understanding that dredgings sediment would likely disperse over the intertidal flats, as argued by Healy (1994). The dredgings mound was observed in the subsequent months after initial dredging was completed in October 1994 to provide a better understanding of how the dredged material behaved once deposited on the intertidal flats and how it eroded. Sediment is entrained into suspension by waves and transported by currents over the intertidal flats discussed in Chapter 4. The direction of transport of entrained sediment is inferred from the tracer studies in this chapter.

The dredge mound was approximately 0.5 m in height and irregularly covered an area of intertidal flats up to 100 m from of the edge of the channel extending beyond the 800 m channel markers along the northern side of the channel (Plates 5.3). The dredge mound was comprised of a matrix of predominantly silt and fine sand sized sediment, supporting gravel to boulder sized fragments of shore platform and abundant shell material (Plate 5.4). The dredgings underwent alternate wetting and drying as the dredge mound was exposed on the intertidal flats at low tide. The development of surficial sediment layer ripples of very fine sand over some areas indicated that sediment was actively moving over the surface of the dredgings. However below the rippled surface, sediment was primarily constituted of silt with high moisture content and was very "boggy" (Plate 5.5).

The dredge mounds reduced in vertical extent after appearing to consolidate initially, and some fine sediment entrained into suspension from the dredge mound was dispersed over the intertidal flats. The dredge mound was not observed to move as a coherent body of sediment; rather it appeared to flatten and spread out around the edges, and an ankle deep layer of fluid-like mud was observed around the mound. Fine (silty) sediment was also observed in troughs of ripples on the intertidal flats to the north and was clearly fine sediment dispersed from the dredgings mound. With increased time after deposition, the fine sediment component of the dredgings material was eroded away, and mounds of gravel to boulder sized fragments of bedrock were left on the intertidal flats as the only indication of where dredgings were deposited (Plate 5.5).

The intertidal flats and dredge mounds along the channel edge were observed to be eroded by water draining off the intertidal flats which scoured small drainage channels from the intertidal flats into the approach channel at various locations. These drainage channels drained some water off the intertidal flats during the ebbing tide and accommodated rainfall runoff from the intertidal flats at low tide. Erosion of dredge mounds was increased with the incision of these drainage channels in the silty material at the channel edge (Plate 5.6).

Drainage channels were not observed on the intertidal flats in November 1994 (Plate 5.7a), however water ponded amongst dredge mounds was observed at low tide. By April 1995 small channels had eroded into the silty sediment and drained water ponded between dredge mounds from the intertidal flats, along with accommodating some ebb tide and rainfall runoff (Plate 5.7b). Moreover the dredge mounds had decreased in height, and gravel to boulder sized fragments of bed rock remained on the dredge mounds. Silt sized sediment from the dredge mounds was dispersed to some extent over the intertidal flats as discussed in Chapter 3, but much of the sediment from the dredge mounds would have been transported back into the channel along with sediment from the intertidal flats.

The intertidal flats at the channel edge slope into the channel suggesting that fine sediment with little structure and support could have slumped back into the channel due to geomechanical failure. The dredgings appeared to be dispersing slowly after the initial period of consolidation and all that remained of the dredge mounds by September 1995 were piles of boulder to pebble sized fragments of shore platform (Plate 5.7c).

Large infrequent waves from the northwest would have had a greater impact on entraining the cohesive muddy dredgings sediment than small high frequency sea waves from the south-west. Waves from the south-west generated by the prevailing south-westerly winds have the greatest day to day impact on the coast (Figure 5.20). However waves generated by high wind speeds from the north-west may produce greater sediment transport towards the south due to the increased orbital velocities under large waves generated over the 10 km fetch, and associated wind driven current (Figure 5.21). The fluorescent tracer experiment indicated that significant concentrations of fluorescent tracer particles released on the northern side of the channel accumulated in the channel within 1 month of tracer release, under strong north-westerly winds.

PLATE 5.3: The dredge mound extending approximately 700 m along the northern intertidal flats adjacent to the approach channel to Pine Harbour Marina, October 1994.

PLATE 5.4: Dredgings mound in November 1994, 1 month after the completion of the dredging works.

PLATE 5.5: Fine sediments were dispersed from the dredge mounds leaving mounds of gravel to boulder sized fragments of bedrock, August 1995.

PLATE 5.6: Small drainage channels were eroded into the silty sediment of the dredge mounds at various locations along the channel edge and would have transported fine sediment back into the channel.

PLATE 5.7: Dredgings mound dispersion through time illustrating the incision of drainage channels into the silty sediment at the channel edge and remnant boulders where fine sediment has been transported away, a) November 1994; b) April 1995; c) September 1995.

5.10.4 Dredge mound stability

Full geomechanical investigation into the post dumping behaviour of the dredgings mound was outside the scope of this investigation. Time series comparisons of particle size, bulk density and moisture content of sediment could have been undertaken to monitor the process of mound consolidation and grain repacking. Investigations into the mechanism of sediment transport from the dredgings mound could also have been explored to identify whether dredge spoil dispersed from the mound by various transportation mechanisms, including: a layer of fluid mud; viscous mass movement; movement of flocculated particles; or failure along stress lines (V. Moon, pers. comm.). Further investigations into the stability of the dredge mound, and mechanism of cohesive sediment movement, could have included the triaxial testing of dredgings sediment, to determine the sediment shear stress, and also the calculation of the viscosity of dredgings sediment. These measures are an indication of the sediments internal cohesive and frictional resistance to flow which can be related to the sediment composition, and could have been utilised in the examination of the geomechnical erosion of the subaerially exposed dredge mound and permitted an examination into the processes involved when dredgings sediment is alternatively wet and dry with exposure on the intertidal flats at low tide.

Dispersion of dredge spoil from the mound is dependent on properties of the dredged sediment, as resuspension is sensitive to the mechanical properties of the sediment. Cohesive coastal and estuarine sediments are generally referred to as "mud", and are a complex mix of materials including water, cohesive sediments consisting of many different clay minerals, organic matter; and small amounts of sand and silt (Dyer, 1986). In cohesive sediments the particles are considered to be flocculated (Mehta & Lee, 1994), and they behave differently to non-cohesive sediments such as sand. Each grain is held by cohesive forces which bond the grain to its neighbours at discrete points of contact (Mehta & Lee, 1994). Thus because of the nature of the grains, cohesive sediments have greater threshold velocities for entrainment of particles into suspension than cohesionless sediments.

5.11 Chapter summary

- The results from the comparison of UV light and AFC methods of tracer concentration analysis have demonstrated that fine tracer particles cannot accurately be determined with UV light. AFC analysis is essential in obtaining accurate results from which to calculate transport rates and infer directions of sediment movement. However, the bulk UV light analysis method may be suitable if the tracer experiment is concerned with the detection of coarse sediments. The artificial tracer particles have been proven to be highly durable with the presence of tracer particles detected at the release site 1 year later. Although the intertidal flats are predominantly exposed to only low wave energy, during storms wave heights and energy increase. The tracer particle durability would make them a suitable tracer material in settings outside intertidal flats such as in higher energy environments.

- Short term tracer mixing in the order of 2-3 cm was observed, this was similar to the results from sedimentation rods and burial of dyed natural sediment. This depth of mixing was expected based on the magnitude of small sediment ripples (h = 1.0-1.5 cm) and low wave energy (H_s = 0.1-0.4 m) for the region. Sampling for tracer particles encompassed this active sediment layer. However detection of tracer particles at depths up to 17 cm in core samples taken after relatively large time intervals following tracer release indicate that biological organisms play a dominant role in vertical sediment movement on the intertidal flats, as bedforms and wave activity in the region were not observed to disturb sediment to these depths.

- The diffusion coefficients indicate that tracer dispersed rapidly soon after release as tracer was primarily dispersed across the sediment surface and mixed to depths between 2.0 and 3.0 cm. During later stages the diffusion coefficient was reduced from 1270.43 m^2day^{-1} to 76.49 m^2day^{-1} which means that tracer movement slowed after reaching an equilibrium level of widespread dispersion following which there was minimal net sediment transport, and that vertical mixing became more important with increased time. The estimated sediment transport rate is an upper limit on the transport of sand grains because the tracer particles were slightly finer and had lower threshold velocities.

- Difficulties were encountered when calculating the sediment transport rate from the tracer concentrations expressed as the number of tracer particles rather than the mass of tracer particles in the sample. High tracer concentration may be representative of an abundance of very fine tracer particles with small mass and could therefore be less significant than lower concentrations of particles with larger grain sizes. In the absence of accurate spatial tracer gradients, tracer size distributions, current measurements and depth of disturbance and speed of tracer penetration into the sediments and without detailed numerical modelling of the processes, an estimate of sediment transport rates is not possible beyond the diffusion coefficients already presented. The numerical modelling was beyond the scope of this thesis.

- Results of the fluorescent tracer experiment are best used as an indicator of the pattern of sediment movement, rather than indicating the exact velocity or quantifying the amount of sediment transported. Knowledge of the pattern of tracer dispersion suffices for many practical purposes where knowledge of the relative magnitudes of tracer in different directions is of primary importance (Bruun, 1990). In this case the pattern of tracer transport and tracer transport rates may be used to give an indication of the direction and magnitude of dredge spoil dispersion over the intertidal flats.

- Fluctuations in tracer particle concentrations at sampling sites indicate that there was minimal net sediment transport over the intertidal flats. The transport rate of tracer particles inferred from the change in tracer particles was greatest at the start of the tracer experiment 1.08×10^{-5} $kg.hr^{-1}$. The highest rate of tracer transport was towards the approach channel to Pine Harbour Marina south of the tracer release site at 4.07×10^{-7} $kg.hr^{-1}$. Overall, the average rate of tracer transport was 1.64×10^{-7} $kg.hr^{-1}$.

- Tracer particles were observed to move towards the south-east and south-west at the beginning of the tracer experiment under the influence of winds up to 15 m/s from the west. Westerly winds create an onshore current which is turned south by the coastline and chenier shell ridge which extends across the intertidal flats. This longshore current towards the south transported sediment entrained by storm waves up to 0.81 m. Highest concentrations of tracer particles were detected in the approach channel to Pine Harbour Marina on 17/1/95 indicating significant movement of fine sediment from the intertidal flats into the channel. This finding supports the conclusion drawn in Chapter 3 that the bulk of the dredgings mound was transported back into the approach channel to Pine Harbour Marina after the dredging works in 1994. During later stages of the tracer experiment the concentration of tracer particles north of the release site began to increase suggesting sediment transport north by the prevailing south-westerly wind driven longshore current.

- Post-deposition observations of the dredgings sediment, along with bulk density and moisture content analysis from Chapter 3, have indicated that the dredgings initially consolidated, as pore water was extruded during grain repacking and fine sediment was slowly dispersed from the mound over the intertidal flats. Rates of consolidation were thought to vary over the dredgings mound as bulk densities and moisture contents of cores varied. Dredge mounds furthest north on the intertidal flats were observed to become flatter with increased time after dredging, possibly due to consolidation at the centre of the mound which caused sediment to spread radially from the centre.

- Dredgings sediment are concluded to have initially consolidated and dispersed to some extent over the intertidal flats north of the approach channel. The dredge mound was observed to be eroded by small drainage channels incised into the intertidal flats and dredge mound at various locations which would have transported fine sediment from the dredge mound and intertidal flats into the approach channel. Some 12 months after dredging the dredge mounds were reduced to piles of shore platform fragments where the mounds of silty sediment were deposited. Most of the dredged sediment deposited in mounds alongside the channel is thought to have been transported away by wave induced erosion and turbulent transport away from the mound, or back into the channel by the slumping of fine sediment close to the channel edge which was unable to support itself. Some suspended sediment washed into the channel as intertidal flats drained during the ebbing tide.

CHAPTER SIX: CONCLUSIONS

6.1 Introduction

This study investigated the nature of sediments, and the role of tides, currents, waves and winds in driving sediment transport on the intertidal flats and shallow subtidal areas in the vicinity of Pine Harbour Marina. The findings, along with the monitoring data from the 1994 dredging operation, have been used to assess the fate of the dredgings dump mound and factors causing the infilling of the navigation approach channel to Pine Harbour Marina. This research has improved our knowledge on sediment transport on intertidal flats. It provides baseline data in order for Pine Harbour Marina to comply with monitoring requirements of the 1994 dredging operation. The findings are of importance for future decision-making by Pine Harbour Marina regarding the long term disposal of dredgings sediment from continued maintenance dredging of the navigation approach channel.

6.2 Sediment transport patterns on the intertidal flats

The sediment transport patterns observed over the intertidal flats fronting Pine Harbour Marina are a result of the forcing processes of wind, waves, currents and the tide which operate in the local embayment. Sediment transport is driven by waves which entrain sediment that is then transported by the net current. Tidal current asymmetry produces a net current towards the north-west with the ebb tide. Wind driven circulation is important over the shallow intertidal flats, producing surficial currents in the direction of the prevailing wind.

Sediment entrainment under waves varies with wave height, sediment grain size, water depth and sediment density. Greater sediment transport occurs over the intertidal region than the subtidal region because sediment threshold velocities are more frequently exceeded in the shallower water depths. Thus sediment deposited in the approach channel to Pine Harbour Marina is infrequently entrained as wave orbital velocities are attenuated before they reach the bed in the deeper water. Greatest near bed orbital velocities and turbulence due to breaking waves occurs at early stages of the tide, maximising sediment transport during this time over the intertidal flats.

Sedimentation rods on the intertidal flats indicate that sediment mixing depths were generally less than 1.5 cm due to shallow disturbance created the movement (h = 1.0-1.5 cm) wave ripples. Depth of sediment disturbance increased to between 2.0 and 3.0 cm associated with storm periods. The maximum sediment mixing depth recorded by sedimentation rods was 6.2 cm on the northern intertidal flats which is exposed to higher wave energy from infrequent north-westerly storms. Similar mixing depths of 2.5 cm were recorded during mixing depth experiments involving short cores through buried dyed sediment and vertical mixing of fluorescent tracer particles. Fluorescent tracer was mixed to a maximum depth of 17 cm, which was not attributed to wave action but rather to bioturbation.

The north-south orientation of Beachlands coastline shelters the embayment and intertidal flats fronting Pine Harbour Marina from wind and waves from the northern and eastern sectors. Wind generated waves are limited by restricted fetch of 4 km to the south and maximum fetch of 10 km to the north-west. The wave climate predicted at Pine Harbour Marina by wave model WGEN3DD is characterised by wave (H_s) between 0.1 m to 0.4 m, and wave periods (T_s) between 1.0 and 2.0 s. Large wave events are rare, but wave heights (H_s) up to 0.5 m and periods (T_s) of 2.5 s are generated by wind speeds (>10 m/s) from the north-west where fetch is greatest.

Suspended sediment is transported downdrift of the prevailing wind. However any synoptic combinations of waves, entraining varying amounts of sediment, and wind from different directions can produce different patterns and magnitudes of sediment transport. Net sediment transport on a day-to-day basis is towards the north, under the combined influence of the prevailing south-westerly winds and tidal asymmetry which produces net flow towards the north-west (Figure 5.20). The westerly winds create an onshore current which is turned towards the south under the influence of the local topography, and transports suspended sediment south towards the approach channel to Pine Harbour Marina (Figure 5.21). During large infrequent storms from the west and north-west waves are capable of entraining and transporting greater volumes of sediment south over shorter time periods.

6.3 Monitoring of 1994 dredging operation

Two resource consents (H/9205 and H/9258) were granted to Pine Harbour Marina in 1994 by the Auckland Regional Council to undertake maintenance dredging to excavate approximately 4,500 m^3 of sediment from the navigation approach channel. In compliance with the resource consents, an extensive monitoring program was instigated to document the dispersion of dredgings sediment from the dump site over the intertidal flats. This monitoring program involved periodic hydrographic surveys; intertidal flat beach surveys; monitoring of sedimentation rods; sediment tracer experiment; hydrodynamic monitoring; long term turbidity monitoring; and photographic record of dredge mound dispersion.

Initially dredgings sediment appeared to consolidate *in situ*, but was also dispersed as a shallow layer extending up to 100 m over the intertidal flats north of the approach channel. The dredge mounds were observed to be eroded by small drainage channels which became incised into the silty sediment and transported fine sediment from the dredge mound and intertidal flats into the approach channel. Some 12 months after dredging, the dredge mounds were dissipated and only remnant blocks of gravel to boulder sized fragments of bed rock were left.

Periodic beach surveys and monitoring of sedimentation rods indicated that a maximum of 2.5 cm of accretion occurred over the mid tide region on the northern intertidal flats. This volume of sediment accretion equates to approximately 2,100 m^3 of sediment which is approximately half of the dredgings material. The remaining dumped sediment was resuspended by wave action and either transported back into the approach channel to Pine Harbour Marina, or removed from the area in suspension.

Hydrographic surveys revealed that in the 9 months following dredging an average of 0.5 m of sediment deposition occurred along the northern side of the landward 700 m of approach channel. This was estimated to be approximately 5,250 $m^3 \pm$ 2,100 m^3 of sediment infilling the channel. This rate of infilling equates to 7,000 m^3 per year. Longer term "natural" sediment accumulation in the approach channel, expected to be approximately 3,000 m^3 by Healy (1994), does not account for this rate of channel infill. The increased rate of sediment infilling the approach channel is attributed to natural sediment accumulation combined with the rapid transportation of some dredgings sediment back into the channel.

These findings conclude that a significant proportion of the dredged sediment dumped adjacent to the channel were transported back into the approach channel within 9 months of the completion of the dredging works.

6.4 Implications for future maintenance dredging at Pine Harbour Marina

The navigation approach channel to Pine Harbour Marina is dredged across the net littoral drift which transports sediment north along the Beachlands coastline. Based on the history of sedimentation in the channel, the approach channel will continue to act as a sediment trap in the future and will require ongoing small scale maintenance dredging of the order of 3,000 to 7,000 m^3 per year.

This investigation has shown that a significant amount of dredge spoil deposited on the northern intertidal flats during the 1994 dredging operation were transported back into the approach channel within 9 months of the completion of the dredging works. An alternate disposal site for future maintenance dredging works in the approach channel at a further distance from the channel edge would reduce the likelihood of "recycling" of dredged material.

Possible alternate disposal options for management of dredge spoil from future maintenance dredging could include:

- Sidecasting disposal further from the channel.
- Offshore disposal site - adjacent or distant.
- Contained disposal.
- Landfill.

6.5 Suggestions for further research

Within the time constraints of the present investigation a considerable amount of data has been collected and an understanding of sediment transport, deposition and forcing mechanism elucidated. However the resulting conceptual models are not unequivocal. Accordingly some additional research would enhance our understanding of the system. In particular the following areas of future research are suggested.

a) In order to calculate sediment transport rates over the intertidal flats several assumptions made during the fluorescent tracer experiment need to be verified and it is necessary to obtain more accurate information on sedimentary processes during tracer experiments including, numerical modelling of spatial tracer gradients, tracer size distributions, and depth of disturbance and speed of tracer penetration into the sediments.

This study involved the use of fluorescent tracer particles to determine sediment transport patterns over the intertidal flats. Analysis of samples using UV light proved to be inaccurate, highlighting the necessity for the analysis of future samples utilising the fluorescent tracer particles with Analytical Flow Cytometry. Tracer concentrations should be output as the mass of tracer instead of the number of particles of tracer to better represent the rate of tracer transport of all particle sizes. In addition, grain size analysis of tracer grains in samples could also be undertaken to determine the rate at which different sized particles are transported over the intertidal flats.

b) The numerical modelling of currents in the embayment and over the intertidal flats is the next progressive step in research to reduce uncertainties and to enhance the overall understanding of the processes in the embayment between Howick and Beachlands Points. Additional current and wave measurements need to be made at various locations over the intertidal flats during different stages of the tide which would be used to calibrate a hydrodynamic model of the embayment, which could be expanded to a sediment transport model to estimate sediment transport rates over the intertidal flats. A numerical model of currents in the embayment may also be applied in the future, with regard to determining the passage of turbid plumes and deposition of fine sediment delivered to the marine environment from sediment erosion in relation to the increasing urban subdivisions and earthworks in Waikopua and Turanga Creek catchments.

c) The processes of salt-fresh water interactions leading to flocculation and deposition of suspended fine sediments in the wave stirred turbid zone from Waikopua Creek are likely to be a contributing factor to fine sediment deposition in the navigation channel to Pine Harbour Marina, and require further research into the deposition processes.

REFERENCES

APHA, 1992. *Standard methods for examination of water and wastewater.* APHA, AWWA, WFF, 18th Ed. p2-54.

Ballance, P., 1994. Source of muddy sediment in Maraetai. Uniservices Report, Auckland University. 3p.

Bioresearches Ltd, 1985. *The effects of the proposed Pine Harbour Marina on aquatic and terrestrial habitats.* Report prepared for Wilkens & Davies Ltd. 81p.

Bioresearches Ltd, 1986. *Pine Harbour Marina: Pre-construction monitoring survey.* Report prepared for Pine Harbour Marina Ltd. 27p.

Bioresearches Ltd, 1988. *Pine Harbour Marina: Post-commissioning monitoring survey No. 1.* Report prepared for Pine Harbour Marina Ltd. 30p.

Bioresearches Ltd, 1989. *Pine Harbour Marina: Post-commissioning monitoring survey No. 2.* Report prepared for Pine Harbour Marina Ltd. 28p.

Bioresearches Ltd, 1991. *Pine Harbour Marina: Post-commissioning monitoring survey No. 3.* Report prepared for Pine Harbour Marina Ltd. 35p.

Bioresearches Ltd, 1993. *Pine Harbour Marina: Post commissioning monitoring survey No. 4.* Report prepared for Pine Harbour Marina Ltd. 38p.

Black, K.P., and Rosenberg, M.A., 1992. Natural stability of beaches around a large bay. *Journal of Coastal Research* 8(2):385-397.

Black, K.P., 1995: *The Hydrodynamic Model 3DD1 and Support Software.* Occasional Report No. 19, Department of Earth Sciences, University of Waikato. 54p.

Black, K.P., and Healy, T.R., 1981. *Computer programs for wave analysis, wind wave generation, wave refraction diagrams, and fast fourier analysis.* Occasional report No. 6, Department of Earth Sciences, University of Waikato. 76p.

Blatt, H., Middleton, G.V., and Murray, R.G., 1980. *Origin of sedimentary rocks,* Englewood Cliffs, NJ: Prentice-Hall. 514p.

Bodge, K.R., 1989. A literature review of the distribution of longshore sediment transport across the surf zone. *Journal of Coastal Research,* 5(2):307-328.

Boggs, S.Jr., 1987. *Principles of sedimentology and stratigraphy.* Merrill Publishing Company, Ohio. 782p.

Bowman, M.J., and Chiswell, S.W., 1982. Numerical tidal simulations within the Hauraki Gulf, New Zealand. *In Hydrodynamics of semi-enclosed seas,* Nihoul, J.C.J.(Ed.), Proceedings of the 13th International Leige Colloquim on Ocean Dynamics. Elsevier Oceanography Series, 34. Elsevier Scientific Publishing Company, Amsterdam. p349-384.

Brenchley, G.A., 1981. Disturbance and community structure: an experimental study of bioturbation in marine soft-bottom environments. *Journal of Marine Research,* 39(4):767-790.

Bruun, P., 1990. *Port engineering: Volume 2: Harbor transportation, fishing ports, sediment transport, geomorphology, inlets and dredging*. Gulf Publishing Company, Houston, Texas. p585-605.

Carter, R.W., 1988. *Coastal Environments: An introduction to the physical, ecological and cultural systems of coastlines.* Academic Press, London. 617p.

Coastal Engineering Center, 1984. Shore Protection Manual, Vol. 1. Department of the Army, Waterways Experiment Station, Corps of Engineers, 4th Ed. 579p.

Davies-Colley, R.J., 1994. Water quality guidelines No. 2: Guidelines for the management of water colour and clarity. Report prepared for the Ministry of Environment, Wellington. 71p.

de Lange, W.P., 1988. Sediment transport within Tauranga Harbour. Unpublished D. Phil thesis, Department of Earth Science, University of Waikato, Hamilton.

de Lange, W.P., Black, K.P., and Hatton, D., 1993. *Programs for the reduction and analysis of tidal data* . VIMS Working Paper No. 27. 43p.

Dolphin, T.J., 1992. Low amplitude multiple bar systems in an intertidal fetch limited environment. Unpublished M.Sc. thesis, University of Auckland. 143p.

Dolphin, T.J., Hume, T.M., and Parnell, K., 1995. Oceanographic processes and sediment mixing on a sand flat in an enclosed sea, Manukau Harbour, New Zealand. *Marine Geology*, 128:169-181.

Dyer, K.R., 1986. *Coastal and estuarine sediment dynamics*. Chichester: John Wiley and Sons. 342p.

Folk, R.L., 1968. *Petrology of Sedimentary Rocks*. Hemphills, Austin Texas.

Fredsoe, J., and Deigaard, R., 1992. *Mechanics of coastal sediment transport*. Vol. 3, Advanced Series on Ocean Engineering, Liu, P. (Ed.). World Scientific, Singapore. 369p.

Gordon, D.A., 1993. A Holocene sediment budget for the Waitemata Harbour. Unpublished M.Sc thesis, Earth Science Department, University of Waikato, Hamilton.

Grant, J., and Daborn, G., 1994. The effects of bioturbation on sediment transport on an intertidal mudflat. *Netherlands Journal of Sea Research*, 32(1):63-72.

Greenwood, B., 1987. Sediment balance and bar morphodynamics in a multiple bar system: Georgian Bay, Canada, in *International Geomorphology 1986 Part I*, Gardiner, V. (Ed.), John Wiley & Sons Ltd, Great Britain. p1119-1143.

Gregory, M.R., and Thompson, S.A., 1973. *Recent sediments of Waitemata Harbour*. Auckland Harbour Board, Auckland Regional Authority. 33p.

Greig, M.J., 1990. Circulation in Hauraki Gulf, New Zealand. *New Zealand Journal of Marine and Freshwater Research,* 24:141-150.

Harris, T.F.W., 1985. North Cape to East Cape. Aspects of the physical oceanography. University of Auckland, Department of Physics and Marine Laboratory. 178p.

Hasselmann, K., Ross, D.B., Müller, P., and Sell, P., 1976. A parametric wave prediction model. *Journal of Physical Oceanography*, 6:200-228.

Healy, T.R., 1994. *Assessment of sedimentation and sediment transport processes in the vicinity of the Pine Harbour Marina and recommendations for future monitoring.* Report prepared for Pine Harbour Marina Ltd. 30p.

Heathershaw, A.D., and Carr, A.P., 1977. Measurements of sediment transport rates using radioactive tracers. In, *Proceedings of Coastal Sediments '77.* 5th Symposium of the Waterway, Port, Coastal & Ocean division of ASCE. New York. p399-416.

Howard, J.D., and Dörjes, J., 1972. Animal-sediment relationships in two beach-related tidal flats; Sapelo Island, Georgia. *Journal of Sedimentary Petrology*, 42(3): 608-623.

Hume, T.M., 1978. Clay petrology of Mesozoic to Recent sediments of central western North Island, New Zealand. Unpublished D.Phil. thesis, University of Waikato, Hamilton, New Zealand.

Hume, T.M., and Nelson, C.S., 1982. *X-ray diffraction analytical procedures and some mineralogical characteristics for south Auckland region sediments, and some sedimentary rocks, with special reference to their clay fraction.* Occasional Report No. 10, University of Waikato, Department of Earth Sciences, Hamilton. 33p.

Hurnard, S.M., 1980. Auckland's Climate. New Zealand Meteorological Service miscellaneous publication. 27p.

Ingle, J.C., 1966. *The movement of beach sand.* Elsevier, New York.

Inman, D.L., Zampol, J.A., White, T.A., Hanes, D.M., Walforf, B.W., and Kastens, K.A., 1980. Field measurements of sand motion in the surf zone. In, *Vol. 2 Proceedings of 17th Coastal Engineering Conference,.* Australia. ASCE Waterway, Port, Coastal & Ocean Division, New York. p1215-1234.

Johnson, R.G., 1967. The vertical distribution of the infauna of a sand flat. *Ecology*, 48(4): 571-578.

Kench, P.S., 1990. The hydrodynamics and morphodynamics of the Waipu tidal inlet, Northland. Unpublished M.A thesis, University of Auckland.

Kermode, L.O., 1992. *Geology of the Auckland urban area.* Scale 1:50 000. Institute of Geological & Nuclear Sciences geological map 2. 1 sheet + 63 p. Institute of Geological & Nuclear Sciences Ltd, Lower Hutt, New Zealand.

King, C.A.M., 1972. *Beaches and Coasts.* Edward Arnold Ltd, London. 570p.

Kingett Mitchell & Associates, 1993a. *Dredging of the approach channel to Pine Harbour Marina: Assessment of effects on the environment under the Resource Management Act 1991.* Report prepared for Pine Harbour Marina Ltd. 31p.

Kingett Mitchell & Associates, 1993b. *Disposal of sediment dredged from the approach channel to Pine Harbour Marina: Assessment of effects on the environment under the Resource Management Act 1991.* Report prepared for Pine Harbour Marina Ltd. 35p.

Knoth, J.S., and Nummedal, D., 1977. Longshore sediment transport using fluorescent tracer. In, *Proceedings of Coastal Sediments '77.* 5th Symposium of the Waterway, Port, Coastal & Ocean division of ASCE. New York. p 383-398.

Komar, P.D., 1976. *Beach Processes and Sedimentation.* Prentice-Hall Inc., New Jersey. 429p.

Komar, P.D., and Inman, D.L., 1970. Longshore sand transport on beaches. *Journal of Geophysical Research*, 75(30):5914-5927.

Komar, P.D., 1990. Littoral sediment transport. In, *Handbook of Coastal and Ocean engineering Vol.2.*, Herbich, J.B. (Ed.). Gulf Publishing Company, Houston. p681-714.

Komar, P.D., and Miller, M.C., 1973. The threshold of sediment movement under oscillatory water waves. *Journal of Sedimentary Petrology*, 43(4):1101-1110.

Komar, P.D., and Miller, M.C., 1975. On the comparison between the threshold of sediment motion under waves and unidirectional currents with a discussion of the practical evaluation of the threshold. *Journal of Sedimentary Petrology*, 45:362-365.

Kraus, N.C., Isobe, M., Igarashi, H., Sasaki, T.O., and Horikawa, K., 1982. Field experiments on longshore sand transport in the surf zone. In, *Proceedings of 18th Coastal Engineering Conference*, South Africa. Edge, B.L. (Ed.), ASCE, New York. p969-989.

Lewis, D.W., and McConchie, D., 1994. *Analytical sedimentology*. Chapman & Hall, London. p92-107.

Madsen, O.S., 1989. Transport determination by tracers: Tracer theory, *in Nearshore sediment transport*, Seymour, R.J. (Ed.). Plenum Press, New York. p103-114.

Masselink, G., and Short, A.D., 1993. The effect of tide range on beach morphodynamics and morphology: A conceptual beach model. *Journal of Coastal Research*, 9(3):785-800.

Meadows, P.S., and Tait, J., 1989. Modification of sediment permeability and shear strength by two burrowing invertebrates. *Marine biology*, 101:75-82.

Mehta, A.J., and Lee, S., 1994. Problems in linking the threshold condition for the transport of cohesionless and cohesive sediment grain. *Journal of Coastal Research*, (10)1: 170-177.

Mei, C.C., 1989. *The applied dynamics of ocean surface waves*. Vol. 1, Advanced Series on Ocean Engineering, Liu, P. (Ed.). World Scientific, Singapore. 740p.

Miller, M.C., McCave, I.N., and Komar, P.D., 1977. Threshold of sediment motion under unidirectional currents. *Sedimentology,* 24:507-527.

Naish, T.R., 1990. Mud sedimentation and diagenesis in Firth of Thames. Unpublished M.Sc thesis, University of Waikato, Hamilton. 136p.

Nielsen, P., 1992. *Coastal bottom boundary layers and sediment transport.*. Vol. 4, Advanced Series on Ocean Engineering, Liu, P. (Ed.). World Scientific, Singapore. 324p.

Nierododa, A W., and Swift, D.J.P., 1991. Shoreface processes. In, *Handbook of Coastal and Ocean Engineering*, Vol. 2, Herbich, J.B. (Ed.). Gulf Publishing Company Houston, Texas. p737-770.

New Zealand Coastal Policy Statement, 1994. Department of Conservation, Wellington. 26p.

Proctor, R., and Greig, M.J.N., 1989. A numerical model investigation of the residual circulation in Hauraki Gulf, New Zealand. *New Zealand Journal of Marine and Freshwater Research*, 23:421-442.

Raudkavi, A.J., 1986. *Hydraulic studies - Pine Harbour Marina EIA*. Report prepared for Pine Harbour Marina. 6p.

Resource Management Act, 1991. New Zealand Government Print, Wellington. 382p.

Sherman, D.J., Nordstrom, K.F., Jackson, N.L., and Allen, J.R., 1994. Sediment mixing depths on a low energy reflective beach. *Journal of Coastal Research*, 10(2):297-305.

Shirley, J.C., 1991. Development of Pine Harbour Marina. In, *"Coastal Engineering - Climate for Change"* proceedings of the 10th Australasian Conference on Coastal and Ocean Engineering, Auckland, 2-6 Dec. 1991. p465-469.

Short, A.D., 1991. Macro-meso tidal beach morphodynamics - An overview. *Journal of Coastal Research,* 7(2):417-436.

Smart, P., and Tovey, N.K., 1981. *Electron microscopy of soils and sediments: Examples*. Clarendon Press, Oxford. 177p.

Sunamura, T. and Kraus, N.C., 1985. Prediction of average mixing depth of sediment in the surf zone. *Journal of Marine Geology*, 62:1-12.

White, T.E., and Inman, D.L., 1989. Application of tracer theory to NSTS experiments. In, *Nearshore sediment transport*. Seymour, R.J., (Ed.). Plenum Press, New York. p133-137.

Whitton, J.S., and Churchman, G.J., 1987. *Standard methods for mineral analysis of soil survey samples for characterisation and classification in NZ Soil Bureau.* NZ Soil Bureau Scientific Report 79, Department of Scientific and industrial Research, Lower Hutt. 18p.

Wilkens & Davies, 1986. *Pine Harbour Marina - Statutory application and environmental impact assessment.* Report prepared for Pine Harbour Marina Ltd.

Wright, L.D., and Short, A.D., 1983. Morphodynamics of beaches and surf zones in Australia. In, *CRC Handbook of Coastal Processes and Erosion*. Komar, P.D., (Ed.), CRC Press Inc. Boca raton, Florida, USA. p35-64.

APPENDIX 1: Sediment textural data

APPENDIX 1.1: Observations of sediment bedforms during surficial sediment sampling of intertidal flats fronting Pine Harbour Marina, February 1995.

Sample Site	Bedform observations
1	Ripple h = 0.5 cm, λ= 5.0 cm, oriented NW-SE.
2	Edge of shell ridge. Shell spp. present *paphies, macomona, austrovenus.* Ripple h = 1.0 cm, λ = 4.0 cm, oriented NW-SE.
3	Ripple h = 1.0 cm, λ = 4.0 cm, oriented NW-SE. Finer sediment in trough.
4	Ripple h = 1.0 cm, λ = 4.0 cm, oriented NW-SE. Finer sediment in trough.
5	Ripple h = 0.5 cm, λ = 3.0 cm, oriented N-E. Finer sediment in trough.
6	Ripple h = 1.0 cm, λ = 6.0 cm, oriented N-S. Finer sediment in trough, no shell hash.
7	Sample taken 75 m from channel on edge of dredgings. Ripple h = 1.0 cm, λ = 5.0-6.0 cm, oriented N-S. Very fine dark sediment on crests, with lighter fine sediment in trough.
8	Sample taken 30 m from channel. Relict ripple marks h <1.0 cm. 1 cm aerobic layer.
9	Sample taken at edge of channel. No bedforms. *Austrovenus* shells, rocks and crabs in dredgings sediment.
10	Ripple h < 1.0 cm, λ = 5.0-6.0 cm. Ripple crest not parallel, oriented roughly NW-SE.
11	Ripple h = 1.0 cm, λ = 3.0-4.0 cm, oriented NW-SE. Finer sediment in trough, no shell hash. Superimposed on these ripples smaller E-W oriented ripples (h = 0.5 cm, λ = 3.0 cm.
12	Sample taken 10 m north of shell ridge (abundant *macomona, austrovenus*). Ripple h = 1.5 cm, λ = 7.0 cm, oriented N-S.
13	Shell ridge approximately 5 m wide, abundant *austrovenus* and *macomona.*
14	20 m from shell ridge. Ripple h = 1.0 cm, λ = 6.0 cm, oriented N-S.
15	50 m from channel, 30 m from dredgings. Irregular ripples.
16	40 m from channel in dredgings. Crab burrows and shells. Dredgings sediment muddy to ankles. Some ripples h = 0.5 cm, λ = 5.0 cm.
17	5 m from channel in dredgings. Rock fragments.
18	10 m from channel. Ripple h = 1.0-1.5 cm, λ = 6.0-7.0 cm, oriented NW-SE. Many *macomona* and *austrovenus* shells.
19	75 m from channel. Ripple h = 1.0 cm, λ = 4.0-5.0 cm, oriented N-S.
20	Flat topped ripples, h = 0.5 cm, λ = 3.0-5.0 cm. Many *austrovenus* and *macomona* shells.
21	Ripple h <1.0 cm, λ = 4.0-5.0 cm, oriented NNW-SSE. Ripple crests vaguely parallel. Less shell material.
22	No bedforms. Abundant polychaete tubes and shell hash.
23	Ripple h = 0.5 cm, λ = 3.0-4.0 cm, show signs of erosion and are not parallel.
24	No bedforms. *Austrovenus* shells.
25	Ripple h = 0.5 cm, λ = 5.0 cm. Ripple crests wavy vaguely oriented NW-SE.
26	Muddy patches, darker sand sized sediment overlying lighter silt sized sediment. Ripple h = 0.5 cm, λ = 1.0-2.0 cm, oriented NW-SE.
27	Ripple h = 1.0 cm, λ = 3.0 cm, oriented NW-SE. Slightly muddy.
28	Ripple h = 1.0 cm, λ = 3.0-6.0 cm. Lunate ripples roughly oriented NW-SE
29	Ripple h = 0.5 cm, λ = 2.0-3.0 cm, oriented NW-SE.
30	Ripple h = 0.5 cm, λ = 2.0-3.0 cm, oriented NW-SE parallel.

APPENDIX 1.1 continued: Observations of sediment bedforms during surficial sediment sampling of intertidal flats fronting Pine Harbour Marina.

Sample site	Bedform observations
31	10 m from channel. Ripples h = 1.5 cm, λ = 8.0 cm, oriented E-W parallel to channel.
32	Mid beach slope, many shells (cockles, clams) and stones.
33	Sample near where stream drains onto tidal flat. Large area of gravel sized sediment veneering shore platform. Beach face covered with shell hash.
34	Shelly beach 8 m wide veneering shore platform. Cockles dominant also pipi and rock fragments in sand. Shell ridge (1 m high, 3 m wide) joins Beachlands coastline.
35	Narrow black sand beach.
36	Sandy bank, few shells against cliff. Drainage rills oriented NW-SE.
37	No bedforms. Abundant shell hash, very old, stained and crumbly.
38	Shell ridge, sandier on north side.
39	Ripple h =1.0 cm, λ = 3.0-4.0 cm, oriented SE-NW. Sandy with abundant *austrovenus* shells.
40	Ripples h = 0.5-1.0 cm, λ = 4.0-5.0 cm, oriented NNW-SSW. Sandy sediment veneers rock 10-20 cm.
41	Broad flat ripples, h = 0.5 cm, λ = 6.0-8.0 cm, oriented SW-NE.
42	No bedforms. Sample located near boat ramp sediment predominantly muddy.
43	Ripples h = 1.0 cm, λ = 3.0-4.0 cm, oriented NW-SE. Few *austrovenus* and *macomona*).
44	Ripple h = 1.0 cm, λ = 3.0-4.0 cm, oriented SSE-NNW. Abundant *austrovenus* shells.
45	Ripple h = 1.0 cm, λ = 3.0-4.0 cm, oriented SSE-NNW. Abundant *austrovenus* shells
46	Sediment predominantly muddy with abundant *austrovenus* shells. Vague irregular ripples, h <1.0 cm, λ = 5.0 cm.
47	Beach face with abundant shell hash.
48	Beach face predominantly sandy with rock fragments.
49	Beach face.
50	Beach near location of stream discharging onto tidal flats..

APPENDIX 1.2: Subtidal sediment observations: A) In the approach channel to Pine Harbour Marina, and B) Along Transects A, B and C.

A) Diver observations and probe measurements of sediment depth on channel floor, 27/9/95. Sample locations illustrated in Figure 3.1b.

Site location	Time	Depth sounder	Diver observations
1 Entrance to marina	11:30	1.5m	Steel rod all the way in (1.4 m) and more, layers of clay (harder to penetrate) in between softer muds.
2 50m seaward of 1st lit beacon	11:55		Diver could stand 1/3 way into channel from south. Rod penetrated 1.4 m before contacting hard layer. No "clay" layers. Dug core out with arm in soft mud.
3 1st unlit starboard marker	12:15	1.6m	Rod (1.4 m) into silt plus up to elbow, could have gone further. Weight sunk into mud.
4 36'53.358'S 174'58.872E	12:55	1.5m middle of channel	> 1.4 m plus arm. Silty mud.
5 2nd unlit starboard marker	12:35	Deeper in middle of channel	> 1.4 m plus arm. Dug arm in to get core out. Silty mud.
6 36'53.341'S 174'58.791'E	1:15	1.8m	> 1.4 m plus arm, harder layers at end. Silty mud.
7 36'53.210'S 174'58.750'E	1:37	1.6m	Rod penetrated 1.35 m then hard bottom. Silty mud.

B) SCUBA observations along Transects A offshore Sunkist Bay, B Motukaraka Island, and C, and the northern intertidal flats, December 1995. All transects start inshore to offshore. Transect locations illustrated in Figure 3.1a.

TRANSECT A: SUNKIST BAY

Distance along transect (m)	Description of sediment	Bedform observations
Start	Fine sand, no mud.	
10	Very fine sand as above.	Ripple h = 2-3 cm, λ ~5 cm.
20	Silty sand, shell fragments.	Ripples not as well defined, h~1 cm.
30	Muddy sand, coarse silt. Abundant worms.	Faint ripple marks h ~1 cm, λ ~5 cm.
40	Very fine sand, coarse silt. Lots of worms and shells.	Vague bedforms h ~1 cm.
50	Coarse silt, same as above	Ripple h = 1-2 cm, finer mud lighter colour in troughs.
70	Muddier than onshore sediments. All silt and some shell fragments.	Small ripple h ~1 cm.
90	Coarse silt with finer sediment in troughs (more lighter coloured finer silt in troughs than previous site).	Irregular ripple h~12 cm, λ~3 cm.
110	Muddier than previous site.	Ripples as above

TRANSECT B: MOTUKARAKA ISLAND

Distance along transect (m)	Description of sediment	Bedform observations
Start	Rocks (shore platform) thinly veneered with silt.	
10	Medium sand with gravel sized shell hash. Mud in troughs.	Ripple h ~3 cm, λ~8 cm
30	Medium sand with gravel sized shell hash. Mud in troughs.	Ripple h ~3 cm, λ~8 cm.
50	Medium sand with shell hash.	Bedforms as above
70	Medium sand.	Ripples h ~ 3 cm, λ ~ 8 cm.
90	Medium sand.	Ripple h ~3 cm, λ ~ 8 cm.
110	Medium/coarse sand. Abundant sand dollars	Large irregular ripples h ~3-4 cm.

TRANSECT C: BETWEEN MARINA APPROACH CHANNEL AND MOTUKARAKA ISLAND

Distance along transect (m)	Description of sediment	Bedform observations
Start	Medium sand.	
20m	All mud, dominantly silt. Sediment sticks together in clumps, slightly coarser underneath.	No bedforms.
40m	Silt/clay very fine sediment	No bedforms.
60m	Same as previous, getting finer.	
80m	Same as previous, very fine and sticky.	
100m	No change, very fine and sticky	
110m	No change, very fine and sticky	

APPENDIX 1.3: Textural parameters of intertidal flat sediments. Sample locations Figure 3.1a.

Sample No.	% Gravel	% Sand	% Mud	Moment method parameters				Textural description
				Mean	Sorting	Skewness	Kurtosis	
1	9.68	86.88	3.45	2.79	0.55	-0.91	7.27	Moderately well sorted, near symmetrical, mesokurtic
2	46.41	51.22	2.37	2.56	0.84	-1.39	6.65	Moderately well sorted, near symmetrical, mesokurtic
3	-	-	-	2.86	0.54	-1.27	10.11	Moderately well sorted, coarse skewed, mesokurtic
4	7.92	88.06	4.02	2.86	0.66	-1.81	11.6	Moderately well sorted, coarse skewed, mesokurtic
5	2.02	88.54	9.45	2.91	0.81	-2.5	12.48	Moderately well sorted, strongly coarse skewed, leptokurtic
6	0.02	90.49	9.50	2.78	0.87	-1.54	7.12	Moderately well sorted, strongly coarse skewed, mesokurtic
7	0.00	81.76	18.24	2.88	0.89	-2.31	11.83	Moderately well sorted, coarse skewed, mesokurtic
9	11.67	41.79	46.53	2.93	0.92	-1.4	5.1	Moderately well sorted, coarse skewed, leptokurtic
10	1.72	95.20	3.08	2.64	0.67	-0.74	5.31	Moderately well sorted, coarse skewed, mesokurtic
11	1.95	93.96	4.09	2.72	0.64	-1.08	5.71	Moderately well sorted, coarse skewed, mesokurtic
12	34.91	62.97	2.11	2.91	0.76	-3.01	17.74	Moderately well sorted, coarse skewed, mesokurtic
13	73.27	24.64	2.09	2.13	1.15	-0.46	2.17	Poorly sorted, coarse skewed, platykurtic
14	2.78	93.96	3.26	2.91	0.53	-0.6	3.43	Moderately well sorted, coarse skewed, mesokurtic
15	0.17	91.45	8.38	2.97	0.59	-0.78	3.95	Moderately well sorted, coarse skewed, mesokurtic
16	1.76	48.46	49.78	3.02	0.76	-1.16	5.58	Moderately well sorted, coarse skewed, leptokurtic
17	29.12	59.53	11.35	2.68	0.82	-1.06	5.32	Moderately well sorted, coarse skewed, mesokurtic
18	11.56	85.88	2.56	2.67	0.63	-0.35	2.34	Moderately well sorted, coarse skewed, platykurtic
19	24.73	72.77	2.50	2.66	0.72	-1.42	7.54	Moderately well sorted, coarse skewed, platykurtic
20	25.67	72.90	1.43	2.55	0.79	-1.76	10.14	Moderately well sorted, near symmetrical, platykurtic
21	1.34	97.38	1.27	2.65	0.6	-0.22	2.52	Moderately well sorted, near symmetrical, platykurtic
22	1.13	96.68	2.19	2.72	0.66	-1.19	6.52	Moderately well sorted, coarse skewed, mesokurtic
23	12.19	78.74	9.07	2.93	0.79	-2.62	14.96	Moderately well sorted, coarse skewed, mesokurtic
24	0.54	98.18	1.27	2.87	0.46	-0.37	4.48	Well sorted, near symmetrical, platykurtic
25	0.00	96.20	3.80	2.88	0.67	-2.78	19.76	Moderately well sorted, coarse skewed, mesokurtic
26	0.68	83.13	16.19	3.02	0.7	-2.25	13.42	Moderately well sorted, coarse skewed, mesokurtic
27	1.35	91.55	7.10	2.89	0.67	-2.07	14.81	Moderately well sorted, near symmetrical, mesokurtic
28	0.01	98.10	1.88	2.65	0.62	-0.48	3.23	Moderately well sorted, coarse skewed, mesokurtic
29	7.28	89.10	3.61	3.01	0.71	-3.11	19.89	Moderately well sorted, near symmetrical, mesokurtic
30	0.12	93.86	6.02	2.91	0.66	-2.26	14.58	Moderately well sorted, coarse skewed, mesokurtic
31	13.06	79.82	7.12	2.85	0.63	-0.85	5.25	Moderately well sorted, coarse skewed, mesokurtic
32	37.95	61.38	0.67	2.08	0.71	-0.84	5.74	Moderately well sorted, near symmetrical, mesokurtic
33	16.91	81.36	1.73	1.47	0.76	0.02	3.23	Moderately sorted, near symmetrical, mesokurtic
34	46.49	52.88	0.63	1.02	0.76	0.25	3.26	Moderately sorted, fine skewed, mesokurtic
35	30.54	68.94	0.53	1.5	0.75	-0.08	5.06	Moderately well sorted, near symmetrical, mesokurtic
36	17.50	79.62	2.88	2.09	0.62	-0.44	5.71	Moderately well sorted, fine skewed, mesokurtic
37	23.75	70.69	5.56	1.97	0.87	0.09	3.09	Moderately sorted, fine skewed, mesokurtic
38	80.80	18.95	0.25	0.47	0.64	0.22	5.36	Moderately well sorted, fine skewed, leptokurtic
39	0.53	95.98	3.50	2.85	0.09	-2.41	10.21	Moderately sorted, strongly coarse skewed, leptokurtic
40	10.38	82.86	6.76	2.41	1.18	-0.81	3.56	Poorly sorted, coarse skewed, mesokurtic
41	0.65	89.81	9.54	2.6	0.76	-0.39	3.3	Moderately sorted, coarse skewed, platykurtic
42	14.43	80.32	5.25	2.54	0.74	-0.28	3.53	Moderately well sorted, near symmetrical, platykurtic
43	5.09	91.08	3.83	2.51	0.86	-0.9	4.82	Moderately sorted, near symmetrical, platykurtic
44	24.01	74.43	1.55	2.18	0.96	-0.34	2.67	Moderately sorted, near symmetrical, platykurtic
45	25.34	71.46	3.20	2.69	0.89	-1.95	9.06	Moderately sorted, coarse skewed, mesokurtic
46	6.95	91.29	1.77	2.99	0.57	-2.38	18.21	Well sorted, coarse skewed, mesokurtic
47	37.13	62.45	0.42	1.39	0.79	0.36	3.55	Moderately sorted, near symmetrical, mesokurtic
48	13.67	85.60	0.73	2.06	0.74	-0.75	7.24	Moderately well sorted, fine skewed, mesokurtic
49	9.46	90.02	0.51	1.76	0.76	0.66	3.77	Moderately well sorted, fine skewed, mesokurtic
50	19.70	79.52	0.78	1.56	0.68	0.23	5.57	Moderately well sorted, fine skewed, mesokurtic

APPENDIX 1.4: Textural composition of subtidal sediments and selected intertidal sediments with high mud content. Sample locations Figure 3.1a & 3.1b.

Sample Number	% Gravel	% Sand	% Silt	% Clay
5	0.02	65.13	26.86	7.99
6	1.99	70.36	21.11	6.54
7	0.02	51.88	38.16	9.94
9	0.48	19.96	62.67	16.90
15	0.00	65.03	26.72	8.25
16	0.87	21.83	60.36	16.94
17	8.05	44.79	37.27	9.90
23	4.80	69.15	19.23	6.82
26	0.09	34.10	24.56	7.35
30	0.06	74.15	19.36	6.43
31	0.22	65.57	26.16	8.05
40	68.05	8.59	17.90	5.46
41	1.46	59.95	30.63	7.96
42	7.88	70.10	16.28	5.74
Dredgings	0.00	19.83	62.69	17.48
Dredgings	0.65	12.42	68.69	18.24
Dredgings core 2	0.00	26.54	54.71	18.74
Dredgings core 4	0.00	17.39	65.38	17.23
Offshore 36'52'530 174'59'220	0.56	23.17	61.02	15.25
A2 36'53'63 175'58'20	0.17	21.46	64.74	13.63
B2 36'53'31 175'58'20	0.54	27.61	59.24	12.61
D2 36'52'66 175'58'20	0.00	9.31	86.47	4.22
Sunkist Bay 36'52'53 174'58'910	0.00	21.88	62.26	15.86
D1 36'52'66 175'58'50	0.00	88.47	8.05	3.48
E1 36'52'34 175'58'50	3.45	40.71	44.47	11.37
A3 36'53'63 175'57'90	0.39	21.77	52.97	11.42
C2 36'52'98 175'58'20	0.28	45.00	40.91	13.81
channel 1	0.00	34.12	51.02	7.43
channel 2	0.00	57.48	31.98	11.44
channel 3	0.00	52.49	35.71	13.66
channel 4	0.00	21.58	61.18	12.43
channel 5	0.00	21.09	62.06	8.24
channel 6	0.00	35.40	49.78	14.18
channel 7	0.00	23.83	62.43	8.34

APPENDIX 2: Turbidity monitoring

APPENDIX 2.1: Short term turbidity monitoring results during 1994 dredging operation at Pine Harbour Marina. (Site A = channel; Site B = control site 200 m upstream).

Date & conditions	Time	Hach 16800 (NTU)		Hach 2100A (NTU)		Suspended solids (mg/l)	
		A	B	A	B	A	B
22/6/94	0825	11.0	6.2	4.7	4.1	-	-
•W to SW wind up to	1005	25.5	6.1	4.0	3.8	-	-
10 knots	1135	21.0	3.6	4.5	4.0	-	-
•Waves 0.3-0.5m	1310	5.6	11.5	7.8	8.3	-	-
•Tide 2.5m @ 1440	1440	9.2	9.2	32.0	-	-	-
• 5.5 mm rain	1615	17.5	11.0	4.3	4.5	-	-
27/9/94 •W wind 15-20 knots	1500 Marina entrance	11	-	-	-	62	-
•Waves 0.25-1.0m •14 mm rain	1505 Adjacent barge	17	-	-	-	28	-
•Tide 1.9m @ 1500	1510 200m seaward of barge	72	-	-	-	205	-
	1517 Site A	13	-	-	-	18	-
11//7/94	1200	-	-	5.9	20.2	12	85
15/7/94	1500	-	-	4.1	4.1	13	13
17/8/94		-	-	4.5	5.0	18	19
10/8/94		-	-	6.1	5.4	37	24

APPENDIX 2.2: Summary of long term turbidity monitoring results from October 1994 to November 1995, and prevailing wind and current conditions during sampling. Sampling sites are located in Figure 3.9. Daily turbidity and suspended solid levels are presented in Figures 1 to 5.

Date	Conditions	Range NTU (Hach 2100A)	Location of highest NTU (Hach 2100A)	Range mg/l	Location of highest mg/l
7/10/94	SW wind 5-10 knots; waves 0.1-0.2m; heavy rainfall; outgoing tide NE current	8-15 NTU	30-37 NTU at sites 6 & 7	5-35 mg/l	65 mg/l at site 6 and 50 mg/l at site 1 & 11
17/1/95	NE 10-15 knots; waves 0.05-0.5 m; no rain; outgoing tide NW current	8-20 NTU	37 NTU at site 3	10-30 mg/l	50 mg/l at site 3
26/4/95	NW wind 5-10 knots; waves 0.2-0.5 m; no rain; incoming tide SE current.	8-15 NTU	24 NTU at site 12	6-18 mg/l	24 mg/l in marina basin 18 mg/l at site 9 and 12
18/7/95	SW wind 5-10 knots; waves 0.1-0.2 m; no rain; outgoing tide NW current	5-13 NTU	13 NTU at site 2	25-75 mg/l	100 mg/l at site 8 and 200 mg/l at site 11
2/11/95	SW wind 20 knots; waves 0.1-0.4 m; no rain; incoming tide SE current	8-15 NTU	25-45 NTU at site 1 & 2	5-20 mg/l	40 mg/l at site 1 & 2

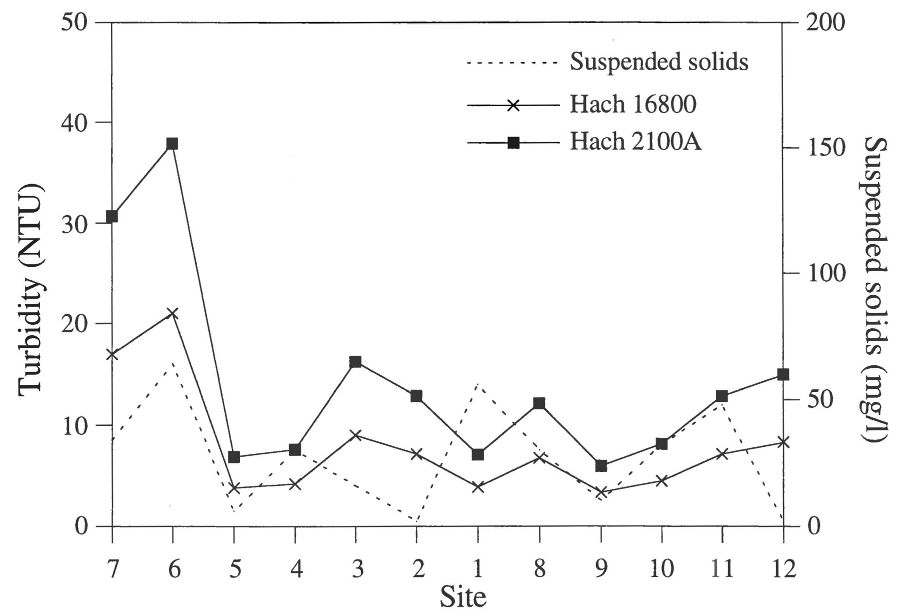

FIGURE 1: Turbidity (NTU) and suspended solids (mg/l) along the Beachlands coastline 7/10/94 after heavy rainfall. Sites 5, 6 & 7 are located near Waikopua Creek, sites 1-4 in the vicinity of Pine Harbour Marina, and sites 8-12 north of Pine Harbour Marina along Sunkist Bay to Shelly Bay.

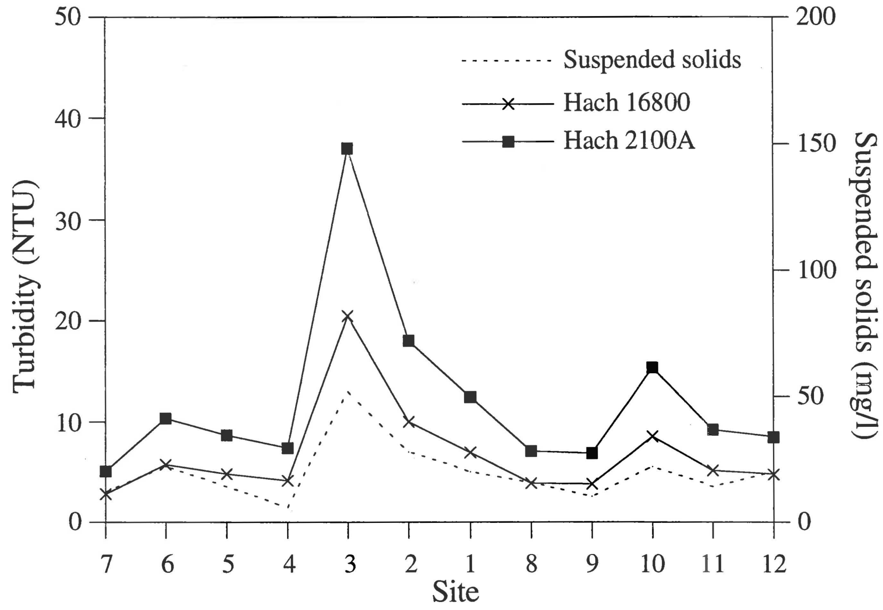

FIGURE 2: Turbidity (NTU) and suspended solids (mg/l) along Beachlands coastline 17/1/95. Sites 5, 6 & 7 are located near Waikopua Creek, sites 1-4 in the vicinity of Pine Harbour Marina, and sites 8-12 north of Pine Harbour Marina along Sunkist Bay to Shelly Bay.

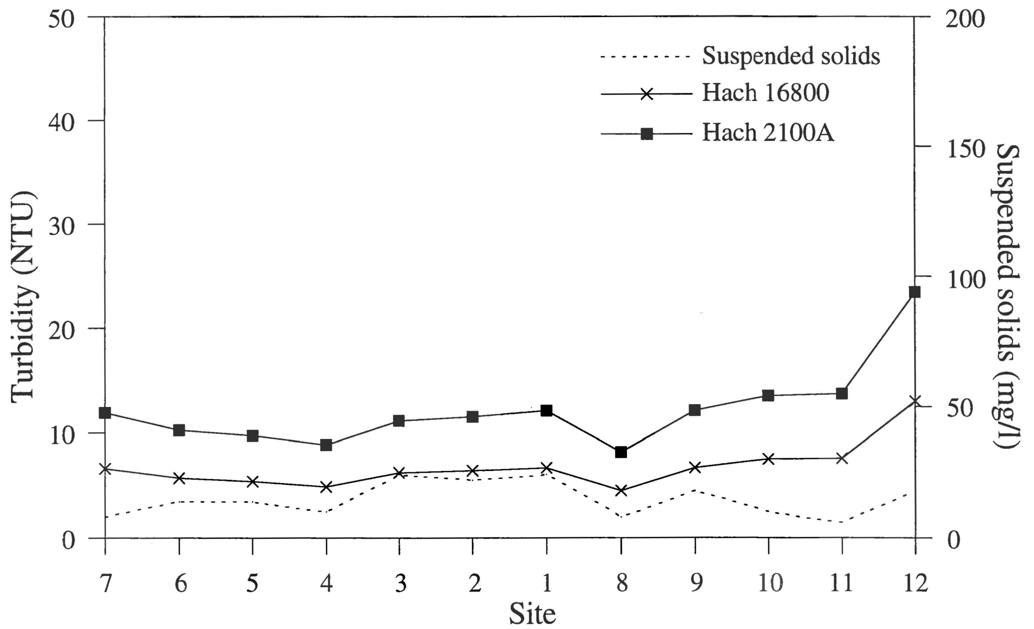

FIGURE 3: Turbidity (NTU) and suspended solids (mg/l) along Beachlands coastline 26/4/95. Sites 5, 6 & 7 are located near Waikopua Creek, sites 1-4 in the vicinity of Pine Harbour Marina, and sites 8-12 north of Pine Harbour Marina along Sunkist Bay to Shelly Bay.

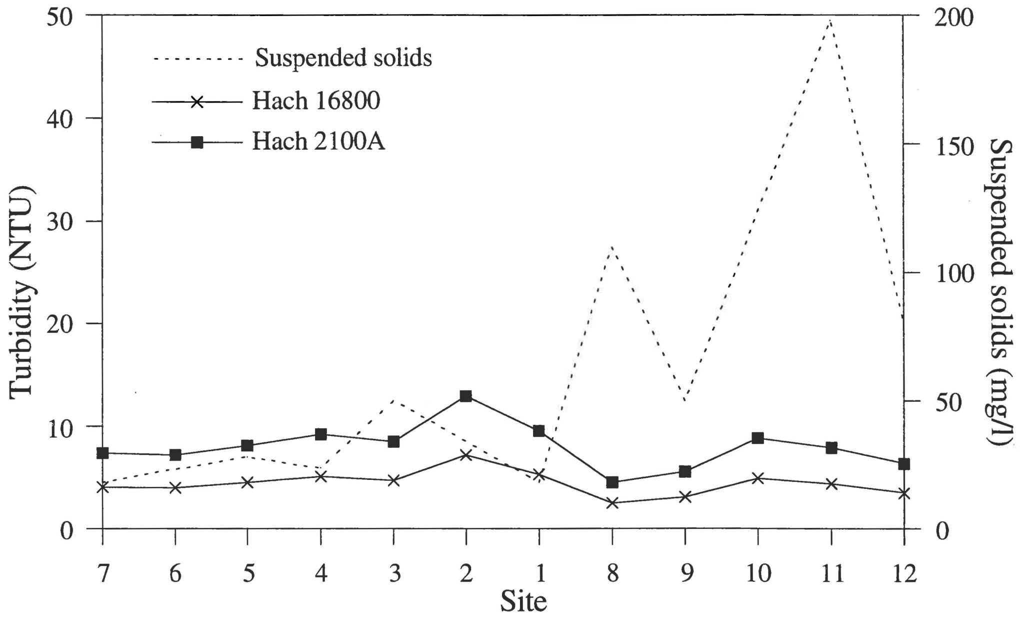

FIGURE 4: Turbidity (NTU) and suspended solids (mg/l) along Beachlands coastline 18/7/95. Sites 5, 6 & 7 are located near Waikopua Creek, sites 1-4 in the vicinity of Pine Harbour Marina, and sites 8-12 north of Pine Harbour Marina along Sunkist Bay to Shelly Bay.

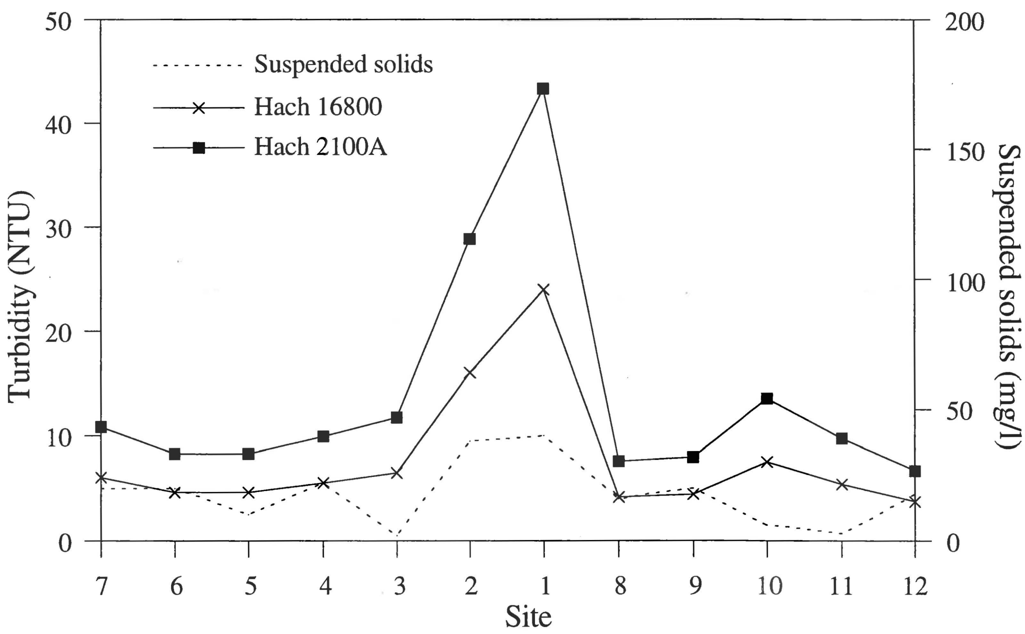

FIGURE 5: Turbidity (NTU) and suspended solids (mg/l) along Beachlands coastline 2/11/95. Sites 5, 6 & 7 are located near Waikopua Creek, sites 1-4 in the vicinity of Pine Harbour Marina, and sites 8-12 north of Pine Harbour Marina along Sunkist Bay to Shelly Bay.

APPENDIX 3: Sedimentation rod results

APPENDIX 3.1: Depths of sediment disturbance (DOD) or mixing recorded by sedimentation rods located across the intertidal flats fronting Pine Harbour Marina from June 1994 to February 1995 (Figure 3.15).

Date	Line 1, rod 1			Line 1, rod 2			Line 1, rod 3			Line 1, rod 4		
	cm to sand	cm to washer	DOD (cm)	cm to sand	cm to washer	DOD (cm)	cm to sand	cm to washer	DOD (cm)	cm to sand	cm to washer	DOD (cm)
1/6/94	-	-	-	-	-	-	-	-	-	-	-	-
3/6/94	21.60	21.60	0.00	10.80	10.80	0.00	27.60	27.60	0.00	-	-	-
22/6/94	23.00	23.00	0.00	11.00	11.00	0.00	missing	missing	-	-	-	-
27/6/94	23.20	23.20	0.00	11.00	11.00	0.00	23.20	23.20	0.00	13.80	13.80	0.00
12/7/94	23.00	23.00	0.00	10.80	10.80	0.00	23.40	24.80	1.40	missing	missing	-
20/9/94	22.20	22.20	0.00	10.80	10.80	0.00	missing	missing	-	missing	missing	-
22/9/94	missing	missing	missing	-	-	-	43.80	43.80	0.00	43.60	43.60	0.00
17/10/94	-	-	-	10.80	10.80	0.00	44.20	47.80	3.60	45.10	49.00	3.90
11/11/94	-	-	-	-	-	-	missing	missing	-	missing	missing	-
29/11/94	-	-	-	10.80	10.80	0.00	-	-	-	46.00	48.20	2.20
5/1/95	-	-	-	10.80	10.80	0.00	-	-	-	missing	missing	-
15/2/95	-	-	-	13.00	missing	-	-	-	-	-	-	-

Date	Line 2, rod 1			Line 2, rod 2			Line 2, rod 3		
	cm to sand	cm to washer	DOD (cm)	cm to sand	cm to washer	DOD (cm)	cm to sand	cm to washer	DOD (cm)
1/6/94	-	-	-	-	-	-	-	-	-
3/6/94	16.80	16.80	0.00	35.40	35.40	0.00	-	-	-
22/6/94	16.60	16.60	0.00	35.20	35.20	0.00	-	-	-
27/6/94	16.40	16.40	0.00	35.80	35.80	0.00	18.00	18.00	0.00
12/7/94	17.00	17.00	0.00	36.00	36.00	0.00	18.80	19.40	0.60
20/9/94	17.00	17.00	0.00	35.40	35.40	0.00	19.40	19.40	0.00
22/9/94	-	-	-	-	-	-	-	-	-
17/10/94	17.80	17.80	0.00	35.80	36.90	1.10	18.00	20.50	2.50
11/11/94	-	-	-	-	-	-	-	-	-
29/11/94	17.80	17.80	0.00	35.50	35.70	0.20	14.60	16.60	2.00
5/1/95	17.60	17.70	0.10	35.80	36.00	0.20	16.80	18.20	1.40
15/2/95	17.60	17.60	0.00	36.00	36.10	0.10	16.00	16.40	0.40

Date	Line 3, rod 1			Line 3, rod 2			Line 3, rod 3			Line 3, rod 4		
	cm to sand	cm to washer	DOD (cm)	cm to sand	cm to washer	DOD (cm)	cm to sand	cm to washer	DOD (cm)	cm to sand	cm to washer	DOD (cm)
1/6/94	24.00	24.00	0.00	19.00	19.00	0.00	60.00	60.00	0.00	24.00	24.00	0.00
3/6/94	23.60	23.60	0.00	19.40	19.40	0.00	55.00	55.00	0.00	24.10	24.10	0.00
22/6/94	24.80	24.80	0.00	20.00	20.00	0.00	55.80	55.80	0.00	25.20	25.20	0.00
27/6/94	24.40	24.50	0.10	19.80	19.80	0.00	56.10	59.60	3.50	25.50	30.04	4.54
12/7/94	24.40	24.40	0.00	20.00	20.00	0.00	missing	missing	-	25.00	27.20	2.20
20/9/94	23.40	23.40	0.00	20.60	20.60	0.00	48.40	51.80	3.40	23.00	27.20	4.20
22/9/94	-	-	-	-	-	-	-	-	-	-	-	-
17/10/94	24.00	24.00	0.00	20.40	20.40	0.00	48.20	54.40	6.20	25.40	29.00	3.60
11/11/94	24.60	24.60	0.00	20.80	20.85	0.05	48.40	49.40	1.00	26.00	28.80	2.80
29/11/94	24.60	24.60	0.00	20.60	20.60	0.00	48.80	49.80	1.00	25.80	25.90	0.10
5/1/95	24.60	24.60	0.00	20.60	20.80	0.20	48.80	49.80	1.00	25.90	26.20	0.30
15/2/95	25.00	25.00	0.00	21.00	21.00	0.00	48.60	49.80	1.20	26.30	26.90	0.60

Date	Line 4, rod 1			Line 4, rod 2			Line 4, rod 3		
	cm to sand	cm to washer	DOD (cm)	cm to sand	cm to washer	DOD (cm)	cm to sand	cm to washer	DOD (cm)
1/6/94	-	-	-	-	-	-	-	-	-
3/6/94	31.18	31.18	0.00	31.19	31.19	0.00	27.78	27.78	0.00
22/6/94	31.80	31.80	0.00	32.00	32.00	0.00	29.00	29.00	0.00
27/6/94	32.20	32.20	0.00	33.60	33.60	0.00	29.90	30.30	0.40
12/7/94	32.00	32.00	0.00	32.60	34.00	1.40	29.40	30.80	1.40
20/9/94	31.80	31.80	0.00	33.80	34.60	0.80	28.90	30.80	1.90
22/9/94	-	-	-	-	-	-	-	-	-
17/10/94	33.20	33.80	0.60	33.60	34.80	1.20	39.40	40.60	1.20
11/11/94	-	-	-	-	-	-	-	-	-
29/11/94	34.20	35.70	1.50	32.90	34.10	1.20	29.60	31.40	1.80
5/1/95	34.40	35.30	0.90	33.60	34.20	0.60	30.08	30.10	0.02
15/2/95	33.60	34.80	1.20	33.60	33.80	0.20	31.20	31.30	0.10

Date	Line 5, rod 1			Line 5, rod 2			Line 5, rod 3		
	cm to sand	cm to washer	DOD (cm)	cm to sand	cm to washer	DOD (cm)	cm to sand	cm to washer	DOD (cm)
1/6/94	-	-	-	-	-	-	-	-	-
3/6/94	29.80	29.80	0.00	43.20	43.20	0.00	33.40	33.40	0.00
22/6/94	30.20	30.20	0.00	43.60	43.60	0.00	33.40	33.40	0.00
27/6/94	31.00	31.40	0.40	43.70	43.70	0.00	33.60	35.00	1.40
12/7/94	30.60	31.40	0.80	43.80	43.80	0.00	33.80	34.20	0.40
20/9/94	30.60	32.10	1.50	43.50	43.50	0.00	33.80	34.50	0.70
22/9/94	-	-	-	-	-	-	-	-	-
17/10/94	30.40	32.20	1.80	43.80	45.40	1.60	33.40	34.40	1.00
11/11/94	-	-	-	-	-	-	-	-	-
29/11/94	31.60	32.80	1.20	44.70	45.40	0.70	34.20	34.70	0.50
5/1/95	31.30	31.80	0.50	44.60	45.80	1.20	34.80	35.30	0.50
15/2/95	32.00	32.00	0.00	45.00	45.50	0.50	34.60	36.30	1.70

Date	Line 6, rod 1			Line 6, rod 2			Line 6, rod 3		
	cm to sand	cm to washer	DOD (cm)	cm to sand	cm to washer	DOD (cm)	cm to sand	cm to washer	DOD (cm)
1/6/94	-	-	-	-	-	-	-	-	-
3/6/94	19.20	19.20	0.00	34.20	34.20	0.00	31.00	31.00	0.00
22/6/94	19.80	19.80	0.00	34.00	34.00	0.00	30.80	31.20	0.40
27/6/94	19.80	19.80	0.00	35.40	35.80	0.40	31.00	31.80	0.80
12/7/94	19.40	19.40	0.00	35.40	36.00	0.60	30.40	33.40	3.00
20/9/94	19.70	19.80	0.10	35.40	36.30	0.90	33.20	34.40	1.20
22/9/94	-	-	-	-	-	-	-	-	-
17/10/94	19.80	19.80	0.00	34.80	37.80	3.00	33.00	36.00	3.00
11/11/94	-	-	-	-	-	-	-	-	-
29/11/94	19.80	19.80	0.00	35.00	35.80	0.80	34.00	34.60	0.60
5/1/95	19.80	19.80	0.00	35.00	36.00	1.00	33.70	35.50	1.80
15/2/95	19.80	19.80	0.00	34.80	36.30	1.50	32.80	34.60	1.80

APPENDIX 4: WGEN3DD wave predictions

APPENDIX 4.1: Offshore wave conditions (H_s and T_s) predicted by wave model WGEN3DD at Site 1 (Figure 4.1) from wind rose data recorded at Pine Harbour Marina 23/11/94 to 17/1/95.

OFFSHORE SIGNIFICANT WAVE HEIGHT (H_s) IN METRES

WIND DIRN	FETCH (km)	EFETCH (km)	WIND SPEED (m/s) 0-1	1-3	3-6	6-10	10-16	16-21	Prob. of occurrence
NNE	3.99	5.15	0.02	0.07	0.14	0.19	0.00	0.00	3.01
NE	1.94	2.80	0.01	0.05	0.12	0.19	0.00	0.00	6.14
ENE	1.68	0.90	0.01	0.05	0.11	0.20	0.00	0.00	6.59
E	1.10	1.00	0.01	0.04	0.09	0.16	0.00	0.00	6.07
ESE	1.36	1.10	0.01	0.04	0.10	0.00	0.00	0.00	3.45
SE	1.79	1.40	0.01	0.05	0.11	0.00	0.00	0.00	7.29
SSE	2.25	2.85	0.01	0.06	0.13	0.22	0.00	0.00	7.15
S	2.80	2.60	0.02	0.06	0.14	0.25	0.39	0.52	11.11
SSW	2.99	3.35	0.02	0.07	0.15	0.26	0.41	0.55	18.55
SW	3.10	3.20	0.02	0.07	0.15	0.27	0.43	0.00	4.44
WSW	3.61	2.85	0.02	0.07	0.16	0.29	0.47	0.00	2.47
W	4.88	3.60	0.02	0.08	0.19	0.34	0.55	0.78	3.09
WNW	6.96	6.65	0.03	0.10	0.23	0.40	0.65	0.00	2.77
NW	8.52	12.70	0.03	0.11	0.25	0.44	0.70	0.00	3.38
NNW	8.01	8.20	0.03	0.11	0.24	0.42	0.66	0.00	11.07
N	6.63	1.00	0.02	0.09	0.18	0.26	0.00	0.00	3.44
Probability of occurrence			2.11	24.45	36.20	29.20	7.79	0.24	100.00

OFFSHORE SIGNIFICANT WAVE PERIOD (T_s) IN SECONDS

WIND DIRN	FETCH (km)	EFETCH (km)	WIND SPEED (m/s) 0-1	1-3	3-6	6-10	10-16	16-21	Prob. of occurrence
NNE	3.99	5.15	1.00	1.22	1.37	1.38	0.00	0.00	3.01
NE	1.94	2.80	1.04	1.04	1.15	1.41	0.00	0.00	6.14
ENE	1.68	0.90	1.00	1.08	1.15	1.32	0.00	0.00	6.59
E	1.10	1.00	1.06	1.08	1.15	1.33	0.00	0.00	6.07
ESE	1.36	1.10	1.01	1.08	1.17	0.00	0.00	0.00	3.45
SE	1.79	1.40	1.02	1.06	1.23	0.00	0.00	0.00	7.29
SSE	2.25	2.85	1.02	1.16	1.25	1.53	0.00	0.00	7.15
S	2.80	2.60	1.06	1.16	1.48	1.67	1.81	2.24	11.11
SSW	2.99	3.35	1.04	1.15	1.38	1.55	1.69	1.67	18.55
SW	3.10	3.20	1.04	1.17	1.57	1.55	1.70	0.00	4.44
WSW	3.61	2.85	1.08	1.16	1.31	1.77	1.89	0.00	2.47
W	4.88	3.60	1.07	1.29	1.51	1.75	2.10	2.34	3.09
WNW	6.96	6.65	1.08	1.52	1.62	1.82	2.27	0.00	2.77
NW	8.52	12.70	1.22	1.45	1.95	1.91	2.14	0.00	3.38
NNW	8.01	8.20	1.08	1.39	1.55	1.91	2.08	0.00	11.07
N	6.63	1.00	1.10	1.41	1.78	1.85	0.00	0.00	3.44
Probability of occurrence			2.11	24.45	36.20	29.20	7.79	0.24	100.00

APPENDIX 4.2: Wave conditions (H_s and T_s) predicted by wave model WGEN3DD at tracer site on the intertidal flats fronting Pine Harbour Marina (Figure 5.1) from wind rose data recorded at Pine Harbour Marina 23/11/94 to 17/1/95.

SIGNIFICANT WAVE HEIGHT (H_s) IN METRES OVER THE INTERTIDAL FLATS

WIND DIRN	FETCH (km)	EFETCH (km)	WIND SPEED (m/s) 0-1	1-3	3-6	6-10	10-16	16-21	Prob. of occurrence
NNE	3.99	5.15	0.02	0.07	0.15	0.24	0.00	0.00	3.01
NE	1.94	2.80	0.02	0.06	0.14	0.25	0.00	0.00	6.14
ENE	1.68	0.90	0.00	0.04	0.08	0.14	0.00	0.00	6.59
E	1.10	1.00	0.00	0.03	0.07	0.13	0.00	0.00	6.07
ESE	1.36	1.10	0.00	0.04	0.08	0.00	0.00	0.00	3.45
SE	1.79	1.40	0.01	0.04	0.10	0.00	0.00	0.00	7.29
SSE	2.25	2.85	0.01	0.05	0.12	0.20	0.00	0.00	7.15
S	2.80	2.60	0.02	0.06	0.13	0.23	0.33	0.42	11.11
SSW	2.99	3.35	0.02	0.07	0.15	0.25	0.36	0.46	18.55
SW	3.10	3.20	0.02	0.07	0.15	0.25	0.36	0.00	4.44
WSW	3.61	2.85	0.02	0.08	0.17	0.30	0.49	0.00	2.47
W	4.88	3.60	0.02	0.09	0.20	0.36	0.57	0.81	3.09
WNW	6.96	6.65	0.03	0.10	0.23	0.41	0.66	0.00	2.77
NW	8.52	12.70	0.03	0.11	0.23	0.38	0.55	0.00	3.38
NNW	8.01	8.20	0.03	0.10	0.20	0.30	0.37	0.00	11.07
N	6.63	1.00	0.02	0.10	0.21	0.36	0.00	0.00	3.44
Probability of occurrence			2.11	24.45	36.20	29.20	7.79	0.24	100.00

SIGNIFICANT WAVE PERIOD (T_s) IN SECONDS OVER INTERTIDAL FLATS

WIND DIRN	FETCH (km)	EFETCH (km)	WIND SPEED (m/s) 0-1	1-3	3-6	6-10	10-16	16-21	Prob. of occurrence
NNE	3.99	5.15	2.03	1.52	1.56	1.52	0.00	0.00	3.01
NE	1.94	2.80	1.82	1.56	1.44	1.52	0.00	0.00	6.14
ENE	1.68	0.90	0.00	1.99	1.48	1.52	0.00	0.00	6.59
E	1.10	1.00	0.00	3.13	1.66	1.46	0.00	0.00	6.07
ESE	1.36	1.10	0.00	1.99	1.42	0.00	0.00	0.00	3.45
SE	1.79	1.40	3.34	1.51	1.59	0.00	0.00	0.00	7.29
SSE	2.25	2.85	2.92	1.64	1.44	1.73	0.00	0.00	7.15
S	2.80	2.60	2.28	1.21	1.32	1.46	1.64	2.02	11.11
SSW	2.99	3.35	1.99	1.47	1.44	1.63	2.03	2.05	18.55
SW	3.10	3.20	1.89	1.20	1.39	1.59	1.81	0.00	4.44
WSW	3.61	2.85	1.84	1.28	1.46	1.54	1.76	0.00	2.47
W	4.88	3.60	1.62	1.52	1.54	2.01	2.07	2.64	3.09
WNW	6.96	6.65	1.55	1.52	1.94	1.95	2.60	0.00	2.77
NW	8.52	12.70	1.41	1.40	1.77	2.08	2.46	0.00	3.38
NNW	8.01	8.20	1.46	1.37	1.77	2.23	2.48	0.00	11.07
N	6.63	1.00	1.45	1.47	1.67	1.92	0.00	0.00	3.44
Probability of occurrence			2.11	24.45	36.20	29.20	7.79	0.24	100.00

APPENDIX 5: Tracer studies

APPENDIX 5.1: Tracer particle grain sizes in sediment samples determined with AFC, indicating most tracer particles were less than 50µm. Sample sites are located in Figures 5.1 & 5.2.

Sample site	Date	% tracer below 0.04 mm (4.5 phi)	AFC assessment mm	AFC assessment Phi
Release pt	21/12/94 am	36.4	50% < 0.05	4.25
E	21/12/94 am	17.7	25% < 0.05	4.25
Release pt	21/12/94 pm	45.7	40% < 0.02	6.00
SE	21/12/94 pm	34.5	-	-
W	21/12/94 pm	13.7	-	-
8	21/12/94 pm	16.8	uniform 0.1-0.01	3.25-6.00
S	22/12/94	28.3	40% < 0.05	4.25
SSW	22/12/94	21.9	-	-
6	22/12/94	17.9	uniform 0.1-0.01	3.25-6.00
ENE	23/12/94	20.6	uniform 0.1-0.01	3.25-6.00
NNW	23/12/94	17.9	uniform 0.1-0.01	3.25-6.00
1	23/12/94	9.2	-	-
SSW	27/12/94	23.7	-	-
5	27/12/94	16.7	-	-
SE	10/1/95	20.6	uniform 0.1-0.01	3.25-6.00
SSE	10/1/95	14.2	70% < 0.04	4.50
W	10/1/95	17.7	30%< 0.04 60% >0.07	30% < 4.50 60% > 3.75
6	10/1/95	11.5	0% < 0.02 uniform 30-100	0% < 4.25 uniform 3.25-5.00
13	10/1/95	14	0%<0.02 uniform 0.03-0.01	0%< 5.00 uniform 5.00-6.00
20	10/1/95	17	uniform 0.1-0.01	uniform 3.25-6.00
22	17/1/95	8.2	70%+ < 0.06	70%+ < 4.00
SSW	27/2/95	16.8	50% < 0.025 50% > 0.06	50% < 5.00 50% > 4.00
8	27/2/95	10.2	85% < 0.06	85% < 4.00

APPENDIX 5.2: Results of fluorescent tracer experiment, with comparative concentrations of tracer particles determined through UV light method and AFC analysis (- denotes sample not analysed with AFC). Sampling locations are shown in Figures 5.1 & 5.2.

Sample No.	UV Light		AFC
	Tracer particles per kg	Tracer particles per g	Tracer particles per g
20/12/94			
Release point	3,140,000	3,140.000	184,240
21/12/94 am (1/2 day)			
Release point	1,520,000	1,520.000	31,652
N	60	0.060	403,859
NNE	-	-	-
NE	49	0.049	-
ENE	-	-	-
E	5,902	5.902	45,917
ESE	-	-	-
SE	5,232	5.232	-
SSE	-	-	-
S	-	-	-
SSW	-	-	-
SW	11	0.011	-
WSW	29	0.029	-
W	223	0.223	-
WNW	35	0.035	-
NW	-	-	-
NNW	-	-	-
21/12/94 pm (1 day)			
Release point	1,250,000	1,250.000	56,650
N	82	0.082	13,800
NNE	27	0.027	-
NE	159	0.159	-
ENE	10	0.010	-
E	55	0.055	-
ESE	64	0.064	-
SE	1,022	1.022	65,013
SSE	106	0.106	-
S	26	0.026	-
SSW	0	0.000	127,066
SW	32	0.032	-
WSW	224	0.224	-
W	513	0.513	75,937
WNW	464	0.464	-
NW	202	0.202	-
NNW	59	0.059	-
1	1	0.001	-
2	0	0.000	-
3	0	0.000	-
4	0	0.000	-
5	0	0.000	-
6	0	0.000	-
7	0	0.000	-
8	15	0.015	23,003
9	0	0.000	-
10	0	0.000	-
22/12/94 (2 days)			
Release point	24,079	24.079	23,029
N	9	0.009	35,077
NNE	5	0.005	-
NE	0	0.000	-
ENE	0	0.000	-
E	14	0.014	-
ESE	0	0.000	-
SE	102	0.102	-
SSE	305	0.305	-
S	1,863	1.863	37,648
SSW	229	0.229	45,089
SW	141	0.141	-
WSW	12	0.012	-
W	62	0.062	-
WNW	69	0.069	-
NW	40	0.040	-
NNW	10	0.010	-
1	0	0.000	-
2	0	0.000	-
3	0	0.000	-
4	7	0.007	-
5	0	0.000	-
6	0	0.000	-
7	0	0.000	-
8	7	0.007	-
9	0	0.000	-
10	0	0.000	-

Sample No.	UV Light		AFC
	Tracer particles per kg	Tracer particles per g	Tracer particles per g
23/12/94 (3 days)			
Release point	10,741	10.741	19,639
N	78	0.078	4,898
NNE	16	0.016	-
NE	70	0.070	15,893
ENE	70	0.070	11,414
E	45	0.045	-
ESE	34	0.034	22,334
SE	563	0.563	-
SSE	156	0.156	41,269
S	862	0.862	-
SSW	54	0.054	28,394
SW	62	0.062	-
WSW	9	0.009	35,866
W	77	0.077	-
WNW	96	0.096	6,183
NW	195	0.195	14,729
NNW	36	0.036	-
1	258	0.258	13,609
2	0	0.000	8,408
3	10	0.010	-
4	0	0.000	-
5	0	0.000	-
6	9	0.009	8,470
7	0	0.000	-
8	49	0.049	-
9	0	0.000	47,188
10	0	0.000	-
27/12/94 (7 days)			
Release point	9,538	9.538	8,901
N	56	0.056	11,489
NNE	37	0.037	-
NE	51	0.051	-
ENE	18	0.018	-
E	104	0.104	-
ESE	16	0.016	-
SE	175	0.175	-
SSE	81	0.081	-
S	421	0.421	-
SSW	177	0.177	51,111
SW	111	0.111	-
WSW	78	0.078	-
W	93	0.093	-
WNW	140	0.140	-
NW	77	0.077	-
NNW	9	0.009	-
1	0	0.000	-
2	0	0.000	-
3	0	0.000	-
4	0	0.000	-
5	0	0.000	27,495
6	0	0.000	-
7	0	0.000	-
8	0	0.000	-
9	0	0.000	-
10	0	0.000	-
10/1/1995 (21 days)			
Release point	8,375	8.375	28,389
N	76	0.076	14,629
NNE	57	0.057	-
NE	110	0.110	-
ENE	25	0.025	-
E	63	0.063	-
ESE	61	0.061	-
SE	225	0.225	-
SSE	0	0.000	24,657
S	169	0.169	-
SSW	17	0.017	-
SW	94	0.094	-
WSW	0	0.000	-
W	9	0.009	-
WNW	19	0.019	-
NW	39	0.039	-
NNW	18	0.018	-

Sample No.	UV Light		AFC
	Tracer particles per kg	Tracer particles per g	Tracer particles per g
10/1/95 (21 days)			
1	10	0.010	-
2	0	0.000	-
3	0	0.000	-
4	0	0.000	-
5	-	-	-
6	0	0.000	85,759
7	0	0.000	-
8	0	0.000	-
9	0	0.000	-
10	0	0.000	-
11	10	0.010	-
12	0	0.000	-
13	0	0.000	-
14	0	0.000	-
15	-	-	-
16	0	0.000	-
17	0	0.000	-
18	17	0.017	-
19	0	0.000	-
20	0	0.000	
17/1/95 (28 days)			
21	10	0.010	847,516
22	93	0.093	727,569
27/2/95 (69 days)			
Release point	3,779	3.779	12,851
N	94	0.094	23,172
NNE	76	0.076	-
NE	41	0.041	13,809
ENE	27	0.027	-
E	55	0.055	-
ESE	23	0.023	16,498
SE	333	0.333	22,259
SSE	91	0.091	20,948
S	358	0.358	-
SSW	129	0.129	86,306
SW	148	0.148	-
WSW	130	0.130	38,761
W	207	0.207	-
WNW	0	0.000	13,814
NW	45	0.045	10,714
NNW	36	0.036	-
1	29	0.029	7,882
2	0	0.000	9,807
3	0	0.000	-
4	0	0.000	-
5	0	0.000	-
6	0	0.000	25,314
7	0	0.000	-
8	0	0.000	183,951
9	0	0.000	30,085
10	0	0.000	-
11	11	0.011	-
12	0	0.000	-
13	0	0.000	-
14	0	0.000	-
15	0	0.000	-
16	0	0.000	-
17	0	0.000	-
18	0	0.000	-
19	0	0.000	12,497
20	0	0.000	9,294
August 1995 - Release pt core			
0-2cm			29,928
2-4cm			37,347
4-6cm			22,839
6-8cm			36,016
8-10cm			105,282
10-12cm			27,962
12-14cm			23,693
14-17cm			132,389
20/12/95			
Release pt			12,435

APPENDIX 5.3: Record of brick chip tracer movement from 29/11/94 to 15/2/95. The number of brick chips to move distances of between 0-1 m, 1-2 m, and > 2 m from the plots were recorded, along with the direction of movement. Brick chip movement was less than 1 m until 15/2/95 when chips moved up to 2 m at Plot A. Location of brick chip plots A, B and C are located in Figure 5.18.

BRICK CHIP PLOT A

DATE	Distance (m)	Direction and number of brick chips moved from plot							
		N	NE	E	SE	S	SW	W	NW
29/11/94	0-1	0	0	0	0	0	0	0	0
3/12/94	0-1	0	0	0	0	0	0	0	0
7/12/94	0-1	0	0	0	0	0	0	0	0
22/12/94	0-1	6	10	8	4	0	0	0	0
5/1/95	0-1	0	4	3	3	0	0	0	3
21/1/95	0-1	2	3	1	0	2	0	3	0
15/2/95	0-1	35	19	6	1	1	0	1	6
	1-2	0	7	2	0	0	0	0	0

BRICK CHIP PLOT B

DATE	Distance (m)	Direction and number of brick chips moved from plot							
		N	NE	E	SE	S	SW	W	NW
29/11/94	0-1	0	0	0	0	0	0	0	0
3/12/94	0-1	0	0	0	0	0	0	0	0
7/12/94	0-1	0	0	0	0	0	0	0	0
22/12/94	0-1	0	0	0	0	0	0	0	0
5/1/95	0-1	2	0	0	0	0	1	0	0
21/1/95	0-1	1	0	0	2	0	1	0	0
15/2/95	0-1	0	0	0	0	0	0	0	0
	1-2	0	0	0	0	0	0	0	0

BRICK CHIP PLOT C

DATE	Distance (m)	Direction and number of brick chips moved from plot							
		N	NE	E	SE	S	SW	W	NW
29/11/94	0-1	0	0	0	0	0	0	0	0
3/12/94	0-1	0	0	0	0	0	0	0	0
7/12/94	0-1	0	0	0	0	0	0	0	0
22/12/94	0-1	0	0	8	0	0	0	0	0
5/1/95	0-1	4	4	2	1	0	0	1	3
21/1/95	0-1	5	2	1	0	0	0	0	3
15/2/95	0-1	10	2	2	0	0	0	3	0
	1-2	0	0	0	0	0	0	0	0